University of Nebraska - Lincoln
DigitalCommons@University of Nebraska - Lincoln

Architectural Engineering -- Dissertations and Student Research

Architectural Engineering

12-2016

An Investigation of DX Cooling Coil Inherent Characteristics

Krittima Santiwattana
University of Nebraska-Lincoln, ksantiwattana@unomaha.edu

Follow this and additional works at: http://digitalcommons.unl.edu/archengdiss

Part of the Architectural Engineering Commons

Santiwattana, Krittima, "An Investigation of DX Cooling Coil Inherent Characteristics" (2016). *Architectural Engineering -- Dissertations and Student Research*. 45.
http://digitalcommons.unl.edu/archengdiss/45

This Article is brought to you for free and open access by the Architectural Engineering at DigitalCommons@University of Nebraska - Lincoln. It has been accepted for inclusion in Architectural Engineering -- Dissertations and Student Research by an authorized administrator of DigitalCommons@University of Nebraska - Lincoln.

AN INVESTIGATION OF DX COOLING COIL INHERENT CHARACTERISTICS

by

Krittima Santiwattana

A THESIS

Presented to the Faculty of

The Graduate College at the University of Nebraska

In Partial Fulfillment of Requirements

For the Degree of Master of Science

Major: Architectural Engineering

Under the Supervision of Professor Haorong Li

Lincoln, Nebraska

December, 2016

AN INVESTIGATION OF DX COOLING COIL INHERENT CHARACTERISTICS

Krittima Santiwattana, M.S.

University of Nebraska, 2016

Advisor: Haorong Li

DX cooling coil (DCC) systems have dominated light commercial and household applications in the U.S for several decades. Approximately 14.5% of energy use is consumed by space cooling in commercial buildings, whereas 87% of households are installed with air-conditioners. Improper installation, poor design, and lack of optimized control/operations incur faults in HVAC systems causing 25% to 50% energy waste in a building. These consequences are subject to inefficient equipment modelling of which is developed from: (1) insufficient understanding in equipment characteristics, (2) uncertainties in testing environment and data, and (3) access and cost limitations. Therefore, in this thesis DCC inherent characteristics are investigated by using manufacturers' data to improve DCC modelling procedures.

Model based control/optimization of DCC methods are: white-box (theoretical-based and physical-based), requiring particular equipment physical geometries, and black-box (empirical-based), requiring high-qualitied data for performance mapping. In practice, physical geometries and laboratory testing data are not always available or not accurate enough to provide robust approximations and validations. A generic rating-data-based (GRDB) model, which can accurately predict roof top unit (RTU) capacities, is derived from readily available manufacturers' data, and the model format is based on measured environment temperatures and air flow rates (CFM).

Accordingly, GRDB will be re-examined and extensively applied to mini-split heat pumps (MSHPs). Unlike RTUs, MSHPs' manufacturing performance data ranges are limited, so intensive understanding of DCC inherent characteristics are essential to create more accurate models. In accordance, the characteristics are examined by air principles and fundamentals of vapor compression cycle (VCC), and illustrated by normalized capacities (NCAPs) and sensible heating ratio (SHR) plots. In addition, new DCC modelling procedures are proposed in this research.

Finally, the improved GRDB for MSHPs, validated by laboratory data, shows relative errors ranged from 12.5% to -8.6%. In addition, the proposed inherent characteristic hypotheses are validated using manufacturers' data from various conditions and systems. The results show correlations in associated with proposed hypotheses. Profound understanding of DCC inherent characteristics in this research could lead to better modelling procedures as it could lessen model complexity and computational processes, which could benefit low-cost sensing and fault detection and diagnostics technologies.

ACKNOWLEDGEMENT

With sincere and most gratitude, the author would like to thank Professor Haorong Li for his continuous support, guidance, and encouragement throughout my graduate life in the University of Nebraska Lincoln, and for offering valuable opportunity to be part of such groundbreaking research areas. Without his thoughtful guidance and patience, this research would not have been proceeded. He patiently trains me with his learning format from the scratch of forming research ideas. Throughout his precious criticism, I am encouraged to craft for the best of my research.

I would like to thank Dr. David Yuill for his comments and suggestions throughout my student life, and for Dr. Avery Schwer and Dr. Bo Shen for serving as my advisory committee and for their valuable suggestions and comments.

I would like extend my gratitude to Dr. Avery Schwer for his guidance for my extracellular market survey projects, Dr. Jay Pucket for giving feedbacks, Dr. Yubin Yu, Mrs. Jeans Waters, Mr. Joshua Nicol-Caddy and Miss Wei Jing for providing information and support throughout the project.

Special thanks for Dr. Denchai Woradechjumroen for introducing such a wonderful study program, for deeply discussion in the pursuit of knowledge, and for his help throughout my first year of studying; for their friendship and intensive discussion to Mr. Yuchen Wang and Mr. Sungmin Yoon, and for friendship and encouragement from my dearest friends from Thailand.

Finally, I devote my effort and this thesis to my dear mother, father and my brother for their love, care, understanding and life-long support.

TABLE OF CONTENT

Acknowledgement iv

Table of content v

List of Table viii

List of Figure x

Nomenclature xiii

Chapter 1. Introduction 15

1.1. Background 15

1.2. Literature Review 19

1.2.1. Residential Air-conditioning Equipment and MSHP 19

1.2.2. Virtual Sensing and FDD Technologies 21

1.2.3. Cooling Performance Models 25

1.3. Motivation and Objectives 27

1.4. Methodology 28

1.5. Thesis Organization 28

Chapter 2. Data Sources 30

2.1. Overview 30

2.2. Laboratory Data 30

2.3. Manufacturing Data 32

2.3.1. Manufacturing data for GRDB 32

2.3.1.1. Mitsubishi FE12NA data 32

2.3.1.2. Fujitsu 12RLS data 32

2.3.2. Other Manufacturing data 33

Chapter 3. Cooling Coil Characteristic analysis and its hypopthesis setup 34

3.1. Cooling Coil Operating Condition 34

3.1.1. Dry Coil 37

3.1.2. Wet coil 38

3.1.3. Actual cooling coil operation 39

3.2. DX Cooling coil model mechanism 41

3.3. Analysis of cooling capacity model mechanism using applied-GRDB for MSHPs 46

3.4. Analysis of Cooling Coil Characteristics Under Fixed OAT and CFM 48

3.4.1. Varying wet-bulb temperature on fixed dry-bulb temperature 49

3.4.2. Varying wet-bulb temperatures under various dry-bulb temperatures . 51

3.4.3. Further analysis cooling coil characteristics based on principles of air 54

3.4.3.1. SHR characteristics' model formulation 55

3.4.3.2. Total cooling capacity characteristics' model formulation 57

3.4.4. Characteristics' model verification using Engineering Equation Solver (EES) and Microsoft Excel. 57

3.5. Analysis of Cooling Coil Characteristics Under Constant Indoor Dry-bulb Temperature (DB) 60

3.5.1. Analysis of Cooling Coil Characteristics Under Fixed DB and CFM .. 60

3.5.2. Analysis of Cooling Coil Characteristics Under Fixed DB and OAT .. 63

3.6. Hypotheses Setup Normalizing and Scaling under Rating Condition 64

Chapter 4. Validation of Normalization and Scalability of DX cooling coil characteristic hypotheses by manufacturing data 67

4.1. GRDB cooling models on MUZ-FE12NA evaluation 67

4.2. Rating Conditions 69

4.3. Manufacturers' performance data evaluation 70

4.3.1. MSHPs 70

4.3.2. Split heat pumps (SHP) 75

4.3.2.1. Fixed DB 77

4.3.2.1. Fixed OAT and CFM 79

4.3.3. Package units 84

4.3.3.1. Fixed DB 84

4.4. Inflection Point Estimation 89

4.4.1. Local Points Estimator 89

4.4.2. Global Estimator 95

Chapter 5. Summaries, Conclusions and Recommendations 98

5.1. Summaries and conclusions 98

5.2. Recommendations and future works 101

List of References 103

APPENDIX A Laboratory testing data for GRDB 107

APPENDIX B Cooling Characteristic plots using psychrometric properties on EES (CODE) 108

APPENDIX C Mini-split system Manufacturers' data 111

APPENDIX D GRDB calculation procedure for MUZ-fe12NA 114

APPENDIX E Split system Manufacturers' data 117

APPENDIX F Package unit Manufacturers' data 152

APPENDIX G Local optimized critical points of various cooling conditions 181

APPENDIX H Global optimized critical points of Carrier model 25hbb18 with fixed DB of 80°F 200

LIST OF TABLE

Table 1-1 Method of implementing seven faults and levels simulated (Chen & Braun, 2000) 23
Table 2-1 Manufacturers' reported data for Fujitsu 12RLS and Mitsubishi FE12NA 31
Table 4-1 Statistical data of errors for all models at maximum speed compressor and DB of 80°F 69
Table 4-2 Manufacturers' reported data 75
Table 4-3 Manufacturers' reported data for Carrier CHP48HE 84
Table 4-4 Critical points of given manufacturing data 93
Table A-1 Trained data of MSHPs MUZ-FR12NA with fixed DB at 80°F 107
Table B-1 Cooling capacities of various DB and WB condition at fixed OAT and WB from psychrometric chart on EES 109
Table C-1 Mitsubishi FE12NA cooling performance data (Fixed DB=80°F) 111
Table C-2 FE12NA cooling performance corrections 111
Table C-3 Trained MUZ-FR12NA data for GRDB where rated CFM is 350 cfm... 112
Table C-4 Fujitsu 12RLS cooling performance data 113
Table C-5 Daikin FTKN12NMVJU + RKN12NMVJU cooling performance data . 113
Table E-1 Goodman DSZ16024-Low cooling performance data 117
Table E-2 Goodman DSZ16024-High cooling performance data 119
Table E-3 Goodman DSZ16036-High cooling performance data 120
Table E-4 Goodman DSZ16048-High cooling performance data 121
Table E-5 Goodman DSZ16060-High cooling performance data 122
Table E-6 Carrier model 25HBB324,36 and 60 cooling performance data 123
Table E-7 York model CZF0- cooling performance data 124
Table F-1 Carrier RTU-CHP48HE004 performance data 152
Table F-2 Carrier RTU-CHP48HE006 performance data 153
Table F-3 Carrier RTU-CHP48HE012 performance data 154
Table F-4 Trane RTU-PRC048-T/YHC037E3 (3 ton) performance data 160
Table F-5 Trane RTU-PRC048-T/YHC047E3 (4 ton) performance data 161
Table F-6 Trane RTU-PRC048-T/YHC067E3 (5 ton) performance data 162
Table G-1 An RTU's cooling performance data..... 181

Table G-2 Critical plots based on local optimization of maximized R square values at 85°f of Outdoor air temperature 182
Table G-3 Critical plots based on local optimization of maximized R square values at 95°f of Outdoor air temperature 186
Table G-4 Critical plots based on local optimization of maximized R square values at 105°F of Outdoor air temperature 191
Table G-5 Critical plots based on local optimization of maximized R square values at 115°F of Outdoor air temperature 195
Table H-1 Cooling Performance data of 25HBB18..... 200
Table H-2 SHR and cooling performance data of 25HBB18 200
Table H-3 Estimated inflection points calculation tables. 201
Table H-4 Estimated inflection points calculation tables. 202
Table H-5 25HBB318 critical point estimation table for normalized plots of Figure F1 209

LIST OF FIGURE

Figure 1-1 Hierarchy scheme of SoVS by Li, et al., 2011 22
Figure 1-2 Generic procedures of FDDs for unitary HVAC system (Katipamula & Brambley, 2005) 23
Figure 1-3 The characteristics of normalized total cooling capacity, sensible heating ratio, and wet-bulb temperature of air entering coil (WB_{aie}) with dry-bulb temperature (T_{aie}), outdoor temperature (OAT) and air flowrate (CFM) (Yang, et al., 2013) 26
Figure 3-1 Schematic of cooling coil process 34
Figure 3-2 Air properties at a fixed pressure. 35
Figure 3-3 Air processing in AC equipment on the psychrometric chart 35
Figure 3-4 Cooling process of dry coil 38
Figure 3-5 Wet-coiled cooling in AC equipment 39
Figure 3-6 Process of air passing through cooling coil 40
Figure 3-7 Actual cooling wet-coil process with bypass air 41
Figure 3-8 An intelligent air-conditioner schematic with enabled virtual sensors 43
Figure 3-9 An air-conditioner enabled with physical and virtual sensors 43
Figure 3-10 Vapor compression cooling system and its inputs and outputs 44
Figure 3-11 Normalized inputs and outputs relationship of VCC cooling system 45
Figure 3-12 VCC cooling coil model 45
Figure 3-13 GRDB model for MSHPs procedure chart 48
Figure 3-14 Characteristics of coil cooling at fixed CFM, DB_{aie} and OAT in relative to varying WB_{aie} 50
Figure 3-15 Cooling capacity and Sensible heating ratio characteristics in relative to WB_{aie} of cooling coil with fixed DB_{aie}, OAT and CFM 51
Figure 3-16 Characteristics of coil cooling at fixed CFM, WB_{aie} and OAT in relative to varying DB_{aie} 52
Figure 3-17 Cooling capacity characteristics while varying DB_{aie} on fixed WB_{aie} line at fixed OAT and CFM 53
Figure 3-18 Cooling capacity and SHR characteristics on fixed OAT and CFM 54
Figure 3-19 Cooling capacity characteristics of varying DB_{aie} on fixed WB_{aie} line at fixed OAT and CFM 55

Figure 3-20 Cooling Capacity characteristics in relative to WB 58
Figure 3-21 SHR characteristics in relative to WB 59
Figure 3-22 Characteristics of cooling coil at constant T_{evap} 59
Figure 3-23 Fundamental of vapor compression cycle illustration 60
Figure 3-24 Cooling capacity characteristics under fixed DB and CFM..... 61
Figure 3-25 Normalized characteristics of cooling coil performance at fixed CFM condition 62
Figure 3-26 Normalized characteristics of cooling coil performance at sixed OAT condition 64
Figure 3-27 Cooling coil characteristics' hypothesis..... 65
Figure 4-1 Actual laboratory data results and model predicted results 69
Figure 4-2Cooling performance of Mitsubishi at fixed DB of 80 F 72
Figure 4-3Cooling performance of Daikin FTXKN 73
Figure 4-4Cooling performance of Fujitsu RLS 74
Figure 4-5 SHR and Cooling performance plots of Carrier 25HBB324 78
Figure 4-6 Normalized plots of Goodman DSZ16024 83
Figure 4-7 The illustration of moving WBcrit correlated with increasing OAT 86
Figure 4-8 SHR and Normalized cooling capacity (NCAP) plots of Carrier CHP48HE060 (5 tons) 88
Figure 4-9 3-local-point estimating method for optimization of maximized R-square value at 85 F of OAT where CFM, DB and OAT are 360, 75, and 85, respectively. 91
Figure 4-10 2-local-point estimating method for optimization of maximized R-square value at 85 F of OAT where CFM, DB and OAT are 360, 80, and 85, respectively. 92
Figure 4-11 Critical Points at (a) 75, (b)80 and (c)85 ^{o}F of dry-bulb temperature..... 94
Figure 4-12 Normalized plots with critical WB of 255HBB18 calculated by using global point-optimization..... 96
Figure D-1Generated two-order polynomial regression by using EES and its coefficients from modified GRDB's method..... 114
Figure D-2 Generated two-order polynomial regression by using EES and its coefficients from original GRDB method..... 115

Figure E-1 York model CZF024 capacity and SHR performance plots at Fixed OAT and DB = 80°F 125
Figure E-2 York model CZF036 capacity and SHR performance plots at Fixed OAT and DB = 80°F 126
Figure E-3 York model CZF060 capacity and SHR performance plots at Fixed OAT and DB = 80°F 127
Figure E-4 Carrier model 25HBB324 capacity and SHR performance plots at Fixed OAT and DB = 80°F 128
Figure E-5 Carrier model 25HBB336 capacity and SHR performance plots at Fixed OAT and DB = 80°F 129
Figure E-6 Carrier model 25HBB360 normalized capacity and SHR performance plots at Fixed OAT and DB = 80°F 130
Figure E-7 Goodman model DAZ16-024 Normalized capacity and SHR performance plots 137
Figure E-8 Goodman model DAZ16-036H Normalized capacity and SHR performance plots 144
Figure E-9 Goodman model DAZ16-060H Normalized capacity and SHR performance plots 151
Figure F-1 Carrier RTU model CHP48H004 Normalized capacity and SHR performance plots 155
Figure F-2 Carrier RTU model CHP48H006 Normalized capacity and SHR performance plots 157
Figure F-3 Carrier RTU model CHP48H012 Normalized capacity and SHR performance plots 159
Figure F-4 Trane RTU model PRC048K T/YHC037E3 model 3 Tons Normalized capacity and SHR performance plots 168
Figure F-5 Trane RTU model PRC048K T/YHC047E3 4 Ton Normalized capacity and SHR performance plots 174
Figure F-6 Trane RTU model PRC048K T/YHC067E3 (5 Ton) Normalized capacity and SHR performance plots 180
Figure H-1 25HBB318 critical point estimation normalized plots 210

NOMENCLATURE

$\dot{m}$	Mass flow rate	*lbm/min*
AC	Air-conditioning	
AEE	Air entering evaporator	
AFDD	Automated fault detection and diagnosis	
AHU	Air handling unit	
BF	Bypass factor	
CAP	Total Cooling capacity	*Btu/lbm*
CFM	Air flow rate	ft^3/min
C_k	Function of throat area and valve parameters	
C_p	Specific heat coefficient	$Btu/(lbm \cdot {}^{o}F)$
DB	Dry-bulb temperature	^{o}F
DHP	Ductless heat pumps	
DP	Dew-point temperature	^{o}F
DX	Direct expansion	
EER	Equipment efficiency ratio	
EES	Engineering Equation Solver	
EEV	Electronic expansion valve	
FDD	Fault detection and diagnosis	
GRDB	Generic-data-rated-based	
h	Enthalpy	*Btu/lbm*
HVAC	Heating, Ventilating, and Air-Conditioning	
MAT	Mixed air temperature	^{o}F
MSHP	Mini-split heat pump	
OAT	Outdoor air temperature	^{o}F
Rel_{er}	Relative error	
RH	Relative humidity	
RTF	Run time fraction	
RTU	Roof top unit	

SAT	Supply air temperature	^{o}F
SHR	Sensible heating ratio	
T	Temperature	
VCC	Vapor compression cycle	
VCCAC	Vapor compression cycle air-conditioning	
VRF	Variable refrigerant flow	
WB	Wet-bulb temperature	^{o}F
$\dot{Q}$	Capacity	*Btu/h*

Greek

ρ	Density	lb/ft^3
ω	Humidity ratio	

Subscripts

a	Air
aie	Air entering evaporator
cond	Condenser
evap	Evaporator
L	Latent
ll	Liquid line
rated	Rated condition
ref	Refrigerant
s	Sensible

CHAPTER 1. INTRODUCTION

1.1. Background

The demand for HVAC equipment in U.S. households rises 6.8% continuously and is expected to reach $20.4 billion in 2019. Unitary heat pumps and room air conditioners will account for $14.8 billion, up to 73% of all HVAC equipment demand in 2019 ("HVAC Equipment," 2015). From a study in 2011, 87% of households in the U.S. have air conditioners (ACs)—an almost 20% increase from 1993 (RECS, 2011). Also, improper installation, poor design, and lack or optimized control/operations incur faults in HVAC systems causing 25% to 50% of energy waste in buildings (Yu, et al., 2014). On the other hand, the trend of energy consumption for space heating and cooling declined from 58% in 1993 to 48% in 2009. Although newly-built homes are larger, they consume less energy than existing homes. The study shows that the average energy consumption per household decreased about 30 million British thermal units (Btu) from 1980 to 2009 (RECS, 2012) due to advances in technology that have increased efficiency in household equipment. Despite the reduction of energy consumption in space heating and cooling, air-conditioning of newly-built homes in 2009 consume 56% more energy in space cooling than that of homes built before 2000. This increase in energy consumption provides an opportunity to improve air conditioning equipment performance.

Space cooling accounts for 14.5% of energy use in the U.S. for commercial buildings (Cheung & Braun, 2014), and 6% of the total primary energy use in the U.S. is consumed by residential buildings. RTUs consume 62% of the total energy use in the commercial sector. More specifically, RTUs account for half of the energy use in light commercial buildings (Woradechjumroen, et al., 2014). In addition, central air

conditioning dominates the majority of AC in U.S. households by 60%, while window- and wall- units account for only 20% of household use (RECS, 2013). A study by the Department of Energy (DOE) shows $29 billion is spent each year to cool down homeowners' spaces (DOE, 2014).

Outdoor air temperature is one of the parameters which impact cooling performance. Although indoor temperature affects the cooling ability of equipment, it typically has a constant temperature setup between 70 to 80°F in summer. In addition, space humidity level has significant impact on both comfort and equipment performance. High relative humidity (RH) results in space overcooling or out-of-comfort-range RH of 30-60% during the summer cooling season (Z. Li & Deng, 2007). Moreover, using multiple linear regression to analyze equipment operation, reducing indoor RH from 55 to 30% could possibly reduce energy consumption (Woradechjumroen et al., 2015). In subtropical and tropical areas that are hot and humid in summer, humidity-control plays an important role in maintaining comfort. Energy efficiency ratio (EER) can be increased by expanding the evaporating surface, thereby reducing the condensing and evaporating temperature (T_{cond} and T_{evap}) gap and decreasing moisture removal capacity in the evaporating coil. However, if the temperature maintained in the conditioned space is satisfactory, RH may not be in control (Li et al., 2006). Another example of humidity impact in commercial buildings by Henderson in 2005 demonstrates that runtime fraction degrades humidity removal in packaged units. When compressors are in the rest state, latent removal ability halts and humidity level will start to accumulate in the spaces due to moisture emission occupants and infiltration (Henderson, 2005). Accordingly, Woradechjumroen studied oversizing effects of 12 big-box suppermarkets, and stated that 40% of studied RTUs are commonly

oversized by 25%, resulting in longer runtime fration (RTF) and leading to humidity addition in stores.

In the 1990's as the cost of measuring devices decreased, fault detection and diagnostics (FDD) research started to grow, though FDD applications have been previously applied in such critical systems that require crucial control and monitoring to which minor failures could lead to loss of life and property (Li & Braun, 2007). In 1998, Breuker and Braun studied common faults in RTUs by surveying and analyzing 6,000 of their recorded fault cases (Breuker & Braun, 1998). Li and Braun developed decoupling features of simultaneous faults in simple vapor compression air conditioners and depicted factors related to the degradation of fault operation in such systems (Li & Braun, 2007b). Although the growth of FDD technologies is astonishing, the study of actual benefits of FDD findings are limited. The benefits of automated FDDs (AFDDs) are not only associated with location and application, it varies by the cost of sensing devices. The cost of some sensing devices are still too expensive to be applicable.

Virtual sensors utilize measurements from other variables associated with mathematical models from other principal sensors to generate desired measurement outputs (Cheung & Braun, 2014). With solid design, the cost of virtual sensors could be relatively low. Virtual sensing technologies have been introduced in the market for decades and widely used in process controls and automobiles, though not many such sensing applications are installed in building systems due to the conventional thought of which physical sensors are more robust and reliable. Li et al., 2011 reviewed virtual sensing techniques in buildings and their benefits in building applications. An example of virtual sensing of supply air flow in RTUs is given (D. Yu et al., 2011), and of virtual cooling

capacity and SHR is given (Yang & Li, 2011). Utilizing low-cost virtual sensors, Li and Braun address the economic impact of AFDDs applied to RTUs in California and found two major savings in service and operating costs that potentially save 70% of annual service cost and $5 to $51/kW·year of operating cost depending on the location and application (H. Li & Braun, 2007).

Present FDDs on the market still needs improvements. Although the technology can detect and diagnose inherent faults, not all the faults require immediate maintenance. Moreover, there are no standard or evaluating tools to measure the performance of FDD. In 2013, Yuill and Braun proposed a method of evaluating the performances of FDD protocol by collecting fault responses relative to the fault's impacts on performance and compare the collected data with fault and un-faulted measurement data. The case study protocol in the paper shows more than 50% of alarms triggered with no fault, 26% with miss diagnosis and 32% with not detecting inherent faults.

In summary, the performance of control and FDD models still needs improvement to be widely implemented. In addition, engineering models or empirical models are the majority of modelling methods that have been implemented because an empirical model can be created without understanding equipment characteristics (input-output). In order to achieve a solid model, understanding of devices' characteristics are required and will be investigated in this research.

1.2. Literature Review

1.2.1. Residential Air-conditioning Equipment and MSHP

AHRI[1] defines small unitary equipment as one piece, a matched split system, or an air source heat pump whose capacity is less than 65,000 Btu/h and most air-conditioning equipped vapor compression devices (AHRI, 2016).

Packaged systems are systems that have an evaporator and condenser combined in one single unit. Packaged systems installed on the rooftop are called RTUs A system requires ductwork and additional fans to deliver air to conditioned spaces. Other packaged units are window types which are installed on perimeter walls adjacent to an outdoor environment and require no ductwork.

Split systems are systems that have two components: an indoor and outdoor unit. The outdoor unit comprises a heat exchanger and compressor while the indoor unit comprises a heat exchanger and expansion device. Heat pumps are included in a split system as well. In addition, split systems can be subdivided into ducted and ductless systems.

Developed in Japan, ductless heat pumps (DHPs) dominate air-conditioning market share in Asian and European countries, but only 1% were installed in the U.S. This system has high efficiency, less complexity and requires less storage space during installation due to the absence of duct work. Also, it has the ability to be individually controlled and operated in specified spaces. Advantages of DHPs include comfort, low electricity consumption, ability to cool and heat in a single unit, and low-cost installation (Hlavinka

[1] Air-Conditioning, Heating, and Refrigeration Institute

et al., 2016). Due to new emerging technology of variable speed compressors and control systems, in 2006, the U.S. started to adopt this technology (Storm & Baylon, 2012). In 2007, approximately 250,000 to 300,000 DHPs were sold in the U.S. despite the reduction of newly-constructed houses in North America due to the system's high efficiency and retrofit application (NAHB, 2008). As a result of this rapid growth, Nation Renewable Energy Laboratory (NREL) performed an investigation of actual systems' performance of installed units in the U.S. and generated performance testing standards for this system. Two mini-split heat pumps (MSHPs) were selected to measure the performance for the first time. In the rated condition, both systems performed as documented by the manufacturers. However, in other humidity and temperature conditions heating and cooling capacities fluctuated 40% above to 54% below the manufacturer reported values (Winkler, 2011).

Multi-split systems are systems that have a single outdoor unit and various indoor units to serve multiple zones used in large residential homes and medium to large commercial buildings. Multi-split systems with variable refrigerant flow (VRF) technologies are utilized to regulate refrigerant flow by using a variable speed compressor and electronic expansion valves (EEVs). Also, a four-way valve is equipped to enable heating and cooling in a single outdoor unit (Aynur, 2010). VRF systems were introduced in Japan more than 20 years ago, and have been widely adopted in European countries since 1987. Half of medium-sized commercial buildings up to 70,000 ft^2 and one-third of large commercial buildings in Japan have adopted this technology (Goetzler, 2007). A recent study by Aynur also shows that a single outdoor unit can serve up to 60 indoor units, a rapid jump from 20 units in 2007. Recently, the author surveyed the air-conditioning market at the ASHRAE expo 2016 in Orlando and found a significant increase in the

number of VRF manufactures attending the EXPO from 2015. Many manufacturer's VRF systems are able to simultaneously operate in both heating and cooling modes. Due to the growth of the VRF market, a new performance rating approach for this system has been suggested by (Su, et al., 2014). Lawrence Berkeley National laboratory also created and validated a new VRF module to replace the existing module in EnergyPlus and has already been intergraded in EnergyPlus 8.4 in 2016 (Hong et al., 2016).

1.2.2. Virtual Sensing and FDD Technologies

Virtual sensing technologies has been developed to tackle difficult-to-measure or expensive sensors by using mathematical models and outputs from other inexpensive sensors. This sensing technology has been extensively used in critical systems and automobiles, but not widely employed in buildings due to insufficient market demands for which factories could not mass produce them (H. Li et al., 2011). In building application, some sensors are sensitive to installation location. For instance, mixed air temperature and supply air temperature sensors are installed in air mixing chambers and supply air ducts, respectively. However, sensors in those locations might incorrectly read the temperatures due to un-uniform air and the radiation of heat generated by fans and coils (D. Yu et al., 2011). In 2009, Wichman and Braun created virtual mixed air temperature (MAT) by using temperature sensors in five points: mixed, supply, return, and outdoor air, and damper positions. Moreover, Yu 2011 suggests virtually calibrated supply air flowrate (SAT) for RTUs by correlating offset errors with available system measurement of outdoor air damper position, manufacturer-installed SAT and outdoor air temperature (OAT). In some cases, it is difficult to install sensors in operating systems without non-invasive approaches. H. Li & Braun, 2009 suggested non-intrusive indirect-measured virtual pressure sensors

for all of the important pressures in vapor-compression cycles which include compressor discharge line, condensing, liquid line, evaporating and suction line pressure points. Conventionally, refrigeration charge could be measured by evacuating system refrigerant and weighing the removed charge and recharge back to the system. Kim & Braun, 2008 suggested low-cost non-invasive refrigerant charge measurement. In addition, compressor power consumption can be virtually measured by using performance mapping equations suggested by ANSI/AHRI Standard 540-2015, 2015. All virtual sensors for buildings can be classified by the hierarchy of systemization of virtual sensors (SoVS) as shown in Figure 1-1 (H. Li et al., 2011).

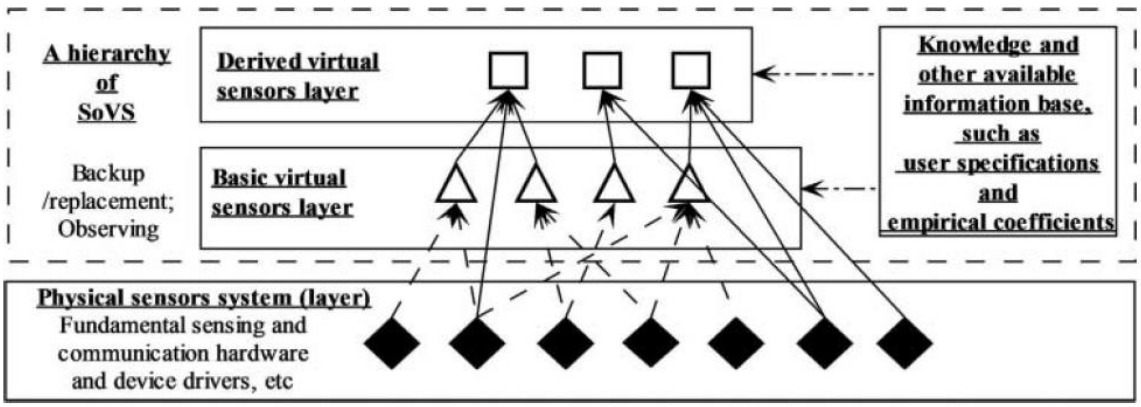

Figure 1-1 Hierarchy scheme of SoVS by Li, et al., 2011

FDD detects early state of identification and isolation of preliminary faults for those that are not violate enough to cause major degradation or failure, and thus preventive actions can be performed beforehand (Li, et al., 2007). Rossi & Braun, 1997 instituted statistical rule-based FDD methods by comparing directional changes of system residuals withaunique sets of rules distinct to each fault. In relation to a previous study, Chen and Braun 2000, purposed a simple FDDmethod for packaged ACs by which seven common faults are implemented in the ACs by physically changing system operating condtions as shown in Table 1-1. Based on sequential steps of FDDs purposed by Rossi, generic

procedures of FDDs for unitary HVAC systems have been purposed as shown in Figure 1-2

Table 1-1 Method of implementing seven faults and levels simulated (Chen & Braun, 2000)

Fault type	Simulation method	Fault level characterization	Fault level simulated				
			1	2	3	4	5
Condenser fouling	Block the condenser coil with paper	% Reduction of the surface area of the condenser coil	0.00%	10.00%	20.00%	30.00%	40.00%
Evaporator fouling	Adjust the air flowrate through the evaporator coils	% Reduction of the air flow rate	0.00%	6.82%	13.64%	20.46%	27.28%
Liquid line restriction	Close partially a needle valve installed in the liquid line	% of the pressure drop from high pressure side to low side	0.00%	4.75%	10.86%	13.07%	18.66%
Compressor wear	Open a bypass valve installed the discharge line and suction line	% Reduction of the volumetric efficiency	0.00%	10.00%	20.00%	30.00%	40.00%
Refrigerant leakage	Discharge some of the refrigerant from the system	% Reduction of the total charge in the system	0.00%	5.00%	10.00%	20.00%	30.00%
Refrigerant overcharge	Overcharge some refrigerant into the system	% Addition of the total charge in the system	0.00%	5.00%	10.00%	20.00%	30.00%
Non-condensable gas	Charge controlled amount of N_2 into the system	% Total refrigerant mass	0.00%	0.03%	0.09%	0.13%	0.17%

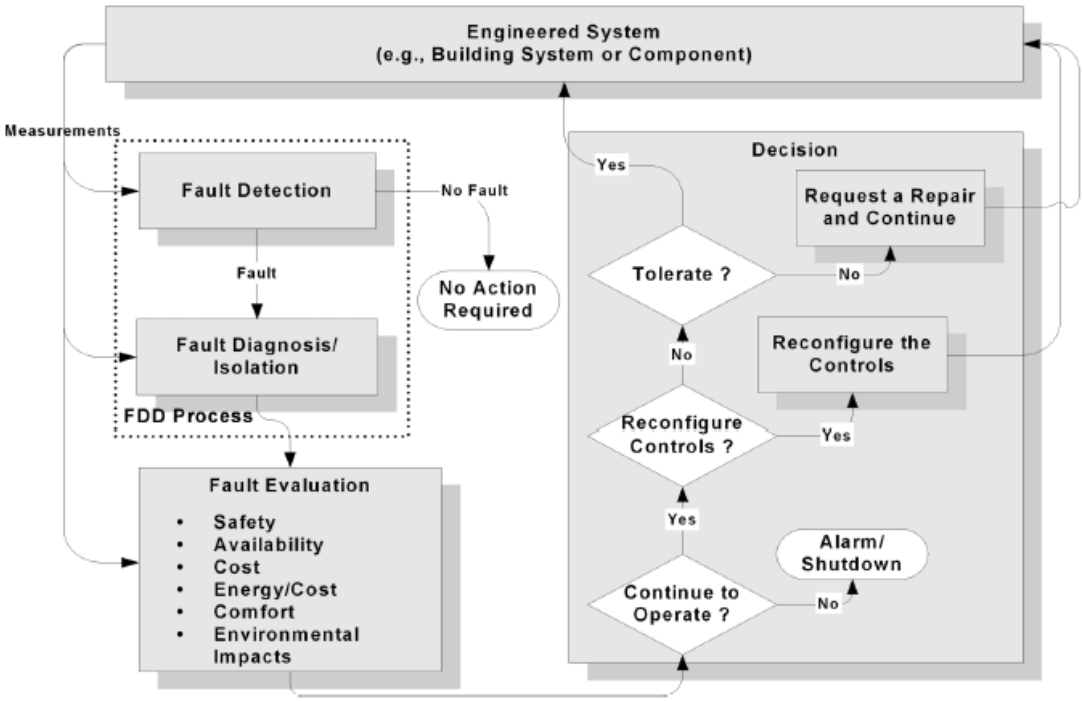

Figure 1-2 Generic procedures of FDDs for unitary HVAC system (Katipamula & Brambley, 2005)

The majority of FDD researches account single faults imposed. However, actual incurred faults in operating units are not straightforward. Antecedent research illustrates

the impact of each fault imposed to a system, wherein the unit shows distinctive performance associated with each fault, which could be used as a standard to verify newly-innovated FDD models. In order to address multiple simultaneous faults, fault-decoupling is necessary (H. Li & Braun, 2007). Accordingly, Li developed model-based FDD based on fault decoupling features and virtual sensors.

Most FDD research publications (45%) focus on air-handling units (AHUs) followed by packaged air-conditioning systems (20%) and chillers (18%) (Li, et al., 2007). Those systems are commonly installed in medium to large commercial buildings. On the other hand, only 2% of publications study other system's FDDs including residential ACs such as heat pumps and split systems. The majority of FDDs in residential heat pumps and split systems come from Korea and Japan who invented split systems. M. Kim et al., 2009 investigated heat pump performance operating in cooling mode with one of seven common faults[1] imposed at a time, and estimated the level of the fault's impact by energy efficiency ratio (EER) following a study of normalized performance of residential heat pumps with a single fault imposed. This study also introduced two additional faults for heat pump systems which are (1) improper electrical line voltage and (2) improper liquid line refrigeration sub cooling (Cho et al., 2014). FDDs for heat pumps based on virtual sensors were introduced by W. Kim, 2013. Also, Cho, et al decribed nine different fault characteristics, and illustrated normalized performance parameters for residential heat pumps in cooling mode with single faults imposed.

1.2.3. Cooling Performance Models

Performance modelling methods can be roughly divided by their methodologies. White box or physical models formulate models based on fundamental theory and physical configurations. Black-box models are based on historical data (data-driven), and utilized statistical methods to generate models. These models typically have no physical meaning (Katipamula & Brambley, 2005). The examples models are as follows:

Purdue University developed ACMODEL to simulate air conditioner and heat pump performance by using VCC component configurations to formulate coil models. Empirical modelling methods are applied to compressor modules to predict mass flow rate and power consumption. CoilDesigner is also a physical-based model developed by the University of Maryland. In addition, NREL developed performance mapping (black-box) to evaluate MSHP's system performance. Wang et al, simplify control and optimization of water-cooled coils by employing hybrid modelling of which the model structures are formulated from physical models or manufacturer's data.

Unlike heating mode operation, AC coils have unique characteristics due to properties of moist air entering evaporating coils (T_{aie}) which possibly formulate two coil operating conditions: wet and dry coils. Wet coils accumulate condensed water in which dew point of T_{aie} is higher than that of coil surface-temperature resulting in water condensate accumulated in the coils. In this condition, SHR is less than 1. On the other hand, dry coil performance is directly associated with sensible cooling where SHR equals 1. In mixed condition where SHR approaches 1 from null, an inflection point is created where coil conditions transform from wet to dry as shown in Figure 1-3.

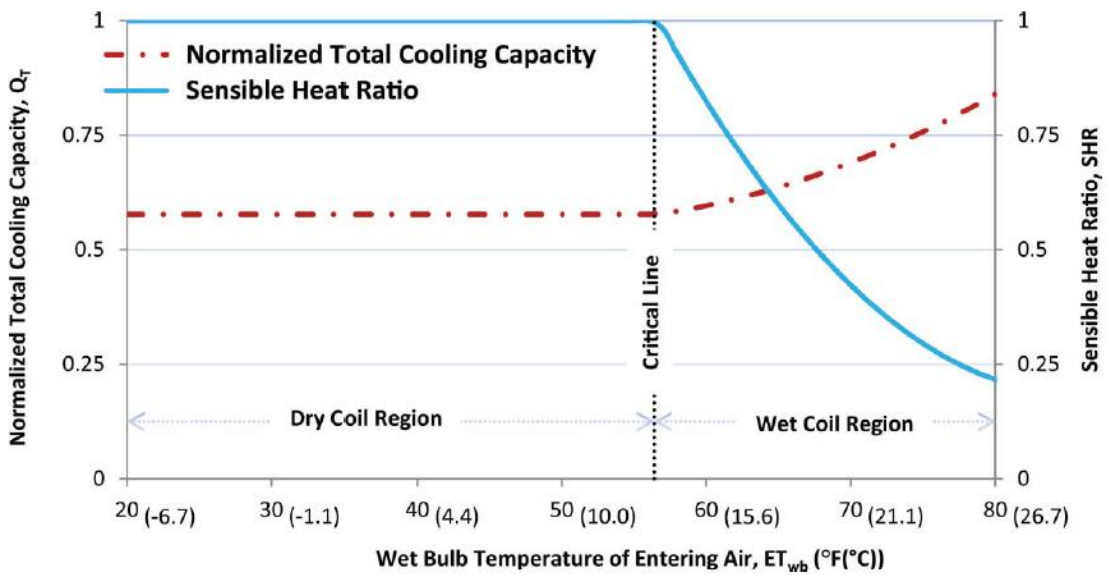

Figure 1-3 The characteristics of normalized total cooling capacity, sensible heating ratio, and wet-bulb temperature of air entering coil (WB_{aie}) with dry-bulb temperature (T_{aie}), outdoor temperature (OAT) and air flowrate (CFM) (Yang, et al., 2013)

Yang et al., 2013 purposed a GRDB coil-modelling method by second order polynomial regression. The model first defines operating conditions by utilizing equipment SHR to separate wet from dry conditions as shown in Figure 1-3. The critical line on Figure 1-3 shows the inflected conditions in which wet coil operating characteristics are distinct and discontinuous.

1.3. Motivation and Objectives

From background and literature review, motivation and objectives of this research can be outlined as follows:

- Equipment having expansion devices are energy efficient devices for heating and cooling in buildings. They are extensively used in a variety of applications for commercial and residential use. Higher capacity units of more than 5 to 20 tons are applied in commercial sections while smaller units of less than 5 tons are applied in light commercial and residential use.
- A cooling operation is a major concern in this study since, though many studies published cooling coil capacity models, there are only few studies concerning cooling coil intrinsic characteristics. Moreover, most cooling equipment in tropical areas concern sensible cooling and meeting temperature set points. In fact, in those tropical zones, humidity accounts for the majority of cooling load in conditioned spaces (Xu, Xia et al., 2010)
- It is difficult and time consuming to find or create accurate laboratory testing data either for modelling or validating aspects.
- The study of cooling coil from Henderson and Yang show normalizing and scaling abilities of cooling coil performance. Those abilities can be utilized to improve cooling coil modelling procedures by reducing model's complexity and computational time.

Consequently, the objectives of the research are: (1) to study the arrangement of available performance rating data of various DX[2]cooling systems from different

[2] Direct expansion air conditioning

manufactures, (2) to investigate cooling coil characteristics using air properties and fundamentals of refrigeration cycle, (3) hypothesize normalizing and scaling ability of cooling coil characteristics, and (4) to validate cooling coil characteristic hypotheses by using manufacturers' data.

1.4. Methodology

The methodology and ideas of research come from the fact that equipment must have its own principles or certain properties based on calculations, statistical analyses, fundamental theories and so on. Therefore, we should be able to trace back to its root characteristics, and thus the equipment can be manipulated and controlled more effectively. To understand equipment characteristics, two analytical methods are employed:

- Theoretical analysis of air principles and refrigeration cycles is utilized in this research to identify DX-cooling coil air conditioning characteristics in order to define essential input and output variables and their relationship.
- Analysis of manufacturer's cooling performance data is employed since they are generic, accurate and freely available. The data is used for both validations of hypotheses graphically and coil characteristics analysis.

1.5. Thesis Organization

With a background in virtual sensing, FDD technologies and capacity modelling methods are described in the literature review of this chapter concerning applications for vapor compression air conditioners. The idea of investigating cooling coil inherent characteristics is developed from mentioned reviews.

Chapter 2 demonstrates data resources, how performance data is displayed, and how to make use of the data for cooling performance analysis. Chapter 3 describes cooling coil characteristics by theoretical and graphical analysis using psychrometric properties, defines input and output variables for DX-cooling coil equipment utilizing air-side properties and refrigerant cycle analysis, and sets up a hypothesis of DX-cooling coil inherent characteristics. Chapter 4 validates the hypothesis from chapter 3 with various types of system data from different manufacturers, and suggests critical point estimating methods. Since cooling coil operating practices passing these critical points produces different capacity throughputs, cooling capacities are handled separately Finally, Chapter 5 summarizes and concludes the contributions from this research as well as recommendations for future studies.

CHAPTER 2. DATA SOURCES

2.1. Overview

In the U.S., there are plenty of test data sets available from previous researches and projects, particularly commercial equipment such as RTUs and AHUs, for the purpose of formulating building-related FDDs techniques and models, and validations. Unfortunately, there are handful publications for residential ACs particularly ductless heat pumps (DHPs) in the U.S. Majority of publications for DHPs are from Asian countries, outstandingly from Korea. National Renewable Energy Laboratory (NREL) acknowledges the importance of systemized codes and standard for this technology; therefore, 2 mini-split heat pumps were tested in regard to existing test standard for heat pump (ANSI/AHRI, 2012). However, those training data sets are not freely available for researchers to access, or though the available data might not match required conditions. For example, large data sets from NREL are conducted according to ANSI/AHRI standard 240, so most of available data is at the standard rating conditions which are inadequate to study the characteristics of cooling coils. Fortunately, in the U.S., manufacturers' data are immensely informative and freely available.

2.2. Laboratory Data

Two sets of MSHPs' testing data under steady state condition for Fujitsu 12RLS and Mitsubishi FE12NA are from Herrick Laboratories. Wide range of test conditions were performed under controlled condition in psychrometric chamber. Table 2-1 shows manufacturers' reported data of those units.

Table 2-1 Manufacturers' reported data for Fujitsu 12RLS and Mitsubishi FE12NA

Model	**Unit**	**Fujitsu 12RLS[3]**	**Mitsubishi FE12NA[4]**
Outdoor Unit	–	ASU12RLS	MUZ-FE12NA
Indoor Unit	–	AOU12RLS	MSZ-FE12NA
Seasonal energy-efficiency ratio (SEER)	Btu/h-W	25	23
Heating seasonal performance factor	Btu/h-W	12	10.6
Rated cooling capacity	Btu/h	12,000	12,000
Cooling capacity range	Btu/h	3,800–14,500	2,800–12,000
Cooling energy efficiency ratio (EER)	Btu/h-W	14.46	12.9
Rated heating capacity	Btu/h	16,000	13,600
Heating capacity range	Btu/h	3,100–24,000	3,000–21,000
Heating coefficient of performance (COP)	–	3.9	4.2
Rated air flow rate	cfm	453	350

A large number of data were performed at: indoor dry-bulb temperature (DB_{aie}) of mostly 80°F within the range of 70 to 86°F, indoor wet-bulb temperature (WB_{aie}) within the range of 45 to 75°F and outdoor temperature (OAT) range of 67 to 11°F. Those conditions were selected based on ANSI/AHRI 240. However, WB_{aie} data from laboratory were not directly measured, so they will be calculated by moist air properties of dew point temperature of air entering evaporator (DP_{aie}) and DB_{aie} in Engineering Equation Solver (EES).

In addition, the units were tested at different air flow rates (CFM) of low, medium, high speeds, and at various compressors speed of minimum, intermediate and high compressor speeds. The CFM_{rated} for each unit are as stated in Table 2-1

[3] Fujitsu Design and Technical manual of ASU09RLS and ASU12RLS
[4] Mitsubishi Electric Submittal: MSZ-FE12NA and MUZ-FE12NA

The provided laboratory data named fan speeds and compressors speed as “intended speed”; however, actual operating conditions might vary regarding the temperature setup conditions. An example of training data is provided in Appendix A.This laboratory data will be used to evaluate GRDB model which will be further described in Chapter 3

2.3. Manufacturing Data

2.3.1. Manufacturing data for GRDB

The study of GRDB model applying to MSHPs system will be performed to evaluate performance of MSHPs at rating conditions. Each manufacturer had its own testing standard. Therefore, each data set should be understood before being utilized.

2.3.1.1. Mitsubishi FE12NA data

Mitsubishi elaborates their cooling performance data by fixed dry-bulb temperature (DB_{aie}) at 80 F, varying wet-bulb (WB_{aie}) temperature of 63, 67 and 71 F, and outdoor temperature (OAT) are at 75, 85, 95, 105 and 115 F (see Table C-1). Also, Mitsubishi provides extended data range for cooling performance (see Table C-2). In addition, laboratory data provided data mostly at rated CFM of 350.

2.3.1.2. Fujitsu 12RLS data

Fujitsu arranges data differently from the Mitsubishi’s. Unlike, the prior manufacturer where dry-bulb temperature (DB) is fixed at 80 ^{o}F for all data, the Fujitsu couples indoor WB and DB, and variates OAT (see Table C-2). In addition, CFM_{rated} data is at 453 cfm.

2.3.2. Other Manufacturing data

Other manufacturers' data sets used in this study are mostly for residential applications (package units and heat pumps) whose performance are below 65,000 Btu/h, and these data sets will be used in normalizing and scaling ability analysis in Chapter 4. Manufacturers' data included in these study are from various makers, i.e. Carrier, Goodman, Lennox, Trane, York, Daikin, Fujitsu and Mitsubishi. All data, used in the analysis Chapter 4, will be divided by types: Mini-split heat pumps (MSHPs), split heat pumps (SHPs) and package units, and are in Appendix C, Appendix E, and Appendix F respectively. The arrangement of data for each manufacture is explained below

- MSHPs data for most systems couples DB_{aie} and WB_{aie} except Mitsubishi's displaying data at fix 80°F of DB_{aie}.
- SHPs data typically fix DB_{aie} at 80°F with various CFMs, OATs and DB_{aie} conditions. However, Goodman provides additional DB data ranges of 70, 75, 80 and 85 ^{o}F.
- All packages units vary WB_{aie} in various fixed CFMs, OATs and DB_{aie} conditions.

CHAPTER 3. COOLING COIL CHARACTERISTIC ANALYSIS AND ITS HYPOPTHESIS SETUP.

3.1. Cooling Coil Operating Condition

Air-conditioning operation is considered a steady state process since an initial condition will not rapidly changed by modifying inputs. As a result, cooling performance can be calculated in steady state conditions. Figure 3-1 represents schematic of cooling coil process and its concerned inputs outputs,

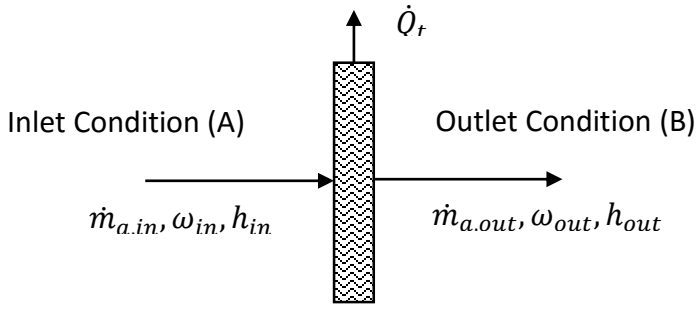

Figure 3-1 Schematic of cooling coil process

where: $\dot{m}$ is mass flow rate, ω is humidity ration, and h is enthalpy of moist air.

Air condition at a fixed pressure can be elaborated on psychrometric chart by a combination point of 2 properties of air as shown in Figure 3-2, and the process of air can be illustrated by lines drawn between 2 condition points. In addition, directions of the plotted lines on the chart represent alteration of initial condition (x) to terminated condition (1-8) of air in the process where Figure 3-3 demonstrates air condition processes by their moving directions.

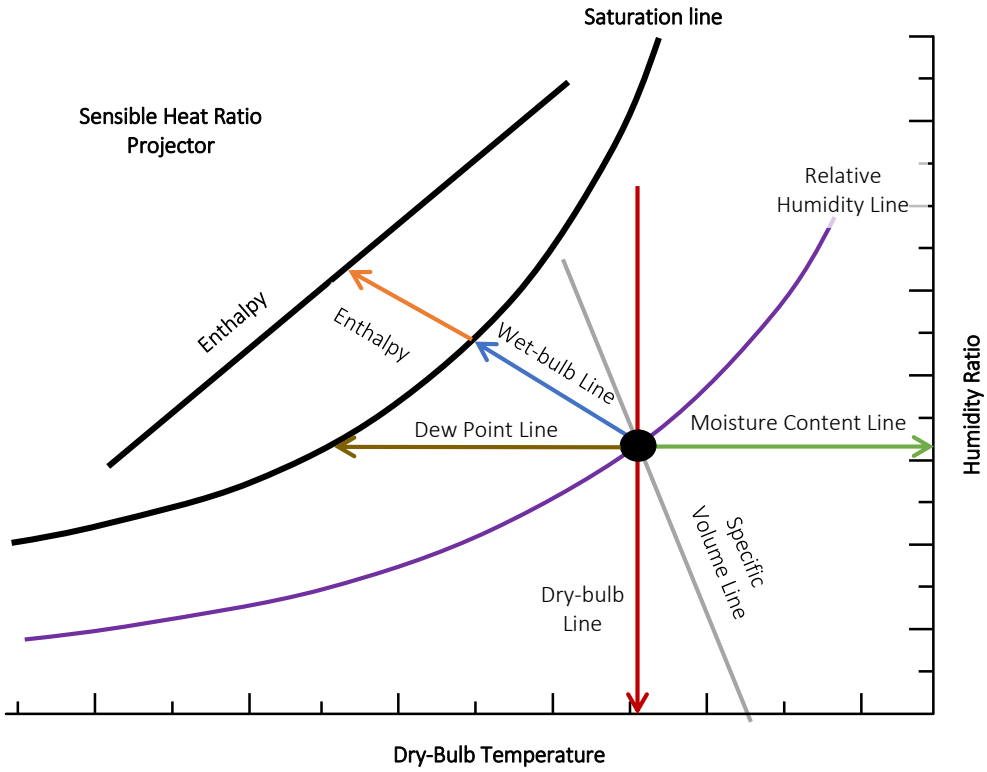

Figure 3-2 Air properties at a fixed pressure.

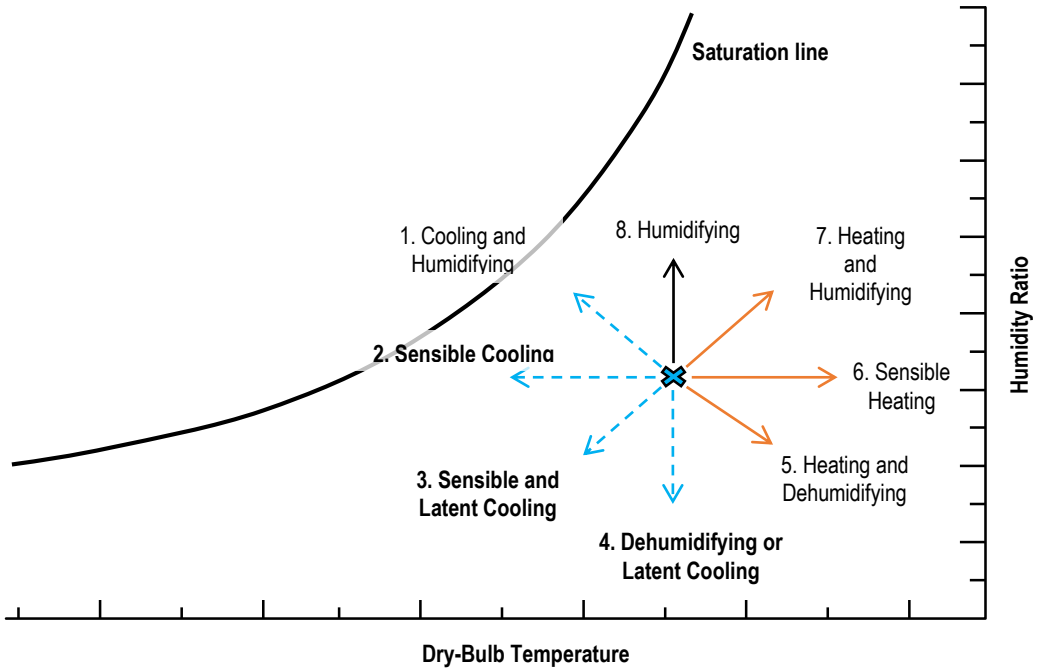

Figure 3-3 Air processing in AC equipment on the psychrometric chart

Left-dashed lines refer to air cooling processes. However, ACs in cooling mode operate on sensible cooling (2) and sensible with latent cooling (3), so cooling coil can dehumidify air without additional equipment. In addition, a fundamental cooling process in a coil can be presented in a triangle on the psychrometric chart. Enthalpy (h) difference of two points is cooling capacity: Horizontal line denotes sensible capacity ($\dot{Q}_s$) and the vertical process denotes latent capacity ($\dot{Q}_L$) (see Figure 3-3). While changing of water content in the process is relatively small and can be neglected, as regards, total cooling, sensible cooling, latent cooling and SHR can be calculated by using enthalpy between two conditions as shown in Equation 3.1, 3.2, 3.3 and 3.4, respectively.

$$\dot{Q}_t = \dot{m}_a(h_A - h_B) \tag{3.1}$$

$$\dot{Q}_s = \dot{m}_a(h_X - h_B) \tag{3.2}$$

$$\dot{Q}_L = \dot{m}_a(h_A - h_X) \tag{3.3}$$

Where $\dot{m}_{a,A} = \dot{m}_{a,B} = \dot{m}_a$

Sensible heating ratio of the equipment (SHR) indicates the ratio of $\dot{Q}_s$ and $\dot{Q}_t$, so then can be calculated by

$$SHR = \frac{\dot{Q}_s}{\dot{Q}_s + \dot{Q}_L} = \frac{\dot{Q}_s}{\dot{Q}_t} \tag{3.4}$$

Cooling operations in AC systems reduce indoor air temperature. There are two operating ranges of wet and dry while removing energy from entering air. Cooling in dry-coiled condition will maintain humidity ratio of air entering evaporator, thereby no dehumidification. On the other hand, cooling in wet-coiled condition, coils inhere ability to remove moisture because of the condensation of which water in the air accumulated in coils.

3.1.1. Dry Coil

Dry-coiled cooling is the process of removing energy and reducing air temperature, meanwhile humidity ratio (ω) remains constant for all ranges of operation. Consequently, $\dot{Q}_s$ and $\dot{Q}_t$ are equivalent.

Where
$$SHR = 1 \tag{3.5}$$

$$\omega_A = \omega_B \tag{3.6}$$

$$\dot{Q}_t = \dot{Q}_s = \dot{m}_a(h_A - h_B) \tag{3.7}$$

Then
$$\dot{Q}_t = \dot{Q}_s = \dot{m}_a C_p(T_A - T_B) \tag{3.8}$$

Equation 3-8 typifies that dry coil cooling is a function of air mass flow rate ($\dot{m}_a$) and dry-bulb temperature elaborated by Figure 3-4, and no dehumidification and moisture addition occurred in this process.

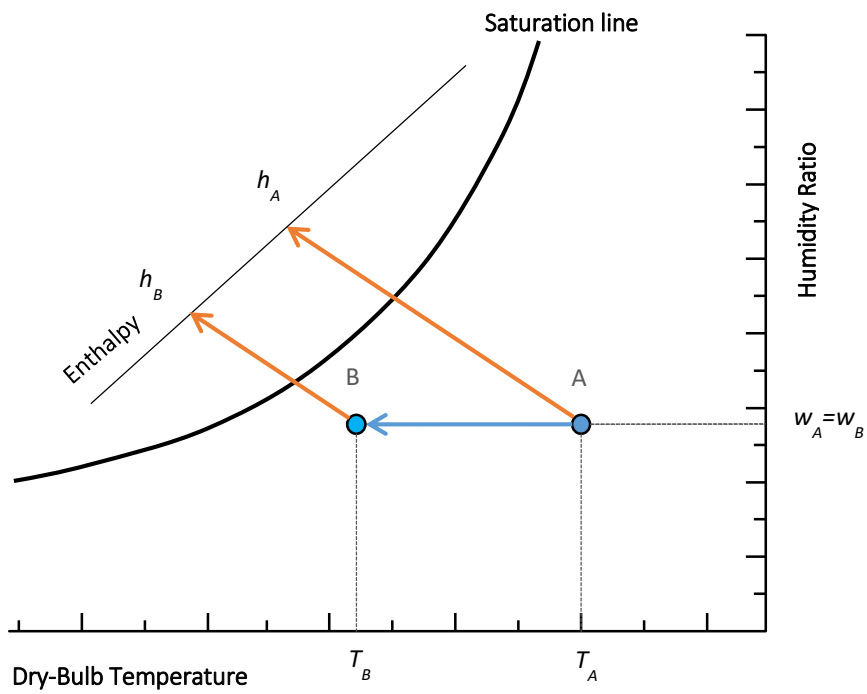

Figure 3-4 Cooling process of dry coil

3.1.2. Wet coil

Wet-coiled cooling withdraws energy from entering air in two ways: sensible cooling, and latent cooling from which moisture is removed. From Equation(3.2), sensible cooling can be rewritten (See Equation (3.9)).

$$\dot{Q}_s = \dot{m}_a(h_X - h_B) \qquad (3.2)$$

$$\dot{Q}_s = \dot{m}_a C_p(T_X - T_B) \qquad (3.9)$$

Total cooling capacity, however, is not affected by varying T_A as shown in Figure 3-5. Though varying T_A, point A will ride on a WB_A line. Therefore, Equation (3.1) can be rewritten as a function of WBs as follows:

$$\dot{Q}_t = \dot{m}_a(h_A - h_B) \qquad (3.1)$$

$$\dot{Q}_t = \dot{m}_a C_{wb@sat}(WB_A - T_B) \qquad (3.10)$$

Where $T_B = WB_B$, and $C_{wb@sat}$ is specific heat of wet coil.

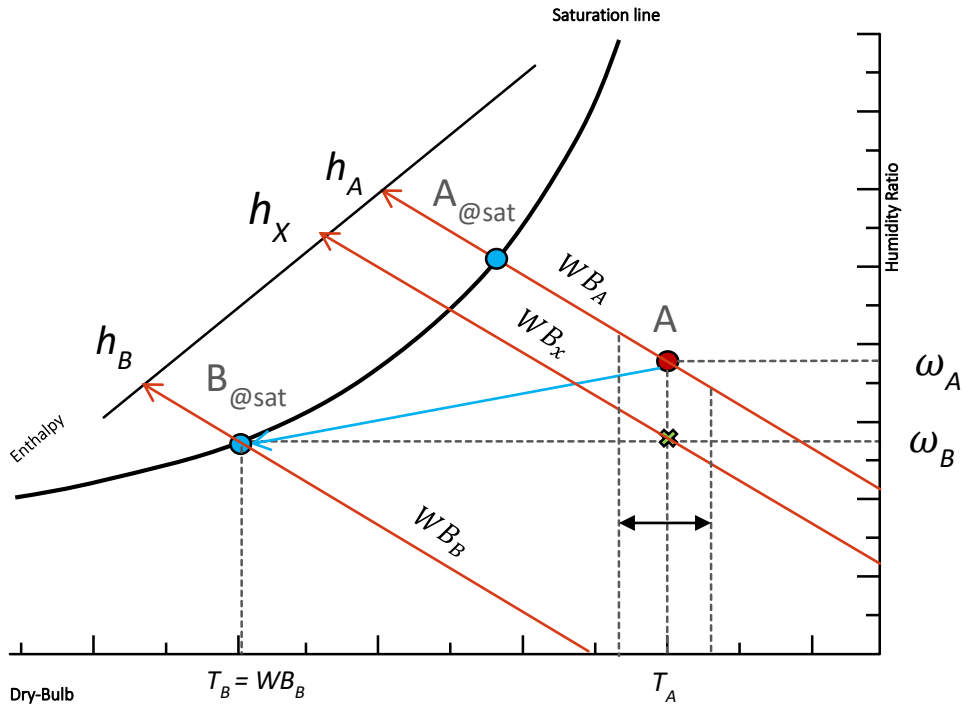

Figure 3-5 Wet-coiled cooling in AC equipment

SHR is the ratio of $\dot{Q}_s$ and $\dot{Q}_t$. From Equation (3.1) and (3.3), SHR can be reformulated as follow (See Figure 3-5).

$$SHR = \frac{\dot{m}_a C_p (T_X - T_B)}{\dot{m}_a (h_A - h_B)} = \frac{C_p (T_X - T_B)}{(h_A - h_B)}$$

Or

$$SHR = \frac{C_p (T_X - T_B)}{C_{wb@sat} (WB_A - T_B)} \qquad (3.11)$$

3.1.3. Actual cooling coil operation

In actual operation, throughputs of air passing cooling coils will not absolutely exchange energy with coils or condensate water. Therefore, the air which is exposure to coils or condensate water will be transformed to saturated air, and some of air which is

partly contact with coil will partially transformed. Finally, bypass air will neither be dehumidified nor processed.

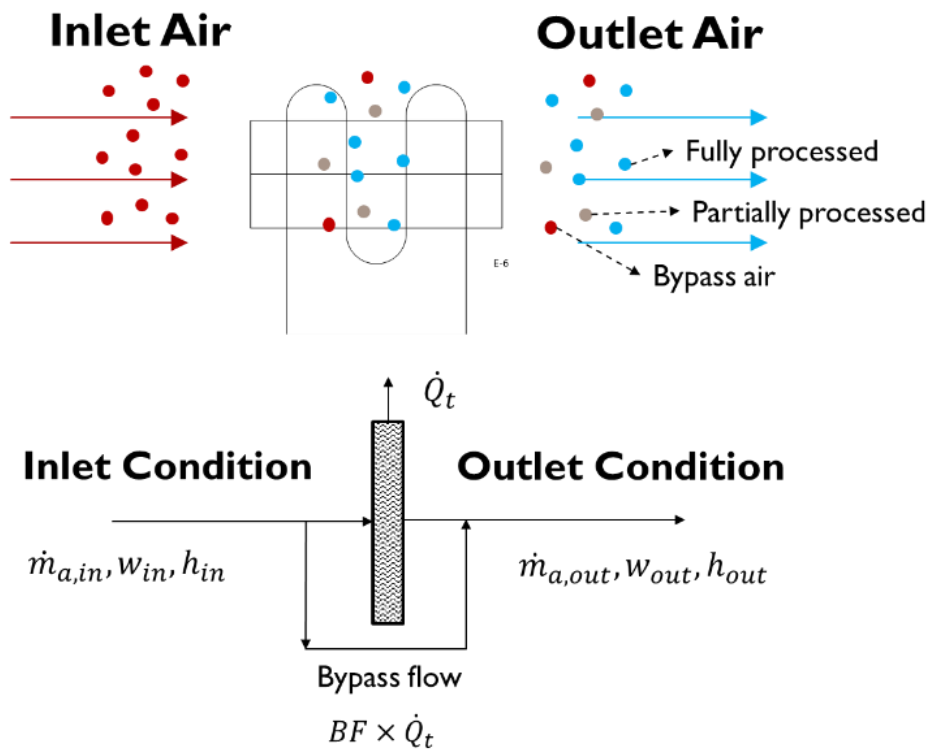

Figure 3-6 Process of air passing through cooling coil

Figure 3-7 illustrates a cooling wet-coil process with air partially bypassing through the coil. The ratio of actual enthalpy changes to ideal non-bypass enthalpy changes.

Therefore, bypass factor (BF) can be calculated by

$$BF = \frac{h_{aoe} - h_{evap}}{h_{aie} - h_{evap}} \tag{3.12}$$

By rules of triangle where the ratio of triangle sharing lines, (BF) can be further calculated by

$$BF = \frac{h_{aoe} - h_{evap}}{h_{aie} - h_{evap}} = \frac{w_{aoe} - w_{evap}}{w_{aie} - w_{evap}} = \frac{DB_{aoe} - T_{evap}}{DB_{aie} - T_{evap}} \tag{3.13}$$

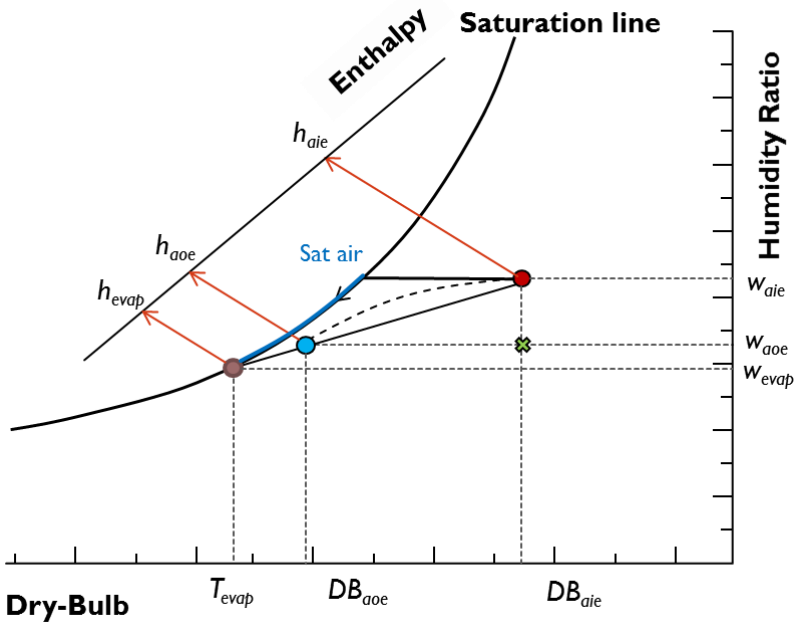

Figure 3-7 Actual cooling wet-coil process with bypass air

Wet coils, where SHR less than 1, will have smaller BF since the saturated or condensate water blocks the inlet air; thus the air cannot clutch through coils and fins thoroughly. On the other hand, dry coils have larger BF due to the fact that no condensate obstructing the air pathway. According to Figure 3-6, considering CFM passing through coil: When CFM increases, BF is relatively increase since coil surface remains constant, thereby enlarging the ratio of bypass air.

3.2. DX Cooling coil model mechanism

A cooling coil model algorithm in this research is based on GRDB developed by Yang, et al., 2010 in which dependent and independent variables of SHR and $\dot{Q}_t$ will be considered based on temperatures and air flow rates. DX cooling components are compressors, comdensers, expansion devices, and evaporators. Thoes components operate depentdently in relative to temperatures, pressures and equipment specifications.

Equipment operates assosiated with equipment's setup and feedbacck signals from various sensors measuring driving conditions for each component. Li et all, determine complete refirgeration cycle driving conditions and their essential enabled physical and virtual sensors as shown in Figure 3-8 and Figure 3-9.

Vapor compression cycle air-conditioning (VCC-AC) components handle refrigerant differently. We can roughly bracket system components by their temperature operating ranges: high temperature and low temperature. The high temperature components are compressors and condensers, and the lower temperature components are expansion devices and evaporators. A compressor will compress low temperature refrigerant leaving an evaporator to high temperature and high energy gas. Then condenser will emit the energy to environment. These two component combinations represent outdoor units. Conversely, an expansion device will expand refrigerant specific volume and reduce temperature simultaneously. Then evaporated refrigerant withdraws energy from a conditioned space in a constant refrigerant phase-changing process through the evaporator. The leaving refrigerant will then enter the compressor and be recirculated in the refrigerant cycle.

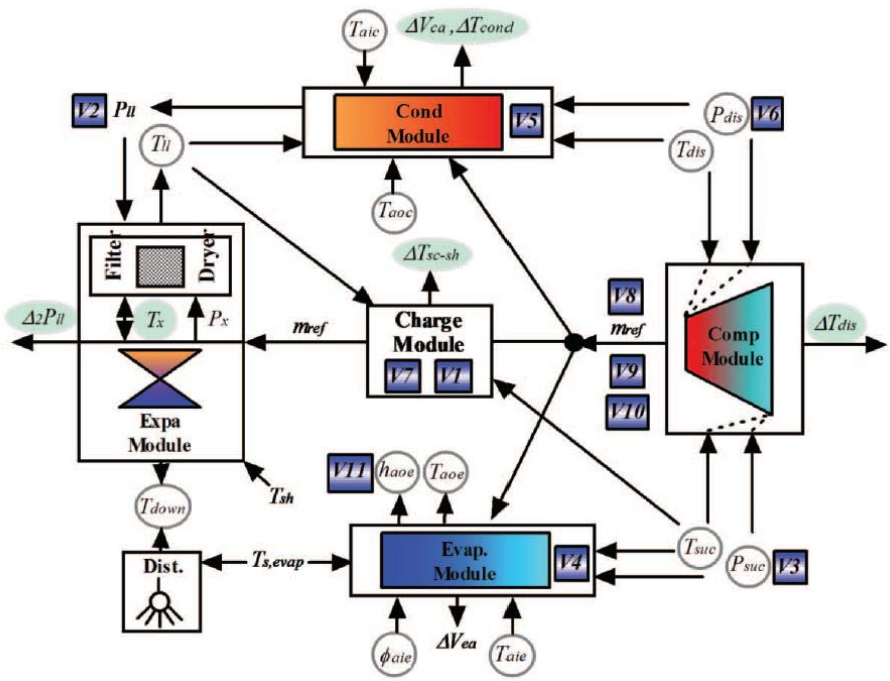

Figure 3-8 An intelligent air-conditioner schematic with enabled virtual sensors

ΔT_{cond}-condenser temperature residual	T_{aoe}-evaporator outlet air temperature
V_{ca}-condenser volumetric air flow rate residual	h_{aoe}-evaporator outlet air humidity
V_{ea}-evaporator volumetric air flow rate residual	T_{down}-expansion device down stream pressure
m_{ref}-refrigerant mass flow rate	T_{suc}-suction temperature
P_{suc}-suction pressure	$\Delta T_{sc\text{-}sh}$-charge level feature
T_{aic}-condenser inlet air temperature	ΔT_{dis}-discharge temperature residual
T_{aoc}-condenser outlet air temperature	$\Delta_2 P_{ll}$-liquid line pressure drop residual
T_{dis}-discharge temperature	P_{ll}-liquid line pressure
T_{sh}-suction superheat	ϕ_{aie}-evaporator inlet air humidity
P_{dis}-discharge pressure	T_{ll}-liqid line temperature
P_x-expansion device upstream pressure	T_x-expansion device upstream temperature

Virtual sensors:

V1-Virtual refrigerant charge sensor	V8-Virtual compressor power consumption sensor
V2-Virtual liquid line pressure sensor	V9-Virtual system coefficient of performance sensor
V3-Virtual suction line pressure sensor	V10-Virtual compressor volumetric efficiency sensor
V4-Virtual evaporating pressure sensor	V11-Virtual supply air humidity sensor
V5-Virtual condensing pressure sensor	
V6-Virtual compressor discharge pressure sensor	
V7-Virtual refrigerant flow rate sensor	

Figure 3-9 An air-conditioner enabled with physical and virtual sensors

Since refrigeration cycles are close-loop systems in which there is no loss in refrigerant during the operation unless refrigerant leakes, so the system manipulates refrigerant according to driving conditions which could be described upon pressure-enthalpy and temperature-entropy diagrams. On the other hand, air-side conditions are

handled with their own properties, and their principles can be delineated on the psychometric chart.

Considering air-side and refrigerant sides of VCC-AC systems, those sides can be sperately evaluated. For a VCCAC equipment, basic schematic with driving variables can be writen as following Figure 3-10.

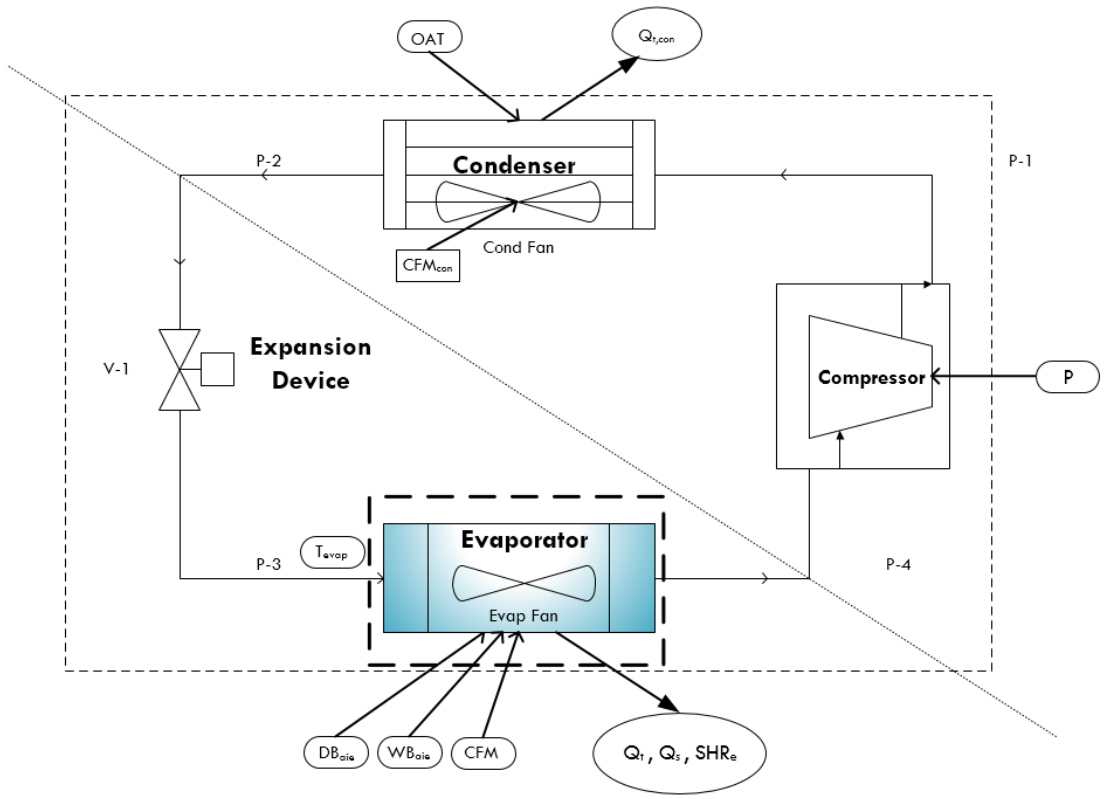

Figure 3-10 Vapor compression cooling system and its inputs and outputs.

Since air conditions are sluggishly reached set points (from minutes up to an hour), thus it could be accounted as a steady state process. Assuming no change in condensing fan speeds, dependent variables at the outside unit depends on OAT only. The indoor unit side, however, includes indoor fan CFMs because they can be regulated in relative to required static pressure in ducts, or for ductless system, in relative to user's and manufacturer's set up. Moreover, CFM effects moisture removal rate of air entering

evaporators. Neglecting internal energy in the system boundary, inputs and outputs of VCC cooling system are described in Figure 3-11. Specifically, we can define evaporator driving conditions and outputs as a function of VCC cooling system inputs; however, dependent variables involving in the VCC must be included. Therefore, the evaporator or VCC cooling coil model inputs can be illustrated (see Figure 3-12).

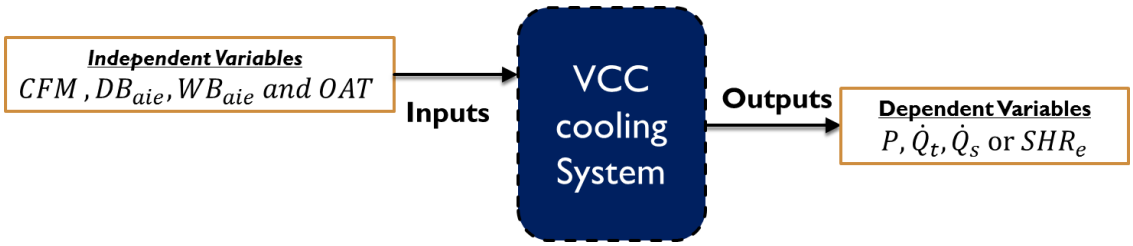

Figure 3-11 Normalized inputs and outputs relationship of VCC cooling system

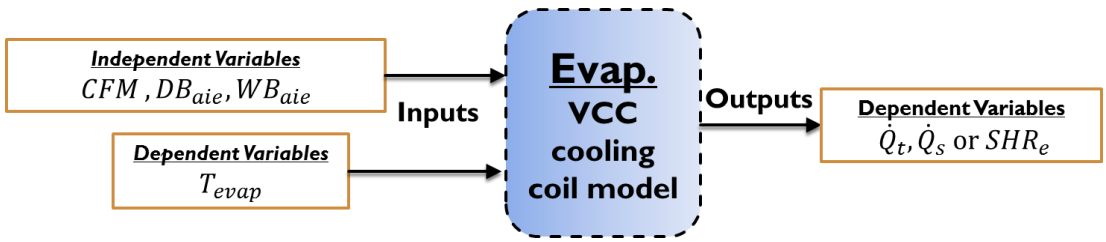

Figure 3-12 VCC cooling coil model

From Figure 3-12, $\dot{Q}_t$ can be rewritten as a function of input variables as shown in Equation (3.14) where specifics cooling (C_p) is constant

$$\dot{Q}_t = f(CFM, DB_{aie}, WB_{aie}, T_{evap}) \qquad (3.14)$$

However, T_{evap} is a function of OAT, CFM and WB_{aie}.

$$T_{evap} = f(CFM, WB_{aie}, OAT) \qquad (3.15)$$

Therefore, $\dot{Q}_t$ can be formulated as a function of independent variables as follows.

$$\dot{Q}_t = f(CFM, DB_{aie}, WB_{aie}, OAT) \qquad (3.16)$$

As described in previous section, cooling coil operates differently regarding coil conditions of wet and dry. Considering those conditions, cooling coil model format are delineated in Equation (3.18) by combining Equation (3.8), (3.10) and (3.11).

$$\dot{m}_a = \rho_a \cdot CFM \tag{3.17}$$

$$Cooling\ coil\ model \begin{cases} wet-coil \begin{cases} \dot{Q}_t = \rho_a \cdot CFM \cdot C_{wb@sat}\left(WB_{aie} - T_{evap}\right) \\ SHR = \dfrac{C_p\left(T_{aie} - T_{evap}\right)}{C_{wb@sat}\left(WB_{aie} - T_{evap}\right)} \\ \dot{Q}_s = SHR \cdot \dot{Q}_t \end{cases}, (SHR < 1) \\ dry-coil \begin{cases} \dot{Q}_t = \rho_a \cdot CFM \cdot C_p\left(T_{aie} - T_{evap}\right) \\ SHR = 1 \\ \dot{Q}_s = SHR \cdot \dot{Q}_t \end{cases}, \quad (SHR = 1) \end{cases} \tag{3.18}$$

Or, in a form of dependent- and independent- variables (see Equation (3.19)).

$$Cooling\ coil\ model \begin{cases} wet-coil \begin{cases} \dot{Q}_t = f(WB_{aie}, CFM, OAT) \\ SHR = f(T_{aie}, WB_{aie}, OAT, CFM) \\ \dot{Q}_s = SHR \cdot \dot{Q}_t \end{cases}, (SHR < 1) \\ dry-coil \begin{cases} \dot{Q}_t = f(T_{aie}, CFM, OAT) \\ SHR = 1 \\ \dot{Q}_s = SHR \cdot \dot{Q}_t \end{cases}, \quad (SHR = 1) \end{cases} \tag{3.19}$$

From the cooling model format, adopting from Yang et al, further analysis of cooling coil model mechanism can be performed in following sections. Firstly, cooling coil model based on GRDB from Yang 2010 appropriately employed to formulate MSHPs' cooling capacities model. In addition to the analysis, assumptions are made to lessen the complexity of the VCC-AC system.

3.3. Analysis of cooling capacity model mechanism using applied-GRDB for MSHPs

As previously described, cooling capacity (CAP) and SHR can be represented as a function of independent variables DB, WB, OAT and CFM, and the coil performing behaviors during wet or dry operation are distinguishable. Yang et al creates cooling performance model by employing compressor performance mapping by using multiple-linear regression (MLR) to fabricate empirical cooling performance model from

manufacturing data. The idea is from the fact that manufactures test their equipment performance and display them following the customary standard of ANSI/AHRI 240. Therefore, tested performance data is assumedly accurate and can be exerted on data mapping to formulate cooling capacity model. From Figure 3-12, Yang applies this model on RTUs and split systems by using this cooling model format to acquire CAP regression:

$$Cooling\ coil\ model \begin{cases} Wet-coil\ \ (SHR<1) \begin{cases} \dot{Q}_t = f(WB, CFM, OAT) \\ \dot{Q}_s = SHR \cdot \dot{Q}_t \end{cases} \\ Dry-coil\ (SHR=1),\ \ \dot{Q}_t = \dot{Q}_s = f(DB, CFM, OAT) \end{cases} \tag{3.20}$$

MUZ-FE12NA and 12RLS models from Mitsubishi and Fujitsu are selected, and the performance rated data are provided in Appendix C. From the data resources, though MSHPs recently install variable speed compressors and variable speed fans, provided performance data captures CAP ranges only at single speed compressor and fan. Since CFMs influence CAP a great deal, to maintain CFM effects in the model, CFMs will be excluded from the regression, but involved in the equation as a multiplier. Therefore, the only regressed data for MLR for MSHPs is WB and OAT, and GRDB's format will be adjusted as follows:

$$Cooling\ coil\ model \begin{cases} Wet-coil\ \ (SHR<1) \begin{cases} \dfrac{\dot{Q}_t}{CFM} = f(WB, OAT) \\ \dot{Q}_s = SHR \cdot \dot{Q}_t \end{cases} \\ Dry-coil\ (SHR=1), \qquad \dfrac{\dot{Q}_t}{CFM} = \dfrac{\dot{Q}_s}{CFM} = f(DB, OAT) \end{cases} \tag{3.21}$$

Then the steps of acquiring CAP model are as follows:

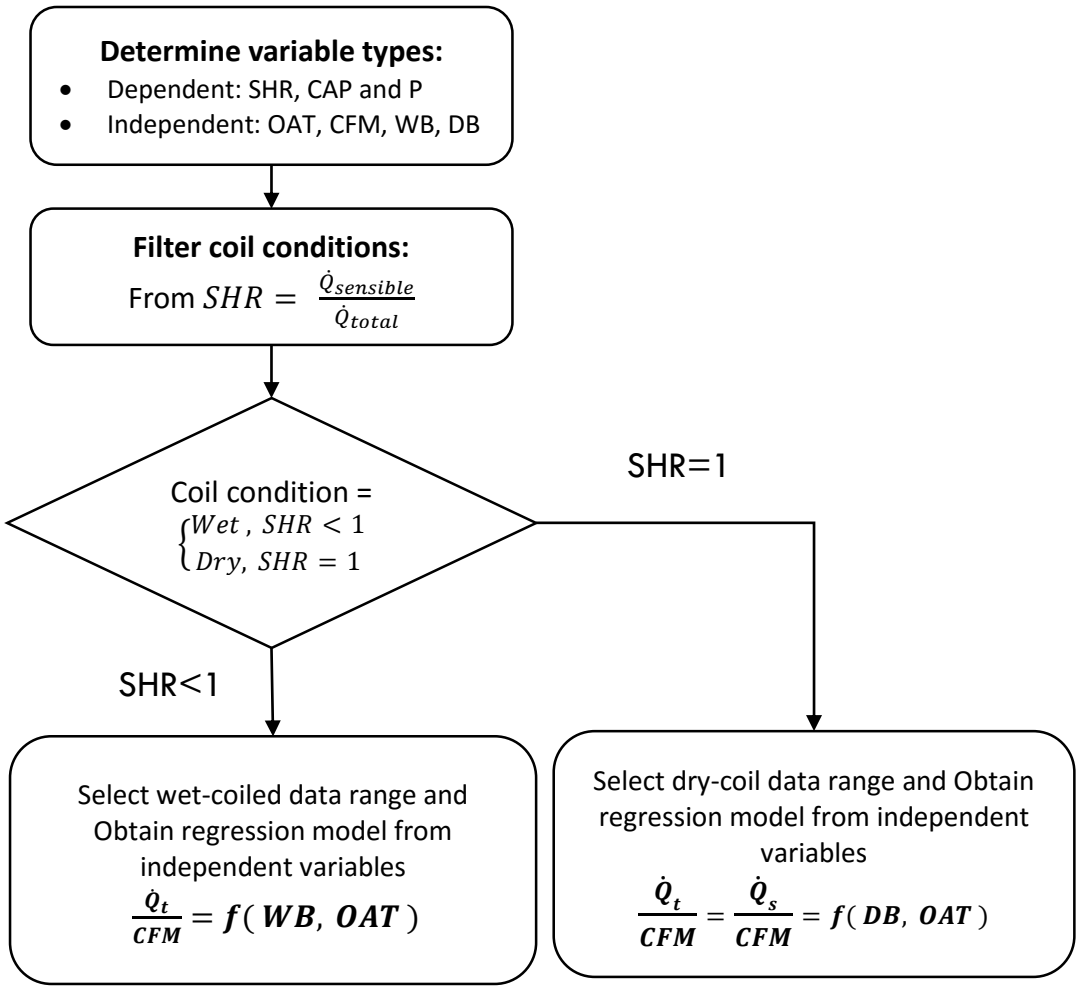

Figure 3-13 GRDB model for MSHPs procedure chart.

The step-by-step example of MUZ-FE12NA is provided in Appendix D, and the validation of the method is performed in Chapter 4.

3.4. Analysis of Cooling Coil Characteristics Under Fixed OAT and CFM

In this section, analysis of cooling coil processes will be formulated upon air-side cooling and its principle outlining on the psychrometric chart. Evaporating coil can be written as a function of inputs in Figure 3-12. Independent driven conditions are CFMs, DB_{aie}, WB_{aie} and a dependent driven condition is evaporating temperature (T_{evap}) of which

is driven by OAT, WB_{aie} and CFM_{cond}. To simplify the analysis upon principle of air, assumptions are made based on a steady-state operation as follows:

- Environment conditions inertly change: OAT and CFM_{cond} are constant.
- Neglecting the effect of WB_{aie} on T_{evap}.
- No bypass air passed through the evaporator.

Regarding the assumptions, T_{evap} is constant, and BF is equal to 0, and the relation of Q_t and SHR are described as following sections.

3.4.1. Varying wet-bulb temperature on fixed dry-bulb temperature

Assuming a steady state condition, DB_{aie} will practically be constant at a certain set point (e.g. 75, 80) as well as CFM, whereas OAT is constant at a certain temperature in associated with outdoor environment. Accordingly, considering the change of WB at fixed CFM, DB_{aie},OAT and BF, wet coil process on psychrometric will practice as following sections (see Figure 3-14.)

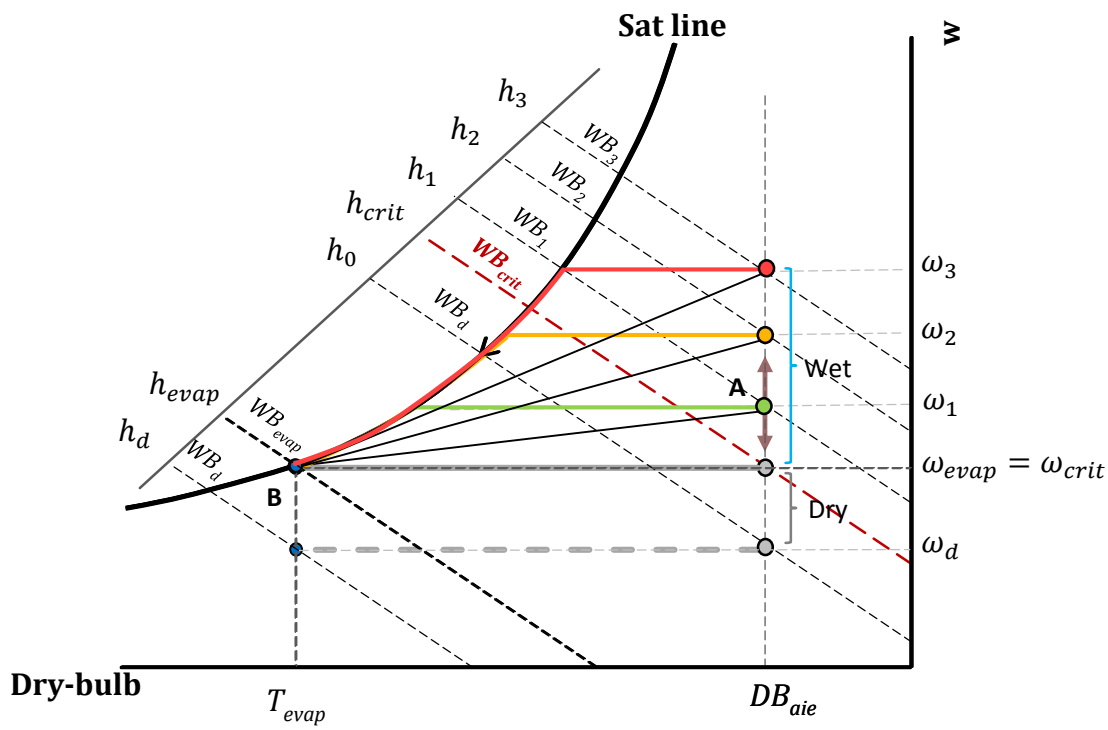

Figure 3-14 Characteristics of coil cooling at fixed CFM, DB_{aie} and OAT in relative to varying WB_{aie}

According to Figure 3-14, point A and point B, referred to air inlet at evaporator (aie) and air outlet at evaporator (aoe) respectively, riding on a constant dry-bulb line as WB_A changes. Considering enthalpy differences ($\Delta h = h_A - h_{evap}$) from Figure 3-14 Δh increases, and the increase rate grows associated with the increase of WB_{aie}. On the other hand, decreasing WB_{aie} on fixed DB_{aie} line to the condition where humidity ratio is constant throughout the process ($\omega_{evap} = \omega_A$) and SHR= 1, WB at this point is determined as critical point (WB_{crit}), whereby sensible cooling and total cooling capacity are equal. From this point forward, the cooling coil is operating dry, and point A will move in parallel with point B on the DB_{aie} line and T_{evap} respectively as shown in Figure 3-14. Consequently, total cooling capacity at dry conditions can be elaborated by dry-bulb temperature difference and will maintain constant as long as DB is fixed in accordance with Equation (3.8) as shown in Figure 3-15.

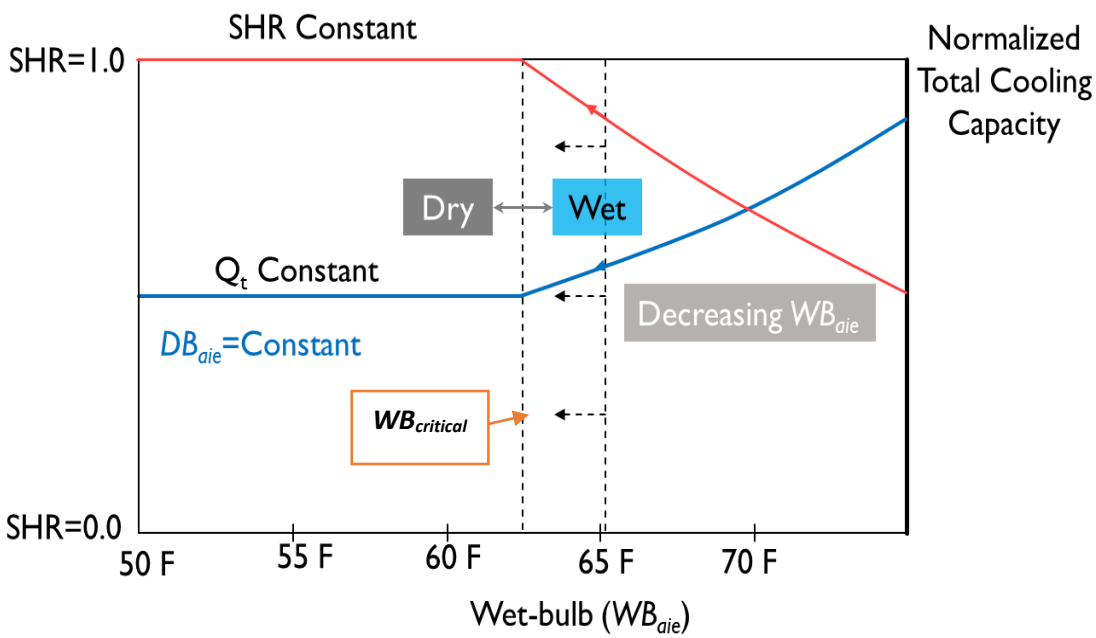

Figure 3-15 Cooling capacity and Sensible heating ratio characteristics in relative to WB_{aie} of cooling coil with fixed DB_{aie}, OAT and CFM

Figure 1-1 and Figure 3-15 represent cooling process of Figure 3-14. While decreasing WB_{aie}, Q_t and Q_L decreases accordingly, in contrast to SHR. As shown in Equation (3.4), when Q_t decreases, SHR increases since SHR is a ratio of dry air cooling to total cooling capacity. Respectively, Q_t and SHR remain constant when SHR is equal to 1 because there is no humidity addition.

$$SHR = \frac{\dot{Q}_s}{\dot{Q}_s + \dot{Q}_L} = \frac{\dot{Q}_s}{\dot{Q}_t} \qquad (3.4)$$

3.4.2. <u>Varying wet-bulb temperatures under various dry-bulb temperatures</u>

From previous section, characteristics of $\dot{Q}_t$ and SHR are elaborated as a function of WB under fixed DB. In this section, DB and WB will be involved under constant CFM, OAT and T_{evap}. The changing in cooling coil characteristics depending upon those conditions will be observed and analyzed.

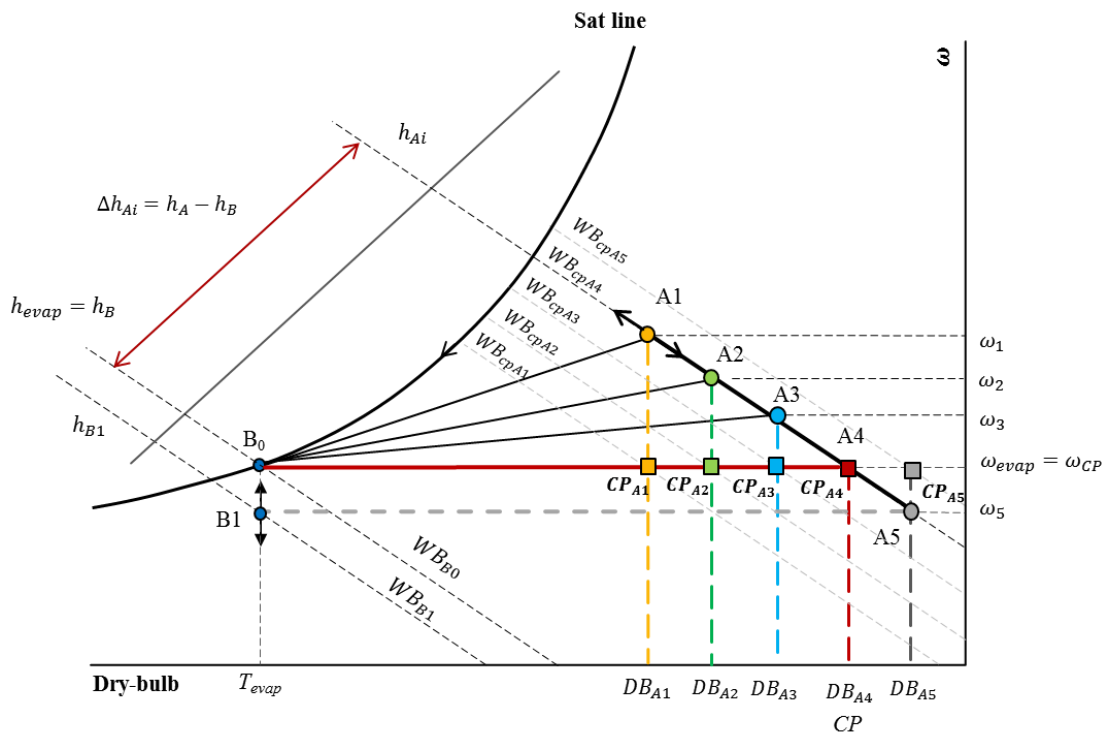

Figure 3-16 Characteristics of coil cooling at fixed CFM, WB_{aie} and OAT in relative to varying DB_{aie}

<u>*Cooling capacity*</u>

Enthalpy difference (Δh) in Figure 3-16 is not effected by varying DB_{Ai} on fixed WB line in wet-coil condition. On the other hand, if DB continues to increase until it converges toward a critical temperature point (CP), the coil turns dry and SHR equals or 1. After this point, the coil will be functioning in dry condition. Then point B is no longer attached the saturation line, and it will move vertically on the T_{evap} line causing alteration in enthalpy. Consequently, cooling capacity, although fixed WB, will continue to rise in relative to increasing DB).

Figure 3-14 demonstrates cooling capacity according to Figure 3-16. At constant WB_{cp} lines, though varying DB, enthalpy differences (Δh) in wet conditions are equal due to no change in enthalpy ($\Delta h_{A1}=\Delta h_{A2}=\Delta h_{A3}=\Delta h_{A4}$). On the other hand, Δh_{A5} is greater than enthalpy at other points because dry coil cooling performance is a function of DB only

as described in previous section. Although, enthalpy at this point is equivalent to other points, however, Δh_{A5} changes associated with moving point B as shown in Figure 3-16.

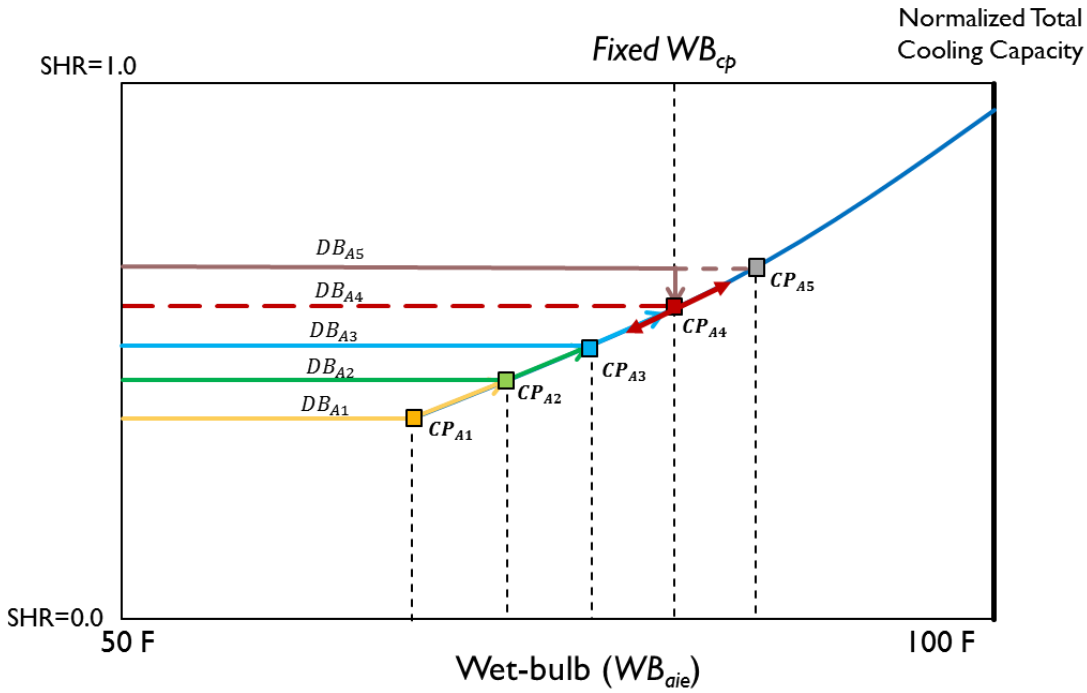

Figure 3-17 Cooling capacity characteristics while varying DB_{aie} on fixed WB_{aie} line at fixed OAT and CFM

In addition, provided all of A_i points proceed on DB_{Ai} vertically to the intersect points where humidity ratios are equal to ω_{evap}. Those intersect points are called wet-bulb critical points (CP_{Ai}) where coil conditions turn dry. Therefore, assumed T_{evap} is constant, each process on DB obtain its own CP on different WB conditions. The WBs which intersect CPs are determined as critical wet-bulb temperature (WB_{crit}).

On the contrary, WB_{crit} of each fixed DB_{Ai} , also appropriately refer to the inflection points of SHRs. Therefore, introducing SHRs to Figure 3-14 will outline relationship of SHR and $\dot{Q}_t$ to WB as following Figure 3-15.

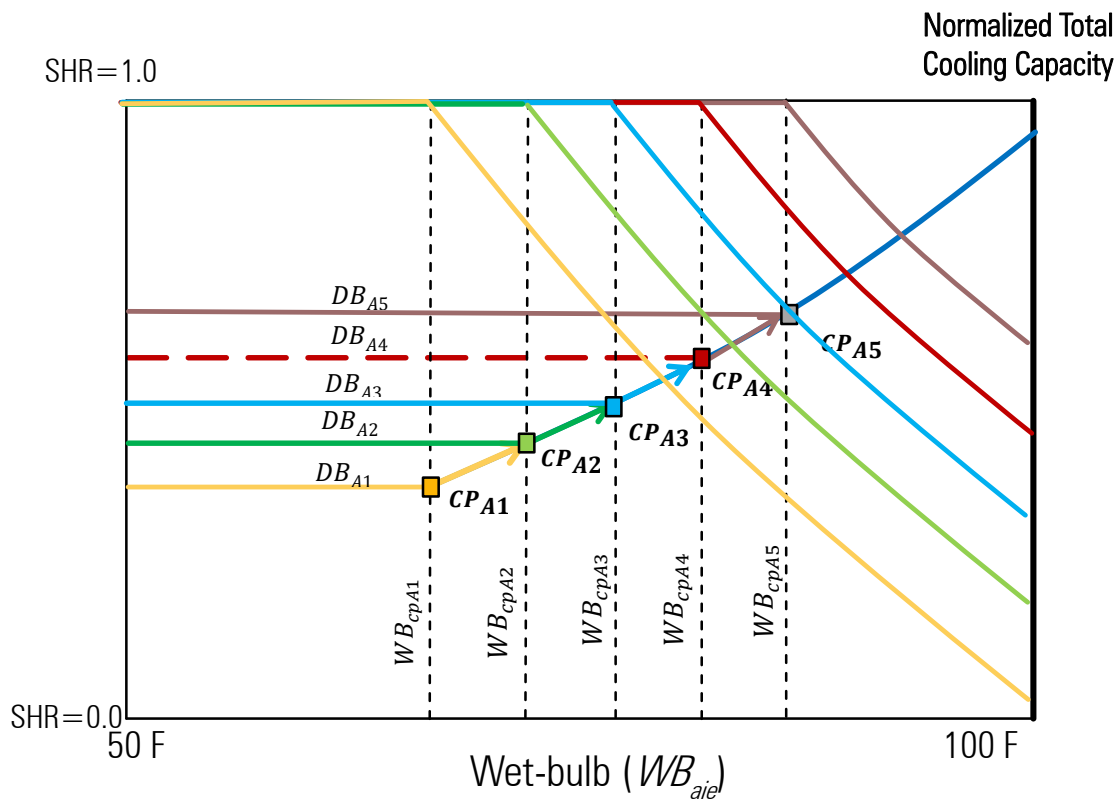

Figure 3-18 Cooling capacity and SHR characteristics on fixed OAT and CFM

3.4.3. Further analysis cooling coil characteristics based on principles of air

The aforementioned section introduces the analysis of cooling capacity and SHR on the psychrometric chart and generalize their relations with regard to WB for different DB conditions under fixed OAT and CFM. However, Figure 3-15 yet cannot determine the exact shapes of both cooling capacity and SHR.

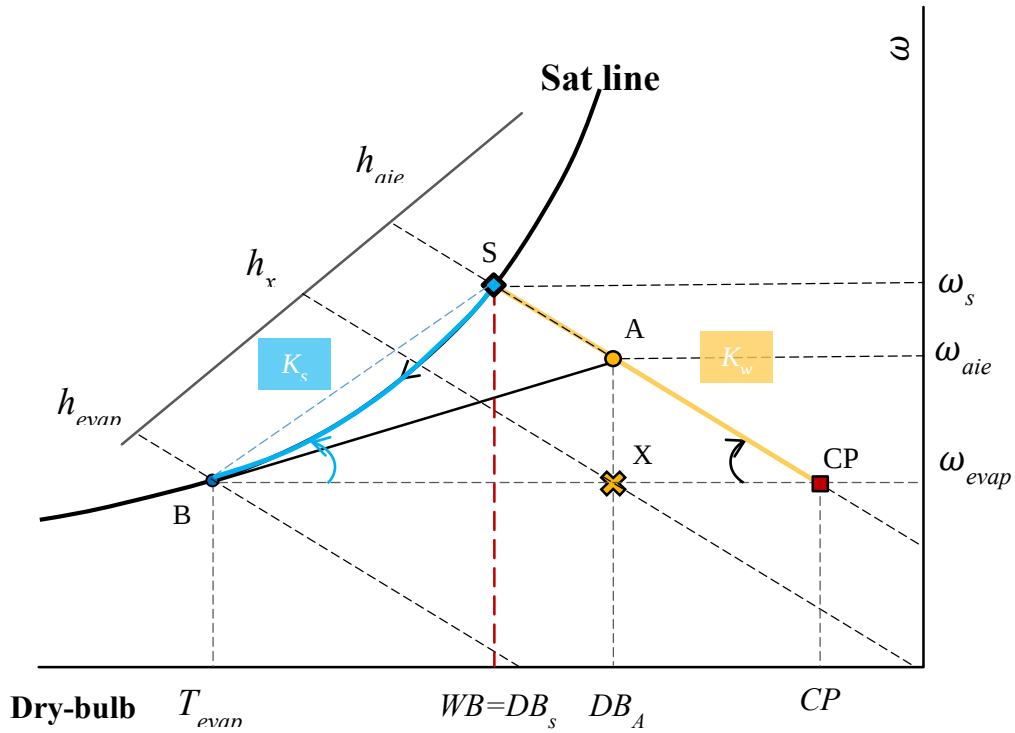

Figure 3-19 Cooling capacity characteristics of varying DB_{aie} on fixed WB_{aie} line at fixed OAT and CFM

3.4.3.1. SHR characteristics' model formulation

Yang, et al., 2010 established SHR and cooling capacity model by generating multiple linear regression models from manufacturers' data for which the capacity model can accurately predict cooling capacity within 10% of relative errors. However, the model requires further investigation to formulate an accurate SHR model. In Figure 3-19, saturated point S and critical point CP are introduced to cooling coil characteristics examining. Saturated point S is the condition in which WB equals DB, and CP is the extending point in which WB line crisscrossed with humidity ratio (ω_{evap}) line of saturated T_{evap}. Since S, A and CP lay on the same WB line, their enthalpies are corresponding. Therefore, Equation (3.11) can be reformulated.

$$\boldsymbol{SHR = \frac{\dot{m}_a C_p (T_X - T_B)}{\dot{m}_a (h_A - h_B)} = \frac{C_p (T_X - T_B)}{(h_A - h_B)}}$$

Where $h_A = h_{cp}$

$$SHR = \frac{C_p(T_X - T_B)}{(h_{cp} - h_B)} = \frac{C_p(DB_A - T_B)}{C_p(CP - T_B)}$$

Then,

$$SHR = \frac{DB_A - T_B}{CP - T_B} \qquad (3.22)$$

Equation (3.22) involves CP to the equation. However, CP can be derived by trinomial relation as a function of *WB* and T_{evap} as follows.

- Step 1: Determine K_t and K_{wb} as slopes of $\overline{BS}$ and $\overline{CP\ S}$ respectively.

  $$K_s = \tan(B) \text{ and } K_{wb} = \tan(CP)$$

  Where $DB_s = WB$

  $$K_s = \frac{\omega_s - \omega_B}{DB_s - T_B} \; and \; K_{wb} = \frac{\omega_s - \omega_B}{CP - DB_s} = \frac{\omega_s - \omega_B}{CP - WB}$$

- Step 2: Determine r as ratio of K_s and K_{wb}

  Then,

  $$r = \frac{k_s}{k_{wb}} \qquad (3.23)$$

  and

  $$r = \frac{DB_s - CP}{DB_s - T_B} = \frac{CP - WB}{WB - T_B}$$

  Then the ratio of slopes r, can be calculated

  $$r = \frac{CP - WB}{WB - T_{evap}} \qquad (3.24)$$

- Step 3: Reform the CP as a function of r and temperatures

  $$CP = (1 + r)WB - rT_{evap} \qquad (3.25)$$

- Step 4: Reform SHR by incorporating Equation (3.22) and (3.25), and calculating SHR as a function of DB and WB

  Where SHR < 1

$$SHR = \frac{DB_A - T_{evap}}{(1+r)(WB - T_{evap})} \tag{3.26}$$

From Equation (3.26), under fixed OAT, CFM and T_{evap}, SHR relation is the function of WB and DB_A as follow:

$$SHR = f(WB^{-1}, DB_A) \tag{3.27}$$

3.4.3.2. Total cooling capacity characteristics' model formulation

To formulate total cooling capacity, under fixed T_{evap} and CFM, from Equation (3.11) and Equation (3.26), total cooling capacity can be derived as follows.

$$SHR = \frac{\dot{m}_a C_p (T_X - T_B)}{\dot{m}_a (h_A - h_B)}$$

Then,

$$(h_A - h_B) = \frac{C_p\left(DB_A - T_{evap}\right)}{SHR} \tag{3.28}$$

And deploy derived SHR from Equation (3.26),

$$(h_A - h_B) = \frac{C_p(DB_A - T_B)}{\frac{DB_A - T_{evap}}{(1+r)(WB - T_{evap})}}$$

Then multiply by air mass flowrate ($\dot{m}_a$).

$$\dot{Q}_t = \dot{m}_a \cdot C_p (1+r)(WB - T_{evap}) \tag{3.29}$$

Equation (3.29), under constant OAT, CFM and T_{evap}, $\dot{Q}_t$ is a function of WB only.

3.4.4. Characteristics' model verification using Engineering Equation Solver (EES) and Microsoft Excel.

To plot SHR and Total cooling capacity ($\dot{Q}_t$), EES is utilized to calculate parameters in associate with the psychrometric chart properties. The plotted conditions consider DB between 70 and 90°F, and WB between 50 and 80 °F depending on the limitation of moist air property (see Appendix B for parametric table of normalized plot of SHR and $\dot{Q}_t$ relative

to WB). To cover all operating conditions, Equation (3.26) and (3.29) are calculated as illustrated in Equation (3.30).

$$Cooling\ coil\ model \begin{cases} Wet-coil\ condition \begin{cases} SHR = \dfrac{DB_{aie} - T_{evap}}{(1+r)(WB_{aie} - T_{evap})} \\ \dot{Q}_t = \dot{m}_a \cdot C_p(1+r)(WB_{aie} - T_{evap}) \end{cases} \\ Dry-coil\ condition \begin{cases} SHR = 1 \\ \dot{Q}_t = \dot{Q}_s = \dot{m}_a C_p(DB_{aie} - T_{evap}) \end{cases} \end{cases} \quad (3.30)$$

Since CFM is constant, From Equation (3.29), the cooling capacity is verified in a form of total cooling capacity per volume of air. Then $\dot{Q}_t$ can be rearranged as a following equation.

$$\frac{\dot{Q}_t}{CFM} = \rho_a(h_A - h_{evap}) = \rho_a \cdot C_p(1+r)(WB - T_{evap}) \quad (3.31)$$

From the calculation table using EES in Appendix B, normalized cooling capacity can be illustrated as follows.

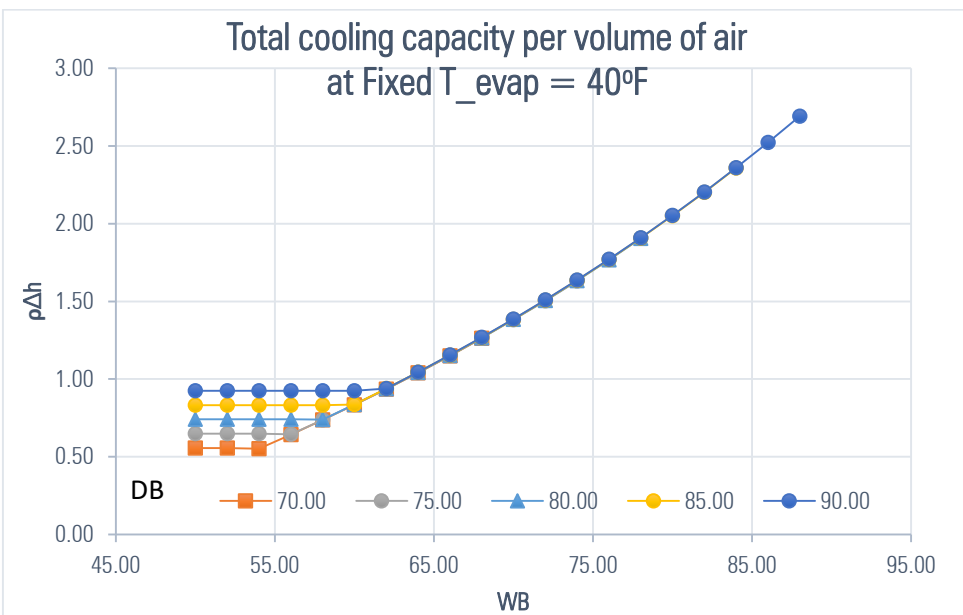

Figure 3-20 Cooling Capacity characteristics in relative to WB

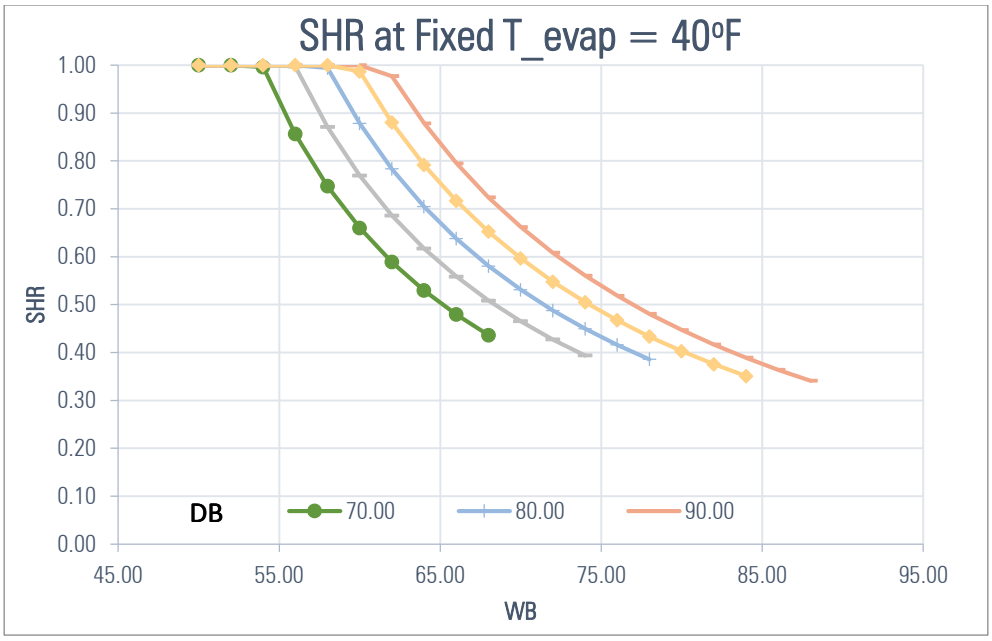

Figure 3-21 SHR characteristics in relative to WB

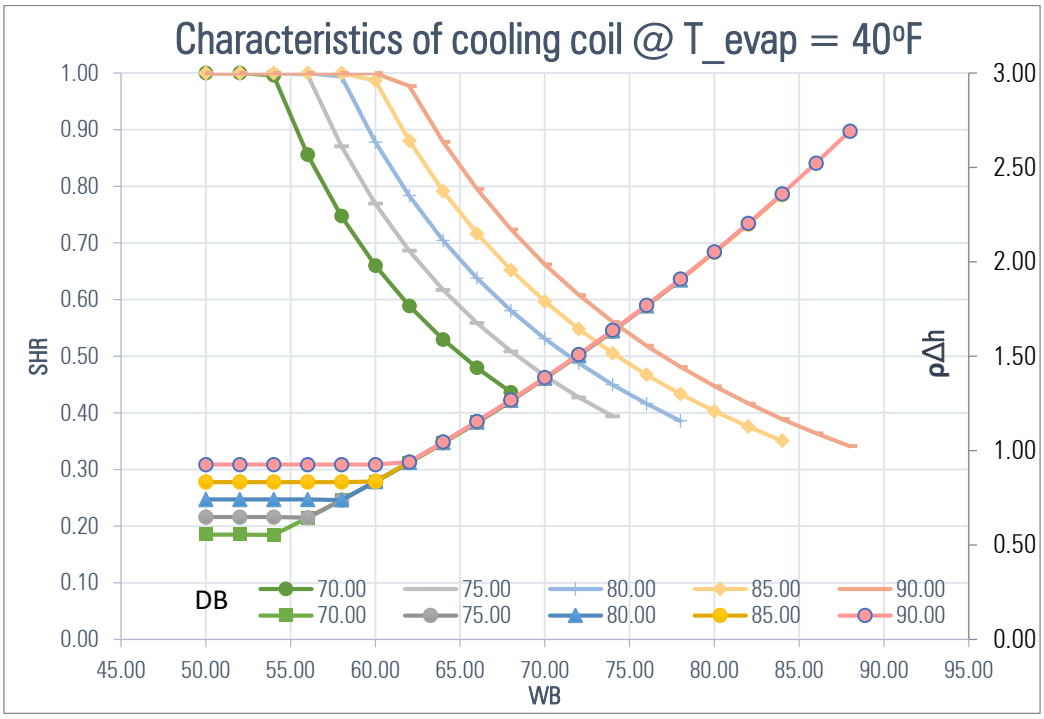

Figure 3-22 Characteristics of cooling coil at constant T_{evap}

3.5. Analysis of Cooling Coil Characteristics Under Constant Indoor Dry-bulb Temperature (DB)

3.5.1. Analysis of Cooling Coil Characteristics Under Fixed DB and CFM

The previously analysis fixes OAT and DFM condition. Thus constant T_{evap} can be deployed to the investigation. However, outdoor environment always changes and is fluctuated. Therefore, the characteristics of cooling coil will be further investigated based on varying OAT. From Equation (3.15), T_{evap} is a function of CFM, WB, and OAT. Provided that CFM and WB conditions are constant. T_{evap} is variated on the saturated line by regulating OAT. Considering fixed orifice expansion device installed in the VCC system, refrigerant mass flowrate is proportional to the throat-area and the square root of the pressure difference. The schematic of an expansion device is illustrated as follows.

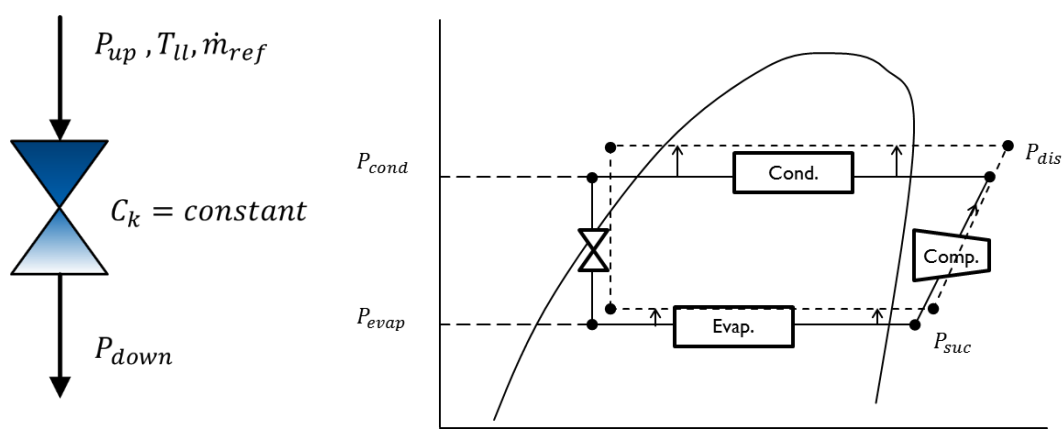

Figure 3-23 Fundamental of vapor compression cycle illustration

Using the nomenclature denoted in Figure 3-23, the refrigerant flowrate of the expansion device has the formula as follows.

$$\dot{m}_{ref} = C_k\sqrt{\rho_{up}(P_{up} - P_{down})} \tag{3.32}$$

Where C_k=function of throat area and valve parameters=constant.

Assuming no loss in heat exchangers and refrigerant pipes, evaporating and condensing pressures remain constant. Therefore, Equation (3.32) can be reformulated as follows.

$$\dot{m}_{ref} = C_k\sqrt{\rho_{up}(P_{cond} - P_{evap})} \tag{3.33}$$

However,

$$P_{cond} = f(T_{cond}) = f(OAT) \tag{3.34}$$

$$P_{evap} = P_{cond} - \dot{m}_{ref}C_k^2 \cdot \frac{1}{\rho_{up}} \tag{3.35}$$

For equation (3.35), evaporating pressure (P_{evap}) is relative to condensing pressure and the device properties. Assuming constant $\dot{m}_{ref}$, from Equation (3.34) and (3.35), $P_{evap} \propto P_{cond}$. In addition, pressures are functions of refrigerant properties and temperature. Therefore, in the constant expansion device, $T_{evap} \propto T_{cond} \propto OAT$.

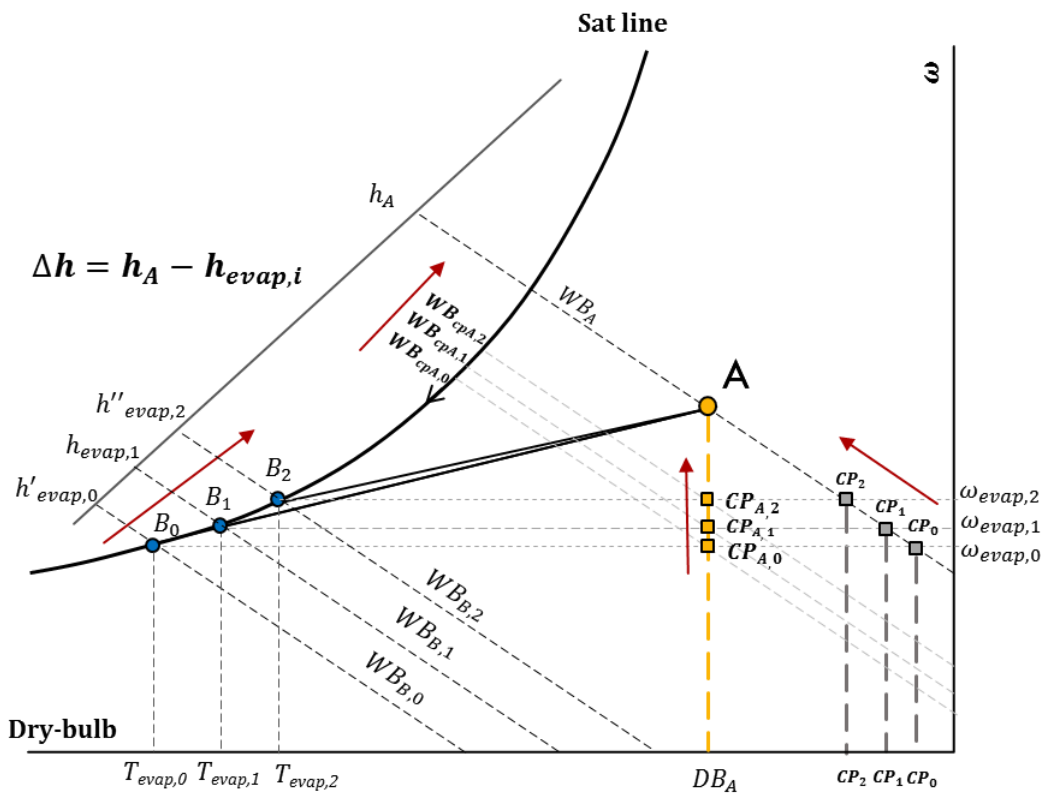

Figure 3-24 Cooling capacity characteristics under fixed DB and CFM

From Figure 3-24 Cooling capacity characteristics under fixed DB and CFM when T_{evap} moves on the air saturation line, CP_A moves correspondingly, changing the critical points where coils turn dry. Since T_{evap} is relative to OAT, enthalpy differences of sensible cooling (h_x-h_{evap}) during which coil is dry will increase in relative to OAT. On the other, when T_{evap} increases according to OAT, CP decrease. However, when coil turns wet sensible cooling remains constant while latent cooling increases corresponding to increasing WB. Furthermore, as shown in Equation (3.22), SHR has opposite relation to CP. Consequently, the increase of CP will oppositely decrease SHR since SHR = f(CP^{-1},T_{evap}).

$$\boldsymbol{SHR = \frac{DB_A - T_B}{CP - T_B}} \qquad (3.22)$$

From the above analysis, characteristic of performance variations of fixed-OAT conditions can be displayed in Figure 3-25.

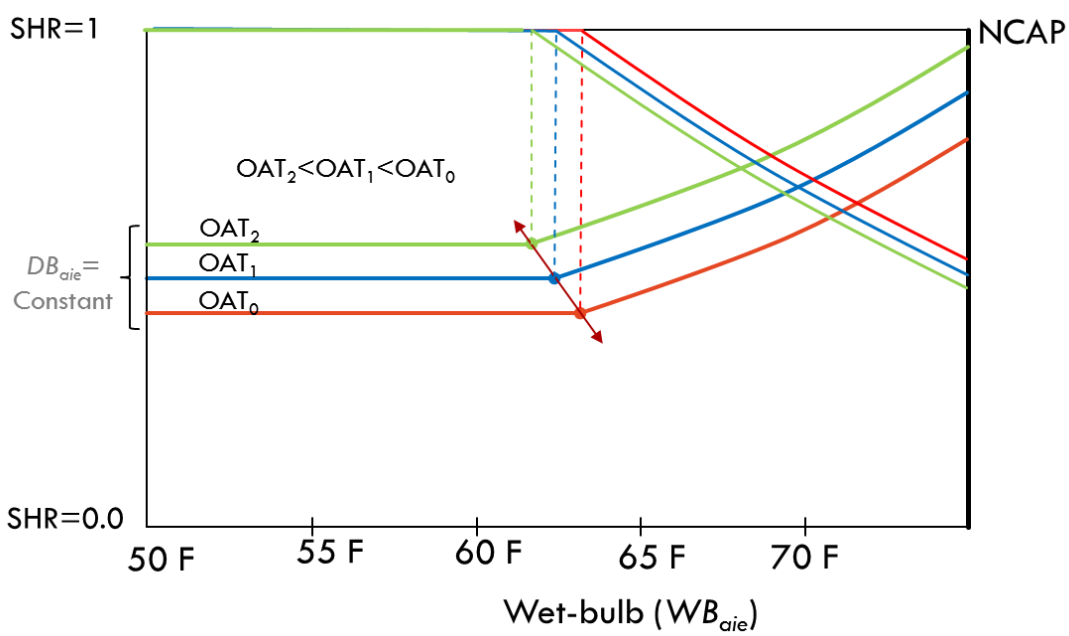

Figure 3-25 Normalized characteristics of cooling coil performance at fixed CFM condition

where NCAP is normalized total cooling capacity which is a proportion of actual cooling capacity over rated cooling capacity. NCAP will be described further in Chapter 4.

3.5.2. Analysis of Cooling Coil Characteristics Under Fixed DB and OAT

For fixed OAT and DB conditions, the effects of CFM on cooling coil condition can be analyzed. According to cooling capacity (Equation (3.1)), cooling capacity is a function of mass flowrate and enthalpy difference.

$$\dot{Q}_t = \dot{m}_a(h_A - h_B) = CFM \cdot \rho_a(h_A - h_B)$$
$$\dot{Q}_t = CFM \cdot \rho_a\left(h_{aie} - h_{evap}\right) \tag{3.36}$$

Therefore, CFM linearly affects total cooling capacity when T_{evap} is constant.

However, in actual operations, T_{evap}= f(CFM, WB_{aie}, OAT). Provided WB_{aie} and OAT are constant, CFM will directly variate T_{evap}. CFM refers to the exchange rate of refrigerant and air passing through coil. Therefore, while increasing CFM, energy exchange rate increase, and refrigerant receives more energy from the air. T_{evap} will slightly increase accordingly. When T_{evap} increases, CP on WB line decreases, in contrast to CP_A point on DB lines, as shown in Figure 3-24. This means that SHR will slightly rise as mentioned correspondingly. Therefore, the impacts of CFM on cooling coil operating characteristics can be concluded as follows:

- Elevate CFM rates will directly increase $\dot{Q}_t$ and SHR, and reduce CFM rates will decrease both $\dot{Q}_t$ and SHR, vice versa.
- Lower the CFM will decrease SHR due to T_{evap} drops, this means that, moisture is removed more effectively in lower CFM.
- CP_A and CP are virtual points on DB and WB lines respectively. Increasing CFM will increase CP_A whereas decreasing CP

From the above conclusions, characteristic of performance variations of fixed-OAT conditions can be displayed in Figure 3-26, where NCFM is normalized CFM which is a proportion of actual CFM over rated CFM.

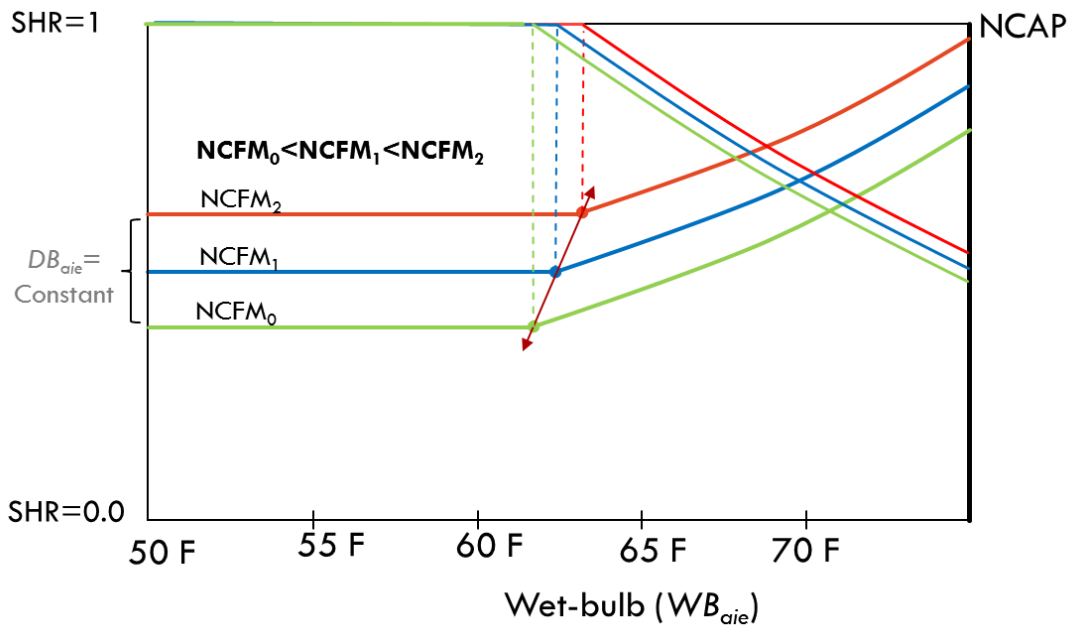

Figure 3-26 Normalized characteristics of cooling coil performance at sixed OAT condition

3.6. Hypotheses Setup Normalizing and Scaling under Rating Condition

Air-conditioning is a steady-state process due the sluggishness of temperature changing in the environment and conditioned spaces (say in minutes to hours). Since all equipment created by humans is based on calculations, assumptions and principles of substances, unlike nature, therefore, the characteristics of equipment could be elaborated and explained.

For cooling coils operations, their performance attributes are the relation of refrigeration cycles and principles of air on the psychrometric chart. The analysis of cooling coil characteristics in this chapter shows that cooling coil performance in steady-state conditions can be normalized and be represented by cooling capacity functions and

SHR lines in relative to wet-bulb temperature (*WB*). The analyses were divided in 3 settings: fixed CFM and OAT, fixed DB and CFM, and fixed DB and OAT. Thus, by combining each analysis from previous sections and their impacts on cooling performance, normalized hypotheses of cooling coil inherent characteristics can be illustrated as following Figure 3-27.

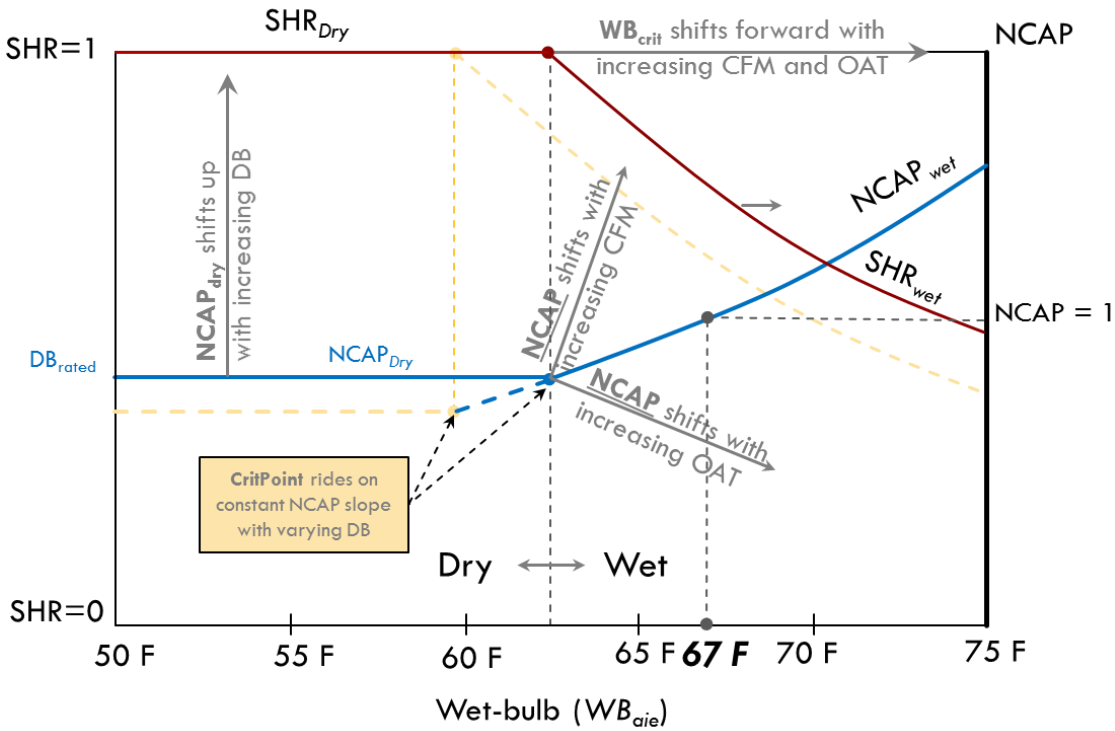

Figure 3-27 Cooling coil characteristics' hypothesis

The critical point in Figure 3-27 represents cooling capacity at fixed dry-bulb condition in which coil condition starts to transform from wet to dry conditions. Those two conditions have significant difference in operating characteristics. When the wet-bulb temperature increases at fixed DB condition passing the critical point from dry to wet, SHR drops non-linearly in contrast to cooling capacity which will increase as increasing WB. Therefore, knowing the critical points behaviors, wet and dry coil condition can be separated precisely which can significantly improve modelling performance.

Since in this analysis, rates of total cooling capacity variate by temperature, CFMs, and equipment sizes, therefore, cooling capacity different representing in this analysis is a proportion of actual capacity over rated capacity as a following equations:

$$NCAP = \frac{Actual\ Cooling\ Capacity\ (CAP)}{Rated\ capacity\ (CAP_{rated})} = \frac{CAP}{CAP_{rated}} \qquad (3.37)$$

CAP_{rated} is total cooling capacity designating sizes and performance of equipment at rated conditioned in manufacturers' manuals which will be explained in Chapter 4.

Hypotheses of Cooling Coil characteristics

- For constant CFM and OAT, increasing DB will shift $NCAP_{dry}$ vertically
    - WB_{crit} decreases with decreasing DB, and increases with increasing DB
    - $NCAP_{wet}$ remain on constant $NCAP_{wet}$ slope.
- For constant DB
    - NCAP and WB_{crit} increase with increasing CFM
    - NCAP decreases with increasing OAT, whereas WB_{crit} increases with increasing CFM.

The hypotheses are developed and upon principal of air, fundamental of refrigerant cycle and graphical observation of cooling coil processing on psychrometric chart. The evaluations and validations of hypotheses are performed in Chapter 4.

CHAPTER 4. VALIDATION OF NORMALIZATION AND SCALABILITY OF DX COOLING COIL CHARACTERISTIC HYPOTHESES BY MANUFACTURING DATA

According to previous section, cooling coil are function of air properties at an evaporator inlet (CFM, DB_{aie},WB_{aie}) and environment temperature (OAT). As cooling coil operation is sluggish, cooling performance and its characteristics will be analyzed in various steady state conditions obtained from manufacturers' data that is: freely available, ready for analyses, generic and accurate (Li, et al., 2007). Data using in this analysis are of mini-split heat pumps (MSHPs), split-system of heat pumps and packages units (roof top units RTUs). First the GRDB model format will be validated by self-validated and laboratory validation methods. Afterward, the validation of cooling coil characteristics hypotheses is evaluated.

4.1. GRDB cooling models on MUZ-FE12NA evaluation

The generated models from the original GRDB and the applied GRDB is validated by laboratory data from Purdue University whose results were used by department of energy (DOE) to evaluate MSHPs performance characteristics in 2011. Purposes of validations is to evaluate model efficiency in various and real operating conditions. In this case, the validations are conducted based on interpolation. As a result, data ranges beyond DB_{aie} of 80 ± 1 ^{o}F of which manufacturer's data does not cover will be excluded from the validations. In addition, only the maximum speed compressor ranges will be evaluated. Laboratory trained data for validation is provided in Appendix A. Errors of total cooling capacity (CAP) are examined by using relative error equation (See Equation (4.1)). Figure 4-1 shows relationship between actual laboratory results and the model predicted results. The

upper and lower dashed lines are the upper and lower bounds of errors, respectively. Table 4-1 display statistical data of calculated errors. The maximum relative errors for the modified and the original are 12.5 % and 15.32%, and the minimum relative errors are -8.6% and –4.2%, respectively. Moreover, the average error of the modified model is 0.0% which is better than that of the original model. The improved model also shows less standard deviation of 0.0312 which is slightly improved. However, the absolute error of the proposed model is 6.2% which is 0.2% more than that of the authentic model. All the validation results are provided in Table 4-1.

$$Rel_{er} = \left[\frac{CAP_{model} - CAP_{actual}}{CAP_{actual}}\right] \times 100 \tag{4.1}$$

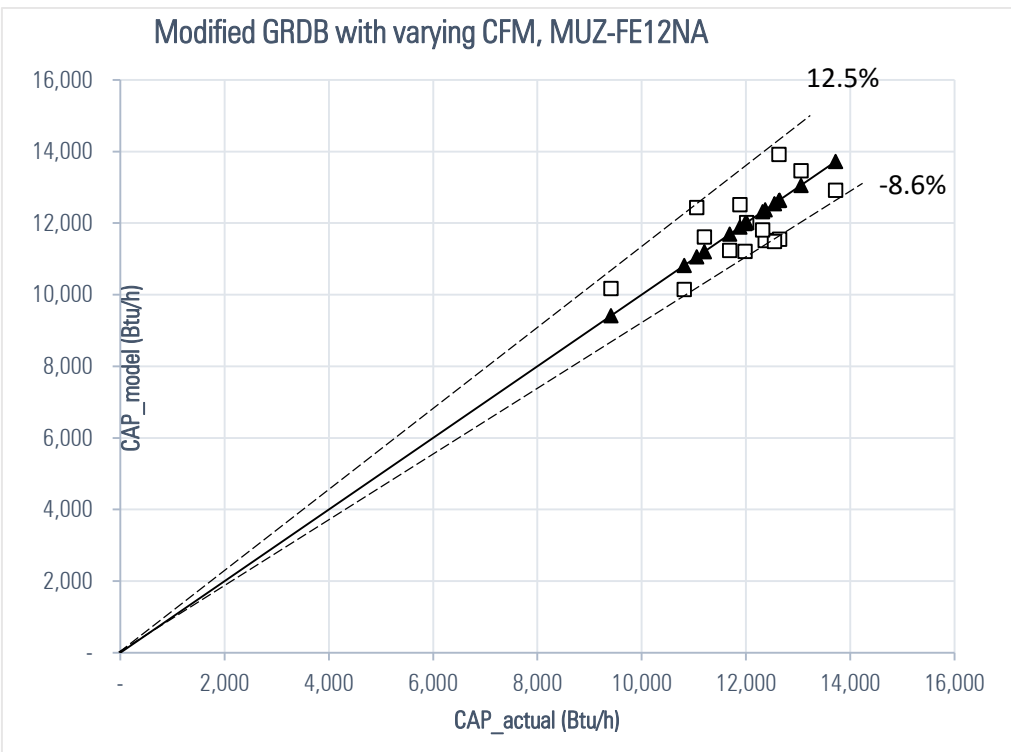

a) Modified model

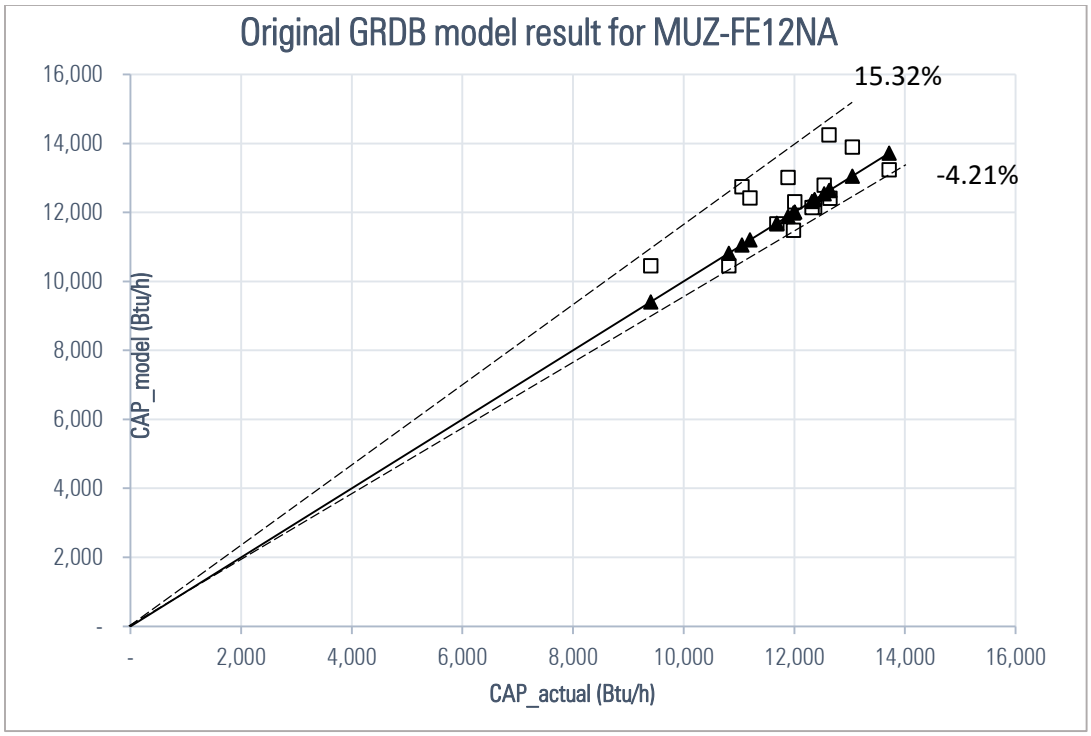

b) Original model

Figure 4-1 Actual laboratory data results and model predicted results

Table 4-1 Statistical data of errors for all models at maximum speed compressor and DB of 80°F

Data types	Set of data	Min	Max	Average	Absolute average	Standard Deviation
Original GRDB	15	-4.21%	15.32%	4.08%	6.0%	0.0478
Modified GRDB	15	-8.6%	12.5 %	0.00	6.2%	0.0312

4.2. Rating Conditions

A rating condition is the condition on which capacity, efficiency and energy consumption are represented. Each manufacture arranges equipment data uniquely, however, standardized according to ANSI/AHRI 240. Rating conditions for cooling systems in steady state are as follows.

- Outdoor temperature (OAT) at 95 F
- Indoor temperatures at dry-bulb (DB) of 80 F and wet-bulb (WB) of 67 F

- Medium setting indoor air flowrate is typically ranged from 350 to 400 cfm/ton.

From above information, normalized cooling capacity settings are determined as follows.

$$NCAP = \frac{Actual\ Cooling\ Capacity\ (CAP)}{Rated\ capacity\ (CAP_{rated})} = \frac{CAP}{CAP_{rated}} \tag{4.2}$$

$$MCFM = \frac{CFM_{rated}}{CAP_{rated}} \times 1\ (\frac{ton}{cfm}) \tag{4.3}$$

$$NCFM = \frac{CFM}{MCFM} \tag{4.4}$$

Where,

NCAP : Normalized cooling capacity

NCFM : Normalized Air flow rate

CFM : Air flow rate (ft^3/mins of cfm)

MCFM : Medium setting indoor air flow rate (typically ranging between 350 and 400 cfm/ton)

CAP : Total cooling capacity at interested condition (Btu/h)

CAP_{rated} : Total cooling capacity at rated condition (Btu/h)

4.3. Manufacturers' performance data evaluation

4.3.1. MSHPs

MSHPs' data used in this section are from Mitsubishi (FE), Fujitsu (RLS) and Daikin (FTXKN). Variables representing in performance tables are wet- and dry- bulb temperature, total cooling capacity and total power consumption (or outdoor unit power consumption) at fixed air flow rates (CFMs). Mitsubishi fixes DB at 80F, while others couple DB and WB (see Appendix C). To analyze cooling coil characteristics, two types

of plots will be performed: plots of relationship between Q_t and WB, and plots of relationships between SHR and WB of various OATs.

For Mitsubishi as shown in Figure 4-2, three sets of capacity ranges in this model are displayed at fixed DB of 80°F. The plots of Q_t and SHR for all rating capacities displaying in Figure 4-2 are in wet conditions where SHR < 1. By varying OAT in the CAP and SHR plots, the behavior of Mitsubishi cooling performance can be elaborated as follows:

- In wet condition, cooling capacity increases in accordance with WB.
- Varying OAT in each plot, the higher the OAT, the lower the capacity.
- SHR decrease in contrast to increasing WB.
- SHR is slightly effected by OAT. However, slopes slightly decrease with increasing OAT.

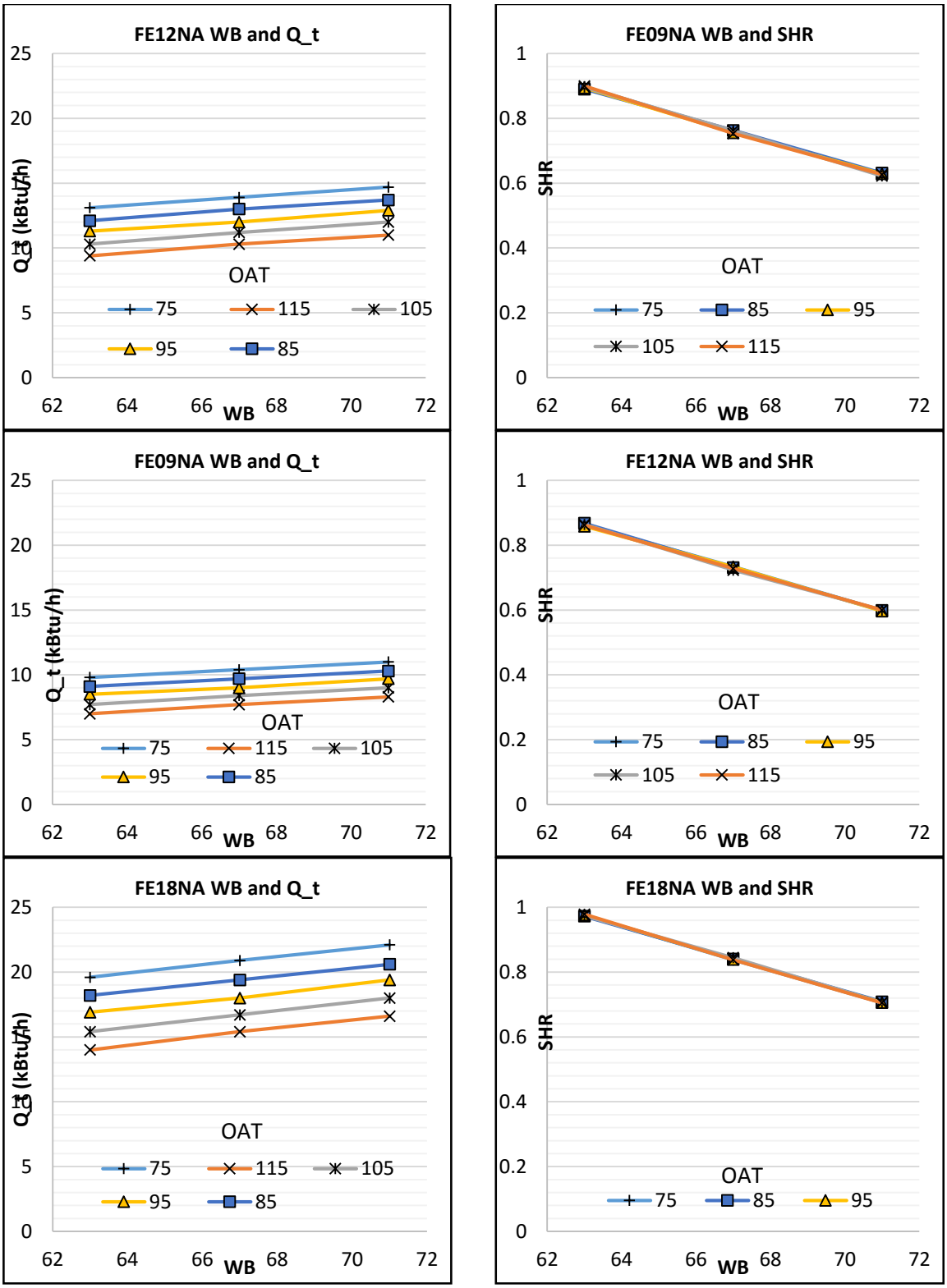

(a) Cooling capacity (Q_t) and Wet-bulb (WB) (b) SHR and Wet-bulb (WB)

Figure 4-2Cooling performance of Mitsubishi at fixed DB of 80 F

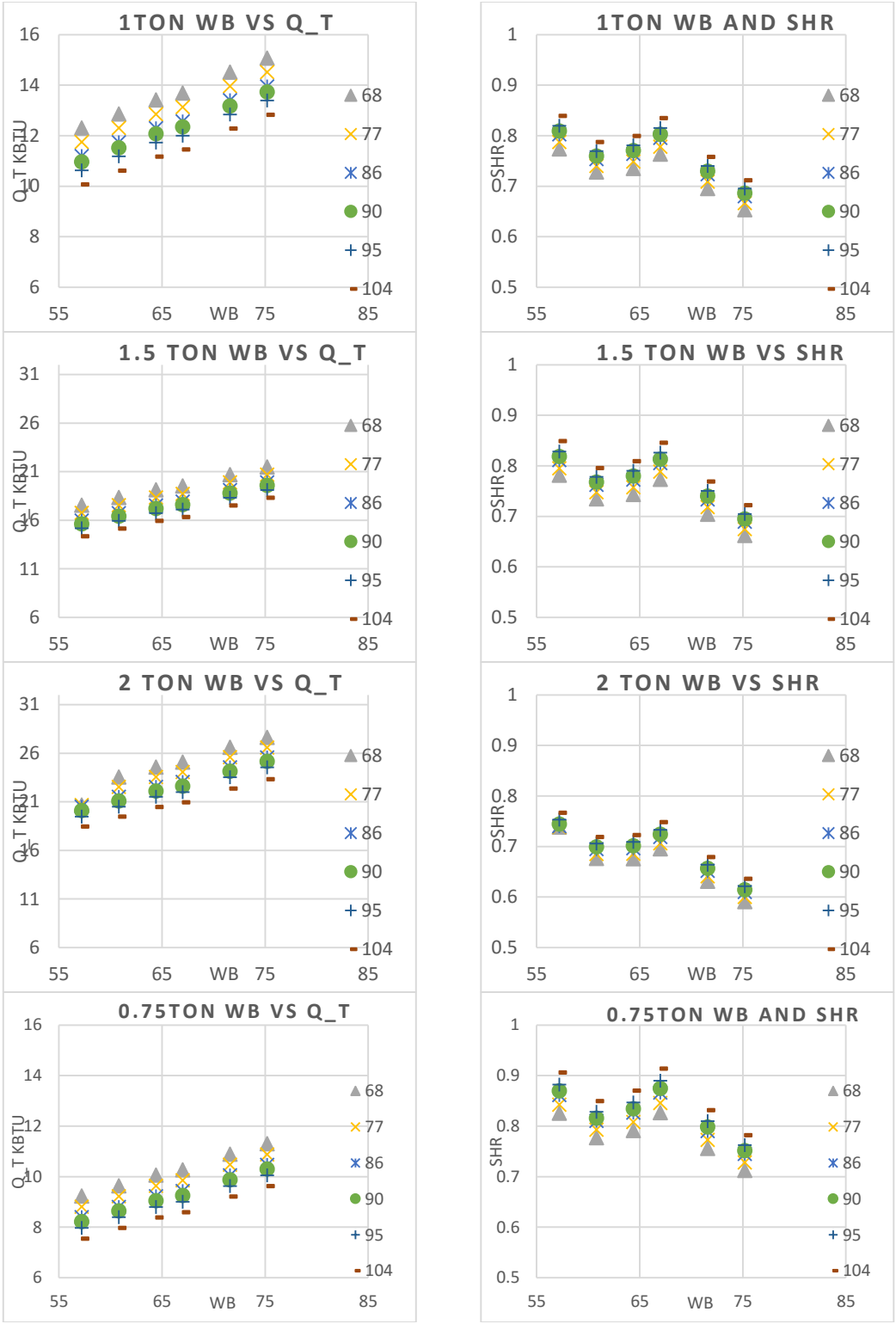

(a) Cooling capacity (Q_t) and Wet-bulb (WB) (b) SHR and Wet-bulb (WB)

Figure 4-3Cooling performance of Daikin FTXKN

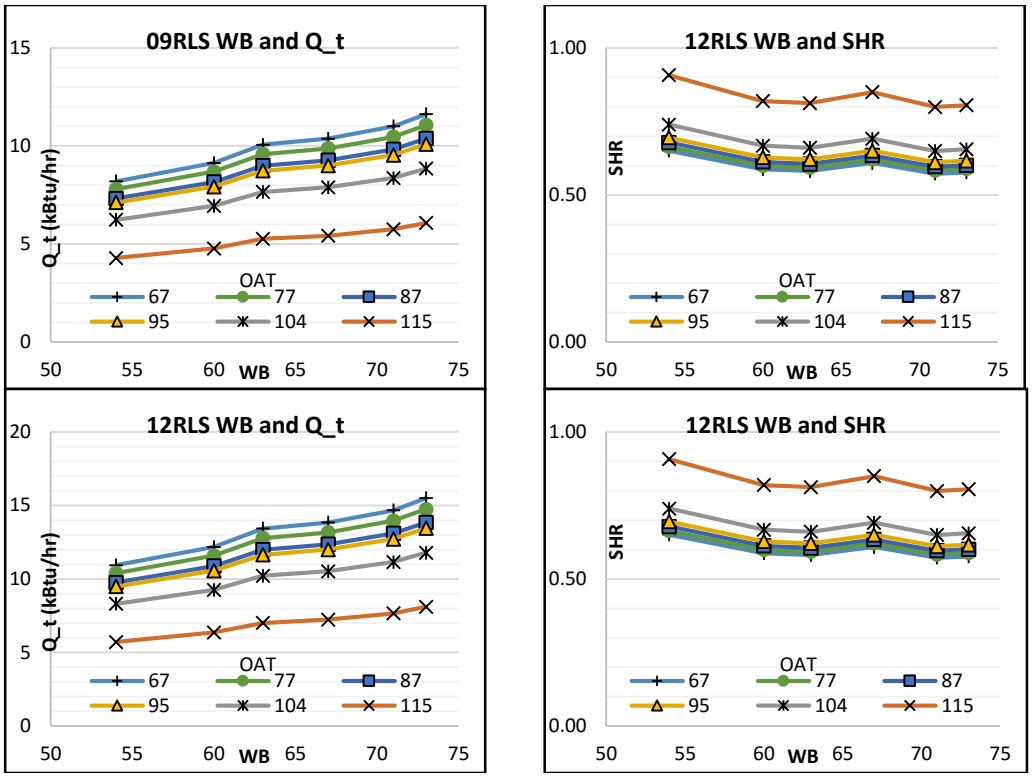

(a) Cooling capacity (Q_t) and Wet-bulb (WB) (b) SHR and Wet-bulb (WB)

Figure 4-4Cooling performance of Fujitsu RLS

For Daikin as shown in Figure 4-3, 4 sets of equipment capacity are given where WBs are 57.2, 60.8, 64.4, 67, 71.6 and 75.2°F, and DBs are 68, 71.6, 77, 80, 86 and 89.6°F, coupled respectively. As previously stated, wet-coil cooling capacity at fixed CFM is varying associated with WB temperature. Therefore, varying OAT at different DB and WB provides similar trends of cooling capacity as seen in Mitsubishis' data. On the other hand, SHR is depending upon both WB and DB according to Equation (3.11). Hence, SHR plots of Daikins' data show results randomly. Likewise, Fujitsu pairs WBs and DBs, and thus SHR plots show unsystematic results as shown in Figure 4-4. However, from Daikins' and Fujisus' plots, it can be observed that increasing of OAT shifts cooling capacity line downward during operating in the same sets of temperature.

4.3.2. Split heat pumps (SHP)

Three split systems' data from Carrier, Goodman and York are selected to evaluate the hypotheses. Carrier and York display their cooling performance data by fixed DB at 80°F, unlike Goodman's performance data in which various DB ranges are provided in the manual. Therefore, the Goodman's data will be major resources for evaluations of split system heat pumps (SHPs) cooling coil characteristics.

Goodman, Carrier and York nominated models are DSZ16, 25HBB3 and CZF, respectively. All selected split system heat pumps (SHPs) sizes are between 1.5 and 5 tons with thermal expansion device (TXV). The comprehensive performance tables of selected models are provided in Appendix C; the essential data for the analyses are given in Table 4-2**.** Since DSZ16 performance table provides various range of DB. It can be propagated to additional comparative plots, i.e. fixed OAT-CFM, fixed OAT-DB, fixed DB-CFM. In addition, normalized plot will be applied for ease of analyses.

Table 4-2 Manufacturers' reported data

(a) Goodman DSZ160 Manufacturers' reported data

Makers	**Units**	**Goodman**				**Goodman**			
Outdoor Models		**DSZ16-Low**				**DSZ16-High**			
Rated capacities	**kBtu/h**	**24**	**36**	**48**	**60**	**24**	**36**	**48**	**60**
Compressor		2 stage Scroll							
CFM (Low)	cfm	569	700	941	1050	766	1006	1356	1600
CFM (Medium)	cfm	**637**	**800**	**1075**	**1150**	**875**	**1150**	**1550**	**1750**
CFM (high)	cfm	731	900	1209	1350	984	1294	1744	2000
Power con.	kW	1.37	1.86	2.53	3.06	2.02	2.78	3.63	4.53
***CAP_{rated}**	kBtu/h	18.1	25.2	34.4	40.2	24	34.6	47.5	57
MCFM	cfm/ton	319	266.7	268.8	230	438	383.3	387.5	350

(b) Carrier 25HBB Manufacturers' reported data

Makers	Units	Carrier						
Outdoor Models		**25HBB-**						
Rated capacities	kBtu/h	**18**	**24**	**30**	**36**	**42**	**48**	**60**
Compressor		Scroll						
CFM (Low)	cfm	525	700	875	1050	1225	1400	1750
CFM (Medium)	cfm	600	800	1000	1200	1400	1600	2000
CFM (high)	cfm	**675**	**900**	**1125**	**1350**	**1575**	**1800**	**2250**
Power con.	kW	1.63	2.16	2.82	3.23	3.9	4.4	5.65
***CAP$_{rated}$**	kBtu/h	17.4	22.9	30.34	34.08	40.87	47.96	59.77
MCFM	cfm/ton	450	450	450	450	450	450	450

(c) York CZF0 Manufacturers' reported data

Makers	Units	York					
Outdoor Models		**CZF0-**					
Rated capacities	**kBtu/h**	**24**	**30**	**36**	**42**	**48**	****60**
Compressor		Scroll					
CFM (Low)	cfm	600	800	1000	1200	1400	1500
CFM (Medium)	cfm	**800**	**1000**	**1200**	**1400**	**1600**	**1700**
CFM (high)	cfm	1000	1200	1400	1600	1800	1900
Power con.	kW	1.93	2.45	2.81	3.39	3.76	4.28
***CAP$_{rated}$**	kBtu/h	23.6	30	34.4	41.5	48	53.5
MCFM	cfm/ton	400	400	400	400	400	340

Notes:

* *Rated in accordance with AHRI Standard 210/240 at DB/WB = 80/67 F and OAT = 95 F*

** *Rated at 1,800 cfm.*

Rated CFM

From Table 4-2**,** all makers apply scroll compressors to SHPs. However, Goodman pertains 2-stage scroll compressors, thus having low- and high- performance tables. Thee CFM settings are used (high, medium and low), and MCFMs for rating are placed between 340 to 450 at rated conditions (at low-staged operation from Goodman obtains MCFM between 230 and 320). York's SHPs provide the highest MCFMs and power consumption among other makers' models in the same size.

To analyze cooling coil characteristics of SHP systems, three sets of graphical elaborations will be plotted to validate the previously mentioned hypotheses.

4.3.2.1. Fixed DB

From the hypotheses in Chapter 3 of which DB and OAT are fixed at certain temperatures, cooling capacity (CAP) and SHR curves shall move as follows.

(a)Fixed OAT plots

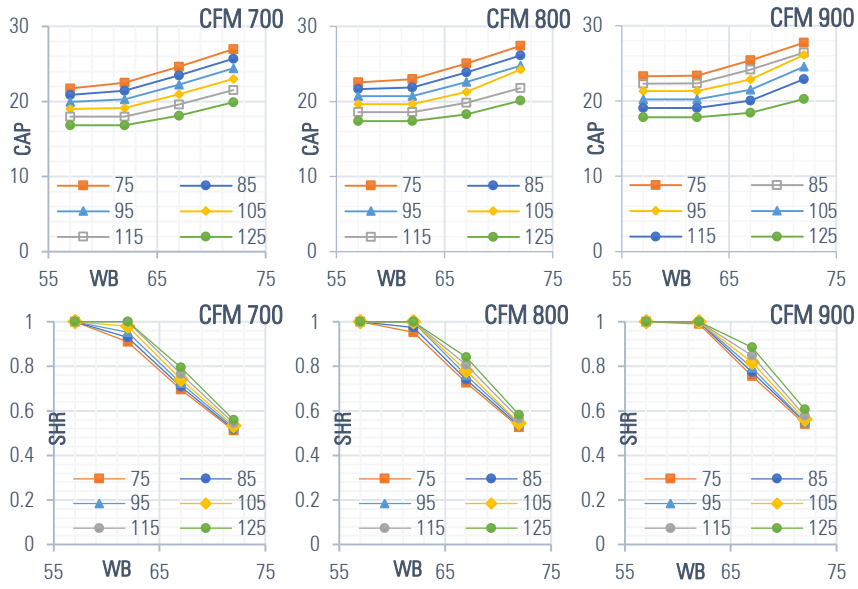

(b)Fixed CFM plots

Figure 4-5 SHR and Cooling performance plots of Carrier 25HBB324

<u>CFM perspective</u>

- From Figure 4-5a, as CFM increases, CAPs increase correspondingly. However, as the OAT increases, the effects of CFM on CAP decreases at higher WB.
- Likewise, increasing CFM causes more bypass air through the coil. Therefore, less moist air is condensed, and thus coil becomes less wet, or drier vice versa.
- Increasing CFM causes higher WB_{crit}, shifting to the right. Considering SHR, from Figure 4-5b, each constant OAT curves from each plot shifts upward. Also, at WB=62°F when CFM = 700, only the condition at which OAT=125°F obtains SHR equals 1. Otherwise, increasing CFM to 900, all conditions become dry at WB=62°F. This means that WB_{crit} increases (or move to the right), as CFM increases.

In conclusion, increasing CFM at any fixed DB and OAT conditions: increases WB_{crit} (move to the right) and increases CAP following the hypothesis as shown in Figure 3-26.

OAT perspective

- As OAT rises, entire CAP lines shifts down. This means that cooling capacity decreases constantly while increasing OAT. From OAT 75°F and OAT 125°F plots, maximum CAP drops from 27 kBtu/h to 20 kBtu, and CAP at dry condition (SHR = 1 see Figure 4-5b) decreases from around 22 kBtu/h to 17 kBtu/h.
- Similarly, WB_{crit} rises according to OAT. On fixed CFM=800 plots (Figure 4-5b) and at WB = 62°F, SHR curve shifts upward constantly while increasing OAT from 75 to 125°F. This means that when WB temperature decreases fixed CFM conditions, coil conditions turn dry faster with higher OAT.

Consequently, cooling capacities have opposite relation with increasing OAT; however, WB_{crit} increases in accordance with OAT as analyzed in Chapter 3 Figure 3-25.

Only Carriers' plots are displayed in this report of hypothesis evaluations. However, all SPHs from other manufacturers provide results correspondingly with previous examining. Additional plots of SPHs according to this implementation are provided in Appendix D.

4.3.2.1. Fixed OAT and CFM

In this section, Goodman's data will be used for hypothesis analysis because it provides data with diverse DB ranges, unlike Carriers' and Yorks' in which only data at DB of 80°F are provided. For this investigation, more impacts on coil's characteristics are presumed, particularly the impacts on sensible cooling or dry coil conditions, since varying

the DB directly affects enthalpy difference. In this case, scaled normalized capacities plots are introduced for better understanding and a prove of scaling ability.

From Goodman reported data in Table 4-2(a), DSZ26024 is selected for hypothesis exploration. Capacity rating for this model is 24 kBtu/h according to ANSI/AHRI 240 standard. NCAPs from Equation (4.2) is obtained to plot normalized capacity curves for comparison and hypothesis examining. Three perspectives of SHR, NCAP and WB_{crit}, will be observed with varying DB from 70 to 85°F on fixed OAT and CFM conditions. Figure 4-6 provides plots for evaluations and comparisons.

SHR

- Apparently, SHRs on constant DB lines shift upward as DB rises from 70 to 85 F for all OAT and CFM conditions. At lowest OAT=65°F and CFM=700 cfm conditions, cooling coil condition remains wet for all DBs ranges, though SHR rises with regard to increasing DB. On the other hand, at OAT=115°F and CFM = 900 cfm, the two-highest DBs conditions (80 and 85°F) obtain dry coil properties after decreasing WB to below 63°F, and at least three of DBs constant lines below WB=57° have dry condition.
- Either raising OAT or CFM causes all-around cooling coil conditions to operate in higher SHR states, thus less moisture removal in the process.
- SHR curves, while increasing WB, move horizontally along with each other, and the lines are linearly stretched with increasing WB. However, the curves' gaps seem smaller at low WB.

NCAP (see Figure 4-6b)

- Unlike SHR lines, NCAP curves are not extensively changed by increasing DB. Nevertheless, at low WB conditions, NCAP lines of each DB conditions are distinct where increasing DB results in increasing NCAP respectively.
- The higher the WB, the higher the NCAP, and the slope of NACPs evidently changed at WB=63°F.
- Unlike increasing CFM or OAT, as aforementioned observation, adjusting CFM and OAT causing deviations of NCAP curves. However, increasing DB in fixed OAT and CFM conditions does not deviate the NCAP lines. Thus, all DB conditions likely to share the same NCAP line. However, the lines in wet conditions slightly vaguely tweaked at higher WB. This refer the impacts of WB on T_{evap} which is subject to WB.
- At very dry conditions (lower WB), the slopes of NCAPs plots are almost zero or horizontal, thereby non or less latent removal.

Wet-bulb Critical (WB_{crit})

Critical WBs move to the right as either CFM or OAT increases. This situation happens regardless of changing in DB. However, at fixed CFM and OAT, DB itself is more powerful dragging WB_{crit}—the higher the DB, the higher the WB_{crit}. Appendix D is provided for additional capacities' plots of split heat pumps system.

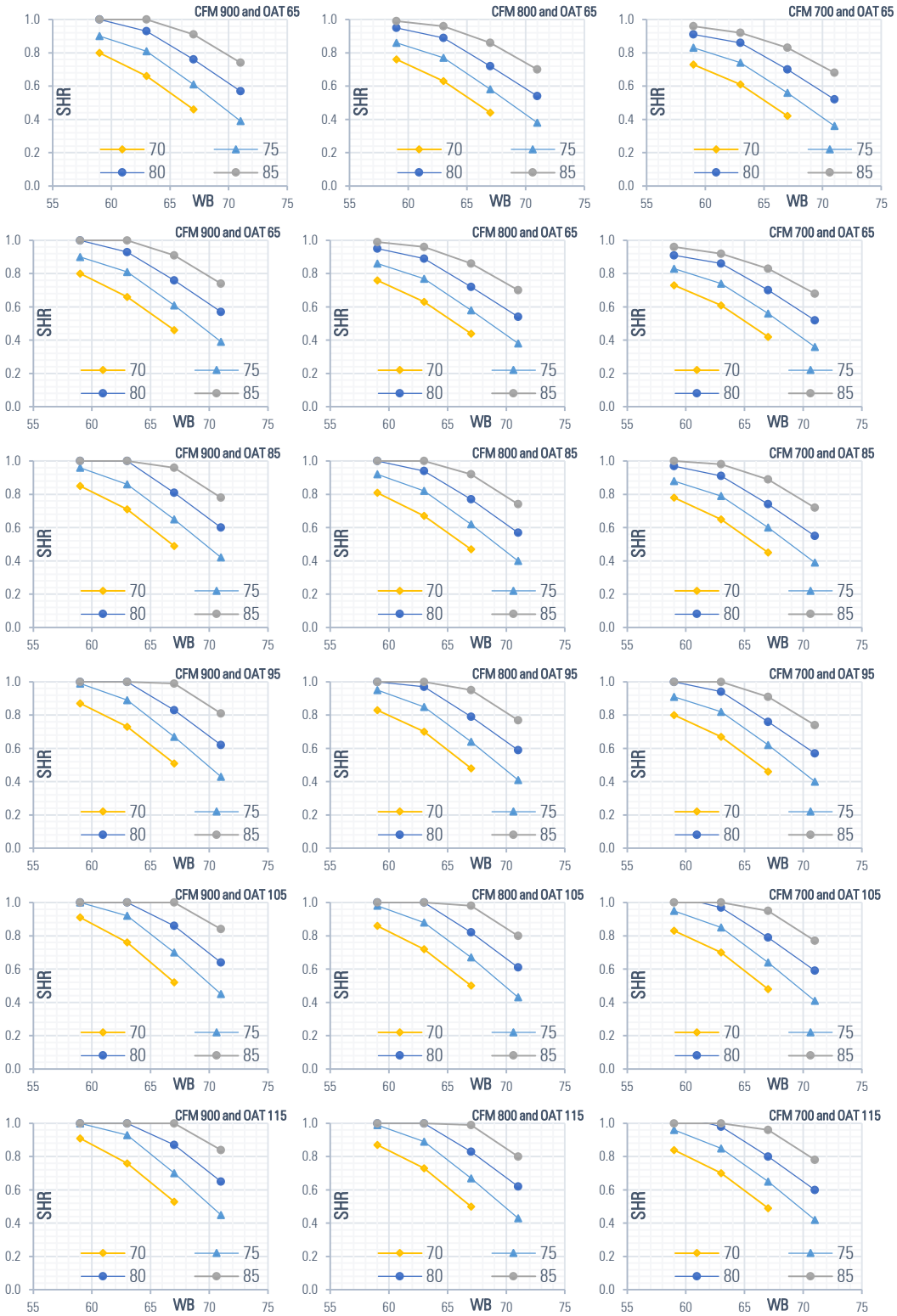

(a)SHR of Fixed OAT and CFM Normalized plots

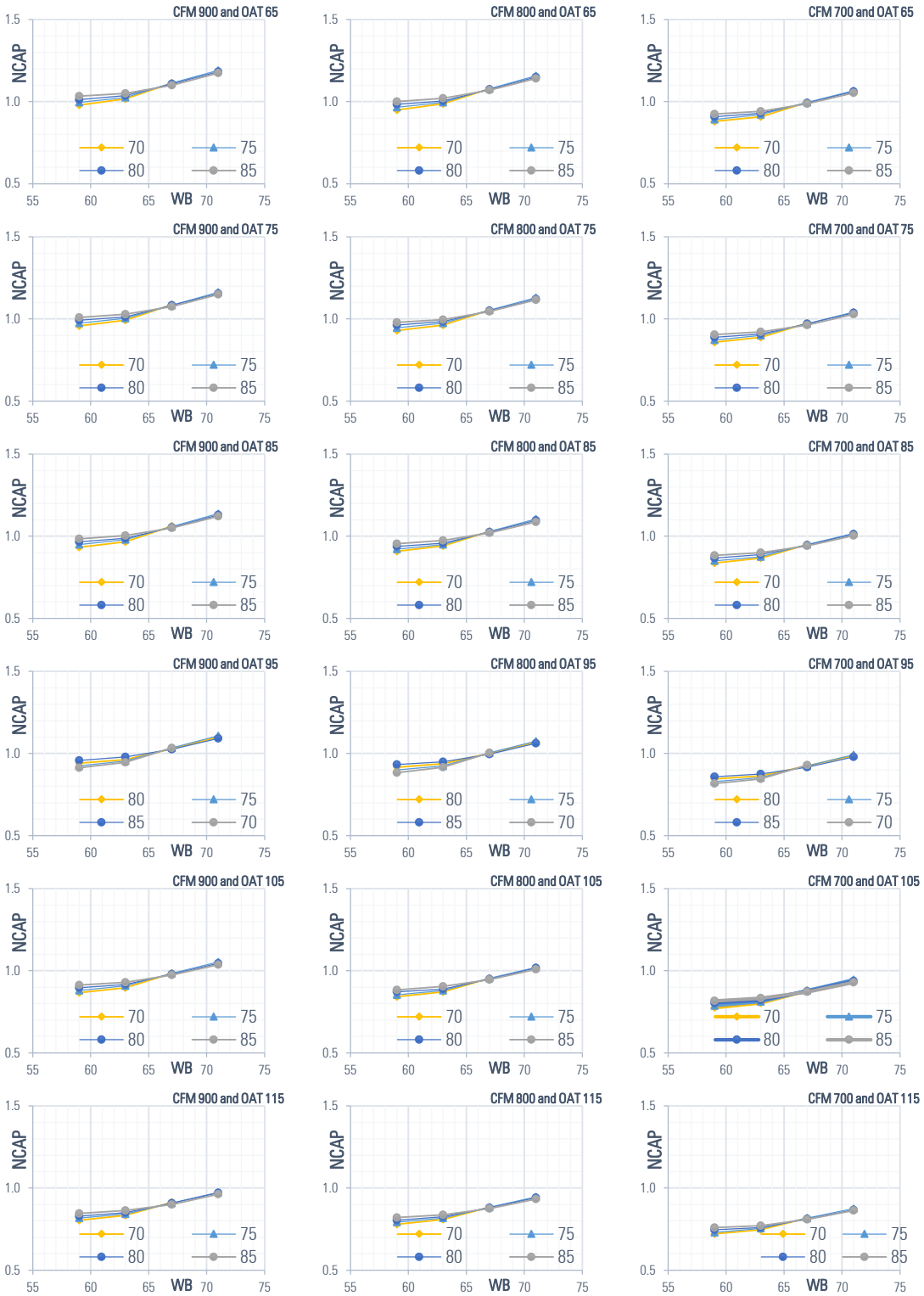

(b)NCAP of Fixed OAT and CFM Normalized plots of Goodman DSZ16024

Figure 4-6 Normalized plots of Goodman DSZ16024

4.3.3. Package units

Unlike split systems, a package unit assemble evaporating coils, expansion devices, condensing coils, fans, and compressors all-inclusively in a single unit which is typically installed outside, or on the roof top of the facility. Nominal tonnages of package units vary from 3 tons up to 20 tons for light to medium commercial applications; nevertheless, typically, the sizes of 3 to 10 tons are applied in residential or light commercial sectors. The performance data is laid out similarly with the Goodman of which additional DB ranges are given. A carrier's RTU model CHP48HE (see Table 4-3) is chosen for the fixed DB analysis since extensive WB points are given in the data (4 points rather than 3 points). Furthermore, Trane data plots of which CFM and OAT are fixed will be scrutinized.

Table 4-3 Manufacturers' reported data for Carrier CHP48HE

Makers	**Units**	**Carrier**			
Package model		**48HE-**			
Rated capacities	**kBtu/h**	**24**	**36**	**48**	**60**
Compressor/refrigerant		Scroll/R22			
CFM	cfm				1500
CFM (Low)	cfm	600	900	1200	1750
CFM (Medium)	**cfm**	**800**	**1200**	**1600**	**2000**
CFM (high)	cfm	1000	1500	2000	2250
Power con*2	kW	1.59	2.56	3.1	4.01
CAP_rated*1	kBtu/h	26	37.7	48.8	62.9
MCFM	cfm/ton	369	378.9	393.4	375

4.3.3.1. Fixed DB

From fixed DB plots two analytical parameters: OAT and CFM impacts on cooling characteristics can be obtained. Table 4-3 shows manufacturer's reported data of 2-5 tons of CHO48HE. The models utilize R-22 as operating refrigerant. Considering OAT effects on CFM plots from Figure 4-8 the intrinsic characteristics of SHR and cooling capacity can be observed.

SHR

- For every condition at WB=57°F, the coil operate in dry condition where SHR = 1 for all given OATs. Then, SHR levels constantly drop after passing WB=63°F for every operating condition since the coil functions in transition states from dry to wet coil.
- The SHR levels are elevated apparently due to increasing OAT.
- Considering SHR levels at WB=63°F, while operating at 1500 cfm, only the condition where OAT equals 125 °F operates with dry coil of which SHR equals 1. However, with increasing CFM from 1500 to 2500 cfm, cooling coil inheres dry conditions for all OAT settings corresponding to SHPs cooling coil properties.
- With higher WB, gaps between each consecutive line are likely to be parallel. Also, increasing WB tends to linearize the SHR curves.

It can be concluded that either increasing CFM or OAT extends the range of dry condition on WB and draws higher WB_{crit} as shown in Figure 4-7. Provided extended lines are drawn from SHR lines, formed by WB=67°F and WB=72°F, to which SHRs are approximately 1, those points are transition or inflection points where coil turns from dry to wet and vice versa. Those points refer to WB_{crit} and they dynamically increase with increasing WB. However, more plots with greater resolutions are required to clarify this problem setting.

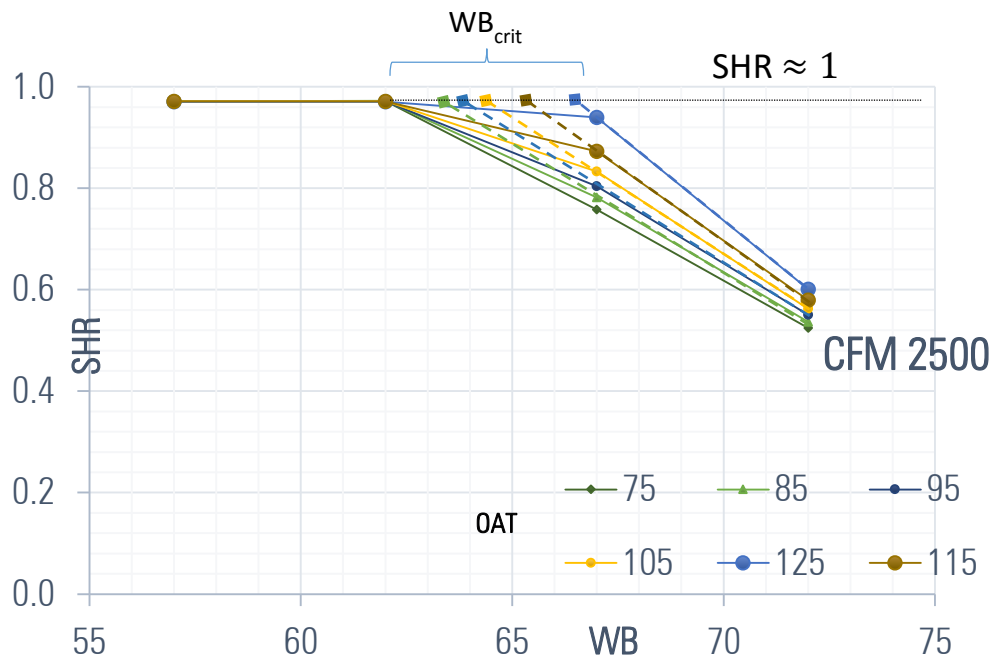

Figure 4-7 The illustration of moving WBcrit correlated with increasing OAT

NCAP

- Figure 4-8, increasing OAT results in lower NCAP for all fixed CFMs since higher OAT leads to increasing T_{evap}, thereby reducing enthalpies differences of air inlet and T_{evap}.
- NCAPs passing the WB=63°F abruptly increase correlated with WB gain, and the curves are straightened as WB increase.
- NCAP lines between 57°F and 63°F WB ranges lay horizontally and in parallel to each other since they are operating in dry condition where cooling capacities remain constant. However, lines are less parallel when CFM degrades because at lower CFM, coils tend to operate in wet condition where moisture removal ability is still active. Therefore, at lower OAT, NCAP lines are not horizontally laid against each other. However, if WB continues to reduce, the coil condition will eventually become dry.

- The gaps of NCAPs operating in dry condition increase accordingly with OAT increase.

In summary, NCAPs decrease with increasing OAT; in contrast, NCAPs rise accordingly with increasing CFM. Furthermore, as the coil turns from dry to wet, NCAPs' slopes instantly increase. Considering the transition points, if straight lines are drawn connecting to NCAP curves with identical slope, those points virtually delineate the dynamic movements of the WB_{crit} points which are corresponding to the hypothesis of normalized cooling coil characteristics as shown in Figure 3-25. However, the relation of WB_{crit} points cannot be defined in this study.

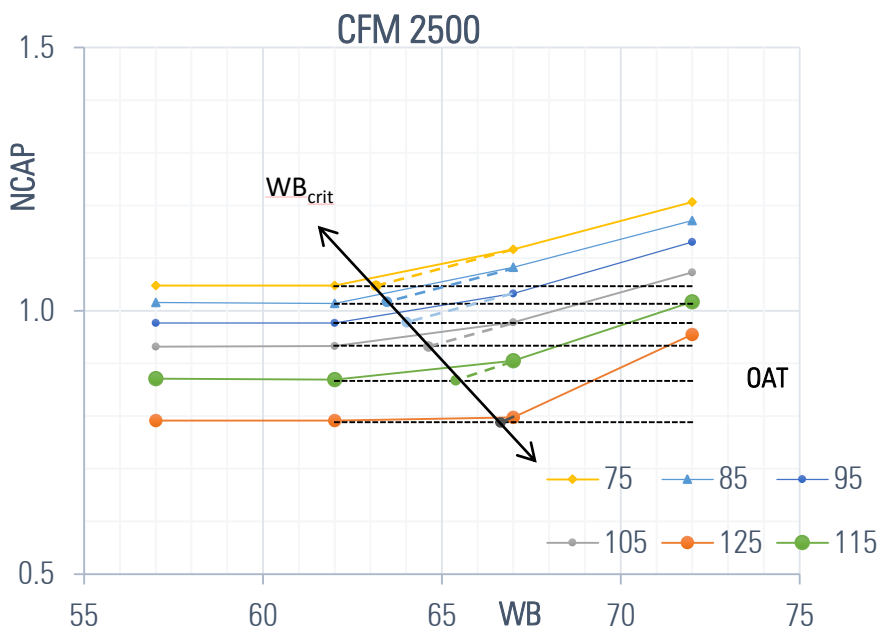

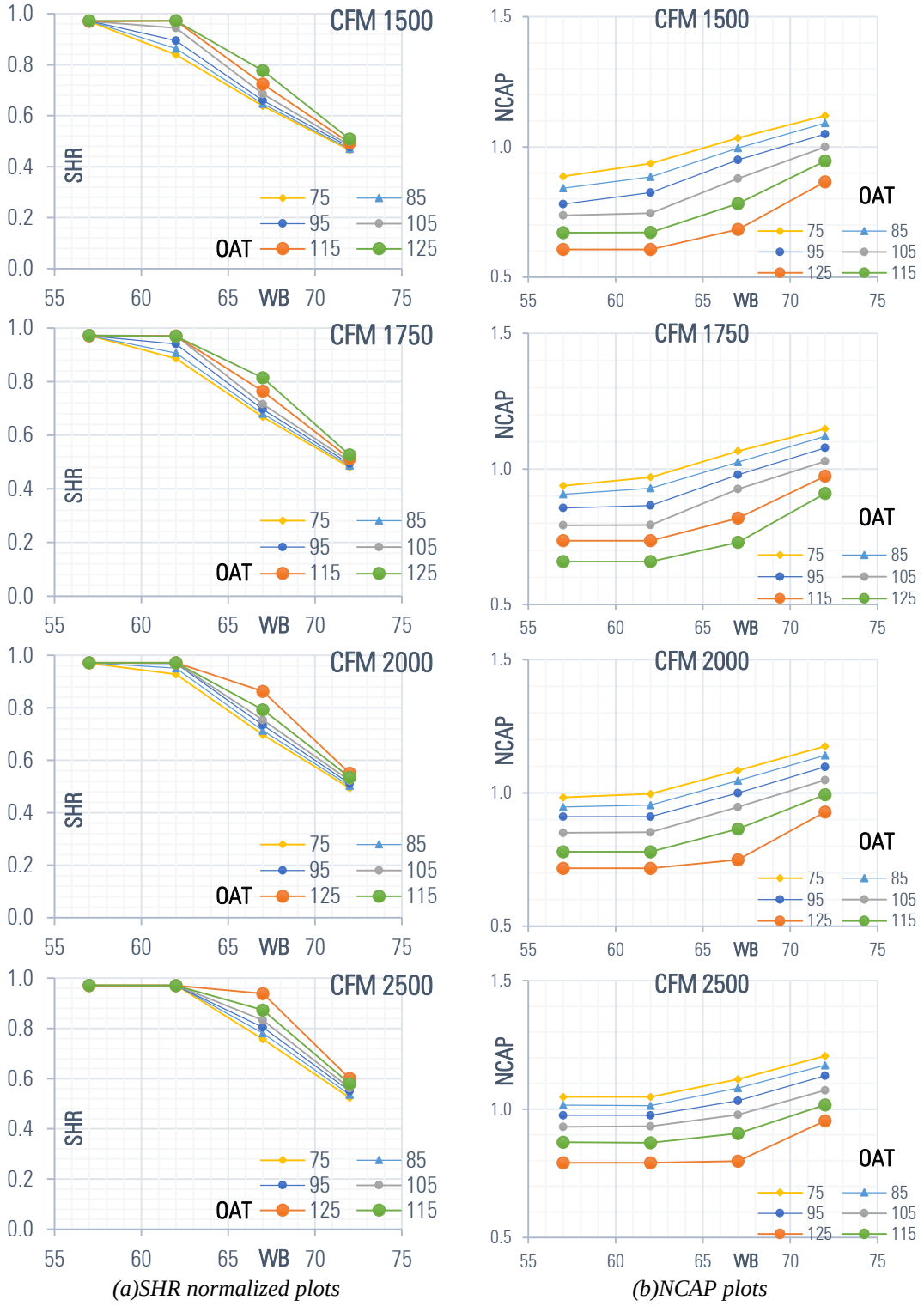

Figure 4-8 SHR and Normalized cooling capacity (NCAP) plots of Carrier CHP48HE060 (5 tons)

The package cooling characteristics of which CFM and OAT are fixed are similar to the SHPs'. Nevertheless, all capacity plots of package units are provided in Appendix E. From observations of cooling performance characteristic from various types of equipment, it can be concluded that inherent characteristics of cooling coil performances exist corresponding to the given hypotheses in Chapter 3. However, more researches are required to explicitly present the relationship of critical points (WB_{crit}) and inputs variables (WB, DB, OAT and CFM). Next, the author will introduce critical point finding methodology based on the analysis cooling coil intrinsic characteristics in Chapter 3.

4.4. Inflection Point Estimation

Inflection points or critical point ($WB_{crit)}$ are points of which coil conditions transform from wet to dry and vice versa. While coils handle dry condition at fixed CFM and OAT, cooling capacities (CAP) are constant, though WB changes. However, dry coil operation is very sensitive to DB temperature. On the other hand, wet coil operations are depending on DB temperature, but vary corresponding to WB states. As such, it is essential to determine inflection points for each operating condition. Nevertheless, critical points are not given in any of manufacturers' data (mostly 3 to 4 points of WBs are displayed). Therefore, critical points must be calculated in relation with existing points. This study points estimator by using slope creating from given points.

4.4.1. Local Points Estimator

The methodology of local point estimate is based on normalized plots and graphical analysis. Figure 4-7 demonstrates that critical points of each condition can be estimated by extending SHR lines on the same slope created by given points from manufacturing data.

Firstly, assumptions must be made in order to define slopes and lines: (1) Assume the points approaching transition conditions have linear relations; and (2) transition conditions from wet to dry occur at SHR approaching 1. RTU data in Appendix G will be used as a calculation example. From the given data in Appendix E. OAT, CFM, WB, CAP and sensible CAP are provided. The calculation process are as follows:

1. Find rated condition associated with ANSI/AHRI 240 to obtain rated cooling capacity CAP_{rated}, which is 210 kBtu/h
2. Select an interested condition, then determine wet points. If there are more than 3 points, apply the condition parameters in Figure 4-9b, else in Figure 4-10b
3. Calculate an initial slope formed by existing wet points of the selected data.
4. Initially guess WB_{crit} which should be lower than the minimum wet points of given data. Then initial optimized slope that includes the guess WB_{crit} value.
5. Utilize excel optimize function to find maximum WB_{crit} which simultaneously maximize R-square value.
6. Plot the result on the normalized cooling capacity plot.

Figure 4-8 shows the calculation example of selected data at a condition of which CFM, DB and OAT are 360, 75, and 85, respectively.

OAT		**85**	**85**	**85**	**85**	**85**	**85**
CFM	**DB**	**61**	**61**	**67**	**67**	**73**	**73**
x100	**F**	**CAP**	**SHC**	**CAP**	**CAP**	**MBH**	**CAP**
63	75	195	171	213	127	224	83

(a)Given capacities of selected condition.

	CFM	DB	OAT	WB	CAP	SHC	NCFM	SHR	NCAP
Guess Val.	6300	75	85	57.87	187	187	360	1	0.89
	6300	75	85	61	195	171	360	0.88	0.93
	6300	75	85	67	213	127	360	0.60	1.01
	6300	75	85	73	224	83	360	0.37	1.07
Critical pt.	6300	75	85	57.87	187	187	360	1	0.89

	NCAP			SHR			Objective
Cond.	m	c	r^2	m	c	r^2	
initial cod	0.012	0.227	0.981	-0.042	3.451	0.981	
Opt cond	0.012	0.206	0.990	-0.042	3.451	0.998	0.998
rel_dev	2.5%	9.1%	0.9%	0.0%	0.0%	1.7%	

(b)Guess values and slope calculation table of local points optimization.

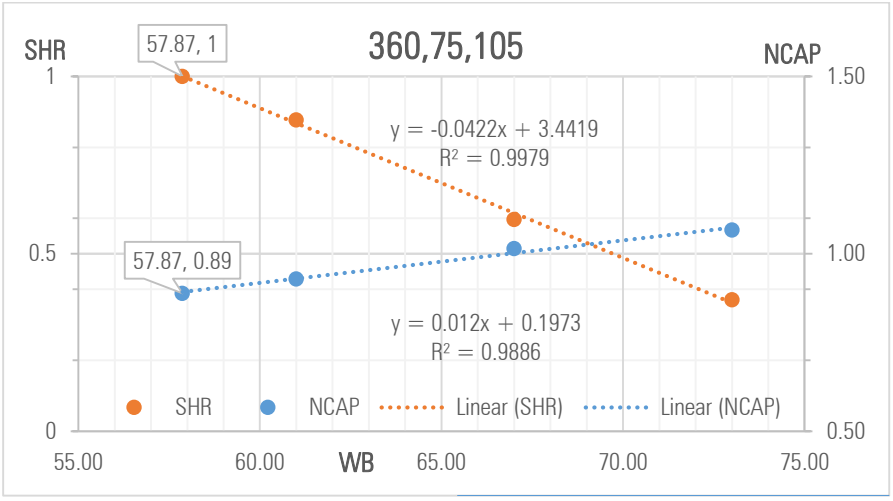

(c)Illustration of critical point finding based on local point optimization.

Figure 4-9 3-local-point estimating method for optimization of maximized R-square value at 85 F of OAT where CFM, DB and OAT are 360, 75, and 85, respectively.

Figure 4-8a is the selected capacities data of the given model. Following Figure 4-8b is the calculation table where NCAPs are calculated by Equation (4.2) with rated capacity of 210 kBtu/h and the last Figure 4-8c is an illustration of critical points calculation where the estimated critical point is at WB_{crit} = 57.87°F.

OAT		**85**	**85**	**85**	**85**	**85**	**85**
CFM	**DB**	**61**	**61**	**67**	**67**	**73**	**73**
x100	**F**	**CAP**	**SHC**	**CAP**	**CAP**	**MBH**	**CAP**
63	80	200	200	214	157	226	114

(a)Given capacities of selected condition.

Cond	CFM	DB	OAT	WB	CAP	SHC	NCFM	SHR	NCAP
	6300	80	85	61	200	200	360	1.00	0.95
Guess	6300	80	85	61.00	200	200	360	1.00	0.95
	6300	80	85	67	214	157	360	0.73	1.02
	6300	80	85	73	226	114	360	0.50	1.08
Crit	6300	80	85	61.00	200	200	360	1	0.95

	NCAP			SHR			Objective
Cond.	m	c	r^2	m	c	r^2	
initial cod.	0.010	0.381	0.998	-0.038	3.293		
Opt cond	0.010	0.323	0.998	-0.041	9.838	0.998	0.998
rel_dev							

(b)Guess values and slope calculation table of local points optimization.

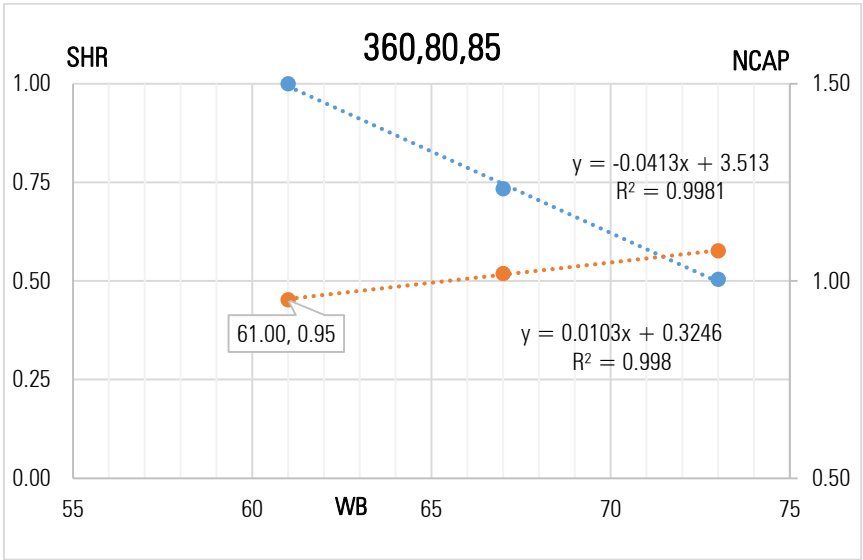

(c)Illustration of critical point finding based on local point optimization.

Figure 4-10 2-local-point estimating method for optimization of maximized R-square value at 85 F of OAT where CFM, DB and OAT are 360, 80, and 85, respectively.

Figure 4-10a is the selected capacities data of the given model. Following Figure 4-10b is the calculation table where NCAPs are calculated by Equation (4.2) with rated capacity of 210 kBtu/h and the last Figure 4-10c is an illustration of critical points calculation where only 2 wet conditions are available. In addition, the estimated critical point is WB_{crit} = 61°F.

This method assumes that cooling capacities have linear relation near transition points. The results of each sample condition are 57.87 and 61°F of WB. To understand the

dynamic of critical points for all conditions of given manufacturing data, inflection points for all condition will be performed. Appendix E provides complete critical points calculation. Also, Table 4-4 shows all critical points for the selected data. The shaded area are the conditions that point estimator method could be utilized since only 1 we point is given in each shaded condition which is not adequate to form virtual slopes. In addition, Table 4-4 shows all critical points for the selected data of various dry-bulb temperature conditions (75, 80 and 85 F).

Table 4-4 Critical points of given manufacturing data

	OAT	**85**	**85**	**95**	**95**	**105**	**105**	**115**	**115**
NCFM	DB	WB_{crit}	NCAP	WB_{crit}	NCAP	WB_{crit} pt.	NCAP	WB_{crit}	NCAP
360	75	57.67	0.89	58.55	0.82	59.40	0.77	60.25	0.72
360	80	61.00	0.95	61.01	0.91	62.06	0.86	62.88	0.80
360	85	63.86	1.00	64.82	0.97	65.65	0.93	66.48	0.88
360	90	66.70	1.04						
400	75	58.71	0.92	59.53	0.87	60.20	0.81	61.00	0.76
400	80	61.07	0.98	62.09	0.94	63.03	0.90	63.88	0.84
400	85	64.67	1.03	65.54	1.00	63.88	0.96		
400	90								
440	75	59.46	0.95	60.35	0.90	61.00	0.85	61.00	0.79
440	80	61.66	1.00	62.92	0.97	63.81	0.92	64.71	0.87
440	85	65.17	1.05	66.18	1.02				
440	90								
480	75	60.00	0.97	61.00	0.93	61.00	0.87	61.43	0.81
480	80	62.20	1.02	63.64	0.99	64.57	0.95	65.42	0.90
480	85	65.72	1.06	66.75	1.03				
480	90								

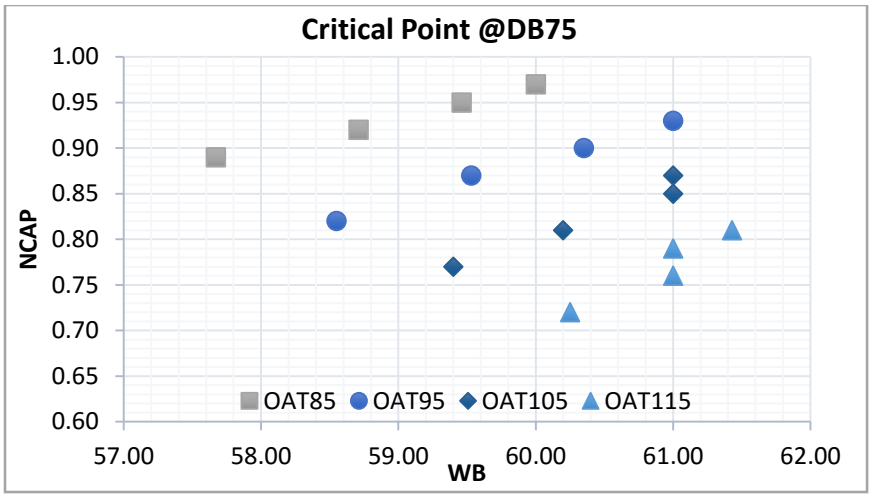

(a)

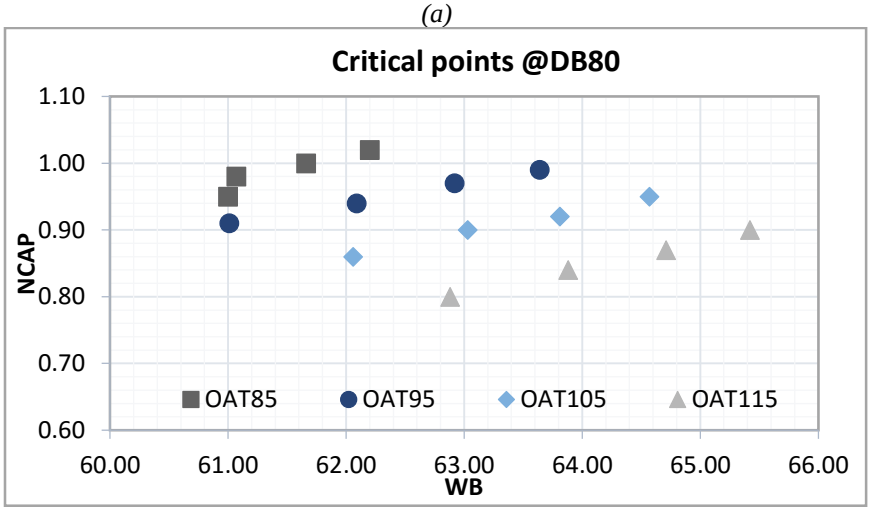

(b)

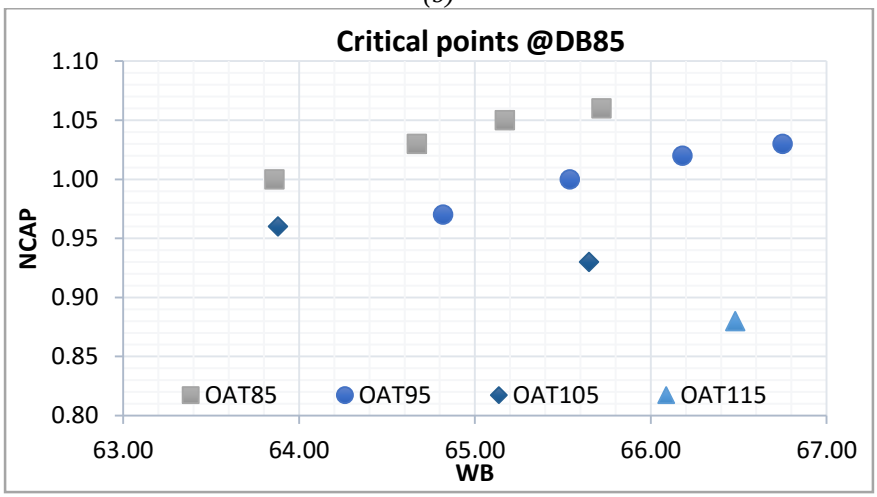

(c)

Figure 4-11 Critical Points at (a) 75, (b)80 and (c)85 °F of dry-bulb temperature

As previously mentioned in Chapter 3, critical points on NCAPs move downward to the right when OAT increases, which inflection points lay on WB and NCAP plots according

to the hypothesis (see Figure 3-25). However, the estimated critical points in higher OAT conditions have undefined relation. This is because of the local point estimator accounts for only single condition regardless of effects and correlation to other points. Therefore, next section will provide the study of global estimation of all point in the selected manufacturer's data.

4.4.2. Global Estimator

The global point estimator calculates critical points based on the similar format as of the local estimator. However, more conditioned relations are introduced to avoid data overlapping. In this section, the data from carrier (25HBB18) is used for calculation example; CAP_{rated} of this model is 17.4 kBtu/h at 675 CFM. The conditioned relations are determined as follows:

1. Inflection points (WB_{crit}) at lower OAT are always less than that of the higher OAT.
2. WB_{crit} at higher CFM always more than that of the lower CFM in similar OAT conditions.
3. SHR slopes in wet condition where SHR<1 decrease while increasing CFM and OAT.

After all conditioned relations are defined, then apply the optimization tool Excel to optimize the product of R-square values for all conditions provided in manufacturer's data. The results of this method are illustrated in Figure 4-12. The calculation materials are given in Appendix F.

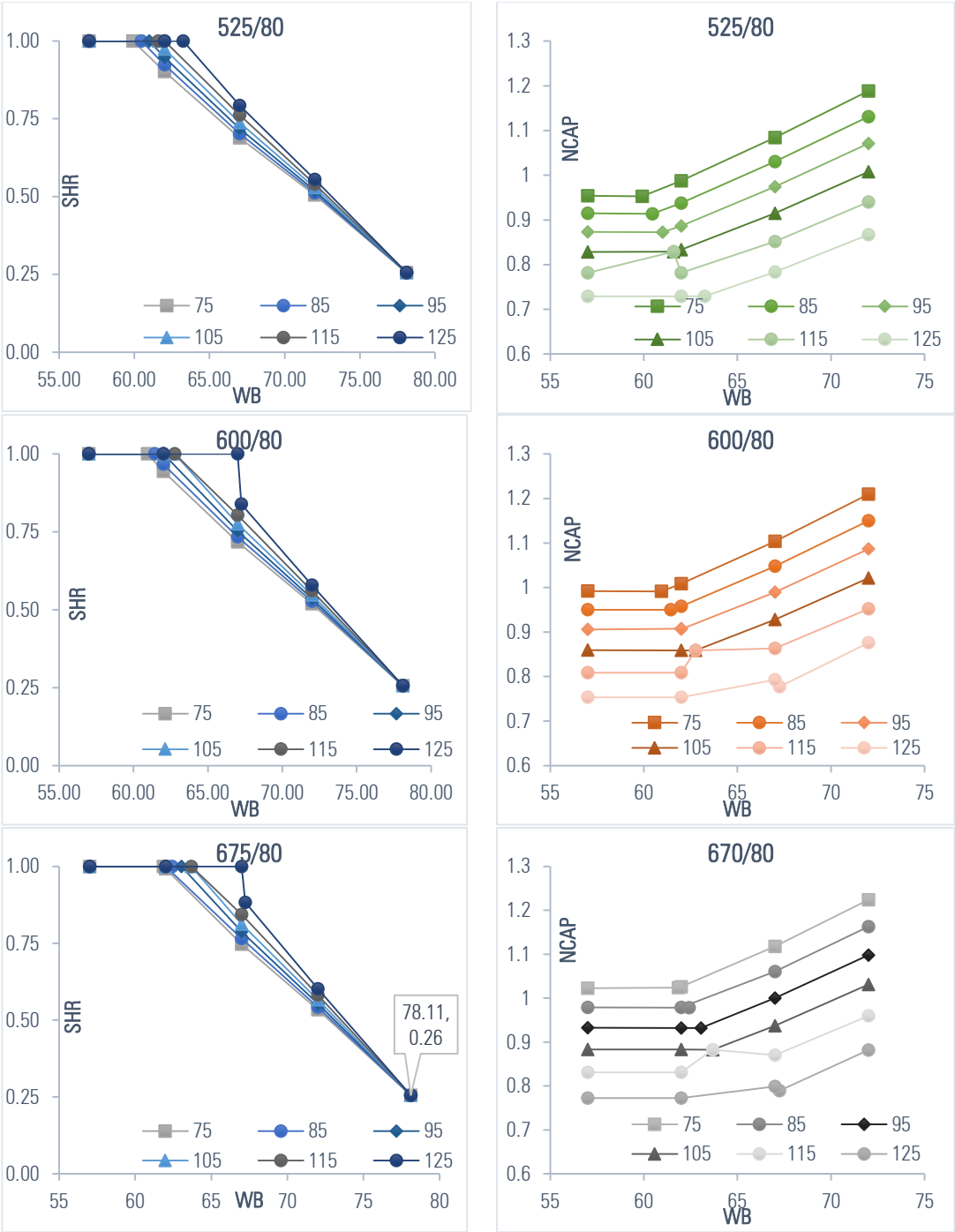

(a)SHR of 25HBB18 with critical points *(b)NCAP of 25HBB18 with critical points*

Figure 4-12 Normalized plots with critical WB of 255HBB18 calculated by using global point-optimization.

As shown in Figure 4-12, considering NCAP plots, critical points move downward to the right with increasing WB_{crit} as OAT rises. Nevertheless, there are several points at

OAT over 115°F. The calculation points distance from their trend lines and overlap other conditions. This means that, at higher OAT conditions, linear relations are not applicable.

CHAPTER 5. SUMMARIES, CONCLUSIONS AND RECOMMENDATIONS

5.1. Summaries and conclusions

DX cooling coil performance analysis is extensively studied by many researchers since DX cooling equipment accounts for many components which operate in different ways and generate different impacts on cooling performance. Yang, et al., 2013 proposed a cooling coil format of which wet and dry conditions are distinguished by using cooling coil characteristics, and calculated differently according to their operating behaviors. In addition, Henderson, 2005 proposed coil moisture removal behavior associated with fan operating modes and compressor runtimes which results in predictable SHR characteristics. Those studies initiate ideas of intrinsic characteristics of cooling coils for further development in two aspects: cooling capacity calculation models and systematic temperature and humidity level control in relation with required cooling loads in conditioned spaces. The investigation of inherent DX-cooling coil characteristics and its normalizing and scaling ability are the main objectives of this research. To achieve those objectives, three analytical tools are utilized:

- Moist air characteristics in cooling mode operation on the psychrometric chart: to elaborate moist air behavior during cooling operation, and to illustrate the impact of input variables on cooling performance.
- Normalized capacity plots: to illustrate that wet- and dry- coil operating conditions provide distinct performance characteristics, and to delineate normalization and performance scalability of DX cooling coils.

- Manufacturer's data and performance plots: to understand the essence of manufacturing data and how to handle diverse data disciplines, and to empirically and graphically validate purposed hypotheses of cooling characteristics.

Drawing attention to investigation of GRDB application of mini-split systems with variable speed compressors, GRDB methods purpose the practice of cooling capacity in relation to SHR degradation by investigating manufacturer's data of packaged unit air-conditioning systems and apply multiple-linear regression using performance data to predict cooling capacity. Characteristics of cooling coils have been exposed while investigating massive manufacturer's data. Extensively, manufacturer's data provide generic, easy-to-understand yet accurate performance data which lessen the effort and time to train data.

In order to develop cooling coil models, inherent characteristics are required to be mastered. Better understanding in its intrinsic properties of DX cooling coil will lead to research and application benefits. Through the investigation, the following can be concluded:

- Air-side cooling performance can be drawn and explained on the psychrometric chart only with air-side variable inputs, and evaporating temperature can represent refrigeration cycle and outdoor air temperature impacts on cooling coils.
- Temperature parameters of WB, OAT, DB and T_{evap} determine cooling load removal ability of the equipment and CFM extends the cooling capacity regarding the size of equipment and cooling load demand which can be displayed as normalized or CFM/ton.

- The effects of varying outdoor air condition (OAT) and air flow rate (CFM) on cooling coil operating characteristic are predictable.
- Cooling performance and air flowrate could be scaled in regard to manufacturer rated conditions under a similar set of compressors and expansion devices. The arrangement of findings is described in each chapter.

Chapter 3 describes the ideas of analyzing DX cooling performance characteristics by: (1) Analyzing and defining input and output independent- and dependent- variables based on GRDB methods, fundamentals of refrigerant cycles and moist-air properties; (2) elaborating cooling process practices on the psychrometric chart and mathematically formulating air-side cooling performance characteristic equations, and verifying the formulas with EES; (3) introducing normalized plots of SHR and normalized cooling capacity and determining cooling characteristic hypotheses based on previous analyses.

Chapter 4 demonstrates implementations, validations and applications of the aforementioned hypotheses by combining findings with manufacturers' data of various air conditioning systems: mini-split heat pumps, split heat pumps and packaged systems. By plotting an immense amount of data and comparing hypotheses, coil characteristics of actual manufacturer's empirical data and purposed hypotheses are correlated. Furthermore, critical point estimating methods are used to find the inflection point of wet-bulb temperature where cooling coil process turns from wet to dry and dry to wet.

In conclusion, the compilation through this research shows that: (1) the hypotheses could capture the effects of air-side variables on DX cooling coils (DCC); (2) the hypotheses expose the actual characteristics of DCC which can be elaborated on proposed normalized plots as shown in Figure 3-27; (3) the research shows that cooling capacities

can be scaled; and (4) the thesis shows that air-side variables can represent DCC inherent characteristics. In addition, the compilation of this research provides the following contributions: (1) Generic inherent characteristics of all DX cooling coils have been devised and (2) the normalizing and scaling ability of cooling coil performance have been developed.

5.2. Recommendations and future works

The contributions and compilations throughout this research could be extended to these future works and applications:

- Equipment performance improvement: in order to improve efficiency of equipment, characteristics of cooling load and equipment itself must be mastered since cooling load not only accounts for sensible cooling but also humidity levels. By knowing the equipment characteristics, humidity control could be effectively manipulated by varying independent variables to obtain proper SHR values. Most cooling equipment only maintain qualifying dry-bulb temperatures, but not humidity level. However, tropical areas typically demand more moisture removal than sensible cooling. If those aspects are desired, potential to maintain temperature humidity level within a comfort zone without sacrificing extra energy could be achieved.
- Application extension:
    - The hypotheses could be applied to other air-cooled systems with cooling coils having other refrigerant substances, in particular water.

  - Proven scaling ability could reduce modelling and computational processes by using rating condition performance to refer to other condition performances within the same equipment.

- Implementation on virtual sensing application: virtual sensors are indirect measuring sensors of which utilize sensing outputs from other sensors processed through certain methods to acquire certain values. In this study, cooling capacities can be calculated based on temperature and air flow rate sensors which are inexpensive and easy to install. However, more studies are required to extensively utilize it as a virtual sensor.
- More studies of inflection point estimators are required to accurately obtain critical condition of cooling coil processes in a certain condition.

LIST OF REFERENCES

AHRI. (2016). Unitary Small Equipment. Retrieved November 15, 2016, from http://www.ahrinet.org/About-Us/Product-Sections/Unitary-Small-Equipment.aspx

ANSI/AHRI. (2012). Standard, Performance Rating of Unitary Air-Conditioning & Air-Source Heat Pump Equipment. *ANSI/AHRI Standard 210/240*. Arlington: Air-Conditioning, Heating and Refrigeration Institute.

ANSI/AHRI Standard 540-2015. (2015). Standard For Performance Rating Of Positive Displacement Refrigerant Compressors And Compressor Units, 1–19.

Aynur, T. N. (2010). Variable refrigerant flow systems: A review. *Energy and Buildings*, *42*(7), 1106–1112. https://doi.org/10.1016/j.enbuild.2010.01.024

Breuker, M. S., & Braun, J. E. (1998). Common faults and their impacts for rooftop air conditioners. *ASHRAE Transactions*, *105*(February). https://doi.org/10.1080/10789669.1998.10391406

Chen, B., & Braun, J. E. (2000). Simple Rule-Baes Methods for Fault Detection and Diagnostics Applies to Packaged Air Conditioners. *ASHRAE Transactions*, *107*(1), 1–10.

Cheung, H., & Braun, J. E. (2014). Purdue e-Pubs Virtual Power Consumption and Cooling Capacity Virtual Sensors for Rooftop Units Virtual Power Consumption and Cooling Capacity Virtual Sensors for Rooftop Units. Retrieved from http://docs.lib.purdue.edu/iracc%5Cnhttp://docs.lib.purdue.edu/iracc/1535

Cho, J. M., Heo, J., Payne, W. V., & Domanski, P. A. (2014). Normalized performance parameters for a residential heat pump in the cooling mode with single faults imposed. *Applied Thermal Engineering*, *67*(1–2), 1–15. https://doi.org/10.1016/j.applthermaleng.2014.03.010

DOE. (2014). Energy Saver 101 Infographic: Home Cooling. Retrieved November 15, 2016, from http://www.energy.gov/articles/energy-saver-101-infographic-home-cooling

Goetzler, W. (2007). Variable refrigerant flow systems. *Digital Scroll Technology · 2nd Generation*, (April). https://doi.org/10.1016/j.enbuild.2010.01.024

Henderson, H. I. (2005). *Understanding Dehumidification Performance at Part Load in Commercial Applications*. Cazenovia.

Hlavinka, A. N., Mjelde, J. W., Dharmasena, S., & Holland, C. (2016). Forecasting the adoption of residential ductless heat pumps. *Energy Economics*, *54*, 60–67. https://doi.org/10.1016/j.eneco.2015.11.020

Hong, T., Sun, K., Zhang, R., Hinokuma, R., Kasahara, S., & Yura, Y. (2016). Development and validation of a new variable refrigerant flow system model in EnergyPlus. *Energy and Buildings*, *117*(February), 399–411. https://doi.org/10.1016/j.enbuild.2015.09.023

HVAC Equipment. (2015). Retrieved November 16, 2016, from http://www.freedoniagroup.com/industry-study/3261/hvac-equipment.htm

Katipamula, S., & Brambley, M. (2005). Review Article: Methods for Fault Detection, Diagnostics, and Prognostics for Building Systems—A Review, Part I. *HVAC&R Research*, *11*(1), 3–25. https://doi.org/10.1080/10789669.2005.10391123

Kim, M., Payne, W., Domanski, P., Yoon, S., & Hermes, C. (2009). Performance of a residential heat pump operating in the cooling mode with single faults imposed. *Applied Thermal Engineering*, *29*(4), 770–778. https://doi.org/10.1016/j.applthermaleng.2008.04.009

Kim, W. (2013). Fault Detection And Diagnosis For Air Conditioners And Heat Pumps Based On Virtual Sensors.

Kim, W., & Braun, J. E. (2008). Performance evaluation of a virtual refrigerant charge sensor. *International Journal of Refrigeration*, *36*(3), 1130–1141. https://doi.org/10.1016/j.ijrefrig.2012.11.004

Li, H., & Braun, J. (2007). A Methodology for Diagnosing Multiple Simultaneous Faults in Vapor-Compression Air Conditioners. *HVAC&R Research*, *13*(2), 369–395. https://doi.org/10.1080/10789669.2007.10390959

Li, H., & Braun, J. (2009). Virtual Refrigerant Pressure Sensors for Use in Monitoring and Fault Diagnosis of Vapor-Compression Equipment. *HVAC&R Research*, *15*(3), 597–616. https://doi.org/10.1080/10789669.2009.10390853

Li, H., & Braun, J. E. (2007). Decoupling features and virtual sensors for diagnosis of faults in vapor compression air conditioners. *International Journal of Refrigeration*, *30*(3), 546–564. https://doi.org/10.1016/j.ijrefrig.2006.07.024

Li, H., & Braun, J. E. (2007). Economic evaluation of benefits associated with automated

fault detection and diagnosis in rooftop air conditioners. *ASHRAE Transactions*, *113 PART 2*(2005), 200–210.

Li, H., Yu, D., & Braun, J. E. (2011). A review of virtual sensing technology and application in building systems. *HVAC&R Research*, *9669*(November 2014), 37–41. https://doi.org/10.1080/10789669.2011.573051

Li, Z., Chen, W., Deng, S., & Lin, Z. (2006). The characteristics of space cooling load and indoor humidity control for residences in the subtropics. *Building and Environment*, *41*(9), 1137–1147. https://doi.org/10.1016/j.buildenv.2005.05.016

Li, Z., & Deng, S. (2007). A DDC-based capacity controller of a direct expansion (DX) air conditioning (A/C) unit for simultaneous indoor air temperature and humidity control - Part II: Further development of the controller to improve control sensitivity. *International Journal of Refrigeration*, *30*(1), 124–133. https://doi.org/10.1016/j.ijrefrig.2006.06.003

NAHB. (2008). *Ductless Heat Pump Market Research and Analysis*. Upper Marlboro.

RECS. (2011). Air conditioning in nearly 100 million U.S. homes. Retrieved November 10, 2016, from http://www.eia.gov/consumption/residential/reports/2009/air-conditioning.php?src=‹ Consumption Residential Energy Consumption Survey (RECS)-f5.

RECS. (2012). RECS data show decreased energy consumption per household. Retrieved November 15, 2016, from http://www.eia.gov/consumption/residential/reports/2009/consumption-down.php?src=‹ Consumption Residential Energy Consumption Survey (RECS

RECS. (2013). State fact sheets on household energy use. Retrieved November 15, 2016, from https://www.eia.gov/consumption/residential/reports/2009/state_briefs/

Rossi, T. M., & Braun, J. E. (1997). A Statistical , Rule-Based Fault Detection and Diagnostic Method for Vapor Compression Air Conditioners A Statistical , Rule-Based Fault Detection and Diagnostic Method for Vapor Compression Air Conditioners. *HVAC and R Research*, *3*(1), 19–37. https://doi.org/10.1080/10789669.1997.10391359

Storm, P., & Baylon, D. (2012). Integrated Ductless Heat Pump Analysis: Developing an Emerging Technology into a Regional Efficiency Resource. *ACEEE Summer Study*

on Energy Efficiency in Buildings, (2), 294–305.

Wichman, A., & Braun, J. E. (2009). A Smart Mixed-Air Temperature Sensor. *HVAC&R Research*, *15*(1), 101–116. https://doi.org/10.1080/10789669.2009.10390827

Winkler, J. (2011). *Laboratory Test Report for Fujitsu 12RLS and Mitsubishi FE12NA Mini-Split Heat Pumps*.

Woradechjumroen, D., Li, H., & Promwattanapakdee, T. (2015). Smart Building Solutions for Investigating Humidity Impact in Supermarkets ETM007, (December), 3–8.

Woradechjumroen, D., Yu, Y., Li, H., Yu, D., & Yang, H. (2014). Analysis of HVAC system oversizing in commercial buildings through field measurements. *Energy and Buildings*, *69*, 131–143. https://doi.org/10.1016/j.enbuild.2013.10.015

Xu, X., Xia, L., Chan, M., & Deng, S. (2010). Inherent correlation between the total output cooling capacity and equipment sensible heat ratio of a direct expansion air conditioning system under variable-speed operation (XXG SMD SHR DX AC unit). *Applied Thermal Engineering*, *30*(13), 1601–1607. https://doi.org/10.1016/j.applthermaleng.2010.03.016

Yang, H., & Li, H. (2011). A Generic Rating-Data-Based (GRDB)DX Coils Modeling Method. *HVAC&R Research*, (MAY 2010), 0–22. https://doi.org/10.1080/10789669.2010.10390908

Yu, D., Li, H., & Yang, M. (2011). A virtual supply airflow rate meter for rooftop air-conditioning units. *Building and Environment*, *46*(6), 1292–1302. https://doi.org/10.1016/j.buildenv.2010.12.017

Yu, Y., Woradechjumroen, D., & Yu, D. (2014). A review of fault detection and diagnosis methodologies on air-handling units. *Energy and Buildings*, *82*, 550–562. https://doi.org/10.1016/j.enbuild.2014.06.042

Yuill, D. P., & Braun, J. E. (2013). Evaluating the performance of fault detection and diagnostics protocols applied to air-cooled unitary air-conditioning equipment. *HVAC&R Research*, *19*(7), 882–891. https://doi.org/10.1080/10789669.2013.808135

APPENDIX A LABORATORY TESTING DATA FOR GRDB

Table A-1 Trained data of MSHPs MUZ-FR12NA with fixed DB at 80°F

	TPC	CFM	SHR	OAT	T_evap	T_oe	DB_aie	DP_aie	T_aoe	DP_aoe	WB_aie	CAP
Indoor Coil	Outdoor unit	Indoor coil	Sensible	Outdoor unit	Indoor coil	Indoor coil	Indoor coil	Indoor coil	Indoor coil	Indoor coil	Indoor coil	Indoor coil
Fan	Total	Air volum.	Heat	Inlet air	Inlet	Outlet	Inlet air	Inlet air	Outlet air	Outlet air	inlet ait	Air-side
Mode	Power	Flow rate	Ratio	Temp.	Temp.	Temp.	Temp.	Dew Point	Temp.	Dew Point	wet bulb	Cooling
Unit	[W]	[cfm]		[F]	[F]	[F]	[F]	[F]	[F]	[F]	[F]	[BTU/h]
High	1032	326.1	0.784	86.34	53.56	42.47	79.25	55.13	52.14	49.80	64.00	12,641.98
High	1071	331.8	0.783	89.74	54.90	43.71	79.54	55.71	53.01	50.56	64.39	12,369.01
High	1330	339.9	0.831	110.84	61.21	48.22	80.37	57.20	55.99	53.71	65.44	10,816.49
High	689	339.9	0.762	73.62	49.13	54.95	80.38	56.70	53.02	50.86	65.19	13,051.44
High	785	342.2	0.510	83.50	51.33	60.48	80.87	69.19	62.91	61.02	72.44	12,628.34
High	787	337.1	0.794	81.66	48.19	54.28	79.75	56.37	53.60	51.80	64.80	11,884.49
High	755	342.0	0.851	81.61	43.06	51.13	80.26	52.90	54.18	49.50	63.27	11,051.93
High	890	341.6	0.502	93.99	62.11	60.08	80.42	69.10	61.27	59.92	72.23	13,716.81
High	828	327.4	0.829	86.25	55.11	46.24	79.30	55.15	53.85	51.53	64.03	11,198.65
High	795	342.0	0.857	85.68	49.16	53.91	80.08	52.59	51.60	49.03	63.06	12,010.74
High	955	314.4	0.528	94.80	61.29	52.99	78.82	66.79	60.24	58.41	70.29	12,543.03
High	814	340.7	0.848	87.87	50.77	53.40	80.40	52.93	51.53	49.06	63.34	12,317.83
High	905	337.1	0.808	95.50	55.36	46.85	79.72	56.21	53.47	52.03	64.71	11,686.59
High	879	341.8	0.866	94.46	53.44	45.44	80.15	52.75	51.46	49.43	63.16	11,983.44
High	1081	340.5	0.887	110.84	62.20	51.30	80.37	57.24	57.67	55.18	65.46	9,407.27
High	639	337.3	0.789	65.82	38.03	50.05	79.74	56.41	56.12	52.20	64.82	10,761.89
High	686	338.0	0.530	74.28	38.30	60.01	80.64	68.32	65.86	62.13	71.83	10,014.64
Mid	540	208.2	0.705	81.63	51.03	45.62	80.94	57.65	49.67	48.53	65.88	9,854.27
Mid	567	209.4	0.735	86.27	52.09	46.11	80.51	56.37	50.29	48.74	65.07	9,096.77
Mid	574	189.4	0.761	86.16	51.13	45.45	79.03	55.00	49.02	48.09	63.86	8,816.97
Mid	656	189.6	0.759	94.78	53.20	47.61	79.93	56.30	51.10	49.97	64.83	8,335.86
Low	296	143.6	0.701	65.01	42.84	48.71	80.58	56.37	48.26	46.31	65.10	6,336.35
Low	338	132.7	0.833	73.51	43.67	40.72	80.87	48.61	43.44	41.84	61.54	6,199.86
Low	368	144.1	0.724	80.71	50.47	47.08	80.67	56.43	49.78	48.07	65.15	5,851.82
Low	368	144.1	0.725	80.71	50.38	47.00	80.58	56.37	49.50	48.00	65.10	5,879.12
Low	395	145.4	0.716	85.89	51.55	47.97	80.29	57.25	50.56	49.14	65.45	5,653.92
Low	397	140.8	0.734	86.04	51.31	47.67	80.67	56.34	50.50	48.61	65.11	5,623.21
Low	449	140.8	0.765	94.71	53.01	49.17	80.62	56.17	51.87	49.94	65.01	5,155.75

APPENDIX B COOLING CHARACTERISTIC PLOTS USING PSYCHROMETRIC PROPERTIES ON EES (CODE)

```
T_evap = 40 [F]
omega_B=humrat(AirH2O,T=T_evap,R=1,P=Po#)
cp=0.240

"Rating condition"
WB_rate = 67
DB_rate = 80
DB_s_rate=WB_rate
omega_sat_rate=humrat(AirH2O,T=WB_rate,B=WB_rate,P=Po#)
omega_A_rate=humrat(AirH2O,T=DB_rate,B=WB_rate,P=Po#)

k_s_rate =(omega_sat_rate-omega_B)/(DB_s_rate-T_evap)
k_wb_rate=(omega_sat_rate-omega_A_rate)/(DB_rate-WB_rate)
r_rate = k_s_rate/k_wb_rate

Duplicate row=1,76
WB[row] = lookup(row,'WB')
DB[row] = lookup(row,'DB')
omega_A[row]=humrat(AirH2O,T=DB[row],B=WB[row],P=Po#)
omega_sat[row]=humrat(AirH2O,T=WB[row],B=WB[row],P=Po#)


k_s[row] =(omega_sat[row]-omega_B)/(WB[row]-T_evap)
k_wb[row]=(omega_sat[row]-omega_A[row])/(DB[row]-WB[row])
r[row] = k_s[row]/k_wb[row]


SHR[row] =(DB[row] - T_evap)/(1+r[row])/(WB[row]-T_evap)

h_A[row]=enthalpy(AirH2O,T=DB[row],B=WB[row],P=Po#)
h_x[row]=enthalpy(AirH2O,T=DB[row],w=omega_B,P=Po#)
h_b[row]=enthalpy(AirH2O,T=t_evap,R=1,P=Po#)
delta_h_l[row]=h_A[row]-h_x[row]

delta_h[row]=cp*(1+r[row])*(WB[row]-T_evap)

delta_h_s[row]= h_x[row]-h_b[row]
delta_hr[row]=h_A[row]-h_b[row]
SHR_r[row]= delta_h_s[row]/delta_hr[row]
End

T_evap[1]=T_evap
T_evap[2]=100
omega_B[1]=omega_B
omega_B[2]=omega_B
```

Table B-1 Cooling capacities of various DB and WB condition at fixed OAT and WB from psychrometric chart on EES

DB	WB	SHR	Δh_l	Δh_s	Δh	Δh_{coil}	**NCAP_r**	**SHR_r**
F	F		Btu/lbm	Btu/lbm	Btu/lbm	Btu/lbm		
70.00	50.00	1.44	-2.28	7.26	4.98	7.26	**0.56**	**1.00**
70.00	52.00	1.18	-1.15	7.26	6.11	7.26	**0.56**	**1.00**
70.00	54.00	1.00	0.03	7.26	7.29	7.29	**0.56**	**1.00**
70.00	56.00	0.86	1.26	7.26	8.52	8.52	**0.65**	**0.85**
70.00	58.00	0.75	2.54	7.26	9.80	9.80	**0.75**	**0.74**
70.00	60.00	0.66	3.88	7.26	11.14	11.14	**0.85**	**0.65**
70.00	62.00	0.59	5.28	7.26	12.54	12.54	**0.96**	**0.58**
70.00	64.00	0.53	6.74	7.26	14.00	14.00	**1.07**	**0.52**
70.00	66.00	0.48	8.27	7.26	15.53	15.53	**1.19**	**0.47**
70.00	68.00	0.44	9.87	7.26	17.13	17.13	**1.31**	**0.42**
75.00	50.00	1.68	-3.51	8.47	4.96	8.47	**0.65**	**1.00**
75.00	52.00	1.38	-2.38	8.47	6.09	8.47	**0.65**	**1.00**
75.00	54.00	1.16	-1.21	8.47	7.26	8.47	**0.65**	**1.00**
75.00	56.00	1.00	0.02	8.47	8.49	8.49	**0.65**	**1.00**
75.00	58.00	0.87	1.30	8.47	9.77	9.77	**0.75**	**0.87**
75.00	60.00	0.77	2.64	8.47	11.11	11.11	**0.85**	**0.76**
75.00	62.00	0.69	4.03	8.47	12.50	12.50	**0.96**	**0.68**
75.00	64.00	0.62	5.49	8.47	13.96	13.96	**1.07**	**0.61**
75.00	66.00	0.56	7.02	8.47	15.49	15.49	**1.18**	**0.55**
75.00	68.00	0.51	8.62	8.47	17.09	17.09	**1.31**	**0.50**
75.00	70.00	0.47	10.29	8.47	18.76	18.76	**1.44**	**0.45**
75.00	72.00	0.43	12.05	8.47	20.52	20.52	**1.57**	**0.41**
75.00	74.00	0.39	13.89	8.47	22.36	22.36	**1.71**	**0.38**
80.00	50.00	1.92	-4.74	9.68	4.94	9.68	**0.74**	**1.00**
80.00	52.00	1.57	-3.62	9.68	6.06	9.68	**0.74**	**1.00**
80.00	54.00	1.33	-2.44	9.68	7.24	9.68	**0.74**	**1.00**
80.00	56.00	1.14	-1.22	9.68	8.46	9.68	**0.74**	**1.00**
80.00	58.00	0.99	0.06	9.68	9.74	9.74	**0.75**	**0.99**
80.00	60.00	0.88	1.39	9.68	11.07	11.07	**0.85**	**0.87**
80.00	62.00	0.78	2.79	9.68	12.47	12.47	**0.95**	**0.78**
80.00	64.00	0.70	4.24	9.68	13.93	13.93	**1.07**	**0.70**
80.00	66.00	0.64	5.77	9.68	15.45	15.45	**1.18**	**0.63**
80.00	68.00	0.58	7.37	9.68	17.05	17.05	**1.30**	**0.57**
80.00	70.00	0.53	9.04	9.68	18.72	18.72	**1.43**	**0.52**
80.00	72.00	0.49	10.79	9.68	20.47	20.47	**1.57**	**0.47**
80.00	74.00	0.45	12.63	9.68	22.31	22.31	**1.71**	**0.43**
80.00	76.00	0.42	14.55	9.68	24.23	24.23	**1.85**	**0.40**
80.00	78.00	0.39	16.57	9.68	26.26	26.26	**2.01**	**0.37**
85.00	50.00	2.16	-5.98	10.89	4.92	10.89	**0.83**	**1.00**
85.00	52.00	1.77	-4.85	10.89	6.04	10.89	**0.83**	**1.00**
85.00	54.00	1.49	-3.68	10.89	7.21	10.89	**0.83**	**1.00**
85.00	56.00	1.28	-2.46	10.89	8.44	10.89	**0.83**	**1.00**
85.00	58.00	1.12	-1.18	10.89	9.71	10.89	**0.83**	**1.00**
85.00	60.00	0.99	0.15	10.89	11.04	11.04	**0.84**	**0.99**
85.00	62.00	0.88	1.54	10.89	12.43	12.43	**0.95**	**0.88**
85.00	64.00	0.79	3.00	10.89	13.89	13.89	**1.06**	**0.78**

DB	WB	SHR	Δh_l	Δh_s	Δh	Δh_{coil}	**NCAP_r**	**SHR_r**
F	F		Btu/lbm	Btu/lbm	Btu/lbm	Btu/lbm		
85.00	66.00	0.72	4.52	10.89	15.41	15.41	**1.18**	**0.71**
85.00	68.00	0.65	6.11	10.89	17.01	17.01	**1.30**	**0.64**
85.00	70.00	0.60	7.78	10.89	18.67	18.67	**1.43**	**0.58**
85.00	72.00	0.55	9.53	10.89	20.42	20.42	**1.56**	**0.53**
85.00	74.00	0.51	11.37	10.89	22.26	22.26	**1.70**	**0.49**
85.00	76.00	0.47	13.29	10.89	24.18	24.18	**1.85**	**0.45**
85.00	78.00	0.43	15.31	10.89	26.20	26.20	**2.00**	**0.42**
85.00	80.00	0.40	17.43	10.89	28.32	28.32	**2.17**	**0.38**
85.00	82.00	0.38	19.66	10.89	30.55	30.55	**2.34**	**0.36**
85.00	84.00	0.35	21.99	10.89	32.89	32.89	**2.52**	**0.33**
90.00	50.00	2.40	-7.21	12.10	4.90	12.10	**0.93**	**1.00**
90.00	52.00	1.96	-6.09	12.10	6.02	12.10	**0.93**	**1.00**
90.00	54.00	1.65	-4.92	12.10	7.19	12.10	**0.93**	**1.00**
90.00	56.00	1.42	-3.70	12.10	8.41	12.10	**0.93**	**1.00**
90.00	58.00	1.24	-2.42	12.10	9.68	12.10	**0.93**	**1.00**
90.00	60.00	1.10	-1.09	12.10	11.01	12.10	**0.93**	**1.00**
90.00	62.00	0.98	0.30	12.10	12.40	12.40	**0.95**	**0.98**
90.00	64.00	0.88	1.75	12.10	13.85	13.85	**1.06**	**0.87**
90.00	66.00	0.80	3.27	12.10	15.37	15.37	**1.18**	**0.79**
90.00	68.00	0.72	4.86	12.10	16.96	16.96	**1.30**	**0.71**
90.00	70.00	0.66	6.53	12.10	18.63	18.63	**1.43**	**0.65**
90.00	72.00	0.61	8.27	12.10	20.38	20.38	**1.56**	**0.59**
90.00	74.00	0.56	10.11	12.10	22.21	22.21	**1.70**	**0.55**
90.00	76.00	0.52	12.03	12.10	24.13	24.13	**1.85**	**0.50**
90.00	78.00	0.48	14.04	12.10	26.15	26.15	**2.00**	**0.46**
90.00	80.00	0.45	16.16	12.10	28.26	28.26	**2.16**	**0.43**
90.00	82.00	0.42	18.38	12.10	30.49	30.49	**2.33**	**0.40**
90.00	84.00	0.39	20.72	12.10	32.82	32.82	**2.51**	**0.37**
90.00	86.00	0.36	23.18	12.10	35.28	35.28	**2.70**	**0.34**
90.00	88.00	0.34	25.76	12.10	37.86	37.86	**2.90**	**0.32**

APPENDIX C MINI-SPLIT SYSTEM MANUFACTURERS' DATA

Table C-1 Mitsubishi FE12NA cooling performance data (Fixed DB=80°F)

TEMP.	OAT														
WB	75			85			95			105			115		
	CAP	SHC	TPC	CAP	SHC	TPC	CAP	SHC	TPC	CAP	SHC	TPC	CAP	SHC	TPC
71	14.7	8.8	0.85	13.7	8.2	0.94	12.9	7.7	1.01	12.0	7.2	1.06	11.0	6.6	1.10
67	13.9	10.2	0.81	13.0	9.5	0.89	12.0	8.8	0.96	11.2	8.1	1.02	10.3	7.5	1.07
63	13.1	11.3	0.77	12.1	10.5	0.85	11.3	9.7	0.92	10.3	8.9	0.98	9.4	8.1	1.02

Table C-2 FE12NA cooling performance corrections

OAT / WB	70	77	81	86	95	104	115
60	1.11	1.06	1.01	0.97	0.91	0.83	0.76
63	1.16	1.1	1.06	1.02	0.96	0.88	0.81
64	1.18	1.13	1.08	1.04	0.98	0.9	0.83
68	1.23	1.18	1.14	1.1	1.03	0.96	0.89
72	1.28	1.23	1.2	1.15	1.09	1.02	0.95
75	1.34	1.29	1.26	1.22	1.15	1.08	1.02
79	1.38	1.34	1.32	1.28	1.21	1.14	1.07

Table C-3 Trained MUZ-FR12NA data for GRDB where rated CFM is 350 cfm.

OAT	**WB**	**CAP**	**CAP/CFM$_{Rated}$**		**OAT**	**WB**	**CAP**	**CAP/CFM$_{Rated}$**
F	F	kBtu/h	kBtu/ft^3/60		**F**	F	kBtu/h	kBtu/ft^3/60
70	60	13.32	38.06		**86**	72	13.8	39.43
70	63	13.92	39.77		**86**	75	14.64	41.83
70	64	14.16	40.46		**86**	79	15.36	43.89
70	68	14.76	42.17		**95**	60	10.92	31.20
70	72	15.36	43.89		**95**	63	11.52	32.91
70	75	16.08	45.94		**95**	64	11.76	33.60
70	79	16.56	47.31		***95***	***67***	***12***	34.29
75	63	13.1	37.43		**95**	68	12.36	35.31
75	67	13.9	39.71		**95**	71	12.9	36.86
75	71	14.7	42.00		**95**	72	13.08	37.37
77	60	12.72	36.34		**95**	75	13.8	39.43
77	63	13.2	37.71		**95**	79	14.52	41.49
77	64	13.56	38.74		**104**	60	9.96	28.46
77	68	14.16	40.46		**104**	63	10.56	30.17
77	72	14.76	42.17		**104**	64	10.8	30.86
77	75	15.48	44.23		**104**	68	11.52	32.91
77	79	16.08	45.94		**104**	72	12.24	34.97
81	60	12.12	34.63		**104**	75	12.96	37.03
81	63	12.72	36.34		**104**	79	13.68	39.09
81	64	12.96	37.03		**105**	63	10.3	29.43
81	68	13.68	39.09		**105**	67	11.2	32.00
81	72	14.4	41.14		**105**	71	12	34.29
81	75	15.12	43.20		**115**	60	9.12	26.06
81	79	15.84	45.26		**115**	63	9.72	27.77
85	63	12.1	34.57		**115**	64	9.96	28.46
85	67	13	37.14		**115**	67	10.3	29.43
85	71	13.7	39.14		**115**	68	10.68	30.51
86	60	11.64	33.26		**115**	71	11	31.43
86	63	12.24	34.97		**115**	72	11.4	32.57
86	64	12.48	35.66		**115**	75	12.24	34.97
86	68	13.2	37.71		**115**	79	12.84	36.69

Table C-4 Fujitsu 12RLS cooling performance data

DB	64			70			75			80			85			90		
WB	54	54	54	60	60	60	63	63	63	67	67	67	71	71	71	73	73	73
OAT	CAP	SHC	TPC	CAP	SHC	TPC	TC	SHC	TPC	TC	SHC	TPC	TC	SHC	TPC	TC	SHC	TPC
67	10.93	7.11	0.55	12.17	7.15	0.55	13.42	7.80	0.56	13.83	8.42	0.57	14.66	8.39	0.57	15.49	8.93	0.58
77	10.40	6.90	0.64	11.58	6.94	0.65	12.77	7.57	0.66	13.16	8.17	0.67	13.95	8.14	0.67	14.74	8.67	0.68
87	9.76	6.62	0.74	10.88	6.66	0.75	11.99	7.26	0.77	12.36	7.84	0.77	13.10	7.81	0.78	13.84	8.32	0.78
95	9.48	6.59	0.80	10.56	6.63	0.81	11.64	7.23	0.83	12.00	7.80	0.83	12.72	7.77	0.84	13.44	8.28	0.85
104	8.31	6.14	0.80	9.26	6.18	0.81	10.21	6.74	0.82	10.52	7.27	0.83	11.15	7.24	0.83	11.78	7.72	0.84
115	5.71	5.18	0.62	6.36	5.21	0.63	7.01	5.69	0.64	7.23	6.14	0.65	7.66	6.12	0.65	8.10	6.52	0.66

Table C-5 Daikin FTKN12NMVJU + RKN12NMVJU cooling performance data

TEMP.		OAT																	
EWB	EDB	68			77			86			90			95			104		
°F	°F	TC	SHC	PI	TC	SHC	PI	TC	SHC	PI	TC	SHC	PI	TC	SHC	PI	TC	SHC	PI
57.2	68.0	12.30	9.52	0.88	11.75	9.25	0.96	11.19	8.98	1.04	10.96	8.87	1.08	10.63	8.71	1.13	10.07	8.45	1.21
60.8	71.6	12.86	9.36	0.88	12.30	9.10	0.97	11.74	8.85	1.05	11.52	8.75	1.08	11.18	8.60	1.13	10.62	8.36	1.22
64.4	77.0	13.41	9.86	0.89	12.85	9.62	0.97	12.29	9.39	1.06	12.07	9.30	1.09	11.73	9.16	1.14	11.17	8.93	1.22
67.0	80.0	13.69	10.45	0.89	13.13	10.22	0.97	12.57	10.00	1.06	12.35	9.91	1.09	12.00	9.78	1.14	11.45	9.56	1.23
71.6	86.0	14.52	10.10	0.90	13.96	9.90	0.98	13.40	9.70	1.07	13.18	9.62	1.10	12.84	9.50	1.15	12.28	9.31	1.23
75.2	89.6	15.07	9.85	0.90	14.51	9.67	0.99	13.95	9.49	1.07	13.73	9.42	1.10	13.39	9.31	1.15	12.83	9.13	1.24

Where

WB : Intake air wet-bulb temperature (F)
CAP : Total cooling capacity (kBtu/h)
SHC : Sensible cooling capacity (Btu/h)
TPC : Total power consumption kW

APPENDIX D GRDB CALCULATION PROCEDURE FOR MUZ-FE12NA

Applied GRDB for MSHPs

- Step 1: From Equation 3.15, independent and depending variables or the manufacturers' data are determined. Since MSHPs' data provided only fixed CFM speed from manufacturer reported condition from Table 2-1, so Equation (3.21) will be appertained.

$$Cooling\ coil\ model \begin{cases} Wet-coil\ \ (SHR<1) \begin{cases} \frac{\dot{Q}_t}{CFM} = f(WB, OAT) \\ \dot{Q}_s = SHR \cdot \dot{Q}_t \end{cases} \\ Dry-coil\ (SHR=1),\ \frac{\dot{Q}_t}{CFM} = \frac{\dot{Q}_s}{CFM} = f(DB, OAT) \end{cases} \quad (3.21)$$

- Step 2: Determine coil condition by using SHR formula from Equation 3.4. If SHR < 1, coil condition is wet, and if SHR = 1, coil condition is dry.
- Step 3: Select wet-coiled data range and obtain multiple-linear regression (MLR) with independent variables WB and OAT from provided in performance data in and with dependent variable CAP from Table C-3. In this study, EES will be utilized to generate MLR equation as shown Figure D-1.

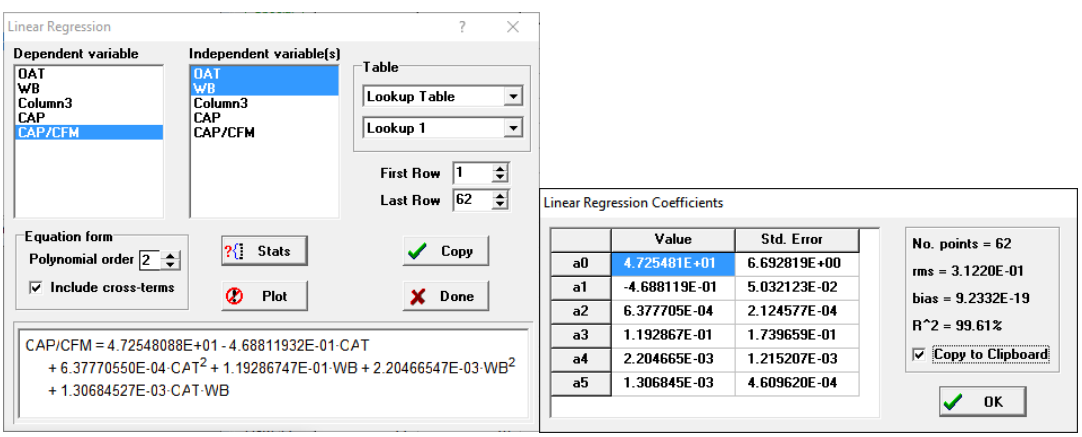

Figure D-1Generated two-order polynomial regression by using EES and its coefficients from modified GRDB's method

Two-polynomial order regression is obtained as follow:

$$\frac{CAP}{CFM} = 4.72548088 \times 10 - 4.68811932 \times 10^{-1} \times OAT + 6.37770550 \times 10^{-4} \times OAT^2 + 1.19286747 \times 10^{(-1)} \times WB + 2.20466547 \times 10^{-03} \times WB^2 + 1.30684527 \times 10^{-03} \times OAT \times WB$$

Or

$$\frac{CAP}{CFM} = 4.72548088E + 01 - 4.68811932E - 01 * OAT + 6.37770550E - 04 * OAT^2 + 1.19286747E - 01 * WB + 2.20466547E - 03 * WB^2 + 1.30684527E - 03 * OAT * WB$$

<u>*Original GRDB*</u>

The original GRDB includes CFM in the regression. As a result, the regression model can be obtained as following steps:

- Repeat all previous mentioned steps, however, substitute Equation 3.21 with Equation 3.20.

$$Cooling\ coil\ model \begin{cases} Wet - coil\ \ (SHR < 1) \begin{cases} \dot{Q}_t = f(WB, CFM, OAT) \\ \dot{Q}_s = SHR \cdot \dot{Q}_t \end{cases} \\ Dry - coil\ (SHR = 1),\ \ \dot{Q}_t = \dot{Q}_s = f(DB, CFM, OAT) \end{cases}$$

Therefore, two-ordered polynomial is obtained from ESS as follows

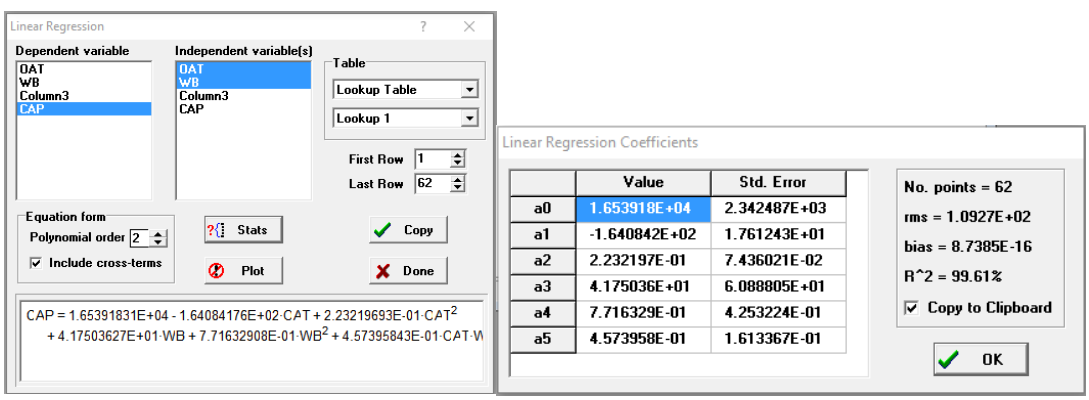

Figure D-2 Generated two-order polynomial regression by using EES and its coefficients from original GRDB method

Two-polynomial order regression is obtained as follow:

$$CAP = 1.65391831E + 04 - 1.64084176E + 02 * OAT + 2.23219693E - 01 * OAT\text{^}2 + 4.17503627E + 01 * WB + 7.71632908E - 01 * WB\text{^}2 + 4.57395843E - 01 * OAT * WB$$

APPENDIX E SPLIT SYSTEM MANUFACTURERS' DATA

Table E-1 Goodman DSZ16024-Low cooling performance data

DSZ16024			Outdoor Ambient Temperature																							
			65ºF				75ºF				85ºF				95ºF				105ºF				115ºF			
			Entering Indoor Wet Bulb Temperature																							
IDB	**Airflow**		**59**	**63**	**67**	**71**	**59**	**63**	**67**	**71**	**59**	**63**	**67**	**71**	**59**	**63**	**67**	**71**	**59**	**63**	**67**	**71**	**59**	**63**	**67**	**71**
		MBh	17.7	18.3	20.1	-	17	18	19.6	-	16.9	17.5	19.2	-	16.5	17.1	18.7	-	15.6	16	18	-	15	15	16.5	-
		S/T	0.79	0.66	0.46	-	0.8	0.7	0.47	-	0.84	0.7	0.48	-	0.86	0.72	0.5	-	0.9	0.8	0.5	-	0.9	0.76	0.52	-
		ΔT	18	15	12	-	18	15	12	-	18	15	12	-	18	15	12	-	18	15	12	-	16	14	11	-
	731	kW	1.06	1.09	1.12	-	1.2	1.2	1.21	-	1.22	1.25	1.29	-	1.29	1.32	1.36	-	1.34	1.4	1.4	-	1.4	1.42	1.47	-
		Amps	4.2	4.3	4.4	-	4.5	4.6	4.8	-	4.9	5	5.2	-	5.2	5.3	5.5	-	5.6	5.7	5.9	-	5.9	6	6.2	-
		Hi PR	209	225	237	-	235	252	266	-	267	287	303	-	304	327	345	-	342	368	388	-	378	406	429	-
		Lo PR	113	121	132	-	120	127	139	-	124	132	144	-	131	139	152	-	137	146	159	-	142	151	164	-
		MBh	17.2	17.8	19.5	-	17	17	19.1	-	16.4	17	18.6	-	16	16.6	18.2	-	15.2	16	17	-	14	14.6	16	-
		S/T	0.75	0.63	0.43	-	0.8	0.7	0.45	-	0.8	0.67	0.46	-	0.82	0.69	0.48	-	0.86	0.7	0.5	-	0.9	0.72	0.5	-
		ΔT	19	16	12	-	19	16	12	-	19	16	12	-	19	16	12	-	19	16	12	-	18	15	12	-
70	**637**	kW	1.06	1.08	1.11	-	1.1	1.2	1.2	-	1.21	1.24	1.28	-	1.28	1.31	1.35	-	1.33	1.4	1.4	-	1.4	1.41	1.46	-
		Amps	4.1	4.2	4.4	-	4.5	4.6	4.7	-	4.8	5	5.1	-	5.2	5.3	5.5	-	5.5	5.6	5.8	-	5.8	6	6.2	-
		Hi PR	207	223	235	-	232	250	264	-	264	284	300	-	301	324	342	-	338	364	384	-	374	402	425	-
		Lo PR	112	119	130	-	118	126	138	-	123	131	143	-	129	138	150	-	136	144	157	-	140	149	163	-
		MBh	16.3	16.9	18.5	-	16	17	18.1	-	15.6	16.1	17.7	-	15.2	15.7	17.2	-	14.4	15	16	-	13	13.9	15.2	-
		S/T	0.72	0.6	0.42	-	0.8	0.6	0.43	-	0.77	0.64	0.44	-	0.79	0.66	0.46	-	0.82	0.7	0.5	-	0.8	0.69	0.48	-
		ΔT	19	16	12	-	19	17	13	-	19	17	13	-	19	17	13	-	19	17	13	-	18	15	12	-
	569	kW	1.04	1.06	1.1	-	1.1	1.1	1.18	-	1.19	1.22	1.26	-	1.26	1.28	1.33	-	1.31	1.3	1.4	-	1.4	1.39	1.43	-
		Amps	4.1	4.2	4.3	-	4.4	4.5	4.6	-	4.8	4.9	5	-	5.1	5.2	5.4	-	5.4	5.5	5.7	-	5.7	5.9	6.1	-
		Hi PR	203	218	230	-	228	245	259	-	259	278	294	-	295	317	335	-	332	357	377	-	366	394	416	-
		Lo PR	110	117	128	-	116	124	135	-	121	128	140	-	127	135	147	-	133	141	154	-	137	146	160	-
		MBh	18	18.5	20.1	21.5	18	18	19.6	21	17.2	17.7	19.1	21	16.7	**17.2**	18.7	20	15.9	16	18	19	15	15.2	16.4	17.6
		S/T	0.9	0.8	0.61	0.39	0.9	0.8	0.63	0.4	0.95	0.85	0.64	0.4	0.98	**0.88**	0.67	0.43	1	0.9	0.7	0.44	1	0.92	0.7	0.5
		ΔT	20	19	15	11	21	19	15	11	21	19	15	11	21	**19**	16	11	20	19	15	11	19	18	14	10.0
	731	kW	1.07	1.1	1.13	1.17	1.2	1.2	1.22	1.3	1.23	1.26	1.3	1.4	1.3	**1.33**	1.37	1.42	1.36	1.4	1.4	1.48	1.4	1.44	1.48	1.5
		Amps	4.2	4.3	4.5	4.6	4.6	4.7	4.8	5	4.9	5.1	5.2	5.4	5.3	**5.4**	5.6	5.8	5.6	5.7	5.9	6.2	5.9	6.1	6.3	6.5
		Hi PR	211	227	240	250	237	255	269	281	269	290	306	319	307	**330**	349	364	345	372	392	409	381	410	433	452.0
		Lo PR	114	122	133	142	121	129	140	150	126	134	146	155	132	**140**	153	163	138	147	161	171	143	152	166	177.0
		MBh	17.5	18	19.5	20.9	17	18	19	20	16.7	17.2	18.6	20	16.3	**16.7**	18.1	19.4	15.4	16	17	18.5	14	14.7	15.9	17.1
		S/T	0.85	0.76	0.58	0.37	0.9	0.8	0.6	0.4	0.91	0.81	0.61	0.4	0.94	**0.84**	0.63	0.41	0.97	0.9	0.7	0.42	1	0.88	0.66	0.4
		ΔT	22	20	16	11	22	20	16	11	22	20	16	11	22	**20**	17	11	22	20	16	11	20	19	15	11.0
75	**637**	kW	1.06	1.09	1.12	1.16	1.2	1.2	1.21	1.3	1.22	1.25	1.29	1.3	1.29	**1.32**	1.36	1.41	1.34	1.4	1.4	1.47	1.4	1.42	1.47	1.5
		Amps	4.2	4.3	4.4	4.6	4.5	4.6	4.8	4.9	4.9	5	5.2	5.4	5.2	**5.3**	5.5	5.7	5.6	5.7	5.9	6.1	5.9	6	6.2	6.5
		Hi PR	209	225	238	248	235	252	267	278	267	287	303	316	304	**327**	345	360	342	368	388	405	378	406	429	448.0
		Lo PR	113	121	132	140	120	127	139	148	124	132	144	154	131	**139**	152	162	137	146	159	169	142	151	165	175.0
		MBh	16.6	17.1	18.5	19.9	16	17	18.1	19	15.8	16.3	17.6	19	15.4	**15.9**	17.2	18.5	14.7	15	16	17.5	14	14	15.1	16.3
		S/T	0.82	0.73	0.55	0.36	0.9	0.8	0.57	0.4	0.87	0.78	0.59	0.4	0.9	**0.8**	0.61	0.39	0.93	0.8	0.6	0.41	0.9	0.84	0.64	0.4
		ΔT	22	20	17	11	22	20	17	12	22	20	17	12	22	**21**	17	12	22	20	17	12	21	19	16	11.0
	569	kW	1.05	1.07	1.1	1.14	1.1	1.2	1.19	1.2	1.2	1.23	1.27	1.3	1.27	**1.29**	1.34	1.38	1.32	1.4	1.4	1.44	1.4	1.4	1.45	1.5
		Amps	4.1	4.2	4.3	4.5	4.4	4.5	4.7	4.9	4.8	4.9	5.1	5.3	5.1	**5.3**	5.4	5.6	5.5	5.6	5.8	6	5.8	5.9	6.1	6.3
		Hi PR	205	220	233	243	230	247	261	272	261	281	297	310	298	**320**	338	353	335	360	381	397	370	398	421	439.0
		Lo PR	111	118	129	137	117	125	136	145	122	130	142	151	128	**136**	149	158	134	143	156	166	139	148	161	172.0

Table E-1 Goodman DSZ16024-Low cooling performance data (continued)

			Outdoor Ambient Temperature																							
			65ºF				75ºF				85ºF				95ºF				105ºF				115ºF			
			Entering Indoor Wet Bulb Temperature																							
IDB	**Airflow**		**59**	**63**	**67**	**71**	**59**	**63**	**67**	**71**	**59**	**63**	**67**	**71**	**59**	**63**	**67**	**71**	**59**	**63**	**67**	**71**	**59**	**63**	**67**	**71**
		MBh	18.3	18.7	20	21.4	18	18	19.5	21	17.5	17.8	19.1	20	17	17.4	18.6	19.9	16.2	17	18	18.9	15	15.3	16.4	17.5
		S/T	1	0.92	0.75	0.56	1	1	0.78	0.6	1	1	0.8	0.6	1	1	0.82	0.61	1	1	0.9	0.64	1	1	0.86	0.64
		ΔT	23	22	19	15	22	22	19	15	22	22	19	15	21	22	19	15	20	21	19	15	19	19	18	14
	731	kW	1.08	1.11	1.14	1.18	1.2	1.2	1.23	1.3	1.24	1.27	1.31	1.4	1.31	1.34	1.38	1.43	1.37	1.4	1.5	1.5	1.4	1.45	1.5	1.55
		Amps	4.3	4.4	4.5	4.7	4.6	4.7	4.9	5	5	5.1	5.3	5.5	5.3	5.4	5.6	5.8	5.7	5.8	6	6.2	6	6.1	6.3	6.6
		Hi PR	213	229	242	253	239	258	272	284	272	293	309	323	310	334	352	367	349	375	396	413	385	415	438	457
		Lo PR	116	123	134	143	122	130	142	151	127	135	147	157	133	142	155	165	140	149	162	173	145	154	168	179
		MBh	17.8	18.2	19.4	20.8	17	18	19	20	17	17.3	18.5	20	16.5	16.9	**18.1**	19.3	15.7	16	17	18.3	15	14.9	15.9	17
		S/T	0.94	0.88	0.72	0.53	1	0.9	0.74	0.6	1	0.93	0.76	0.6	1	0.96	**0.78**	0.59	1	1	0.8	0.61	1	1	0.82	0.61
		ΔT	24	23	20	16	24	23	20	16	24	23	20	16	24	24	**20**	16	23	23	20	16	21	21	19	15
80	**637**	kW	1.07	1.1	1.13	1.17	1.2	1.2	1.22	1.3	1.23	1.26	1.3	1.4	1.3	1.33	**1.37**	1.42	1.36	1.4	1.4	1.48	1.4	1.44	1.48	1.54
		Amps	4.2	4.3	4.5	4.6	4.6	4.7	4.8	5	4.9	5.1	5.2	5.4	5.3	5.4	**5.6**	5.8	5.6	5.7	5.9	6.2	5.9	6.1	6.3	6.5
		Hi PR	211	227	240	250	237	255	269	281	269	290	306	319	307	330	**349**	364	345	372	392	409	381	411	433	452
		Lo PR	114	122	133	142	121	129	140	150	126	134	146	155	132	140	**153**	163	138	147	161	171	143	152	166	177
		MBh	16.9	17.3	18.4	19.7	17	17	18	19	16.1	16.5	17.6	19	15.7	16.1	17.2	18.3	14.9	15	16	17.4	14	14.1	15.1	16.1
		S/T	0.9	0.84	0.69	0.51	0.9	0.9	0.71	0.5	0.95	0.89	0.73	0.5	0.98	0.92	0.75	0.56	1.02	1	0.8	0.58	1	0.97	0.79	0.59
		ΔT	25	23	20	16	25	24	21	17	25	24	21	17	25	24	21	17	25	24	21	16	23	22	19	15
	569	kW	1.06	1.08	1.11	1.15	1.1	1.2	1.2	1.2	1.21	1.24	1.28	1.3	1.28	1.31	1.35	1.4	1.33	1.4	1.4	1.46	1.4	1.41	1.46	1.51
		Amps	4.1	4.2	4.4	4.5	4.5	4.6	4.7	4.9	4.8	5	5.1	5.3	5.2	5.3	5.5	5.7	5.5	5.6	5.8	6	5.8	6	6.2	6.4
		Hi PR	207	223	235	245	232	250	264	275	264	284	300	313	301	324	342	356	338	364	384	401	374	402	425	443
		Lo PR	112	119	130	139	118	126	138	147	123	131	143	152	129	138	150	160	136	144	157	168	140	149	163	173
		MBh	18.6	19	19.9	21.2	18	19	19.4	21	17.8	18.1	19	20	17.3	17.7	18.5	19.7	16.5	17	18	18.8	15	15.6	16.3	17.4
		S/T	1	0.99	0.9	0.73	1	1	0.93	0.8	1	1	0.95	0.8	1	1	0.98	0.8	1	1	1	0.83	1	1	1	0.84
		ΔT	23	24	22	19	23	23	23	20	22	23	23	20	22	22	23	20	21	21	22	20	19	20	20	18
	731	kW	1.09	1.11	1.15	1.19	1.2	1.2	1.24	1.3	1.25	1.28	1.32	1.4	1.32	1.35	1.4	1.44	1.38	1.4	1.5	1.51	1.4	1.46	1.51	1.56
		Amps	4.3	4.4	4.5	4.7	4.6	4.7	4.9	5.1	5	5.1	5.3	5.5	5.4	5.5	5.7	5.9	5.7	5.8	6	6.3	6	6.2	6.4	6.6
		Hi PR	215	232	245	255	242	260	275	286	275	296	312	326	313	337	356	371	352	379	400	417	389	419	442	461
		Lo PR	117	124	136	144	123	131	143	153	128	136	149	159	135	143	156	167	141	150	164	175	146	155	170	181
		MBh	18.1	18.4	19.3	20.6	18	18	18.9	20	17.3	17.6	18.4	20	16.8	17.2	18	19.2	16	16	17	18.2	15	15.1	15.8	16.9
		S/T	0.98	0.95	0.86	0.69	1	1	0.89	0.7	1	1	0.91	0.7	1	1	0.94	0.76	1	1	1	0.79	1	1	0.98	0.8
		ΔT	26	25	24	21	26	26	24	21	25	25	24	21	24	25	24	21	23	24	24	21	21	22	22	19
85	**637**	kW	1.08	1.11	1.14	1.18	1.2	1.2	1.23	1.3	1.24	1.27	1.31	1.4	1.31	1.34	1.38	1.43	1.37	1.4	1.5	1.5	1.4	1.45	1.5	1.55
		Amps	4.3	4.4	4.5	4.7	4.6	4.7	4.9	5	5	5.1	5.3	5.5	5.3	5.4	5.6	5.8	5.7	5.8	6	6.2	6	6.1	6.3	6.6
		Hi PR	213	229	242	253	239	258	272	284	272	293	309	323	310	334	352	367	349	375	396	413	385	415	438	457
		Lo PR	116	123	134	143	122	130	142	151	127	135	147	157	133	142	155	165	140	149	162	173	145	154	168	179
		MBh	17.2	17.5	18.4	19.6	17	17	17.9	19	16.4	16.7	17.5	19	16	16.3	17.1	18.2	15.2	16	16	17.3	14	14.3	15	16
		S/T	0.94	0.91	0.82	0.66	1	0.9	0.85	0.7	1	0.96	0.87	0.7	1	1	0.9	0.73	1	1	0.9	0.76	1	1	0.94	0.76
		ΔT	26.1	26	24	21	26	26	25	21	26	26	25	21	26	26	25	21	25	25	24	21	23	23	23	20
	569	kW	1.06	1.09	1.12	1.16	1.2	1.2	1.21	1.3	1.22	1.25	1.29	1.3	1.29	1.32	1.36	1.41	1.34	1.4	1.4	1.47	1.4	1.42	1.47	1.52
		Amps	4.2	4.3	4.4	4.6	4.5	4.6	4.8	4.9	4.9	5	5.2	5.4	5.2	5.3	5.5	5.7	5.6	5.7	5.9	6.1	5.9	6	6.2	6.5
		Hi PR	209	225	237	248	235	252	266	278	267	287	303	316	304	327	345	360	342	368	388	405	378	406	429	448
		Lo PR	113	121	132	140	120	127	139	148	124	132	144	154	131	139	152	162	137	146	159	169	142	151	164	175

Table E-2 Goodman DSZ16024-High cooling performance data

DSZ16024H			Outdoor Ambient Temperature																							
			65ºF				75ºF				85ºF				95ºF				105ºF				115ºF			
			Entering Indoor Wet Bulb Temperature																							
DB	CFM		59	63	67	71	59	63	67	71	59	63	67	71	59	63	67	71	59	63	67	71	59	63	67	71
70	984	CAP	24	24	27	-	23	24	26	-	22	23	26	-	22	22.7	24.8	-	21	22	24	-	19	20	22	-
		SHR	0.8	0.7	0.5	-	0.8	0.7	0.5	-	0.9	0.7	0.5	-	0.9	0.73	0.51	-	0.9	0.8	0.5	-	0.9	0.8	0.5	-
		ΔT	17	15	11	-	18	15	12	-	18	15	12	-	18	15	12	-	18	15	12	-	16	14	11	-
		TPC	1.6	1.6	1.7	-	1.7	1.7	1.8	-	1.8	1.8	1.9	-	1.9	1.93	2	-	2	2	2.1	-	2	2.1	2.2	-
	875	CAP	23	24	26	-	22	23	25	-	22	23	25	-	21	22	24.1	-	20	21	23	-	19	19	21	-
		SHR	0.8	0.6	0.4	-	0.8	0.7	0.5	-	0.8	0.7	0.5	-	0.8	0.7	0.48	-	0.9	0.7	0.5	-	0.9	0.7	0.5	-
		ΔT	18	16	12	-	18	16	12	-	18	16	12	-	19	16	12	-	18	16	12	-	17	15	11	-
		TPC	1.6	1.6	1.6	-	1.7	1.7	1.8	-	1.8	1.8	1.9	-	1.9	1.92	1.98	-	2	2	2.1	-	2	2.1	2.1	-
	766	CAP	21	22	24	-	21	21	23	-	20	21	23	-	20	20.3	22.3	-	19	19	21	-	17	18	20	-
		SHR	0.7	0.6	0.4	-	0.8	0.6	0.4	-	0.8	0.7	0.5	-	0.8	0.67	0.46	-	0.8	0.7	0.5	-	0.8	0.7	0.5	-
		ΔT	19	16	12	-	19	16	12	-	19	16	12	-	19	16	12	-	19	16	12	-	17	15	11	-
		TPC	1.5	1.5	1.6	-	1.6	1.7	1.7	-	1.7	1.8	1.8	-	1.8	1.87	1.93	-	1.9	2	2	-	2	2	2.1	-
75	984	CAP	24	25	27	29	23	24	26	28	23	24	25	27	22	22.9	24.8	27	21	22	24	25	20	20	22	23
		SHR	0.9	0.8	0.6	0.4	0.9	0.8	0.6	0.4	1	0.9	0.7	0.4	1	0.89	0.67	0.4	1	0.9	0.7	0.5	1	0.9	0.7	0.5
		ΔT	20	19	15	11	20	19	15	11	20	19	15	11	21	19	16	11	20	19	15	11	18	17	14	10
		TPC	1.6	1.6	1.7	1.7	1.7	1.7	1.8	1.9	1.8	1.9	1.9	2	1.9	1.95	2.02	2.1	2	2	2.1	2.2	2.1	2.1	2.2	2.3
	875	CAP	23	24	26	28	23	23	25	27	22	23	25	27	22	**22.2**	24.1	26	21	21	23	25	19	20	21	23
		SHR	0.9	0.8	0.6	0.4	0.9	0.8	0.6	0.4	0.9	0.8	0.6	0.4	1	**0.85**	0.64	0.4	1	0.9	0.7	0.4	1	0.9	0.7	0.4
		ΔT	21	19	16	11	21	20	16	11	21	20	16	11	21	**20**	16	11	21	20	16	11	20	18	15	10
		TPC	1.6	1.6	1.7	1.7	1.7	1.7	1.8	1.8	1.8	1.8	1.9	2	1.9	**1.93**	2	2.1	2	2	2.1	2.2	2	2.1	2.2	2.2
	766	CAP	21	22	24	26	21	22	23	25	20	21	23	24	20	20.5	22.2	24	19	20	21	23	18	18	20	21
		SHR	0.8	0.7	0.6	0.4	0.9	0.8	0.6	0.4	0.9	0.8	0.6	0.4	0.9	0.82	0.62	0.4	1	0.9	0.6	0.4	1	0.9	0.7	0.4
		ΔT	21	20	16	11	22	20	16	11	22	20	16	11	22	20	16	11	22	20	16	11	20	19	15	10
		TPC	1.5	1.6	1.6	1.7	1.6	1.7	1.7	1.8	1.8	1.8	1.9	1.9	1.8	1.88	1.95	2	1.9	2	2	2.1	2	2	2.1	2.2
80	984	CAP	24	25	27	28	24	24	26	28	23	24	25	27	23	23.1	24.7	26	22	22	24	25	20	20	22	23
		SHR	1	0.9	0.8	0.6	1	1	0.8	0.6	1	1	0.8	0.6	1	1	0.83	0.6	1	1	0.9	0.6	1	1	0.9	0.7
		ΔT	23	22	19	15	22	22	19	15	22	22	19	15	21	22	19	15	20	21	19	15	19	19	18	14
		TPC	1.6	1.6	1.7	1.7	1.7	1.8	1.8	1.9	1.8	1.9	1.9	2	1.9	1.97	2.03	2.1	2	2.1	2.1	2.2	2.1	2.1	2.2	2.3
	875	CAP	24	24	26	28	23	24	25	27	23	23	25	26	22	22.5	**24**	26	21	21	23	24	19	20	21	23
		SHR	1	0.9	0.7	0.5	1	0.9	0.8	0.6	1	0.9	0.8	0.6	1	0.97	**0.79**	0.6	1	1	0.8	0.6	1	1	0.8	0.6
		ΔT	24	23	20	16	24	23	20	16	24	23	20	16	23	23	**20**	16	22	22	20	16	20	21	18	15
		TPC	1.6	1.6	1.7	1.7	1.7	1.7	1.8	1.9	1.8	1.9	1.9	2	1.9	1.95	**2.02**	2.1	2	2	2.1	2.2	2.1	2.1	2.2	2.3
	766	CAP	22	22	24	26	21	22	23	25	21	21	23	24	20	20.7	22.2	24	19	20	21	23	18	18	20	21
		SHR	0.9	0.9	0.7	0.5	1	0.9	0.7	0.5	1	0.9	0.7	0.6	1	0.94	0.76	0.6	1	1	0.8	0.6	1.1	1	0.8	0.6
		ΔT	24	23	20	16	24	23	20	16	24	23	20	16	24	23	20	16	24	23	20	16	22	22	19	15
		TPC	1.5	1.6	1.6	1.7	1.7	1.7	1.8	1.8	1.8	1.8	1.9	1.9	1.9	1.9	1.96	2	1.9	2	2.1	2.1	2	2.1	2.1	2.2
85	984	CAP	25	25	26	28	24	25	26	28	24	24	25	27	23	23.5	24.6	26	22	22	23	25	20	21	22	23
		SHR	1	1	0.9	0.7	1	1	0.9	0.8	1	1	1	0.8	1	1	0.99	0.8	1	1	1	0.8	1	1	1	0.8
		ΔT	23	24	22	19	23	23	23	20	22	22	23	20	22	22	23	20	20	21	22	19	19	19	20	18
		TPC	1.6	1.6	1.7	1.7	1.7	1.8	1.8	1.9	1.8	1.9	1.9	2	1.9	1.98	2.05	2.1	2	2.1	2.1	2.2	2.1	2.1	2.2	2.3
	875	CAP	24	25	26	27	24	24	25	27	23	23	25	26	22	22.8	23.9	26	21	22	23	24	20	20	21	22
		SHR	1	1	0.9	0.7	1	1	0.9	0.7	1	1	0.9	0.7	1	1	0.95	0.8	1	1	1	0.8	1	1	1	0.8
		ΔT	25	25	23	20	25	25	24	20	24	25	24	20	24	24	24	21	22	23	23	20	21	21	22	19
		TPC	1.6	1.6	1.7	1.7	1.7	1.8	1.8	1.9	1.8	1.9	1.9	2	1.9	1.97	2.03	2.1	2	2.1	2.1	2.2	2.1	2.1	2.2	2.3
	766	CAP	22	23	24	25	22	22	23	25	21	22	23	24	21	21	22	24	20	20	21	22	18	19	19	21
		SHR	1	0.9	0.8	0.7	1	1	0.9	0.7	1	1	0.9	0.7	1	1	0.91	0.7	1	1	1	0.8	1	1	1	0.8
		ΔT	25	25	24	21	26	25	24	21	25	25	24	21	25	25	24	21	24	24	24	21	22	22	22	19
		TPC	1.6	1.6	1.6	1.7	1.7	1.7	1.8	1.8	1.8	1.8	1.9	1.9	1.9	1.92	1.98	2.1	2	2	2.1	2.1	2	2.1	2.1	2.2

Table E-3 Goodman DSZ16036-High cooling performance data

DSZ16036H			Outdoor Ambient Temperature																							
			65ºF				75ºF				85ºF				95ºF				105ºF				115ºF			
			Entering Indoor Wet Bulb Temperature																							
DB	CFM		59	63	67	71	59	63	67	71	59	63	67	71	59	63	67	71	59	63	67	71	59	63	67	71
70	1294	CAP	34	35	39	-	33	34	38	-	32	34	37	-	32	32.7	35.8	-	30	31	34	-	28	29	32	-
		SHR	0.7	0.6	0.4	-	0.8	0.6	0.4	-	0.8	0.7	0.5	-	0.8	0.67	0.47	-	0.8	0.7	0.5	-	0.9	0.7	0.5	-
		ΔT	18	15	12	-	18	16	12	-	18	16	12	-	18	16	12	-	18	15	12	-	17	14	11	-
		TPC	2.2	2.2	2.3	-	2.3	2.4	2.5	-	2.5	2.5	2.6	-	2.6	2.67	2.76	-	2.7	2.8	2.9	-	2.8	2.9	3	-
	1150	CAP	33	34	37	-	32	33	37	-	31	33	36	-	31	31.7	34.8	-	29	30	33	-	27	28	31	-
		SHR	0.7	0.6	0.4	-	0.7	0.6	0.4	-	0.8	0.6	0.4	-	0.8	0.64	0.45	-	0.8	0.7	0.5	-	0.8	0.7	0.5	-
		ΔT	18	16	12	-	19	16	12	-	19	16	12	-	19	16	12	-	19	16	12	-	17	15	11	-
		TPC	2.1	2.2	2.3	-	2.3	2.4	2.4	-	2.5	2.5	2.6	-	2.6	2.65	2.73	-	2.7	2.8	2.9	-	2.8	2.9	3	-
	1006	CAP	30	32	35	-	30	31	34	-	29	30	33	-	28	29.3	32.1	-	27	28	31	-	25	26	28	-
		SHR	0.7	0.6	0.4	-	0.7	0.6	0.4	-	0.7	0.6	0.4	-	0.7	0.62	0.43	-	0.8	0.6	0.5	-	0.8	0.7	0.5	-
		ΔT	19	16	12	-	19	16	13	-	19	16	13	-	19	17	13	-	19	16	12	-	18	15	12	-
		TPC	2.1	2.1	2.2	-	2.3	2.3	2.4	-	2.4	2.5	2.5	-	2.5	2.58	2.66	-	2.6	2.7	2.8	-	2.7	2.8	2.9	-
75	1294	CAP	35	36	38	41	34	35	38	40	33	34	37	39	32	33	35.7	38	31	31	34	36	28	29	32	34
		SHR	0.8	0.8	0.6	0.4	0.9	0.8	0.6	0.4	0.9	0.8	0.6	0.4	0.9	0.82	0.62	0.4	1	0.9	0.7	0.4	1	0.9	0.7	0.4
		ΔT	21	19	15	11	21	19	16	11	21	19	16	11	21	19	16	11	21	19	16	11	19	18	15	10
		TPC	2.2	2.2	2.3	2.4	2.4	2.4	2.5	2.6	2.5	2.6	2.6	2.7	2.6	2.69	2.78	2.9	2.7	2.8	2.9	3	2.8	2.9	3	3.1
	1150	CAP	34	35	37	40	33	34	36	39	32	33	36	38	31	**32.1**	34.7	37	30	31	33	35	27	28	31	33
		SHR	0.8	0.7	0.5	0.4	0.8	0.7	0.6	0.4	0.9	0.8	0.6	0.4	0.9	**0.78**	0.59	0.4	0.9	0.8	0.6	0.4	0.9	0.8	0.6	0.4
		ΔT	21	20	16	11	22	20	16	11	22	20	16	11	22	**20**	16	11	22	20	16	11	20	18	15	10
		TPC	2.2	2.2	2.3	2.4	2.3	2.4	2.5	2.5	2.5	2.5	2.6	2.7	2.6	**2.67**	2.76	2.9	2.7	2.8	2.9	3	2.8	2.9	3	3.1
	1006	CAP	31	32	34	37	30	31	34	36	30	30	33	35	29	29.6	32	34	27	28	30	33	25	26	28	30
		SHR	0.8	0.7	0.5	0.3	0.8	0.7	0.5	0.4	0.8	0.7	0.6	0.4	0.8	0.76	0.57	0.4	0.9	0.8	0.6	0.4	0.9	0.8	0.6	0.4
		ΔT	22	20	16	11	22	20	17	11	22	20	17	11	22	20	17	12	22	20	16	11	20	19	15	11
		TPC	2.1	2.2	2.2	2.3	2.3	2.3	2.4	2.5	2.4	2.5	2.6	2.6	2.5	2.6	2.69	2.8	2.7	2.7	2.8	2.9	2.8	2.8	2.9	3
80	1294	CAP	35	36	38	41	34	35	37	40	34	34	37	39	33	33.4	35.6	38	31	32	34	36	29	29	31	34
		SHR	0.9	0.9	0.7	0.5	1	0.9	0.7	0.5	1	0.9	0.7	0.6	1	0.94	0.77	0.6	1	1	0.8	0.6	1	1	0.8	0.6
		ΔT	23	22	19	15	23	22	19	15	24	22	19	15	23	22	19	16	22	23	19	15	20	21	18	14
		TPC	2.2	2.2	2.3	2.4	2.4	2.4	2.5	2.6	2.5	2.6	2.7	2.8	2.7	2.71	2.8	2.9	2.8	2.8	2.9	3	2.9	2.9	3	3.1
	1150	CAP	34	35	37	40	33	34	36	39	33	33	36	38	32	32.4	**34.6**	37	30	31	33	35	28	29	30	33
		SHR	0.9	0.8	0.7	0.5	0.9	0.9	0.7	0.5	0.9	0.9	0.7	0.5	1	0.9	**0.73**	0.6	1	0.9	0.8	0.6	1	0.9	0.8	0.6
		ΔT	24	23	20	16	24	23	20	16	24	23	20	16	24	23	**20**	16	24	23	20	16	22	21	19	15
		TPC	2.2	2.2	2.3	2.4	2.4	2.4	2.5	2.6	2.5	2.6	2.6	2.7	2.6	2.69	**2.78**	2.9	2.7	2.8	2.9	3	2.8	2.9	3	3.1
	1006	CAP	31	32	34	37	31	31	34	36	30	31	33	35	29	29.9	31.9	34	28	28	30	32	26	26	28	30
		SHR	0.8	0.8	0.6	0.5	0.9	0.8	0.7	0.5	0.9	0.8	0.7	0.5	0.9	0.87	0.71	0.5	1	0.9	0.7	0.6	1	0.9	0.7	0.6
		ΔT	24	23	20	16	25	24	20	16	25	24	20	16	25	24	21	16	24	23	20	16	23	22	19	15
		TPC	2.1	2.2	2.2	2.3	2.3	2.3	2.4	2.5	2.4	2.5	2.6	2.7	2.6	2.62	2.71	2.8	2.7	2.7	2.8	2.9	2.8	2.8	2.9	3
85	1294	CAP	36	36	38	41	35	36	37	40	34	35	36	39	33	33.9	35.5	38	32	32	34	36	29	30	31	33
		SHR	1	0.9	0.8	0.7	1	1	0.9	0.7	1	1	0.9	0.7	1	1	0.92	0.8	1	1	1	0.8	1	1	1	0.8
		ΔT	24	24	23	20	25	24	23	20	24	24	23	20	24	24	23	20	22	23	23	20	21	21	21	18
		TPC	2.2	2.3	2.3	2.4	2.4	2.4	2.5	2.6	2.5	2.6	2.7	2.8	2.7	2.74	2.83	2.9	2.8	2.9	3	3.1	2.9	3	3.1	3.2
	1150	CAP	35	35	37	40	34	35	36	39	33	34	35	38	32	32.9	34.4	37	31	31	33	35	28	29	30	32
		SHR	0.9	0.9	0.8	0.7	1	0.9	0.8	0.7	1	0.9	0.9	0.7	1	0.97	0.88	0.7	1	1	0.9	0.7	1	1	0.9	0.7
		ΔT	25	25	24	20	26	25	24	21	26	25	24	21	26	26	24	21	24	25	24	21	23	23	22	19
		TPC	2.2	2.2	2.3	2.4	2.4	2.4	2.5	2.6	2.5	2.6	2.7	2.8	2.7	2.71	2.8	2.9	2.8	2.8	2.9	3	2.9	2.9	3	3.1
	1006	CAP	32	33	34	36	31	32	33	36	31	31	33	35	30	30.3	31.8	34	28	29	30	32	26	27	28	30
		SHR	0.9	0.9	0.8	0.6	0.9	0.9	0.8	0.7	0.9	0.9	0.8	0.7	1	0.94	0.85	0.7	1	1	0.9	0.7	1	1	0.9	0.7
		ΔT	26	25	24	21	26	26	24	21	26	26	24	21	26	26	25	21	26	26	24	21	24	24	23	20
		TPC	2.1	2.2	2.3	2.3	2.3	2.4	2.4	2.5	2.5	2.5	2.6	2.7	2.6	2.64	2.73	2.8	2.7	2.8	2.9	3	2.8	2.9	3	3.1

Table E-4 Goodman DSZ16048-High cooling performance data

DSZ16048H			Outdoor Ambient Temperature																							
			65ºF				75ºF				85ºF				95ºF				105ºF				115ºF			
			Entering Indoor Wet Bulb Temperature																							
DB	CFM		59	63	67	71	59	63	67	71	59	63	67	71	59	63	67	71	59	63	67	71	59	63	67	71
70	1744	CAP	47	48	53	-	46	47	52	-	44	46	50	-	43	44.9	49.2	-	41	43	47	-	38	40	43	-
		SHR	0.8	0.6	0.4	-	0.8	0.7	0.5	-	0.8	0.7	0.5	-	0.8	0.7	0.48	-	0.9	0.7	0.5	-	0.9	0.7	0.5	-
		ΔT	19	16	12	-	19	16	12	-	19	16	12	-	19	16	12	-	19	16	12	-	18	15	11	-
		TPC	2.8	2.9	3	-	3	3.1	3.2	-	3.2	3.3	3.4	-	3.4	3.48	3.6	-	3.6	3.6	3.8	-	3.7	3.8	3.9	-
	1550	CAP	45	47	51	-	44	46	50	-	43	45	49	-	42	43.6	47.7	-	40	41	45	-	37	38	42	-
		SHR	0.7	0.6	0.4	-	0.8	0.6	0.4	-	0.8	0.6	0.4	-	0.8	0.66	0.46	-	0.8	0.7	0.5	-	0.8	0.7	0.5	-
		ΔT	19	17	13	-	20	17	13	-	20	17	13	-	20	17	13	-	20	17	13	-	18	16	12	-
		TPC	2.8	2.9	3	-	3	3.1	3.2	-	3.2	3.3	3.4	-	3.4	3.45	3.57	-	3.5	3.6	3.7	-	3.7	3.7	3.9	-
	1356	CAP	42	43	47	-	41	42	46	-	40	41	45	-	39	40.2	44.1	-	37	38	42	-	34	35	39	-
		SHR	0.7	0.6	0.4	-	0.7	0.6	0.4	-	0.7	0.6	0.4	-	0.8	0.64	0.44	-	0.8	0.7	0.5	-	0.8	0.7	0.5	-
		ΔT	20	17	13	-	20	17	13	-	20	17	13	-	20	17	13	-	20	17	13	-	19	16	12	-
		TPC	2.7	2.8	2.9	-	2.9	3	3.1	-	3.1	3.2	3.3	-	3.3	3.37	3.48	-	3.4	3.5	3.6	-	3.6	3.6	3.8	-
75	1744	CAP	47	49	53	57	46	48	52	55	45	47	50	54	44	45.3	49.1	53	42	43	47	50	39	40	43	46
		SHR	0.9	0.8	0.6	0.4	0.9	0.8	0.6	0.4	0.9	0.8	0.6	0.4	1	0.85	0.64	0.4	1	0.9	0.7	0.4	1	0.9	0.7	0.4
		ΔT	22	20	16	11	22	20	16	11	22	20	16	11	22	20	17	11	22	20	16	11	20	19	15	11
		TPC	2.9	2.9	3	3.1	3.1	3.1	3.2	3.3	3.3	3.3	3.5	3.6	3.4	3.51	3.63	3.8	3.6	3.7	3.8	3.9	3.7	3.8	3.9	4.1
	1550	CAP	46	47	51	55	45	46	50	54	44	45	49	52	43	**44**	47.6	51	41	42	45	49	38	39	42	45
		SHR	0.8	0.7	0.6	0.4	0.9	0.8	0.6	0.4	0.9	0.8	0.6	0.4	0.9	**0.81**	0.61	0.4	0.9	0.8	0.6	0.4	0.9	0.8	0.6	0.4
		ΔT	22	21	17	12	23	21	17	12	23	21	17	12	23	**21**	17	12	23	21	17	12	21	19	16	11
		TPC	2.8	2.9	3	3.1	3	3.1	3.2	3.3	3.2	3.3	3.4	3.5	3.4	**3.48**	3.6	3.7	3.6	3.6	3.8	3.9	3.7	3.8	3.9	4
	1356	CAP	42	44	47	51	41	43	46	50	40	42	45	48	40	40.6	44	47	38	39	42	45	35	36	39	42
		SHR	0.8	0.7	0.5	0.4	0.8	0.7	0.6	0.4	0.8	0.8	0.6	0.4	0.9	0.78	0.59	0.4	0.9	0.8	0.6	0.4	0.9	0.8	0.6	0.4
		ΔT	23	21	17	12	23	21	17	12	23	21	17	12	23	21	18	12	23	21	17	12	21	20	16	11
		TPC	2.8	2.8	2.9	3	3	3	3.1	3.2	3.2	3.2	3.3	3.4	3.3	3.4	3.51	3.6	3.5	3.5	3.7	3.8	3.6	3.7	3.8	3.9
80	1744	MBh	48	49	53	56	47	48	51	55	46	47	50	54	45	45.8	48.9	52	43	44	47	50	39	40	43	46
		S/T	1	0.9	0.7	0.5	1	0.9	0.8	0.6	1	0.9	0.8	0.6	1	1	0.79	0.6	1	1	0.8	0.6	1	1	0.8	0.6
		ΔT	24	23	20	16	25	23	20	16	24	23	20	16	24	24	20	16	22	23	20	16	21	21	19	15
		kW	2.9	2.9	3	3.1	3.1	3.2	3.3	3.4	3.3	3.4	3.5	3.6	3.5	3.54	3.66	3.8	3.6	3.7	3.8	4	3.7	3.8	4	4.1
	1550	MBh	47	48	51	55	46	47	50	53	45	46	49	52	44	44.5	**47.5**	51	41	42	45	48	38	39	42	45
		S/T	0.9	0.9	0.7	0.5	0.9	0.9	0.7	0.5	1	0.9	0.7	0.6	1	0.93	**0.76**	0.6	1	1	0.8	0.6	1	1	0.8	0.6
		ΔT	25	24	21	17	25	24	21	17	25	24	21	17	26	24	**21**	17	25	24	21	17	23	23	20	16
		kW	2.9	2.9	3	3.1	3.1	3.1	3.2	3.3	3.3	3.3	3.5	3.6	3.4	3.51	**3.63**	3.8	3.6	3.7	3.8	3.9	3.7	3.8	3.9	4.1
	1356	MBh	43	44	47	50	42	43	46	49	41	42	45	48	40	41	43.8	47	38	39	42	45	35	36	39	41
		S/T	0.9	0.8	0.7	0.5	0.9	0.9	0.7	0.5	0.9	0.9	0.7	0.5	1	0.89	0.73	0.5	1	0.9	0.8	0.6	1	0.9	0.8	0.6
		ΔT	25	24	21	17	26	25	21	17	26	25	21	17	26	25	22	17	26	25	21	17	24	23	20	16
		kW	2.8	2.8	2.9	3	3	3.1	3.2	3.3	3.2	3.3	3.4	3.5	3.4	3.43	3.54	3.7	3.5	3.6	3.7	3.8	3.6	3.7	3.8	4
85	1744	MBh	49	50	52	56	48	49	51	55	47	48	50	53	46	46.5	48.7	52	43	44	46	49	40	41	43	46
		S/T	1	1	0.9	0.7	1	1	0.9	0.7	1	1	0.9	0.7	1	1	0.95	0.8	1	1	1	0.8	1	1	1	0.8
		ΔT	26	25	24	21	25	26	24	21	25	25	24	21	24	25	24	21	23	23	24	21	21	22	22	19
		kW	2.9	3	3.1	3.2	3.1	3.2	3.3	3.4	3.3	3.4	3.5	3.6	3.5	3.57	3.69	3.8	3.6	3.7	3.9	4	3.8	3.9	4	4.1
	1550	MBh	48	49	51	54	47	47	50	53	45	46	48	52	44	45.1	47.3	50	42	43	45	48	39	40	42	44
		S/T	1	0.9	0.8	0.7	1	1	0.9	0.7	1	1	0.9	0.7	1	1	0.9	0.7	1	1	0.9	0.8	1	1	1	0.8
		ΔT	27	26	25	21	27	27	25	22	27	27	25	22	26	27	25	22	25	25	25	22	23	24	23	20
		kW	2.9	2.9	3	3.1	3.1	3.2	3.3	3.4	3.3	3.4	3.5	3.6	3.5	3.54	3.66	3.8	3.6	3.7	3.8	4	3.7	3.8	4	4.1
	1356	MBh	44	45	47	50	43	44	46	49	42	43	45	48	41	41.7	43.6	47	39	40	41	44	36	37	38	41
		S/T	0.9	0.9	0.8	0.6	1	0.9	0.8	0.7	1	0.9	0.8	0.7	1	0.97	0.87	0.7	1	1	0.9	0.7	1	1	0.9	0.7
		ΔT	27	27	25	22	27	27	26	22	28	27	26	22	28	27	26	22	26	27	25	22	24	25	24	21
		kW	2.8	2.9	3	3.1	3	3.1	3.2	3.3	3.2	3.3	3.4	3.5	3.4	3.45	3.57	3.7	3.5	3.6	3.7	3.9	3.7	3.7	3.9	4

Table E-5 Goodman DSZ16060-High cooling performance data

DSZ16060H			Outdoor Ambient Temperature																							
			65ºF				75ºF				85ºF				95ºF				105ºF				115ºF			
			Entering Indoor Wet Bulb Temperature																							
IDB	Airflow		59	63	67	71	59	63	67	71	59	63	67	71	59	63	67	71	59	63	67	71	59	63	67	71
70	2000	CAP	56	58	63	-	55	57	62	-	53	55	61	-	52	53.9	59	-	49	51	56	-	46	47	52	-
		SHR	0.7	0.6	0.4	-	0.8	0.6	0.4	-	0.8	0.7	0.5	-	0.8	0.68	0.47	-	0.8	0.7	0.5	-	0.9	0.7	0.5	-
		ΔT	19	16	13	-	19	17	13	-	19	17	13	-	19	17	13	-	19	17	13	-	18	15	12	-
		TPC	3.6	3.6	3.7	-	3.8	3.9	4	-	4.1	4.1	4.3	-	4.3	4.36	4.5	-	4.4	4.5	4.7	-	4.6	4.7	4.9	-
	1750	CAP	54	56	62	-	53	55	60	-	52	54	59	-	50	52.3	57.3	-	48	50	54	-	44	46	50	-
		SHR	0.7	0.6	0.4	-	0.7	0.6	0.4	-	0.8	0.6	0.4	-	0.8	0.65	0.45	-	0.8	0.7	0.5	-	0.8	0.7	0.5	-
		ΔT	20	17	13	-	20	18	13	-	20	18	13	-	21	18	14	-	20	18	13	-	19	16	12	-
		TPC	3.5	3.6	3.7	-	3.8	3.9	4	-	4	4.1	4.2	-	4.2	4.32	4.46	-	4.4	4.5	4.7	-	4.6	4.7	4.8	-
	1600	CAP	53	55	61	-	52	54	59	-	51	53	58	-	50	51.5	56.4	-	47	49	54	-	44	45	50	-
		SHR	0.7	0.6	0.4	-	0.7	0.6	0.4	-	0.7	0.6	0.4	-	0.8	0.62	0.43	-	0.8	0.7	0.5	-	0.8	0.7	0.5	-
		ΔT	21	18	14	-	21	18	14	-	21	18	14	-	21	18	14	-	21	18	14	-	20	17	13	-
		TPC	3.5	3.6	3.7	-	3.7	3.8	3.9	-	4	4.1	4.2	-	4.2	4.26	4.4	-	4.3	4.4	4.6	-	4.5	4.6	4.7	-
75	2000	CAP	57	59	63	68	56	57	62	66	54	56	60	65	53	54.4	58.9	63	50	52	56	60	47	48	52	56
		SHR	0.8	0.8	0.6	0.4	0.9	0.8	0.6	0.4	0.9	0.8	0.6	0.4	0.9	0.83	0.63	0.4	1	0.9	0.7	0.4	1	0.9	0.7	0.4
		ΔT	22	20	17	11	22	21	17	12	22	21	17	12	22	21	17	12	22	20	17	12	21	19	16	11
		TPC	3.6	3.7	3.8	3.9	3.9	3.9	4.1	4.2	4.1	4.2	4.3	4.5	4.3	4.39	4.53	4.7	4.5	4.6	4.7	4.9	4.6	4.7	4.9	5.1
	1750	CAP	55	57	62	66	54	56	60	64	53	54	59	63	51	**52.8**	57.2	61	49	50	54	58	45	47	50	54
		SHR	0.8	0.7	0.5	0.4	0.8	0.7	0.6	0.4	0.9	0.8	0.6	0.4	0.9	**0.79**	0.6	0.4	0.9	0.8	0.6	0.4	0.9	0.8	0.6	0.4
		ΔT	23	21	18	12	24	22	18	12	24	22	18	12	24	**22**	18	12	23	22	18	12	22	20	17	11
		TPC	3.6	3.6	3.7	3.9	3.8	3.9	4	4.2	4.1	4.1	4.3	4.4	4.3	**4.36**	4.5	4.6	4.4	4.5	4.7	4.8	4.6	4.7	4.9	5
	1600	CAP	54	56	61	65	53	55	59	64	52	53	58	62	51	52	56.3	60	48	49	54	57	45	46	50	53
		SHR	0.8	0.7	0.5	0.3	0.8	0.7	0.5	0.4	0.8	0.7	0.6	0.4	0.9	0.76	0.58	0.4	0.9	0.8	0.6	0.4	0.9	0.8	0.6	0.4
		ΔT	24	22	18	13	24	23	18	13	25	23	18	13	25	23	19	13	24	22	18	13	23	21	17	12
		TPC	3.5	3.6	3.7	3.8	3.8	3.9	4	4.1	4	4.1	4.2	4.4	4.2	4.3	4.43	4.6	4.4	4.5	4.6	4.8	4.5	4.6	4.8	4.9
80	2000	CAP	58	59	63	68	57	58	62	66	55	56	60	64	54	55	58.7	63	51	52	56	60	47	48	52	55
		SHR	0.9	0.9	0.7	0.5	1	0.9	0.7	0.6	1	0.9	0.8	0.6	1	0.95	0.77	0.6	1	1	0.8	0.6	1	1	0.8	0.6
		ΔT	25	24	20	16	25	24	21	17	25	24	21	17	25	24	21	17	23	24	21	16	22	22	19	15
		TPC	3.6	3.7	3.8	3.9	3.9	4	4.1	4.2	4.1	4.2	4.3	4.5	4.3	4.43	4.57	4.7	4.5	4.6	4.8	4.9	4.7	4.8	4.9	5.1
	1750	CAP	56	57	61	66	55	56	60	64	54	55	58	63	52	53.4	**57**	61	50	51	54	58	46	47	50	54
		SHR	0.9	0.8	0.7	0.5	0.9	0.9	0.7	0.5	0.9	0.9	0.7	0.5	1	0.91	**0.74**	0.6	1	0.9	0.8	0.6	1	1	0.8	0.6
		ΔT	26	25	22	17	26	25	22	18	26	25	22	18	27	25	**22**	18	26	25	22	17	24	23	20	16
		TPC	3.6	3.7	3.8	3.9	3.9	3.9	4.1	4.2	4.1	4.2	4.3	4.5	4.3	4.39	**4.53**	4.7	4.5	4.6	4.7	4.9	4.6	4.7	4.9	5.1
	1600	CAP	55	57	60	65	54	55	59	63	53	54	58	62	51	52.6	56.1	60	49	50	53	57	45	46	49	53
		SHR	0.9	0.8	0.7	0.5	0.9	0.8	0.7	0.5	0.9	0.9	0.7	0.5	0.9	0.87	0.71	0.5	1	0.9	0.7	0.6	1	0.9	0.7	0.6
		ΔT	27	26	23	18	27	26	23	18	27	26	23	18	28	26	23	18	27	26	23	18	25	24	21	17
		TPC	3.5	3.6	3.7	3.8	3.8	3.9	4	4.1	4	4.1	4.3	4.4	4.2	4.33	4.47	4.6	4.4	4.5	4.7	4.8	4.6	4.7	4.8	5
85	2000	CAP	59	60	63	67	58	59	61	65	56	57	60	64	55	55.8	58.4	62	52	53	56	59	48	49	51	55
		SHR	1	0.9	0.8	0.7	1	1	0.9	0.7	1	1	0.9	0.7	1	1	0.93	0.8	1	1	1	0.8	1	1	1	0.8
		ΔT	26	26	24	21	26	26	25	21	26	26	25	21	25	26	25	22	24	24	25	21	22	23	23	20
		TPC	3.6	3.7	3.8	4	3.9	4	4.1	4.3	4.2	4.2	4.4	4.5	4.4	4.46	4.61	4.8	4.6	4.7	4.8	5	4.7	4.8	5	5.1
	1750	CAP	57	58	61	65	56	57	60	64	55	56	58	62	53	54.2	56.7	61	51	51	54	58	47	48	50	53
		SHR	0.9	0.9	0.8	0.7	1	0.9	0.8	0.7	1	1	0.9	0.7	1	0.98	0.88	0.7	1	1	0.9	0.7	1	1	0.9	0.8
		ΔT	28	27	26	22	28	28	26	23	28	28	26	23	28	28	26	23	27	27	26	22	25	25	24	21
		TPC	3.6	3.7	3.8	3.9	3.9	4	4.1	4.2	4.1	4.2	4.3	4.5	4.3	4.43	4.57	4.7	4.5	4.6	4.8	4.9	4.7	4.8	4.9	5.1
	1600	CAP	56	57	60	64	55	56	59	63	54	55	57	61	52	53.3	55.9	60	50	51	53	57	46	47	49	52
		SHR	0.9	0.9	0.8	0.6	0.9	0.9	0.8	0.7	1	0.9	0.8	0.7	1	0.94	0.85	0.7	1	1	0.9	0.7	1	1	0.9	0.7
		ΔT	29	28	27	23	29	29	27	23	29	29	27	23	29	29	27	24	29	29	27	23	26	27	25	22
		TPC	3.6	3.6	3.8	3.9	3.8	3.9	4	4.2	4.1	4.2	4.3	4.4	4.3	4.37	4.51	4.7	4.5	4.6	4.7	4.9	4.6	4.7	4.9	5

Table E-6 Carrier model 25HBB324,36 and 60 cooling performance data

Model 25HBB3-	EVAP Air		CONDENSER ENTERING AIR TEMPERATURES ° F (° C)																	
			75			85			95			105			115			125		
		WB	Capacity MBtuh		Total System KW**	Capacity MBtuh		Total System KW**	Capacity MBtuh		Total System KW**	Capacity MBtuh		Total System KW**	Capacity MBtuh		Total System KW**	Capacity MBtuh		Total System KW**
	CFM	F	Total	Sens‡		Total	Sens‡		Total	Sens‡		Total	Sens‡		Total	Sens‡		Total	Sens‡	
25HBB324		72	26.97	13.8	1.66	25.72	13.32	1.86	24.41	12.81	2.09	23.03	12.29	2.34	21.54	11.73	2.61	19.91	11.13	2.91
	700	67	24.65	17.15	1.66	23.49	16.65	1.86	22.26	16.12	2.09	20.97	15.57	2.34	19.59	15	2.62	18.09	14.38	2.92
		62	22.5	20.46	1.66	21.42	19.93	1.86	20.3	19.36	2.09	19.14	18.75	2.34	17.96	17.96	2.62	16.82	16.82	2.92
		57	21.73	21.73	1.66	20.87	20.87	1.86	19.96	19.96	2.09	19	19	2.34	17.96	17.96	2.62	16.82	16.82	2.92
		72	27.42	14.42	1.69	26.13	13.93	1.9	24.76	13.42	2.12	24.27	13.23	2.06	21.8	12.33	2.65	20.12	11.72	2.94
	800	67	25.09	18.2	1.69	23.88	17.68	1.9	22.6	17.15	2.12	21.27	16.6	2.37	19.84	16.01	2.65	18.29	15.38	2.95
		62	22.96	21.88	1.69	21.86	21.3	1.9	20.72	20.69	2.13	19.67	19.67	2.38	18.57	18.57	2.65	17.37	17.37	2.95
		57	22.57	22.57	1.69	21.66	21.66	1.9	20.7	20.7	2.13	19.67	19.67	2.38	18.57	18.57	2.65	17.37	17.37	2.95
		72	27.75	15.01	1.73	26.42	14.51	1.93	26.1	14.39	1.86	24.55	13.82	2.09	22.87	13.22	2.36	20.25	12.28	2.98
	900	67	25.4	19.19	1.73	24.16	18.68	1.93	**22.85**	**18.13**	**2.16**	21.48	17.57	2.41	20.02	16.97	2.69	18.43	16.31	2.98
		62	23.36	23.12	1.73	22.32	22.31	1.93	21.3	21.3	2.16	20.23	20.23	2.41	19.07	19.07	2.69	17.81	17.81	2.99
		57	23.27	23.27	1.73	22.31	22.31	1.93	21.3	21.3	2.16	20.23	20.23	2.41	19.07	19.07	2.69	17.81	17.81	2.99
25HBB336		72	40.35	20.31	2.51	38.48	19.62	2.8	36.5	18.89	3.11	34.43	18.14	3.45	32.16	17.33	3.83	29.64	16.44	4.23
	1050	67	37.01	25.58	2.51	35.27	24.86	2.79	33.42	24.11	3.1	31.48	23.33	3.45	29.38	22.49	3.82	27.05	21.56	4.22
		63	34.54	24.77	2.5	32.9	24.03	2.79	31.16	23.28	3.1	29.32	22.48	3.44	27.34	21.63	3.81	25.16	20.69	4.21
		62	33.94	30.74	2.5	32.35	29.94	2.79	30.69	29.07	3.1	28.99	28.99	3.44	27.35	27.35	3.81	25.55	25.55	4.21
		57	33.16	33.16	2.5	31.86	31.86	2.78	30.46	30.46	3.1	28.98	28.98	3.44	27.35	27.35	3.81	25.55	25.55	4.21
	1200	67	37.51	27.1	2.57	35.71	26.37	2.85	33.8	25.6	3.16	31.81	24.81	3.51	29.64	23.95	3.88	27.26	22.99	4.28
		63	35.04	26.19	2.57	33.34	25.45	2.85	31.54	24.68	3.16	29.65	23.87	3.5	27.61	22.99	3.87	25.38	22.02	4.27
		62	34.55	32.68	2.56	32.93	32.93	2.85	31.42	31.42	3.16	29.85	29.85	3.5	28.14	28.14	3.88	26.23	26.23	4.28
		57	34.28	34.28	2.56	32.89	32.89	2.85	31.42	31.42	3.16	29.86	29.86	3.5	28.15	28.15	3.88	26.24	26.24	4.28
	1350	67	37.88	28.58	2.63	36.03	27.84	2.91	**34.08**	**27.06**	**3.23**	32.04	26.24	3.57	29.83	25.34	3.94	27.41	24.33	4.34
		63	35.42	27.58	2.63	33.67	26.83	2.91	31.82	26.03	3.22	29.89	25.19	3.56	27.81	24.27	3.94	25.54	23.24	4.34
		62	35.17	35.17	2.63	33.73	33.73	2.91	32.18	32.18	3.22	30.55	30.55	3.57	28.77	28.77	3.94	26.77	26.77	4.34
		57	35.18	35.18	2.63	33.73	33.73	2.91	32.19	32.19	3.22	30.55	30.55	3.57	28.77	28.77	3.94	26.77	26.77	4.34
25HBB360		72	70.34	35.38	4.52	67.1	34.14	4.98	63.63	32.83	5.48	60.01	31.48	6.03	56.06	30.03	6.63	51.7	28.45	7.27
	1750	67	64.72	44.25	4.46	61.72	42.98	4.92	58.5	41.62	5.42	55.15	40.23	5.97	51.5	38.73	6.57	47.5	37.11	7.21
		63	60.52	42.98	4.41	57.68	41.67	4.87	54.66	40.31	5.37	51.5	38.9	5.92	48.09	37.4	6.52	44.37	35.78	7.17
		62	59.39	53.03	4.4	56.6	51.67	4.86	53.67	50.23	5.36	50.63	48.68	5.91	47.46	47.46	6.51	44.4	44.4	7.17
		57	57.36	57.36	4.38	55.12	55.12	4.84	52.73	52.73	5.35	50.21	50.21	5.9	47.45	47.45	6.51	44.4	44.4	7.17
	2000	67	65.71	46.88	4.58	62.6	45.59	5.03	59.26	44.22	5.53	55.79	42.8	6.08	52.01	41.28	6.69	47.89	39.62	7.33
		63	61.54	45.45	4.53	58.58	44.14	4.99	55.44	42.75	5.49	52.17	41.32	6.04	48.63	39.78	6.64	44.8	38.11	7.28
		62	60.48	56.64	4.52	57.63	55.18	4.98	54.66	54.31	5.48	51.85	51.85	6.03	48.91	48.91	6.64	45.66	45.66	7.3
		57	59.46	59.46	4.51	57.07	57.07	4.97	54.53	54.53	5.48	51.85	51.85	6.03	48.92	48.92	6.64	45.67	45.67	7.3
	2250	67	66.4	49.38	4.7	63.21	48.09	5.15	**59.77**	**46.69**	**5.65**	56.21	45.25	6.2	52.34	43.69	6.8	48.13	41.98	7.44
		63	62.26	47.81	4.65	59.21	46.48	5.1	55.98	45.06	5.6	52.62	43.6	6.15	49	42.02	6.75	45.07	40.3	7.4
		62	61.41	59.8	4.64	58.65	58.65	5.1	55.97	55.97	5.61	53.15	53.15	6.16	50.06	50.06	6.77	46.64	46.64	7.42
		57	61.16	61.16	4.64	58.65	58.65	5.1	55.97	55.97	5.61	53.16	53.16	6.16	50.07	50.07	6.77	46.65	46.65	7.42

Table E-7 York model CZF0- cooling performance data

Model CZF0-	EVAPORATOR AIR			CONDENSER ENTERING AIR TEMPERATURES ° F (° C)																			
				65			75			85			95			105			115			125		
		DB	WB	Capacity MBtuh		Total System	Capacity MBtuh		Total System	Capacity MBtuh		Total System	Capacity MBtuh		Total System	Capacity MBtuh		Total System	Capacity MBtuh		Total System	Capacity MBtuh		Total System
	CFM	F	F	Total	Sens‡	KW**	Total	Sens‡	KW**	Total	Sens‡	KW**	Total	Sens‡	KW**	Total	Sens‡	KW**	Total	Sens‡	KW**	Total	Sens‡	KW**
	YORK split system CZF02413(C) Outdoor Section With FC/MC/PC35 Indoor Section																						
CZF024	600	80	57	20	20	1.32	19	19	1.5	18	18	1.68	17	17	1.87	16.1	16.1	2.24	15.2	15.2	2.61	14.3	14.3	2.97
	600	80	62	22	19.1	1.3	21.2	18.7	1.49	20.3	18.3	1.69	19.5	17.9	1.88	18.3	17.2	2.23	17.1	16.5	2.57	15.9	15.8	2.91
	600	75	62	22.8	16.8	1.3	21.6	16.1	1.49	20.4	15.4	1.68	19.3	14.7	1.88	18.1	14.2	2.22	17	13.6	2.56	15.9	13.1	2.9
	600	80	67	25.2	16.7	1.31	24.2	16.1	1.49	23.1	15.5	1.67	22	14.9	1.85	20.8	14.4	2.17	19.6	13.9	2.49	18.4	13.4	2.8
	600	80	72	28.1	13.4	1.3	26.9	12.9	1.49	25.7	12.4	1.67	24.4	11.9	1.85	23.2	11.4	2.15	22	10.9	2.44	20.8	10.4	2.73
	800	80	57	21.7	21.7	1.38	20.6	20.6	1.56	19.5	19.5	1.75	18.4	18.4	1.93	17.4	17.4	2.27	16.5	16.5	2.6	15.5	15.5	2.93
	800	80	62	23.5	22.1	1.37	22.6	21.6	1.56	21.8	21.1	1.75	20.9	20.7	1.94	19.6	19.6	2.27	18.3	18.3	2.59	17	17	2.91
	800	75	62	24.1	18.8	1.37	23.1	18.2	1.56	22	17.6	1.75	21	17	1.94	19.6	16.4	2.27	18.3	15.8	2.6	17	15.2	2.92
	800	80	67	27.1	19.1	1.38	26	18.4	1.56	24.8	17.7	1.74	**23.6**	**17**	**1.93**	22.3	16.5	2.24	21	15.9	2.54	19.8	15.4	2.84
	800	80	72	30.1	14.7	1.37	28.9	14.2	1.55	27.7	13.8	1.73	26.5	13.4	1.91	25.1	12.8	2.21	23.7	12.2	2.5	22.4	11.6	2.79
	1000	80	57	23.4	23.4	1.44	22.2	22.2	1.63	21.1	21.1	1.81	19.9	19.9	2	18.8	18.8	2.31	17.8	17.8	2.6	16.7	16.7	2.9
	1000	80	62	25	25	1.45	24.1	24.1	1.63	23.2	23.2	1.81	22.4	22.4	1.99	20.9	20.9	2.3	19.5	19.5	2.6	18.1	18.1	2.9
	1000	75	62	25.4	20.9	1.44	24.5	20.4	1.63	23.6	19.8	1.82	22.7	19.3	2	21.1	18.6	2.33	19.6	17.9	2.64	18.1	17.2	2.95
	1000	80	67	29.1	21.4	1.45	27.8	20.7	1.63	26.5	19.9	1.82	25.2	19.1	2	23.8	18.5	2.3	22.5	18	2.59	21.2	17.5	2.87
	1000	80	72	32.1	16	1.45	31	15.6	1.62	29.8	15.2	1.8	28.6	14.8	1.98	27.1	14.1	2.27	25.5	13.5	2.56	24	12.8	2.85
CZF036	1000	80	57	33.1	33.1	1.92	32.2	32.2	2.22	31.3	31.3	2.51	30.4	30.4	2.8	28.8	28.8	3.27	27.3	27.3	3.73	25.8	25.8	4.19
	1000	80	62	35	30.1	1.92	33.7	29.6	2.21	32.4	29.1	2.51	31	28.6	2.81	29.4	27.6	3.29	27.8	26.5	3.76	26.3	25.5	4.22
	1000	75	62	34.7	25.6	1.91	33.3	25	2.21	31.9	24.5	2.51	30.5	23.9	2.81	28.7	23.1	3.3	26.9	22.3	3.78	25.2	21.5	4.26
	1000	80	67	38.3	25.2	1.93	36.8	24.6	2.22	35.2	24	2.52	33.6	23.5	2.81	31.6	22.8	3.28	29.7	22.2	3.73	27.8	21.5	4.19
	1000	80	72	40	20.9	1.96	38.8	20	2.25	37.6	19.1	2.53	36.4	18.2	2.82	34.3	17.7	3.27	32.3	17.3	3.71	30.3	16.9	4.15
	1200	80	57	34.2	34.2	1.93	33.4	33.4	2.22	32.6	32.6	2.5	31.8	31.8	2.79	30.2	30.2	3.26	28.5	28.5	3.71	26.9	26.9	4.16
	1200	80	62	36.2	32.8	1.92	34.9	32.2	2.21	33.6	31.5	2.51	32.3	30.8	2.8	30.6	29.5	3.27	29.1	28.2	3.73	27.5	27	4.18
	1200	75	62	35.7	27.8	1.91	34.2	27.2	2.21	32.7	26.7	2.5	31.2	26.1	2.8	29.5	25.2	3.29	27.8	24.2	3.76	26.1	23.3	4.23
	1200	80	67	39.3	27.4	1.93	37.7	26.8	2.22	36	26.2	2.52	**34.4**	**25.6**	**2.81**	32.3	25	3.27	30.3	24.3	3.73	28.2	23.7	4.18
	1200	80	72	41.5	22.1	1.97	40	21.3	2.25	38.5	20.5	2.54	37.1	19.6	2.83	35	19	3.28	33	18.4	3.71	30.9	17.8	4.15
	1400	80	57	35.2	35.2	1.93	34.6	34.6	2.22	33.9	33.9	2.5	33.3	33.2	2.79	31.5	31.5	3.24	29.8	29.8	3.68	28.1	28.1	4.12
	1400	80	62	37.4	35.6	1.92	36.1	34.7	2.21	34.8	33.9	2.5	33.5	33.1	2.79	31.8	31.5	3.25	30.3	29.9	3.69	28.7	28.4	4.14
	1400	75	62	36.7	30	1.91	35.2	29.4	2.2	33.6	28.9	2.5	32	28.3	2.8	30.3	27.3	3.28	28.7	26.2	3.74	27	25.1	4.2
	1400	80	67	40.3	29.6	1.93	38.6	29	2.22	36.9	28.3	2.52	35.2	27.7	2.81	33	27.1	3.27	30.8	26.5	3.72	28.7	25.9	4.17
	1400	80	72	43	23.3	1.98	41.3	22.6	2.26	39.5	21.8	2.54	37.7	21.1	2.83	35.6	20.3	3.28	33.6	19.6	3.71	31.6	18.8	4.15
CZF060	1500	80	57	54.9	52	3.02	51.9	49.2	3.41	48.8	46.4	3.8	45.7	43.6	4.19	43.8	41.7	4.84	42	39.9	5.47	40.2	38.1	6.1
	1500	80	62	58	45.1	3.04	54.9	44.2	3.43	51.7	43.3	3.82	48.6	42.4	4.21	44.8	40.1	4.87	41.1	37.9	5.51	37.4	35.7	6.15
	1400	75	62	53	39.2	3.03	50.7	37.9	3.43	48.4	36.7	3.82	46.1	35.5	4.22	43.5	33.7	4.89	41	32	5.54	38.5	30.3	6.2
	1500	80	67	59	37.3	3.06	56.5	36.5	3.44	54	35.8	3.82	51.5	35.1	4.2	48.9	33.8	4.85	46.4	32.6	5.47	43.9	31.4	6.1
	1500	80	72	63.9	30.2	3.09	61.7	29.4	3.47	59.4	28.6	3.84	57.2	27.8	4.22	54.7	26.4	4.85	52.3	25.1	5.47	49.9	23.8	6.08
	1700	80	57	56.8	53.5	3.11	53.8	50.9	3.5	50.8	48.3	3.88	47.8	45.6	4.27	45.7	43.5	4.91	43.6	41.5	5.52	41.5	39.5	6.14
	1700	80	62	58.9	48.2	3.12	55.7	47.1	3.51	52.4	46	3.9	49.2	44.9	4.28	45.4	42	4.92	41.8	39.2	5.55	38.1	36.4	6.17
	1400	75	62	54.4	41	3.11	52.1	39.9	3.5	49.8	38.9	3.9	47.5	37.9	4.29	44.9	36.2	4.96	42.4	34.5	5.6	39.9	32.8	6.25
	1700	80	67	60.1	39.5	3.14	57.9	38.8	3.52	55.7	38.1	3.9	**53.5**	**37.4**	**4.28**	50.5	36	4.92	47.7	34.7	5.54	44.8	33.4	6.16
	1700	80	72	66.6	31.8	3.18	63.5	30.9	3.55	60.5	30	3.92	57.4	29.1	4.3	55.3	27.7	4.93	53.3	26.4	5.54	51.2	25.1	6.15
	1900	80	57	58.6	55.1	3.2	55.8	52.6	3.58	52.9	50.2	3.96	50	47.7	4.35	47.5	45.3	4.97	45.2	43.1	5.58	42.8	40.8	6.18
	1900	80	62	59.7	51.2	3.21	56.4	50	3.59	53.1	48.7	3.97	49.8	47.5	4.35	46.1	44	4.98	42.5	40.5	5.58	38.9	37.1	6.19
	1400	75	62	55.7	42.7	3.19	53.5	41.9	3.58	51.2	41.1	3.97	49	40.2	4.36	46.4	38.6	5.02	43.8	37	5.66	41.3	35.3	6.3
	1900	80	67	61.3	41.8	3.22	59.3	41.1	3.6	57.4	40.4	3.98	55.5	39.7	4.36	52.2	38.2	4.99	48.9	36.8	5.61	45.7	35.4	6.22
	1900	80	72	69.3	33.5	3.26	65.4	32.4	3.64	61.6	31.4	4.01	57.7	30.3	4.38	55.9	29	5	54.2	27.7	5.61	52.5	26.4	6.21

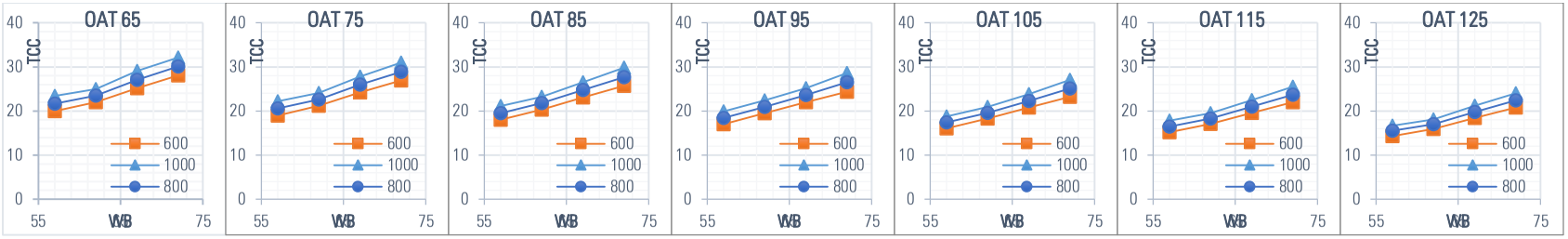

(a) Fixed OAT Cooling capacity plots

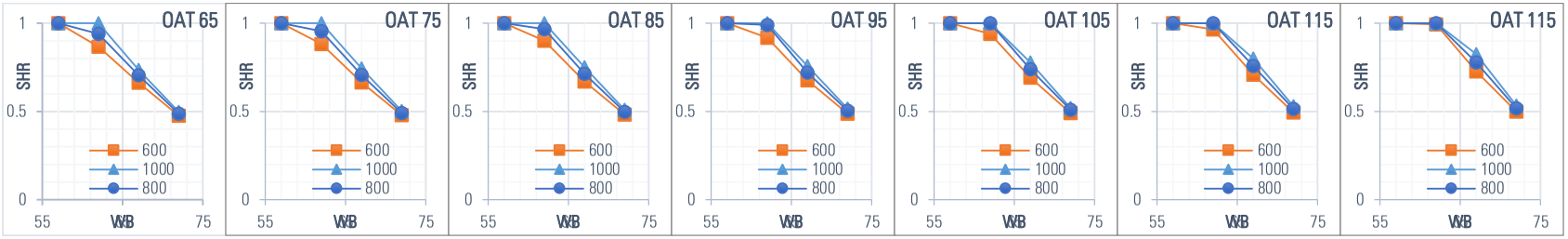

(b) Fixed OAT SHR plots

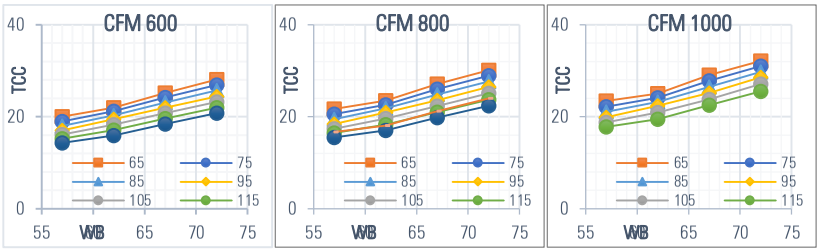

(c) Fixed CFM Cooling capacity plots

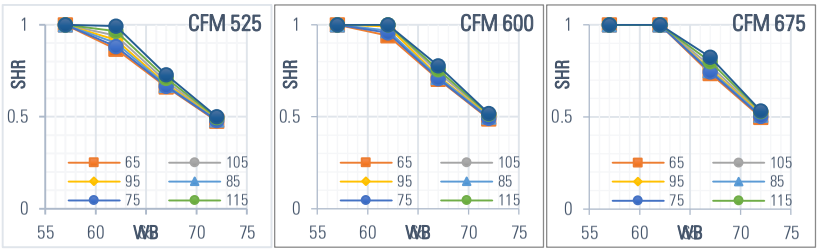

(d) Fixed CFM SHR plots

Figure E-1 York model CZF024 capacity and SHR performance plots at Fixed OAT and DB = 80°F

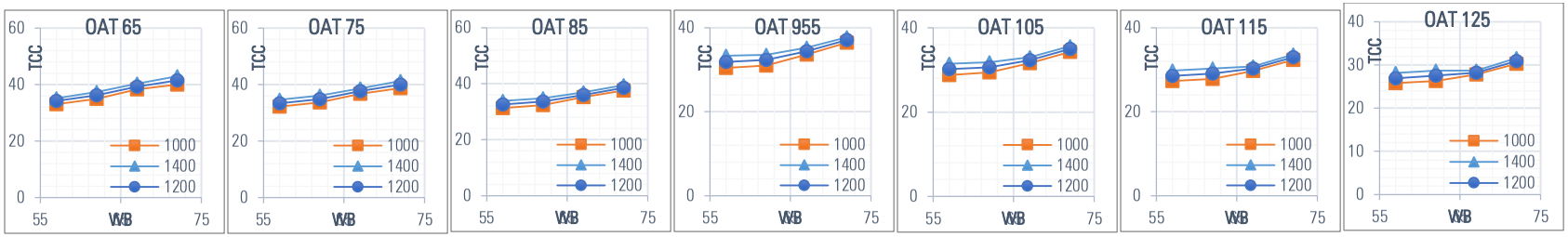

(a) Fixed OAT Cooling capacity plots

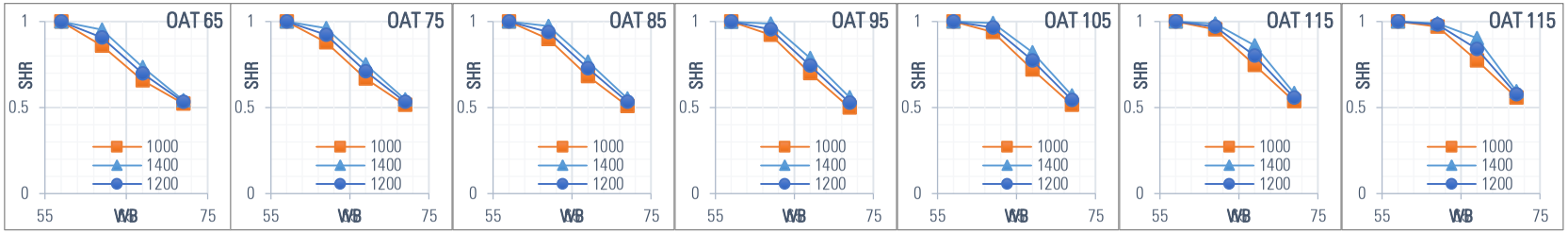

(b) Fixed OAT SHR plots

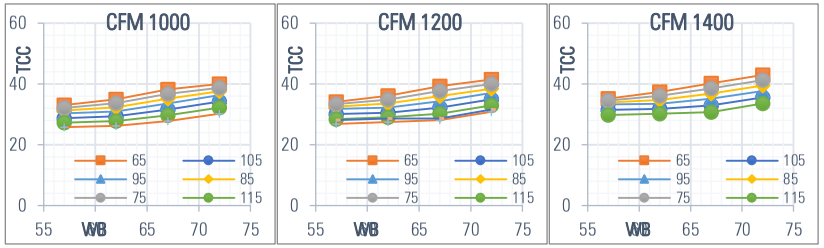

(c) Fixed CFM Cooling capacity plots

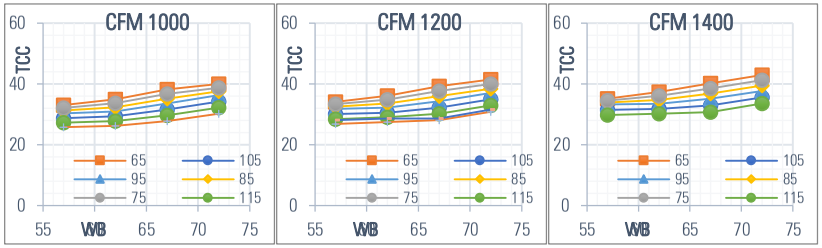

(d) Fixed CFM SHR plots

Figure E-2 York model CZF036 capacity and SHR performance plots at Fixed OAT and DB = 80°F

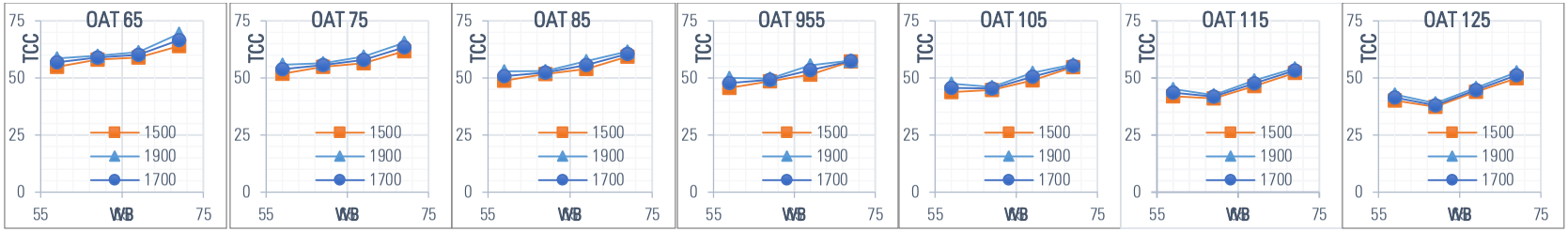

(a) Fixed OAT Cooling capacity plots

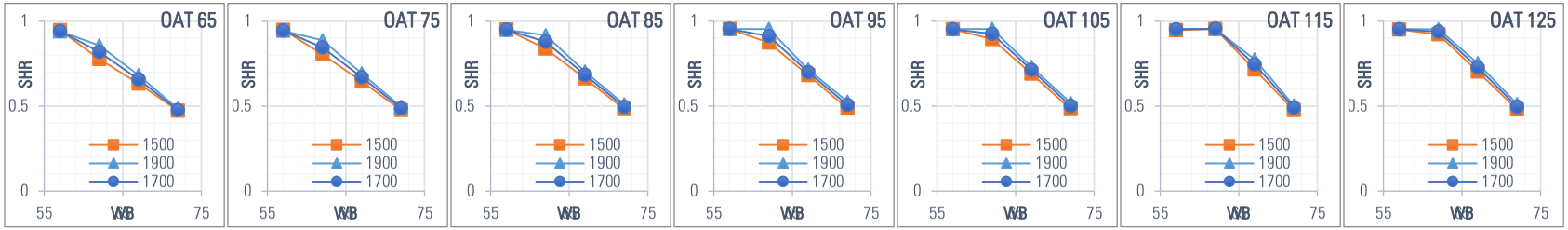

(b)Fixed OAT SHR plots

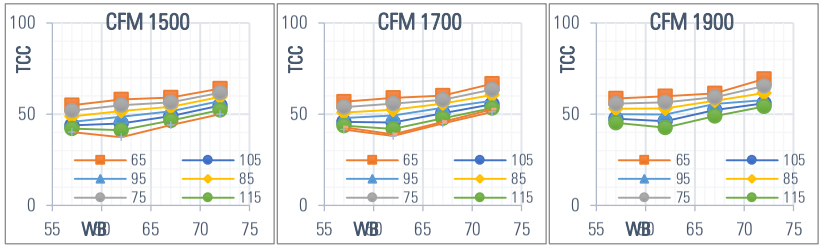

(c) Fixed CFM Cooling capacity plots

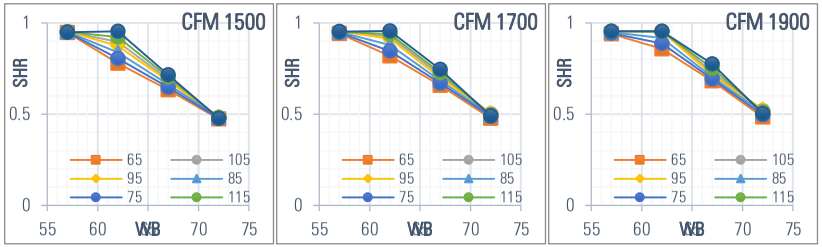

(d) Fixed CFM SHR plots

Figure E-3 York model CZF060 capacity and SHR performance plots at Fixed OAT and DB = 80°F

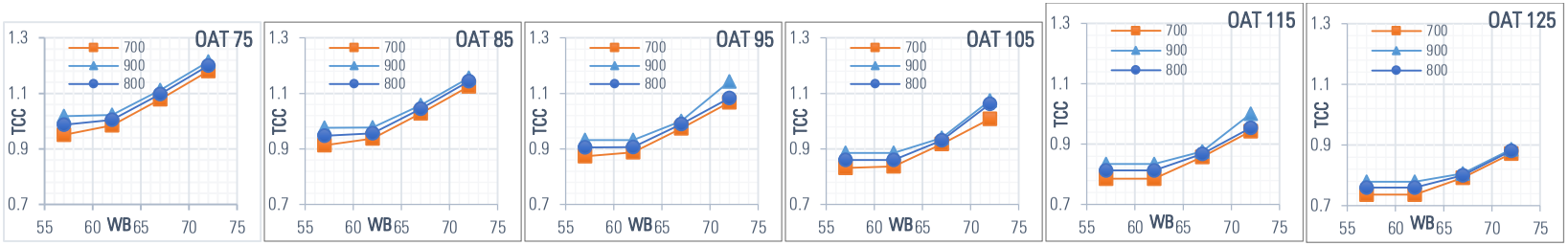

(a) Fixed OAT Cooling capacity plots

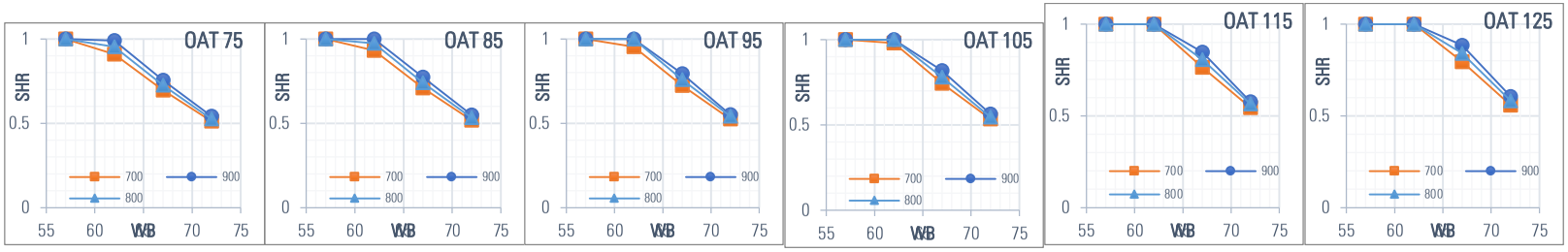

(b)Fixed OAT SHR plots

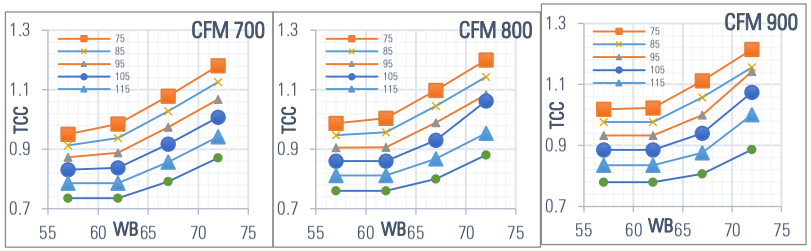

(c) Fixed CFM Cooling capacity plots

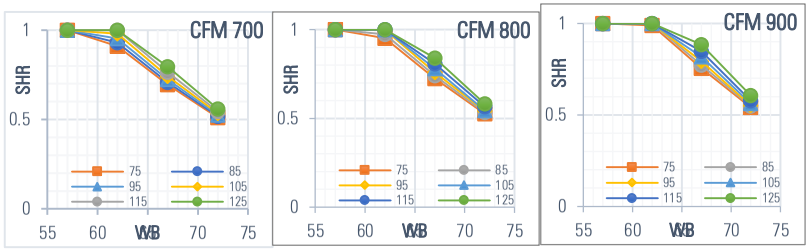

(d) Fixed CFM SHR plots

Figure E-4 Carrier model 25HBB324 capacity and SHR performance plots at Fixed OAT and DB = 80°F

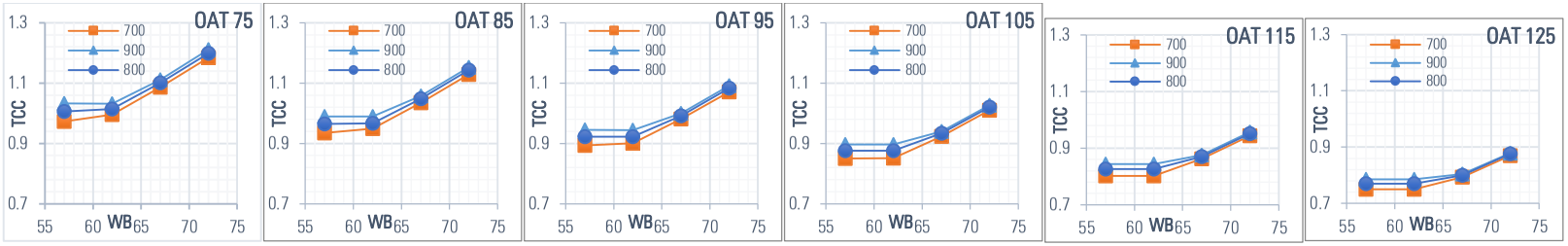

(a) Fixed OAT Cooling capacity plots

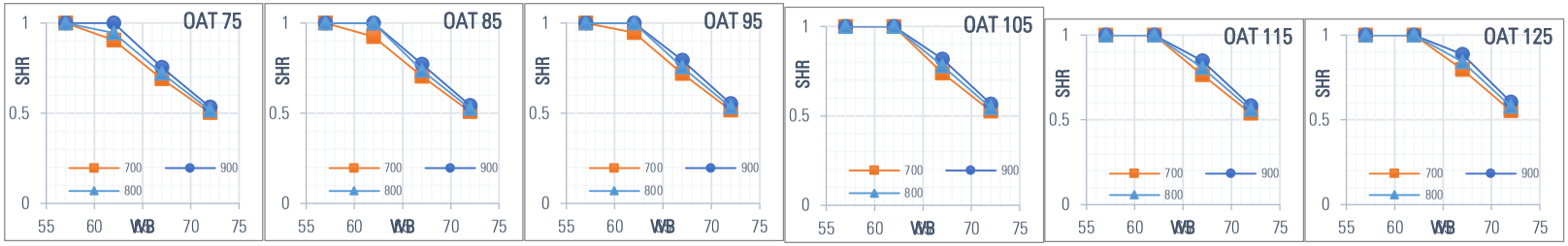

(b)Fixed OAT SHR plots

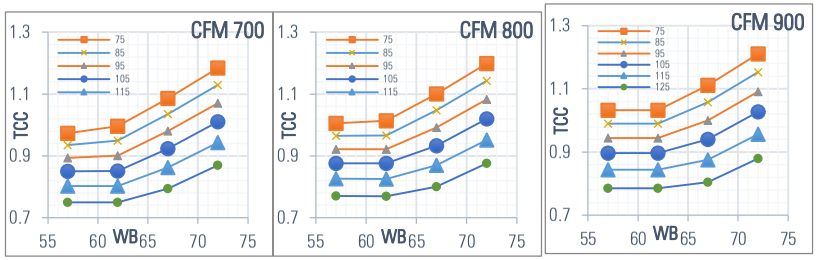

(c) Fixed CFM Cooling capacity plots

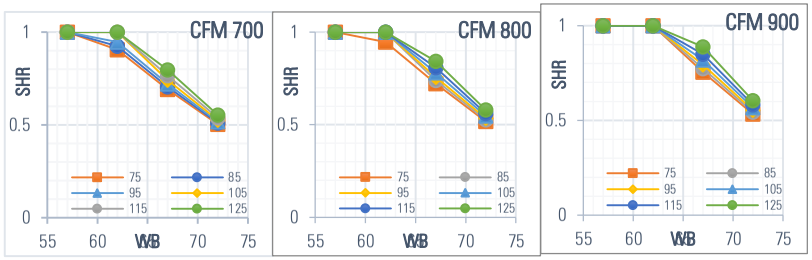

(d) Fixed CFM SHR plots

Figure E-5 Carrier model 25HBB336 capacity and SHR performance plots at Fixed OAT and DB = 80°F

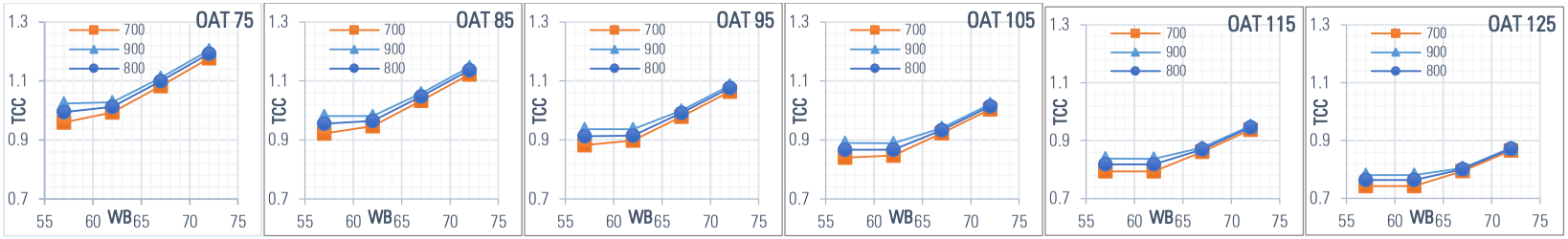

(a) Fixed OAT Cooling capacity plots

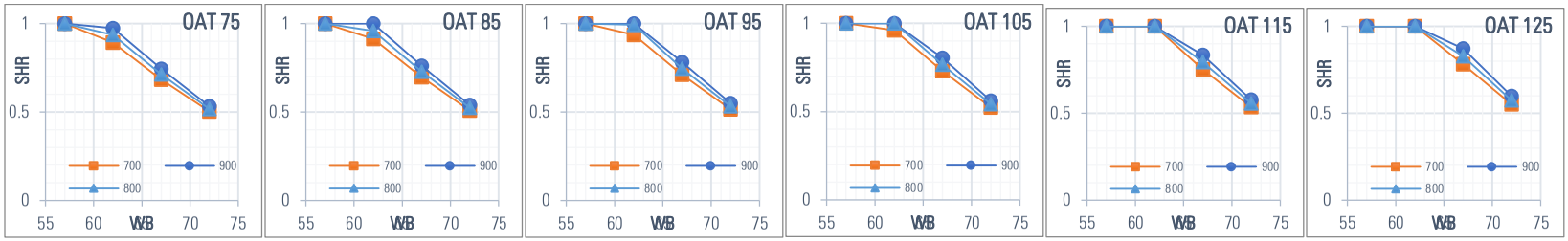

(b)Fixed OAT SHR plots

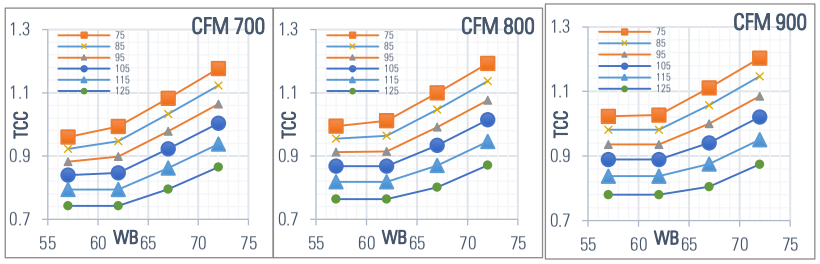

(c) Fixed CFM Cooling capacity plots

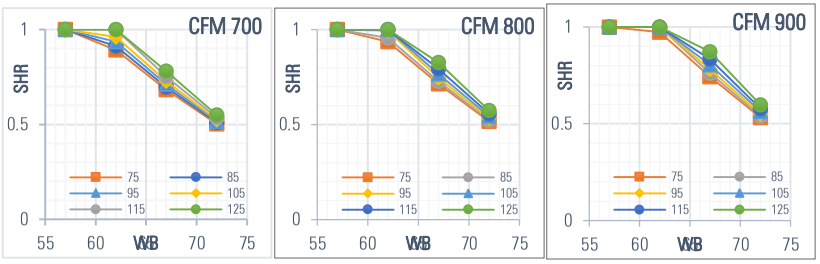

(d) Fixed CFM SHR plots

Figure E-6 Carrier model 25HBB360 normalized capacity and SHR performance plots at Fixed OAT and DB = 80°F

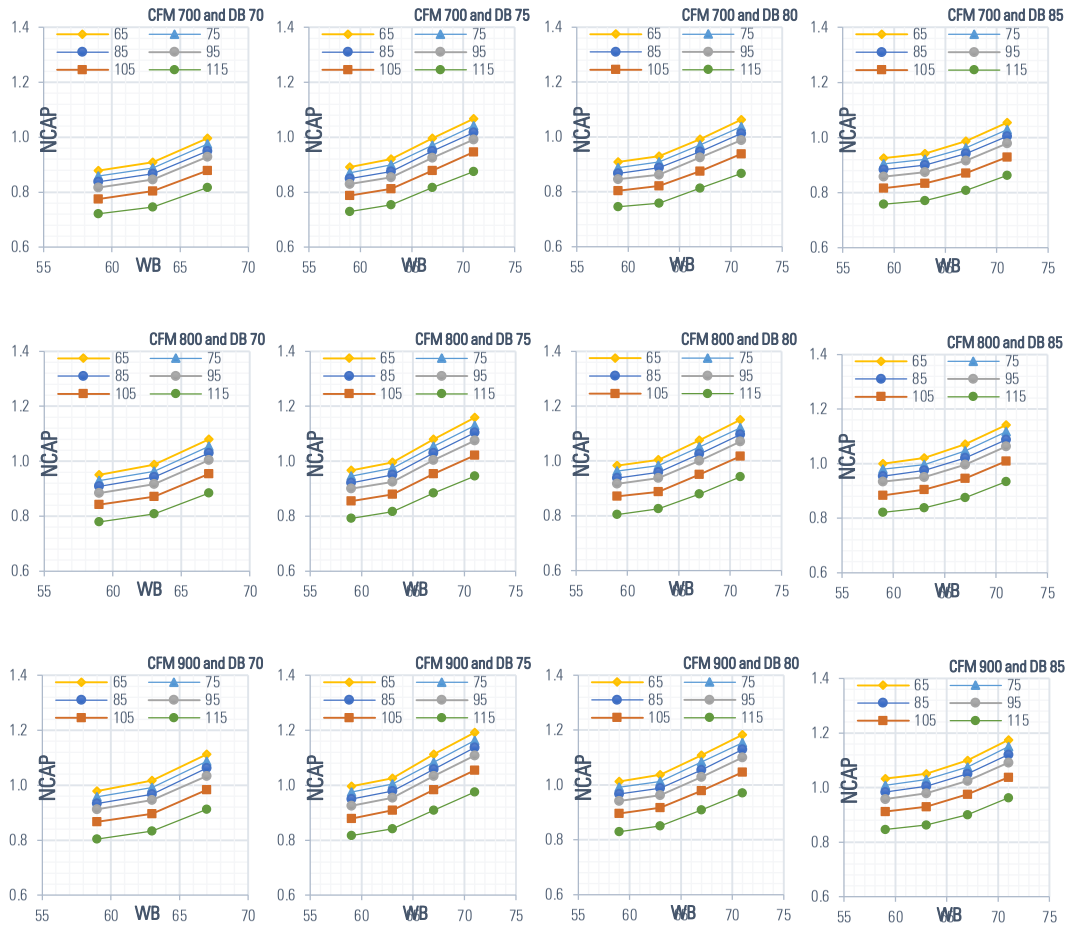

(a) Fixed CFM and DB, vary OAT: Cooling capacity plots

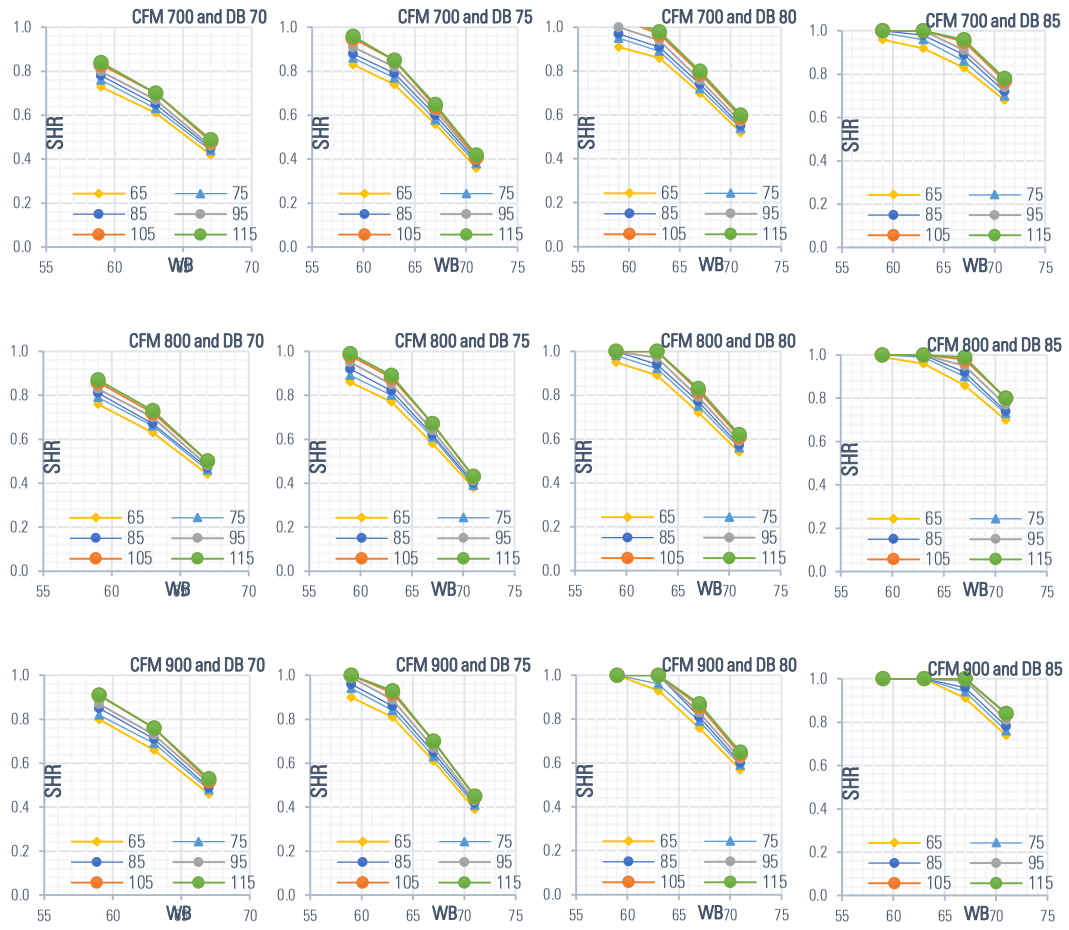

(b) Fixed CFM and DB, vary OAT: Cooling capacity plots

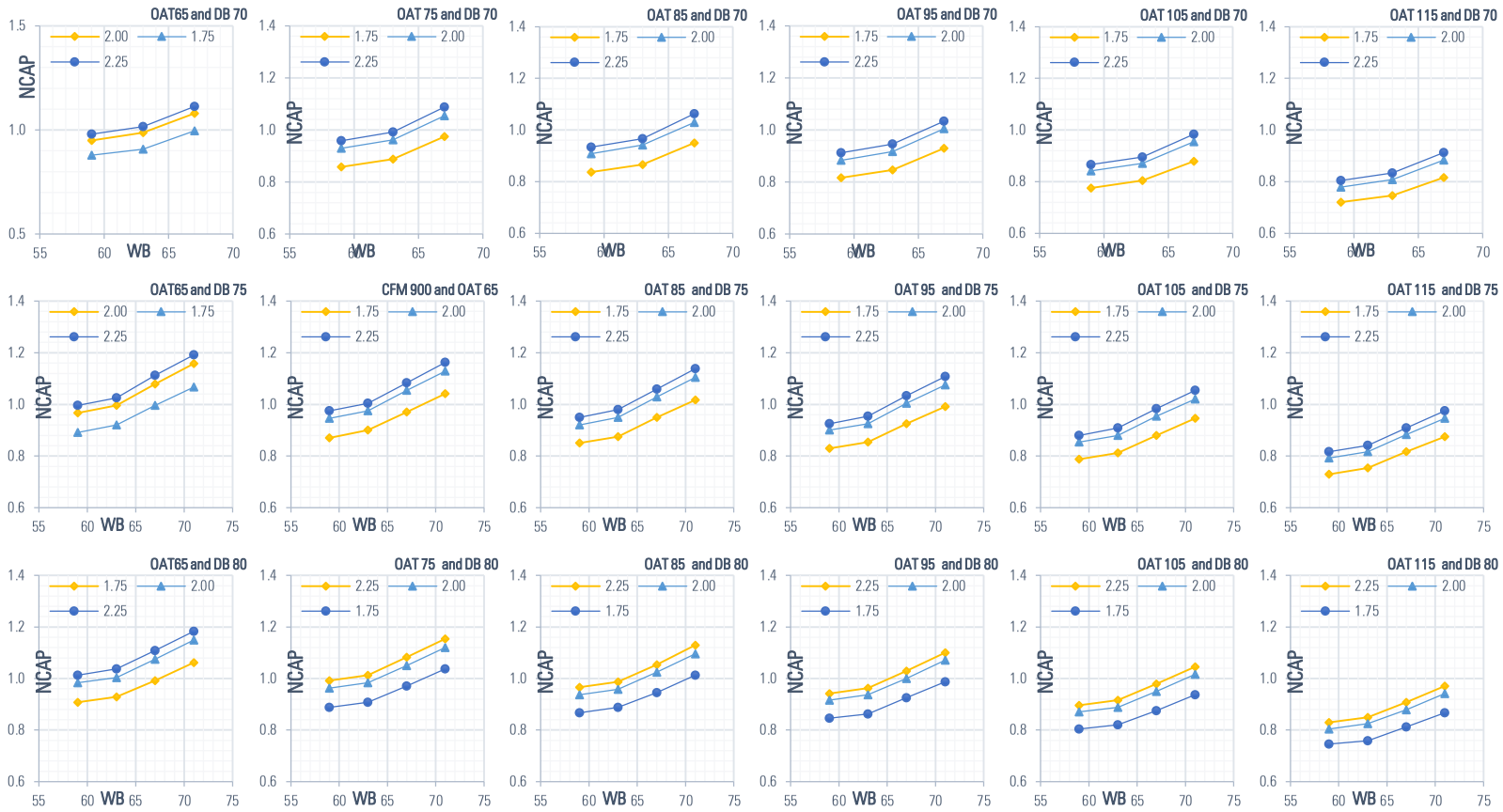
OAT65 and DB 70
2.00
1.75
2.25
NCAP
WB
OAT 75 and DB 70
1.75
2.00
2.25
OAT 85 and DB 70
OAT 95 and DB 70
OAT 105 and DB 70
OAT 115 and DB 70
OAT65 and DB 75
CFM 900 and OAT 65
OAT 85 and DB 75
OAT 95 and DB 75
OAT 105 and DB 75
OAT 115 and DB 75
OAT65 and DB 80
OAT 75 and DB 80
OAT 85 and DB 80
OAT 95 and DB 80
OAT 105 and DB 80
OAT 115 and DB 80

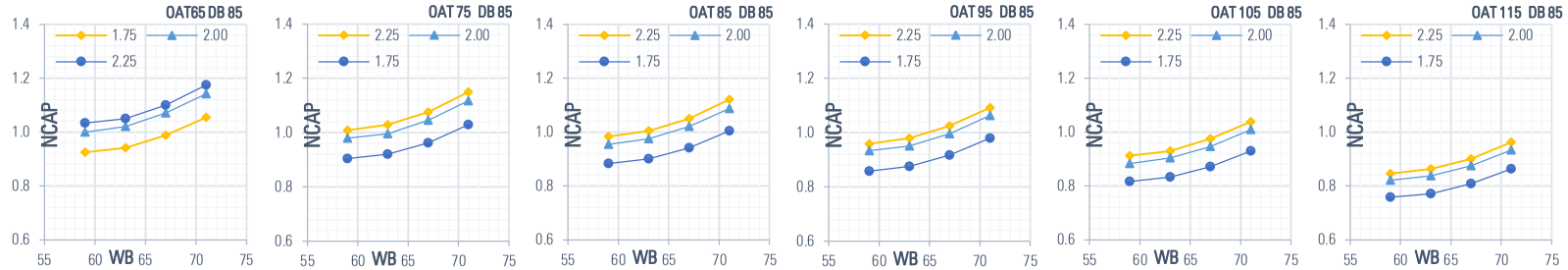

(c) Fixed OAT and DB, vary CFM: Cooling capacity plots

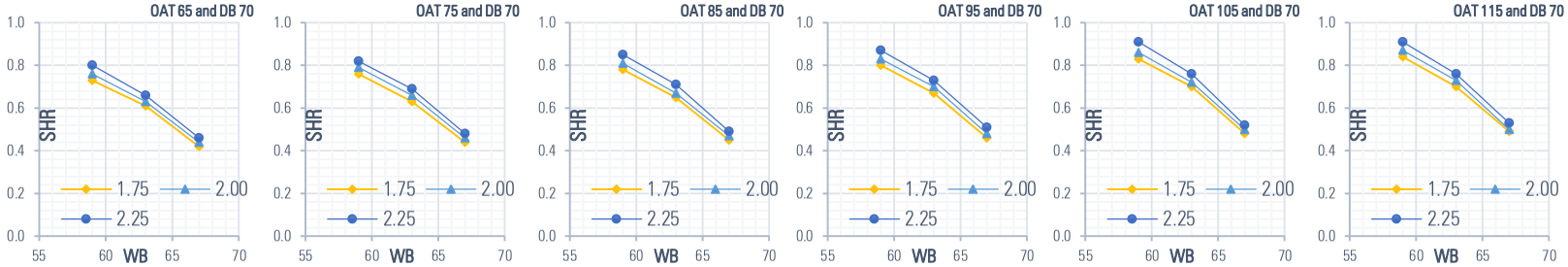

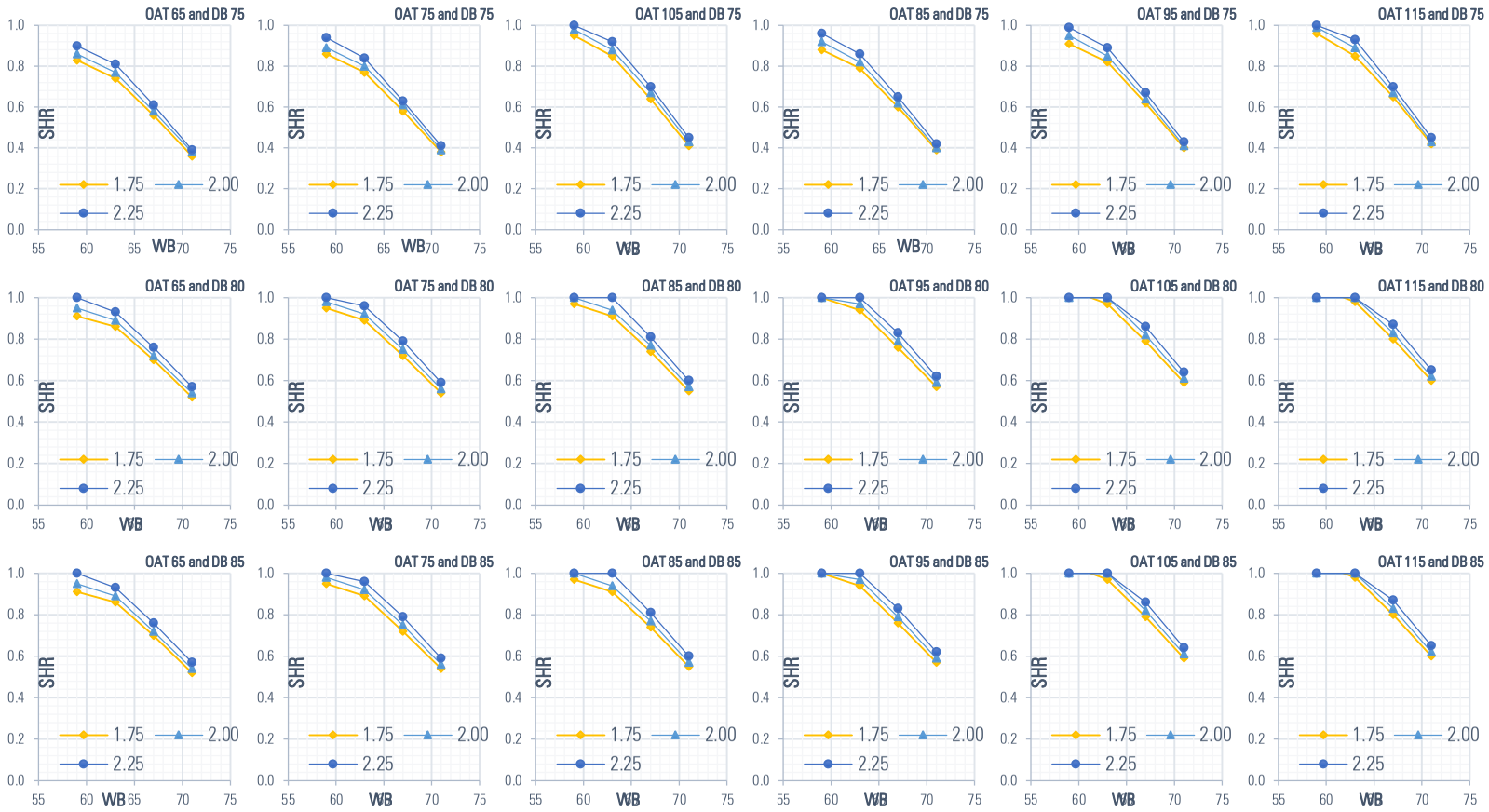

(d) Fixed OAT and DB, vary CFM: Cooling capacity plots

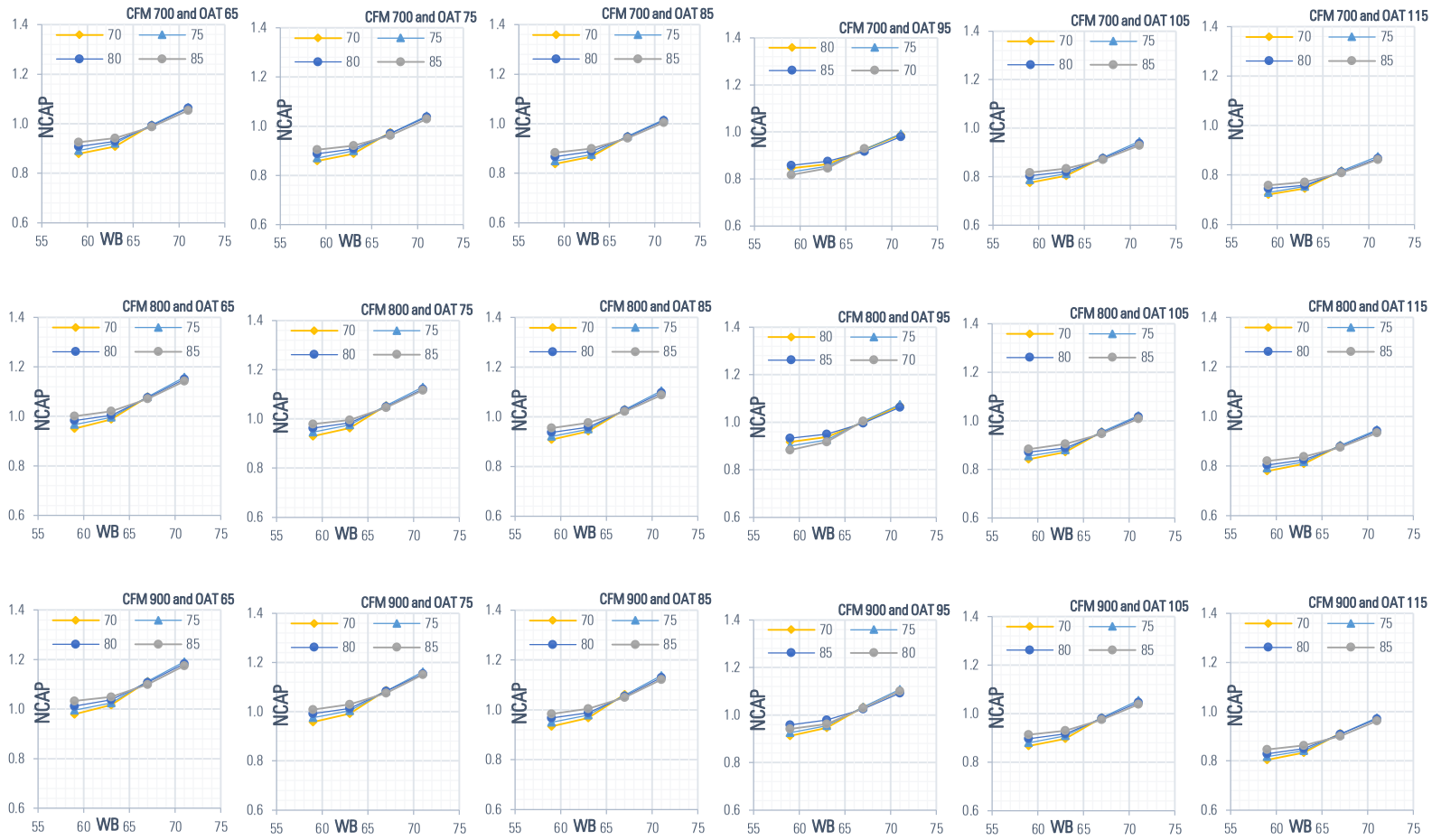

(e) Fixed OAT and CFM, vary DB: Cooling capacity plots

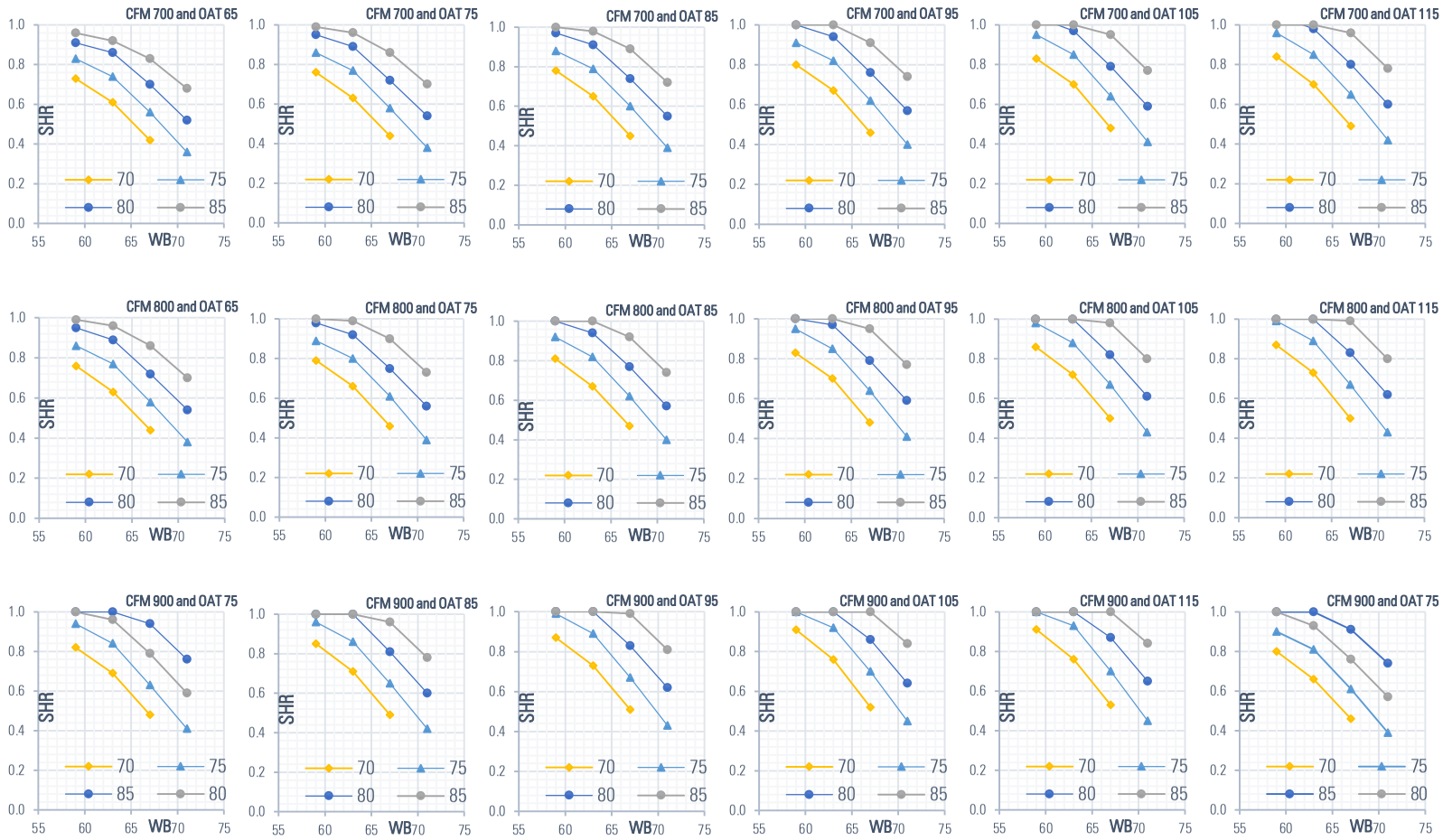

(f) Fixed OAT and CFM, vary DB: SHR plots

Figure E-7 Goodman model DAZ16-024 Normalized capacity and SHR performance plots

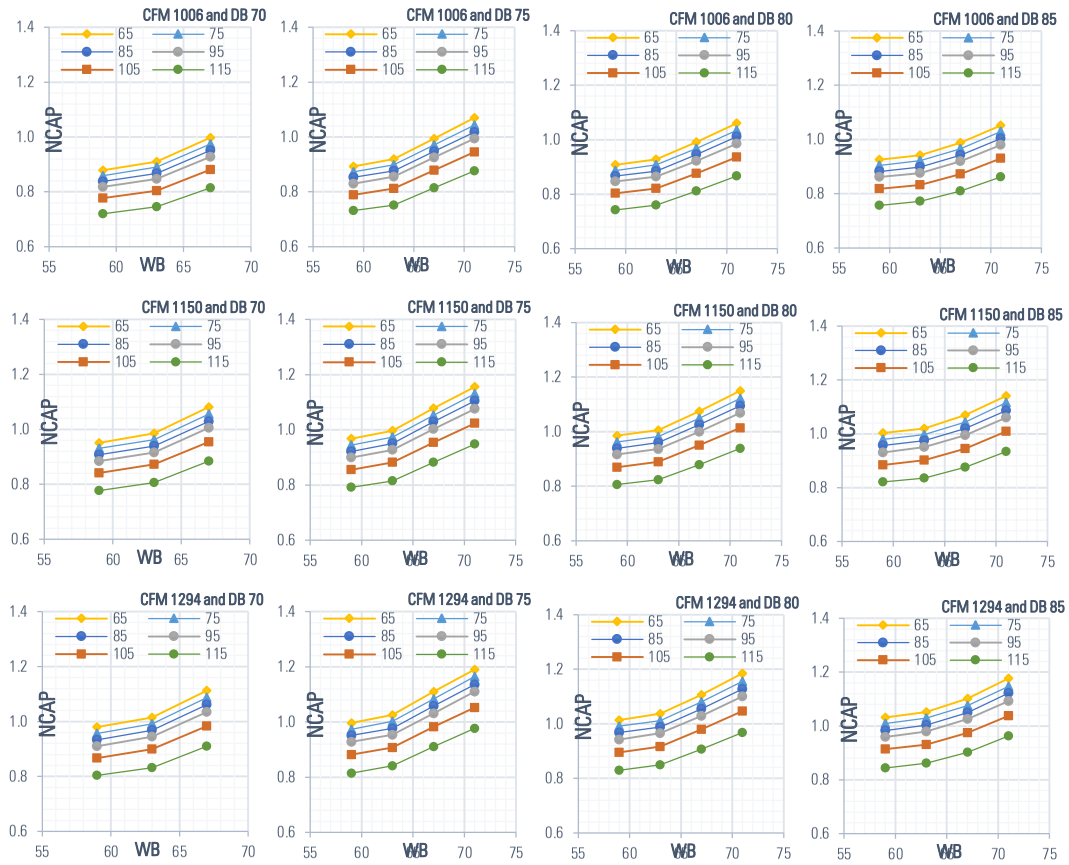

(a) Fixed CFM and DB, vary OAT: Cooling capacity plots

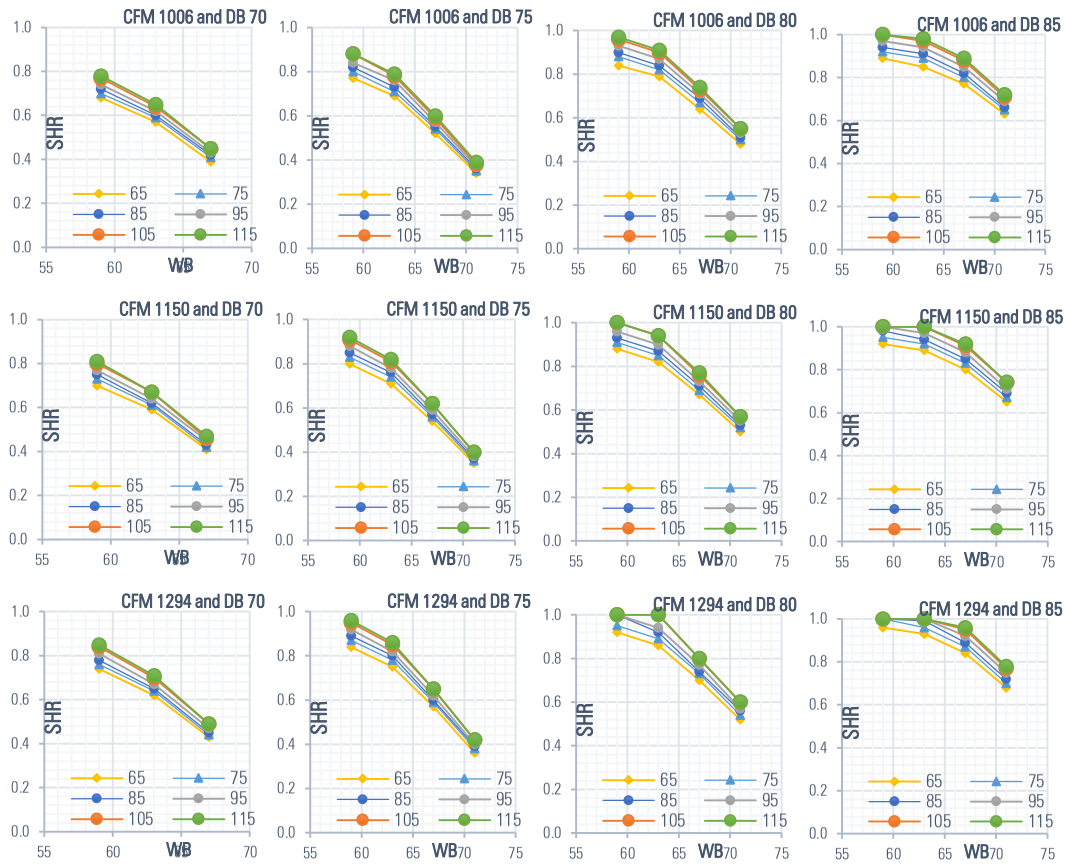

(b) Fixed CFM and DB, vary OAT: SHR plots

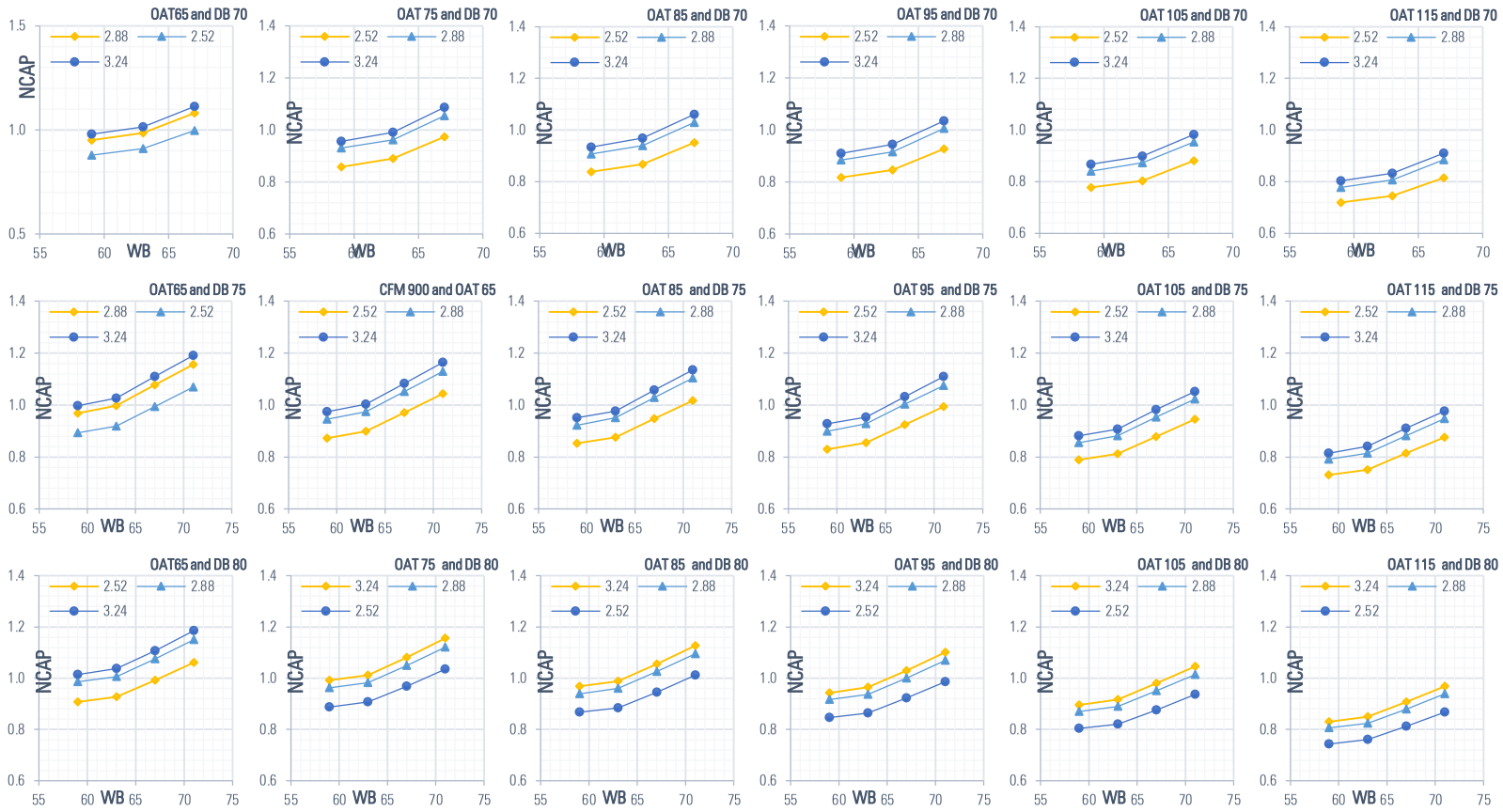
OAT65 and DB 70
2.88
2.52
3.24
OAT 75 and DB 70
2.52
2.88
3.24
OAT 85 and DB 70
2.52
2.88
3.24
OAT 95 and DB 70
2.52
2.88
3.24
OAT 105 and DB 70
2.52
2.88
3.24
OAT 115 and DB 70
2.52
2.88
3.24
OAT65 and DB 75
2.88
2.52
3.24
CFM 900 and OAT 65
2.52
2.88
3.24
OAT 85 and DB 75
2.52
2.88
3.24
OAT 95 and DB 75
2.52
2.88
3.24
OAT 105 and DB 75
2.52
2.88
3.24
OAT 115 and DB 75
2.52
2.88
3.24
OAT65 and DB 80
2.52
2.88
3.24
OAT 75 and DB 80
3.24
2.88
2.52
OAT 85 and DB 80
3.24
2.88
2.52
OAT 95 and DB 80
3.24
2.88
2.52
OAT 105 and DB 80
3.24
2.88
2.52
OAT 115 and DB 80
3.24
2.88
2.52
NCAP
WB

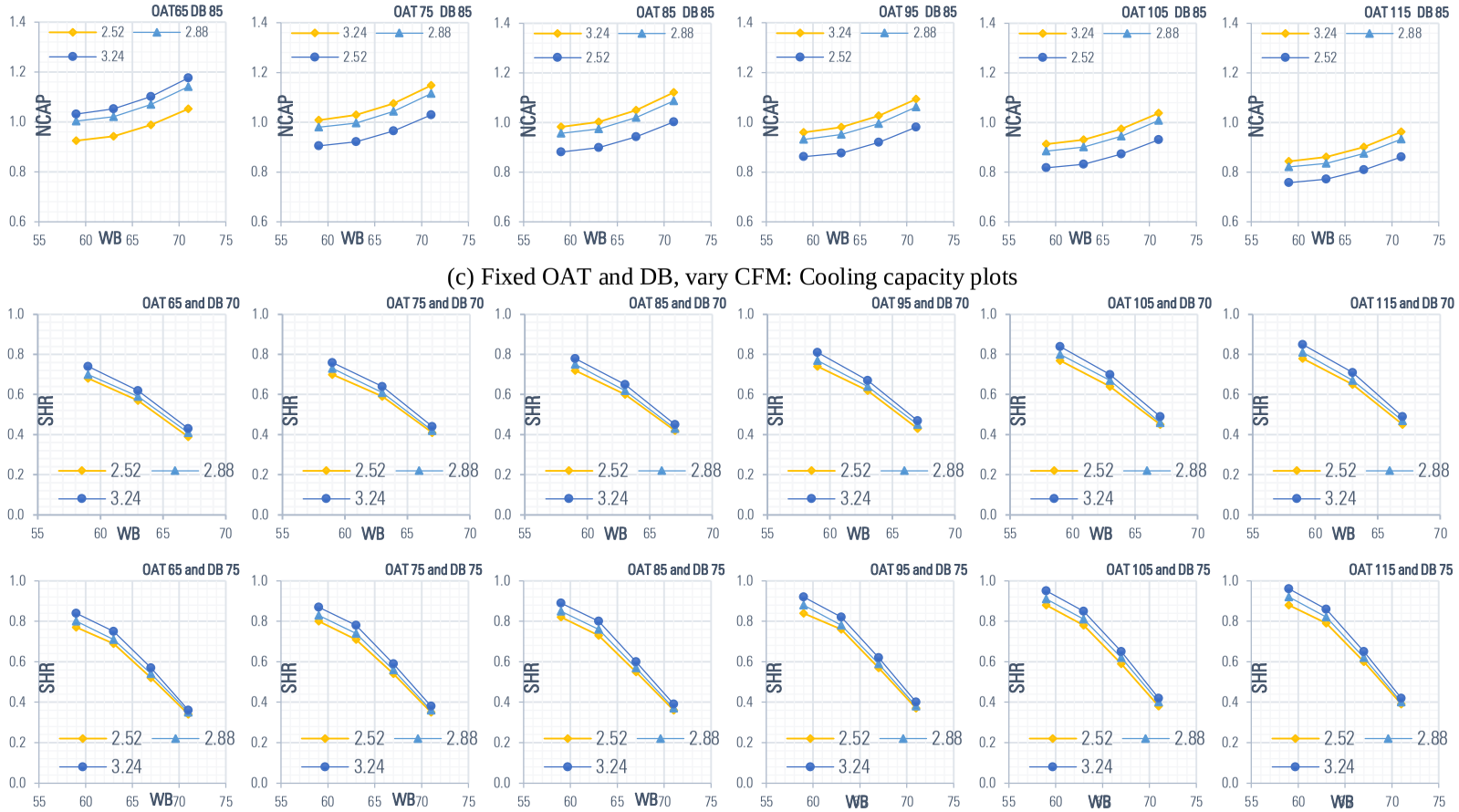

(c) Fixed OAT and DB, vary CFM: Cooling capacity plots

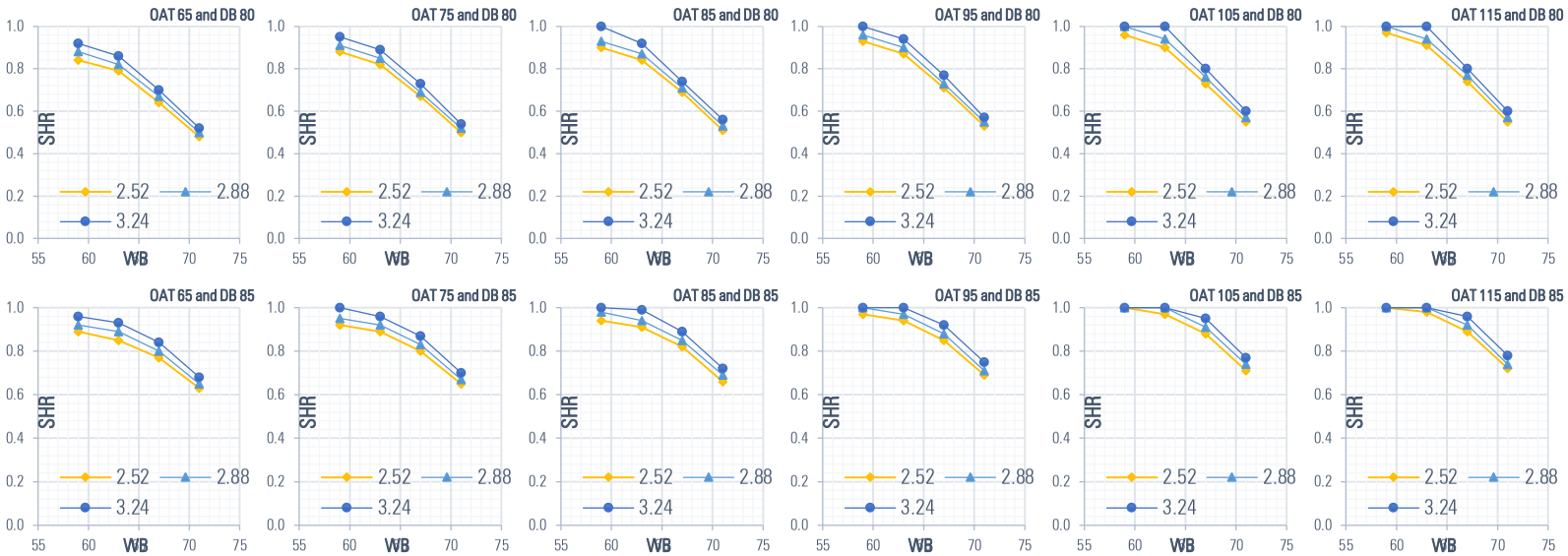

(d) Fixed OAT and DB, vary CFM: SHR plots

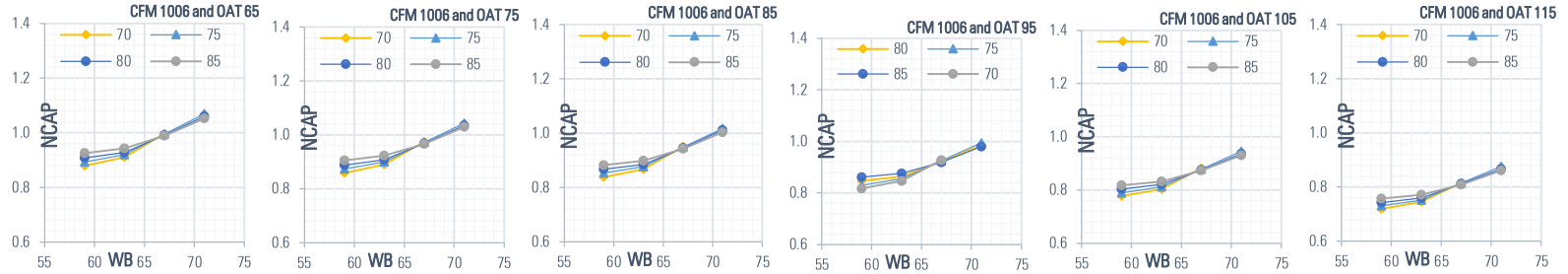

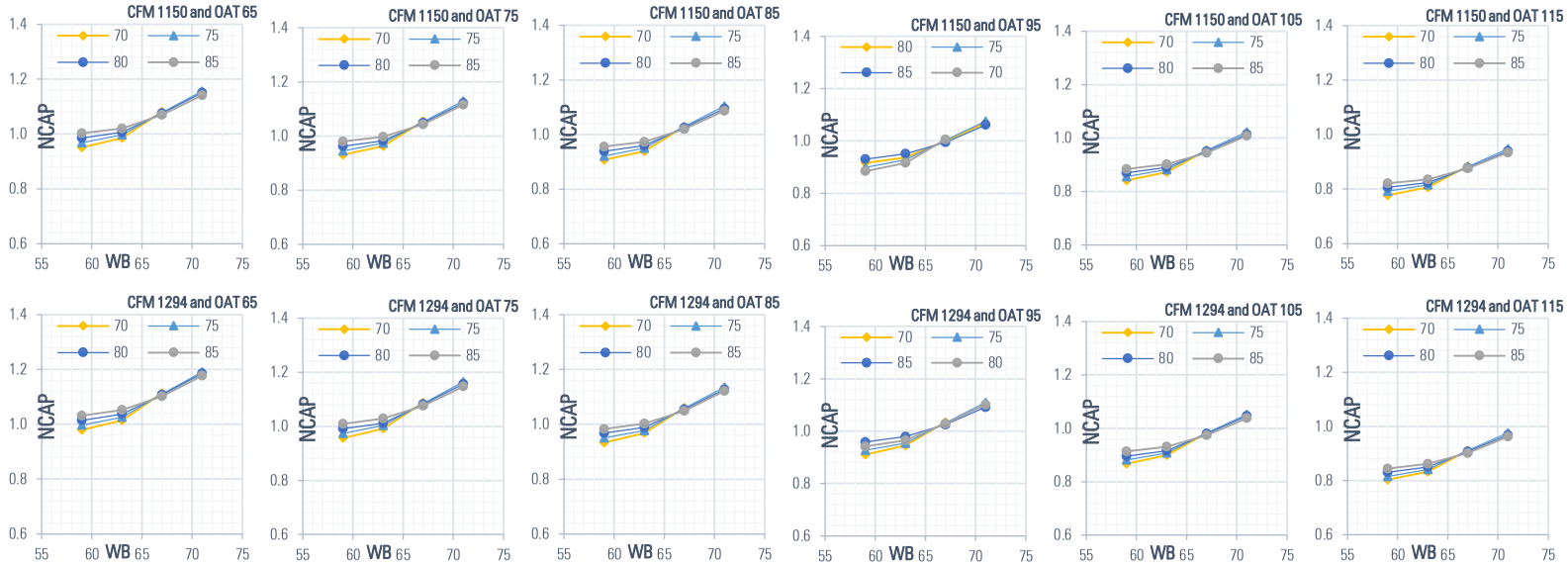

(e) Fixed OAT and CFM, vary DB: Cooling capacity plots

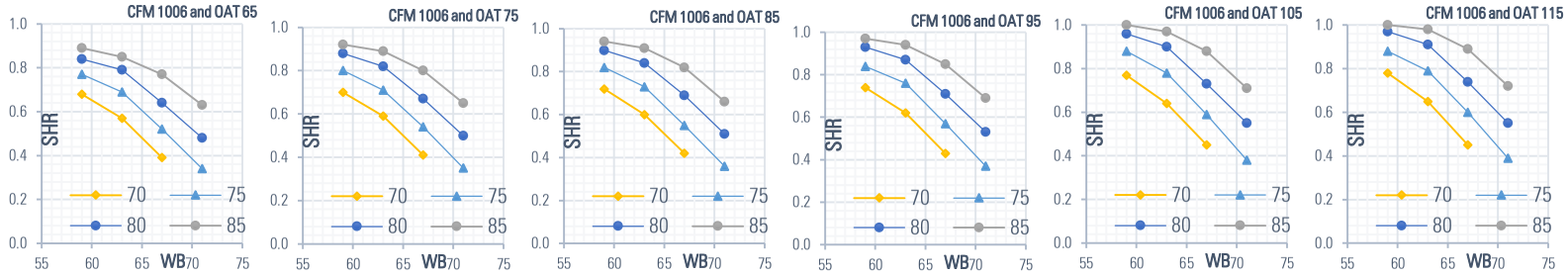

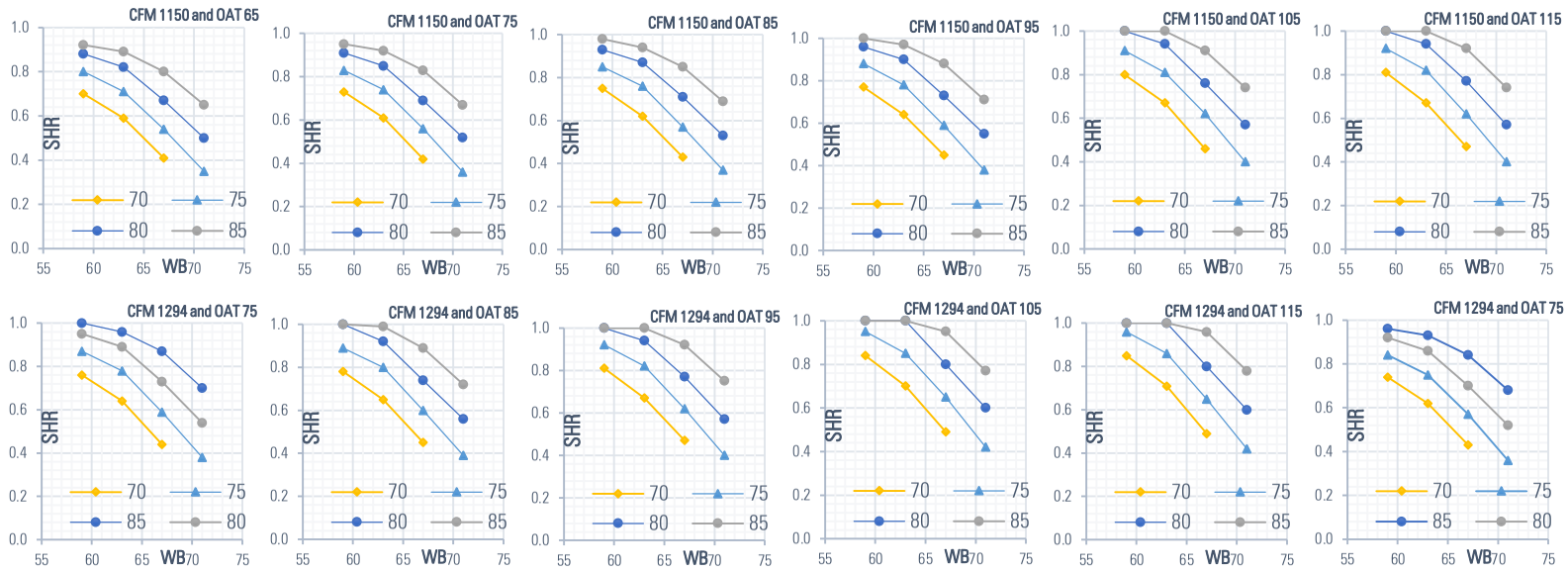

(f) Fixed OAT and CFM, vary DB: SHR plots

Figure E-8 Goodman model DAZ16-036H Normalized capacity and SHR performance plots

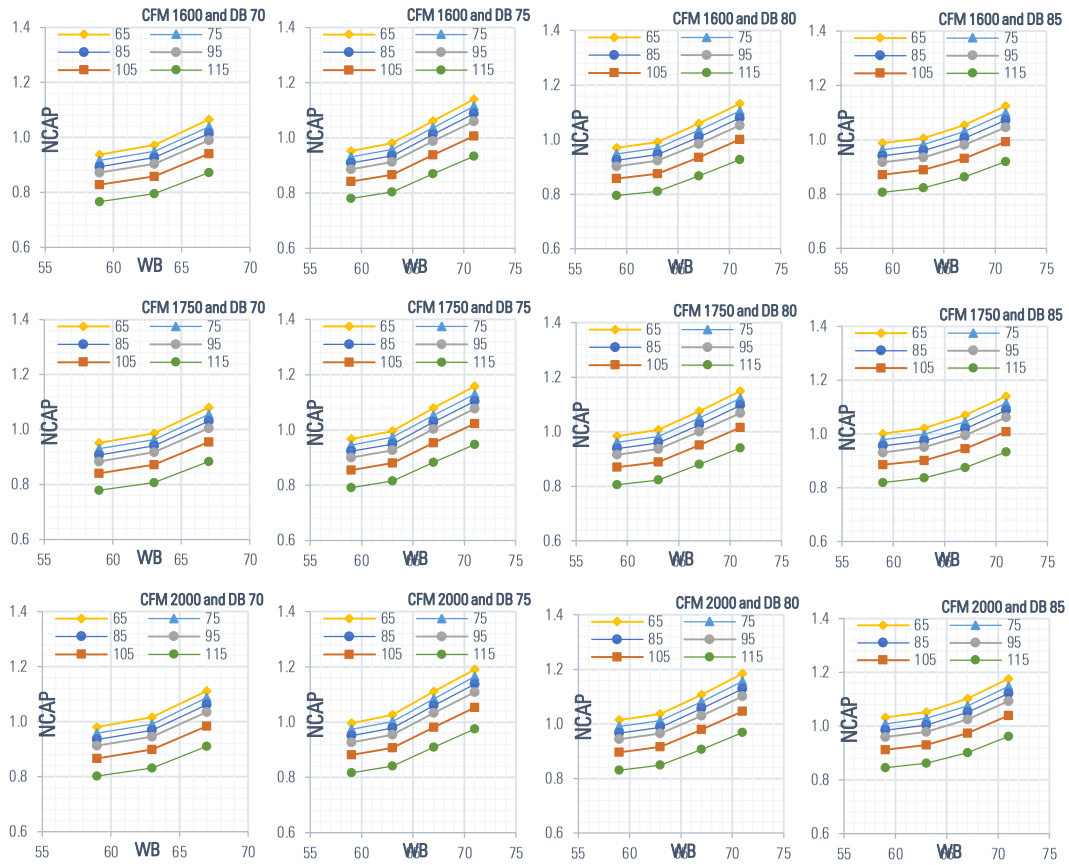

(a) Fixed CFM and DB, vary OAT: Cooling capacity plots

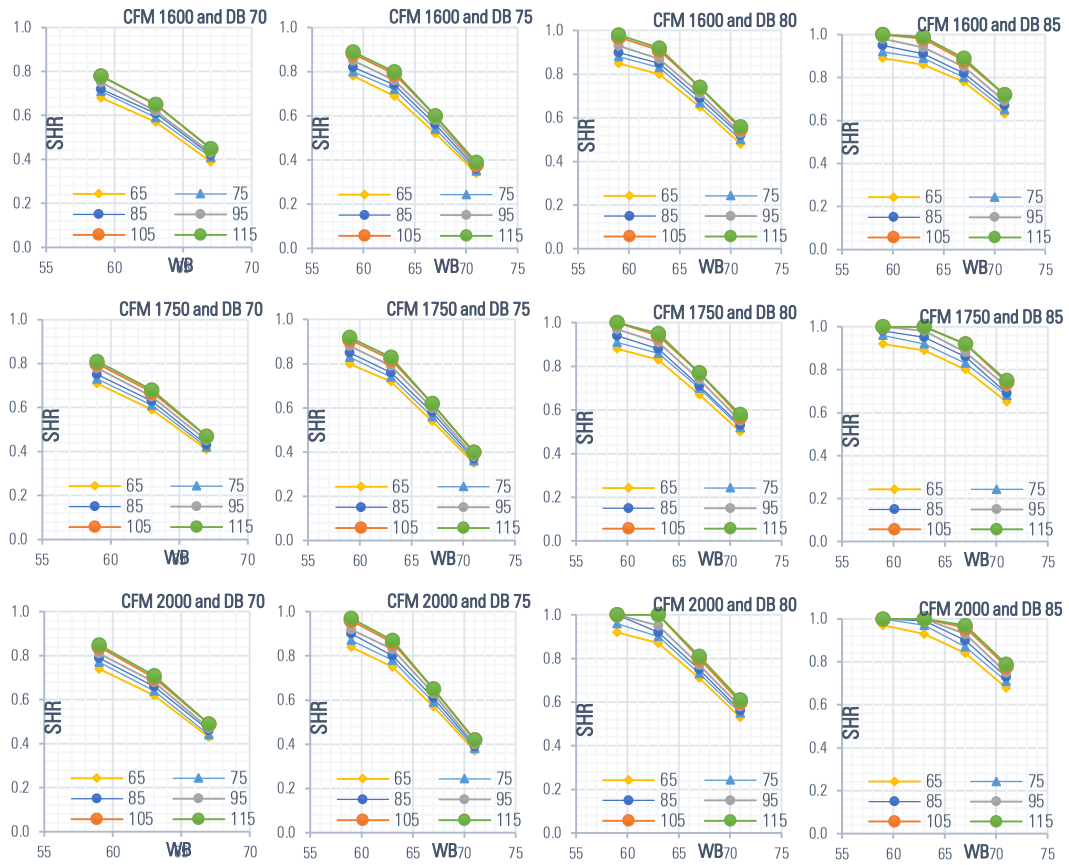

(b) Fixed CFM and DB, vary OAT: SHR plots

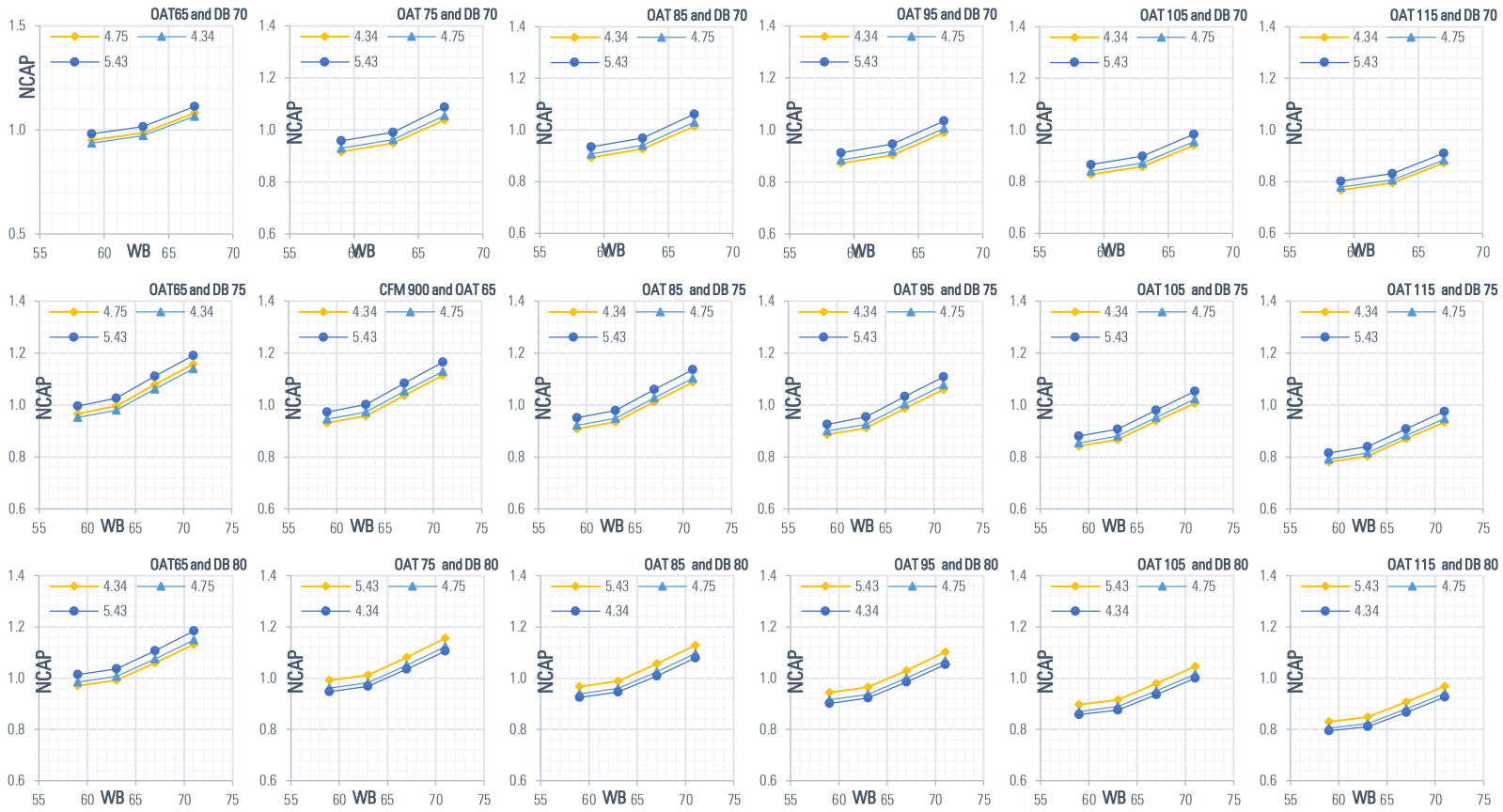
OAT65 and DB 70
4.75
4.34
5.43
NCAP
WB
OAT 75 and DB 70
4.34
4.75
5.43
OAT 85 and DB 70
OAT 95 and DB 70
OAT 105 and DB 70
OAT 115 and DB 70
OAT65 and DB 75
CFM 900 and OAT 65
OAT 85 and DB 75
OAT 95 and DB 75
OAT 105 and DB 75
OAT 115 and DB 75
OAT65 and DB 80
5.43
4.75
4.34
OAT 75 and DB 80
OAT 85 and DB 80
OAT 95 and DB 80
OAT 105 and DB 80
OAT 115 and DB 80

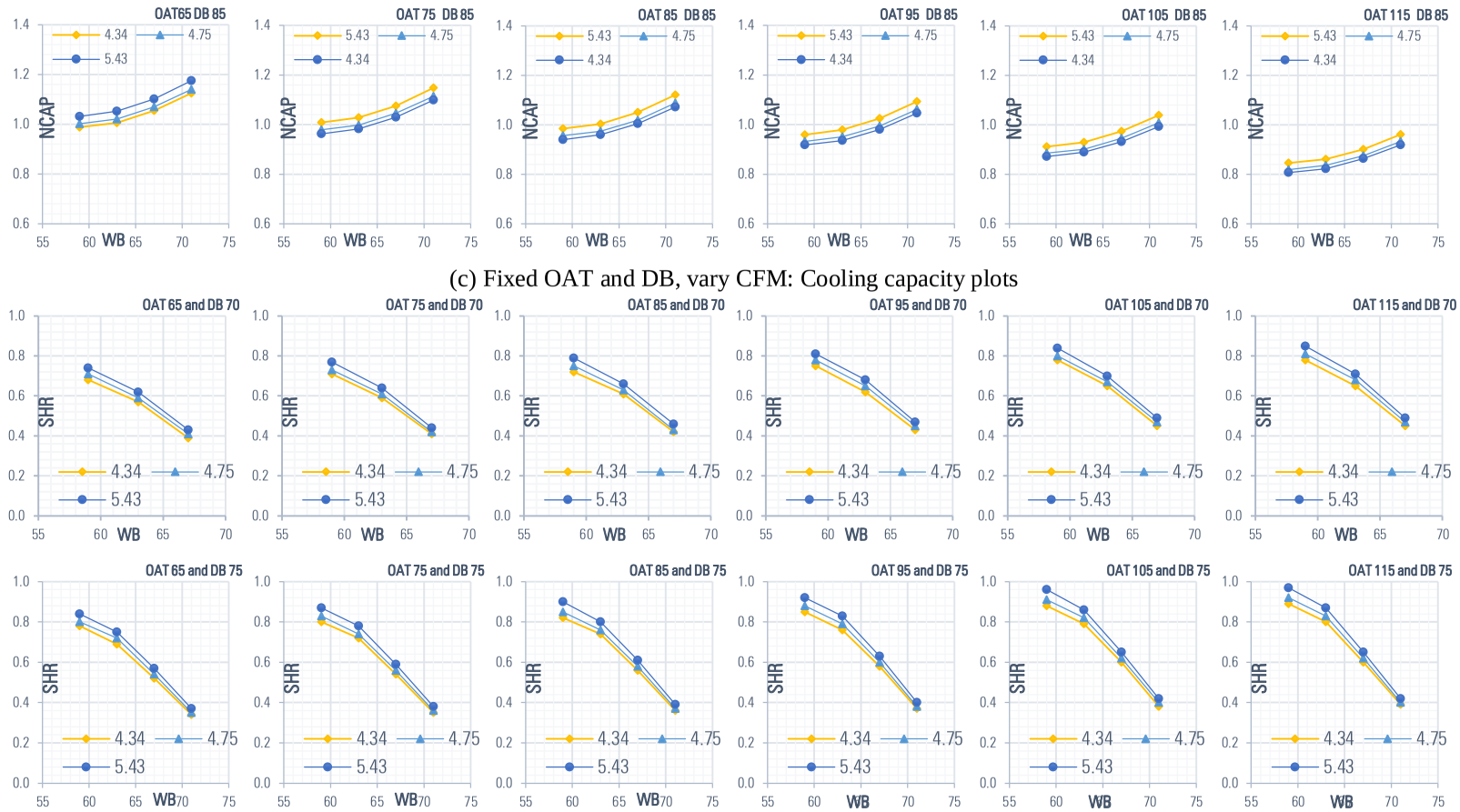

(c) Fixed OAT and DB, vary CFM: Cooling capacity plots

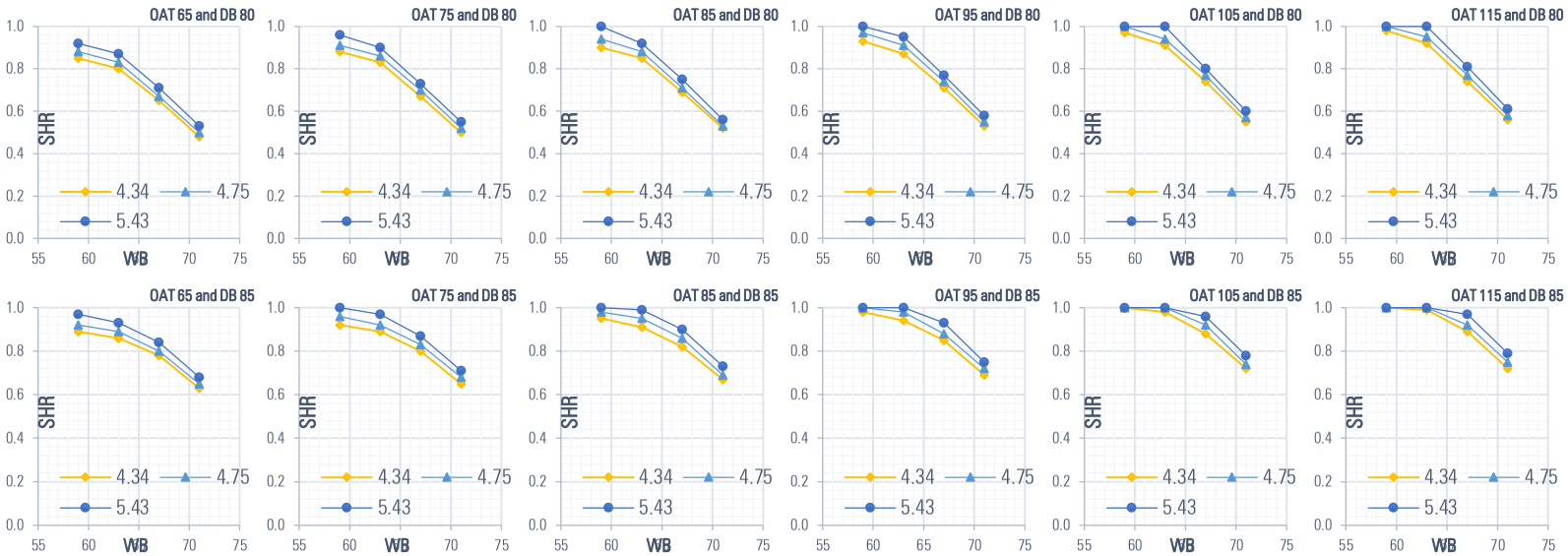

(d) Fixed OAT and DB, vary CFM: SHR plots

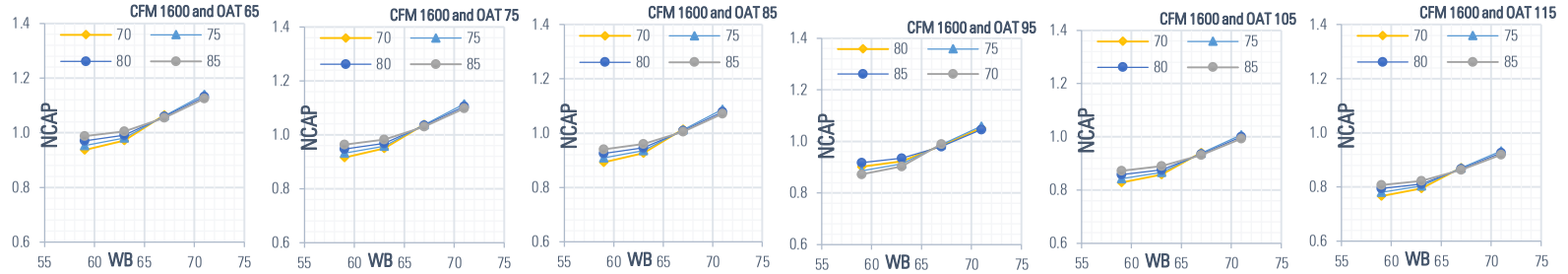

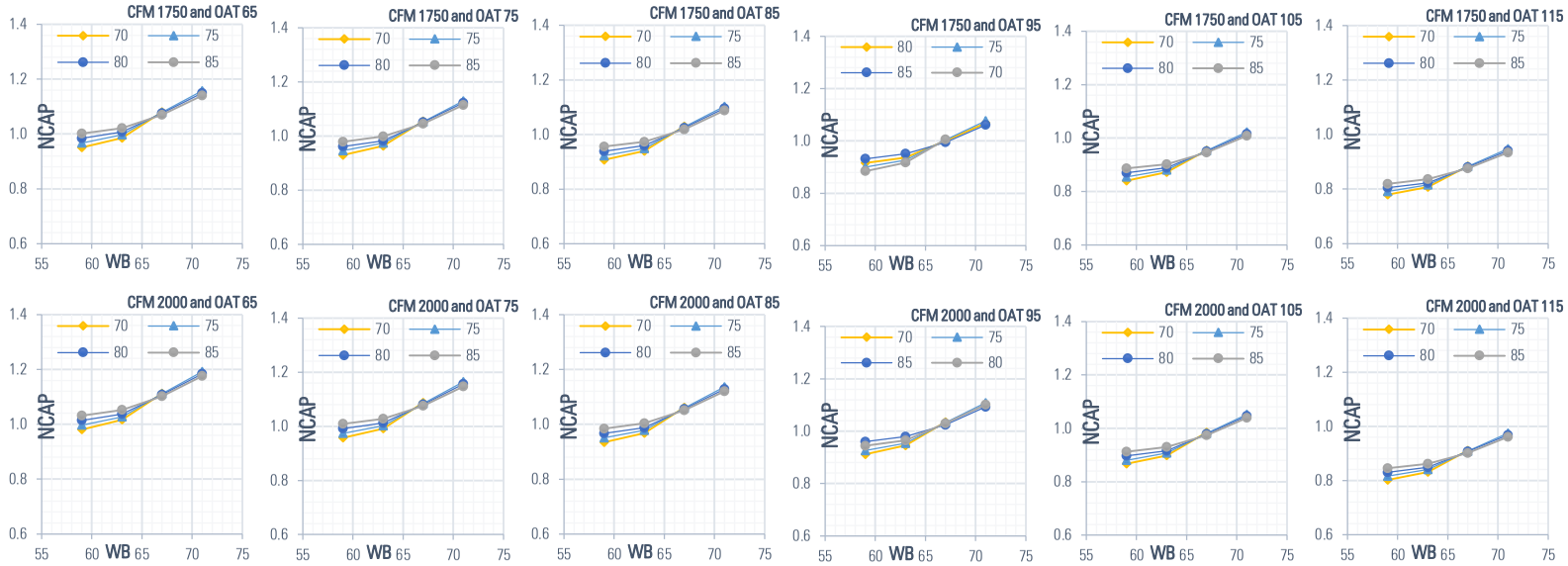

(e) Fixed OAT and CFM, vary DB: Cooling capacity plots

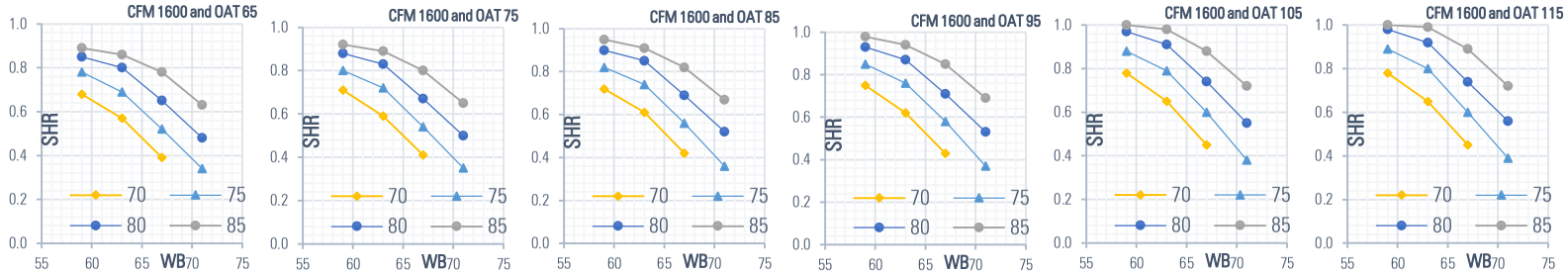

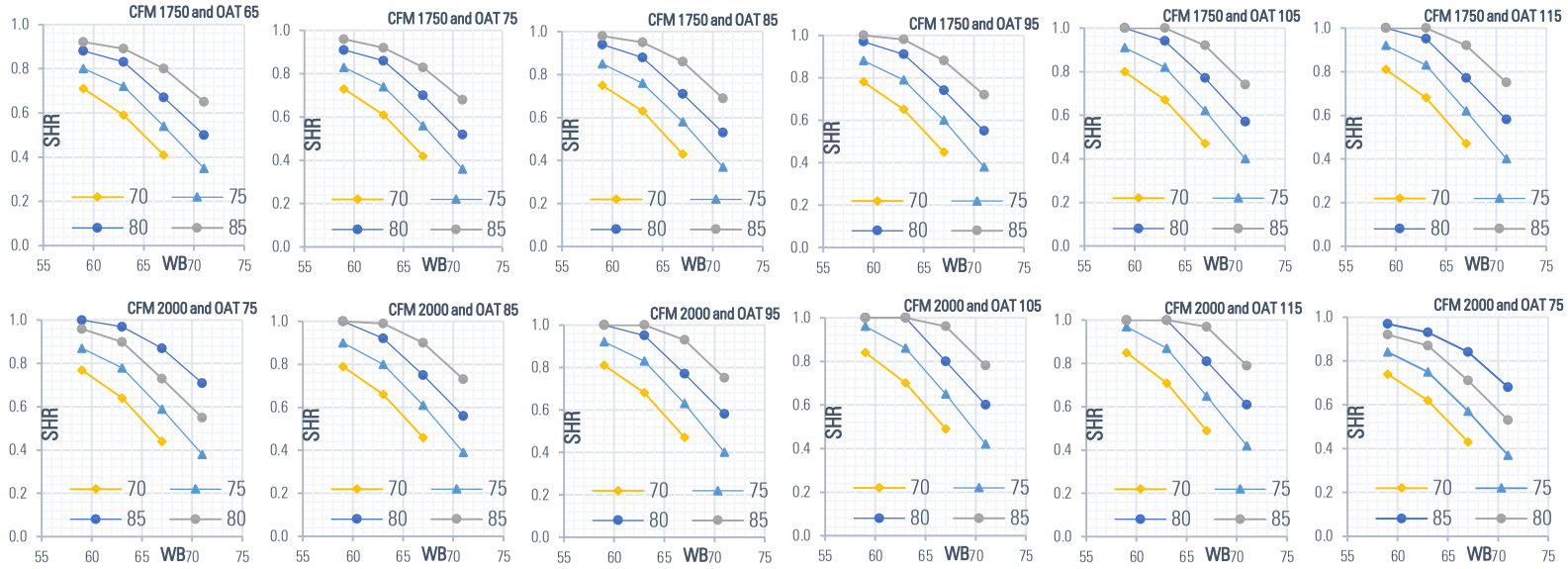

(f) Fixed OAT and CFM, vary DB: SHR plots

Figure E-9 Goodman model DAZ16-060H Normalized capacity and SHR performance plots

APPENDIX F PACKAGE UNIT MANUFACTURERS' DATA

Table F-1 Carrier RTU-CHP48HE004 performance data

48HE004 (3 Tons)		Air Entering Evaporator -- CFM/BF											
		900/0.10				1200/0.13				1500/0.16			
		Air Entering Evaporator -- WB (F)											
DB (F)		57	62	67	72	57	62	67	72	57	62	67	72
75	TCG	32	34.5	38.9	42.8	35.1	37.1	40.9	44.9	38.1	38.5	42.2	45.9
75	SHG	32	28.9	25	20.4	35.1	33.6	28.3	22.3	38.1	37.4	31.2	23.9
75	SHR	1.00	0.84	0.64	0.48	1.00	0.91	0.69	0.50	1.00	0.97	0.74	0.52
75	CMP	1.94	1.96	1.98	2	1.96	1.97	1.99	2.01	1.98	1.98	2	2.02
85	TCG	30.9	33.2	37.5	41.4	33.8	34.9	39.4	43.3	36.9	37	40.5	44.3
85	SHG	30.9	28.3	24.5	19.8	33.8	32.5	27.8	21.8	36.9	36.7	30.7	23.3
85	SHR	1.00	0.85	0.65	0.48	1.00	0.93	0.71	0.50	1.00	0.99	0.76	0.53
85	CMP	2.19	2.21	2.24	2.26	2.22	2.23	2.25	2.27	2.24	2.24	2.26	2.28
95	TCG	29.5	31.4	35.4	39.7	31.8	32.3	***37.7***	41.5	35.1	35.2	38.8	42.5
95	SHG	29.5	27.3	23.6	19.2	31.8	31.2	***27.2***	21.2	35	35.2	30	22.8
95	SHR	1.00	0.87	0.67	0.48	1.00	0.97	***0.72***	0.51	1.00	1.00	0.77	0.54
95	CMP	2.47	2.49	2.52	2.54	2.5	2.51	***2.54***	2.56	2.53	2.53	2.54	2.56
105	TCG	28	29.5	33	38	29.5	29.5	34.7	39.7	32.3	32.2	36.8	40.8
105	SHG	28	26.4	22.6	18.6	29.4	29.4	26	20.7	32.3	32.2	29.5	22.5
105	SHR	1.00	0.89	0.68	0.49	1.00	1.00	0.75	0.52	1.00	1.00	0.80	0.55
105	CMP	2.78	2.79	2.83	2.86	2.81	2.81	2.85	2.87	2.84	2.84	2.86	2.88
115	TCG	26.3	27.1	30.7	35.2	27.6	27.6	31.1	37.6	29.6	29.5	32.9	38.5
115	SHG	26.3	25.3	21.7	17.7	27.6	27.6	24.5	20	29.6	29.5	27.8	21.9
115	SHR	1.00	0.93	0.71	0.50	1.00	1.00	0.79	0.53	1.00	1.00	0.84	0.57
115	CMP	3.1	3.11	3.16	3.2	3.15	3.15	3.18	3.22	3.17	3.17	3.2	3.23
125	TCG	24.4	24.7	28.1	32.1	25.5	25.5	27.5	33.7	27	27	28.5	35.8
125	SHG	24.4	24.1	20.7	16.6	25.5	25.4	22.9	18.8	27	27	26	21.2
125	SHR	1.00	0.98	0.74	0.52	1.00	1.00	0.83	0.56	1.00	1.00	0.91	0.59
125	CMP	3.45	3.46	3.51	3.56	3.51	3.51	3.53	3.59	3.53	3.53	3.55	3.6

Table F-2 Carrier RTU-CHP48HE006 performance data

48HE006 (5 Tons)		Air Entering Evaporator -- CFM/BF															
		1500/0.26				1750/0.31				2000/0.35				2500/0.45			
		Air Entering Evaporator -- Ewb (F)															
DB		**57**	**62**	**67**	**72**	**57**	**62**	**67**	**72**	**57**	**62**	**67**	**72**	**57**	**62**	**67**	**72**
75	**CAP**	57	60.2	66.5	72	60.3	62.3	68.5	73.8	63.2	64.1	69.7	75.6	67.4	67.4	71.8	77.6
75	**SCC**	55.3	50.5	42.4	33.5	58.6	55.2	45.7	35.4	61.3	59.5	48.6	37.4	65.5	65.5	54.4	40.7
75	**SHR**	0.97	0.84	0.64	0.47	0.97	0.89	0.67	0.48	0.97	0.93	0.70	0.49	0.97	0.97	0.76	0.52
75	**TPC**	3.1	3.11	3.12	3.14	3.11	3.12	3.13	3.15	3.11	3.12	3.13	3.16	3.12	3.12	3.14	3.17
85	**CAP**	54.1	56.9	64	70.2	58.3	59.7	65.9	72	60.9	61.4	67.3	73.4	65.3	65.2	69.6	75.3
85	**SCC**	52.6	49.1	41.4	33	56.6	54.1	44.8	35	59.2	58.4	48	36.9	63.4	63.4	54.4	40.4
85	**SHR**	0.97	0.86	0.65	0.47	0.97	0.91	0.68	0.49	0.97	0.95	0.71	0.50	0.97	0.97	0.78	0.54
85	**TPC**	3.5	3.52	3.54	3.56	3.52	3.53	3.54	3.57	3.53	3.54	3.54	3.58	3.54	3.54	3.56	3.59
95	**CAP**	50.2	53	61.1	67.5	55	55.6	62.9	69.3	58.6	58.6	***64.3***	70.6	62.8	62.8	66.4	72.7
95	**SCC**	48.8	47.4	40.3	32.2	53.4	52.3	43.8	34.2	56.9	56.8	***47.2***	36.1	61	61	53.4	40
95	**SHR**	0.97	0.89	0.66	0.48	0.97	0.94	0.70	0.49	0.97	0.97	***0.73***	0.51	0.97	0.97	0.80	0.55
95	**TPC**	3.94	3.95	3.99	4.02	3.97	3.97	4.01	4.03	3.99	3.99	***4.02***	4.03	4.01	4.01	4.02	4.05
105	**CAP**	47.4	47.9	56.5	64.3	50.9	51	59.5	66.1	54.7	54.8	60.9	67.4	59.9	60	62.9	69
105	**SCC**	46	45.2	38.7	31.1	49.5	49.5	42.6	33.2	53.1	53.2	45.9	35.2	58.2	58.3	52.4	38.8
105	**SHR**	0.97	0.94	0.68	0.48	0.97	0.97	0.72	0.50	0.97	0.97	0.75	0.52	0.97	0.97	0.83	0.56
105	**TPC**	4.42	4.42	4.48	4.51	4.44	4.44	4.5	4.53	4.47	4.47	4.51	4.54	4.5	4.5	4.52	4.54
115	**CAP**	43.1	43.2	50.3	60.8	47.3	47.3	52.6	62.6	50.1	50.1	55.6	63.9	56	55.9	58.2	65.4
115	**SCC**	41.8	42	36.4	30	45.9	45.9	40.2	32.1	48.7	48.7	44.1	34.2	54.4	54.3	50.8	37.9
115	**SHR**	0.97	0.97	0.72	0.49	0.97	0.97	0.76	0.51	0.97	0.97	0.79	0.54	0.97	0.97	0.87	0.58
115	**TPC**	4.92	4.92	4.98	5.05	4.96	4.96	5	5.07	4.98	4.98	5.02	5.08	5.03	5.03	5.05	5.08
125	**CAP**	39	39	43.9	55.7	42.3	42.3	46.9	58.5	46.1	46.1	48.2	59.7	50.9	50.9	51.3	61.4
125	**SCC**	37.9	37.9	34.1	28.3	41.1	41	38.2	30.8	44.8	44.8	41.6	32.9	49.4	49.4	48.2	36.9
125	**SHR**	0.97	0.97	0.78	0.51	0.97	0.97	0.81	0.53	0.97	0.97	0.86	0.55	0.97	0.97	0.94	0.60
125	**TPC**	5.47	5.46	5.52	5.62	5.51	5.51	5.55	5.64	5.54	5.54	5.56	5.66	5.59	5.59	5.59	5.66

Table F-3 Carrier RTU-CHP48HE012 performance data

48HE012 (10 Tons)		Air Entering Evaporator -- CFM/BF															
		2550/0.11				3000/0.12				3400/0.13				4250/0.17			
		Air Entering Evaporator — WB (F)															
DB		57	62	67	72	57	62	67	57	62	67	72	57	62	67	72	57
75	CAP	95	101	110	119.2	100	104.4	113.4	121.8	104	106.8	115.8	123.4	110	111	119	125.8
75	SCC	95	84.4	69.4	54.4	100	92.4	75	57.2	104	99	80	59.8	110	110	89.4	64.2
75	SHR	1.00	0.84	0.63	0.46	1.00	0.89	0.66	0.47	1.00	0.93	0.69	0.48	1.00	0.99	0.75	0.51
75	TPC	5.7	5.76	5.76	5.82	5.74	5.76	5.8	5.86	5.74	5.76	5.82	5.88	5.76	5.78	5.84	5.9
85	CAP	91	97.4	106.8	115.8	97.4	101	110	119.6	101	103	112	121.6	108	108	116	123.4
85	SCC	91	83	68.8	53.2	97.4	91.2	74.2	57	101	97.6	78.8	59.6	108	108	89.4	64.2
85	SHR	1.00	0.85	0.64	0.46	1.00	0.90	0.67	0.48	1.00	0.95	0.70	0.49	1.00	1.00	0.77	0.52
85	TPC	6.5	6.5	6.52	6.58	6.5	6.52	6.54	6.6	6.5	6.52	6.54	6.64	6.54	6.54	6.6	6.64
95	CAP	85	91.4	103	112.8	93.4	96.6	***106.2***	116	98.2	99.2	108.4	117.8	105	105	111.6	121.2
95	SCC	85	80.4	67.2	52.6	93.4	89.4	***73***	55.8	98.2	96.2	78.2	58.8	105	105	88	64.6
95	SHR	1.00	0.88	0.65	0.47	1.00	0.93	***0.69***	0.48	1.00	0.97	0.72	0.50	1.00	1.00	0.79	0.53
95	TPC	7.2	7.28	7.36	7.42	7.3	7.32	***7.38***	7.44	7.34	7.36	7.4	7.46	7.36	7.36	7.42	7.5
105	CAP	80	82.2	98.6	108.6	87	87.8	101.6	111.8	93.4	93.6	103.8	114	101	101	106.8	116.6
105	SCC	80	76.6	65.6	51.2	87	85.6	71.6	54.8	93.4	93.2	76.6	57.8	101	101	86.8	63.6
105	SHR	1.00	0.93	0.67	0.47	1.00	0.97	0.70	0.49	1.00	1.00	0.74	0.51	1.00	1.00	0.81	0.55
105	TPC	8.1	8.12	8.26	8.32	8.16	8.16	8.28	8.36	8.2	8.2	8.3	8.38	8.28	8.28	8.3	8.4
115	CAP	74	74.6	89.4	103.4	81	81.2	95.2	106.4	86.2	86.2	98.4	108.4	96.4	96.4	101.6	111.8
115	SCC	74	73	62.2	49.6	81	81.2	69.4	53	86.2	86.2	75	56.4	96.4	96.4	85.4	62.8
115	SHR	1.00	0.98	0.70	0.48	1.00	1.00	0.73	0.50	1.00	1.00	0.76	0.52	1.00	1.00	0.84	0.56
115	TPC	9	9	9.16	9.28	9.08	9.08	9.22	9.3	9.14	9.14	9.26	9.34	9.22	9.22	9.3	9.38
125	CAP	69	68.6	80.2	98.2	74.4	74.4	84	101	79.2	79.2	86.8	102.8	88	88	93.8	105.6
125	SCC	69	68.6	59	48	74.4	74.4	65.4	51.6	79.2	79.2	71	54.6	88	88	82.8	61
125	SHR	1.00	1.00	0.74	0.49	1.00	1.00	0.78	0.51	1.00	1.00	0.82	0.53	1.00	1.00	0.88	0.58

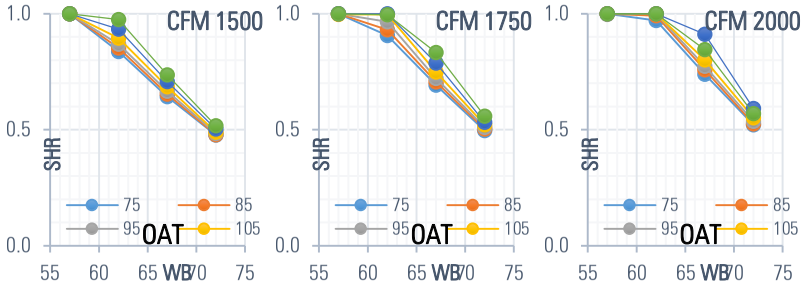

(a) Fixed CFM and DB, vary OAT: Cooling capacity plots

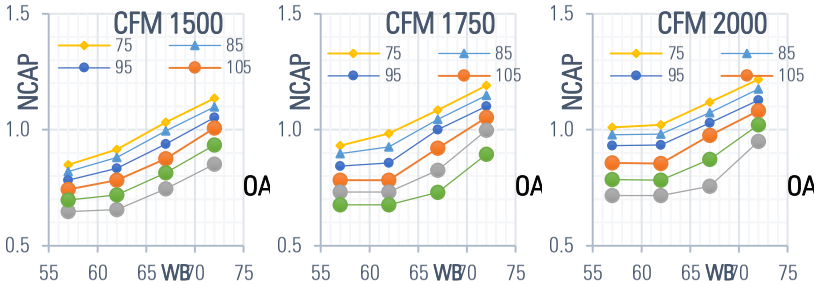

(b) Fixed CFM and DB, vary OAT: SHR plots

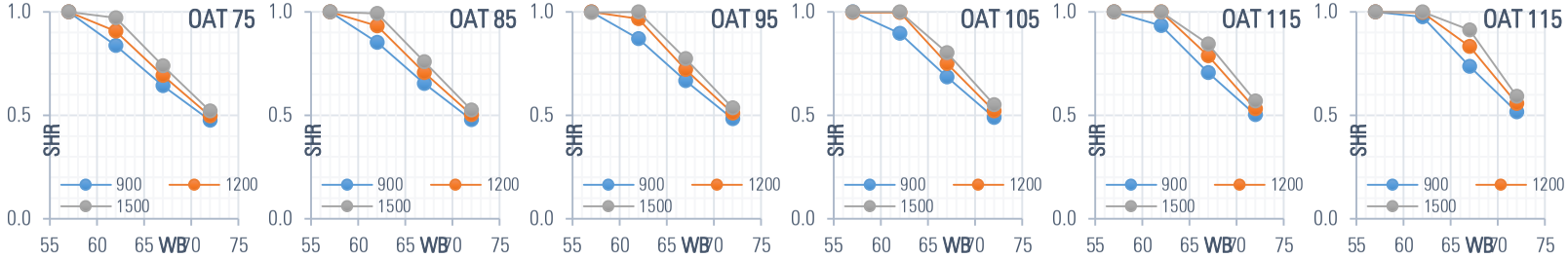

(c) Fixed OAT and DB, vary CFM: SHR plots

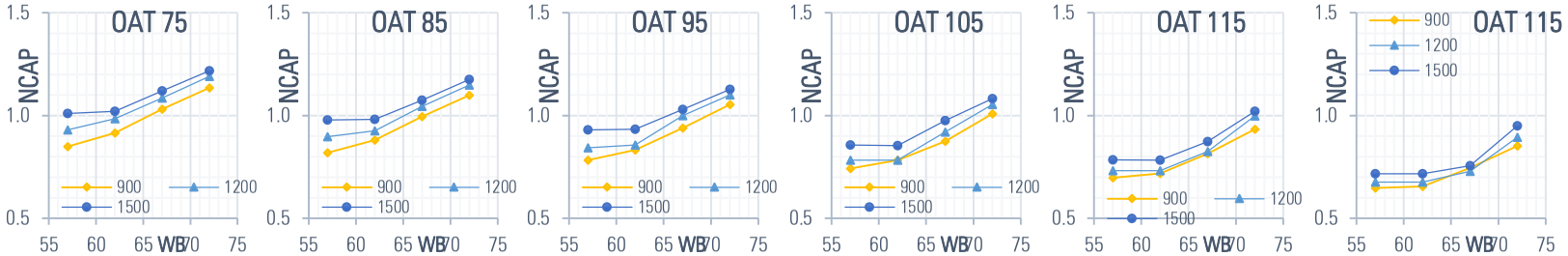

(d) Fixed OAT and DB, vary CFM: Cooling capacity plots

Figure F-1 Carrier RTU model CHP48H004 Normalized capacity and SHR performance plots

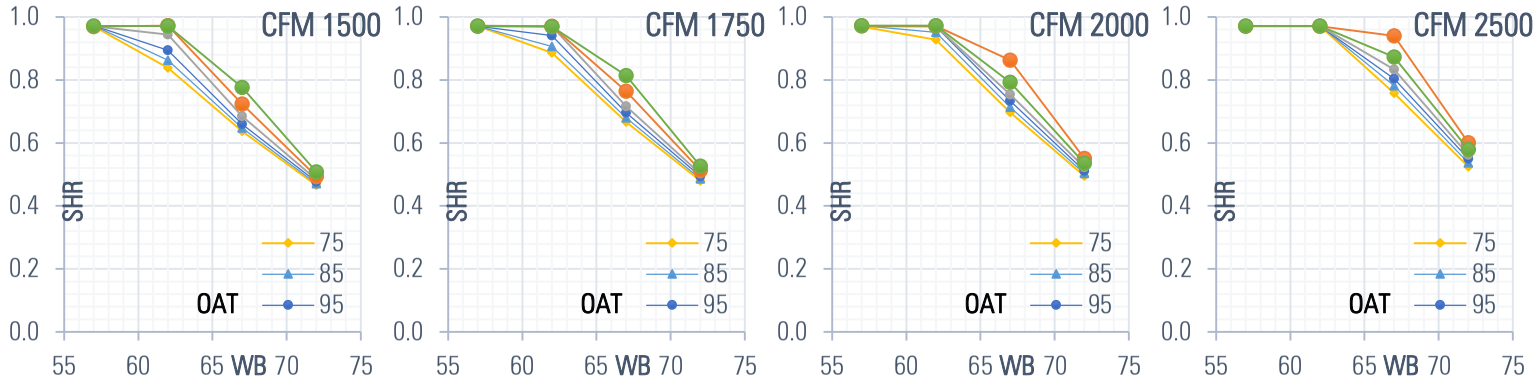

(a) Fixed CFM and DB, vary OAT: SHR plots

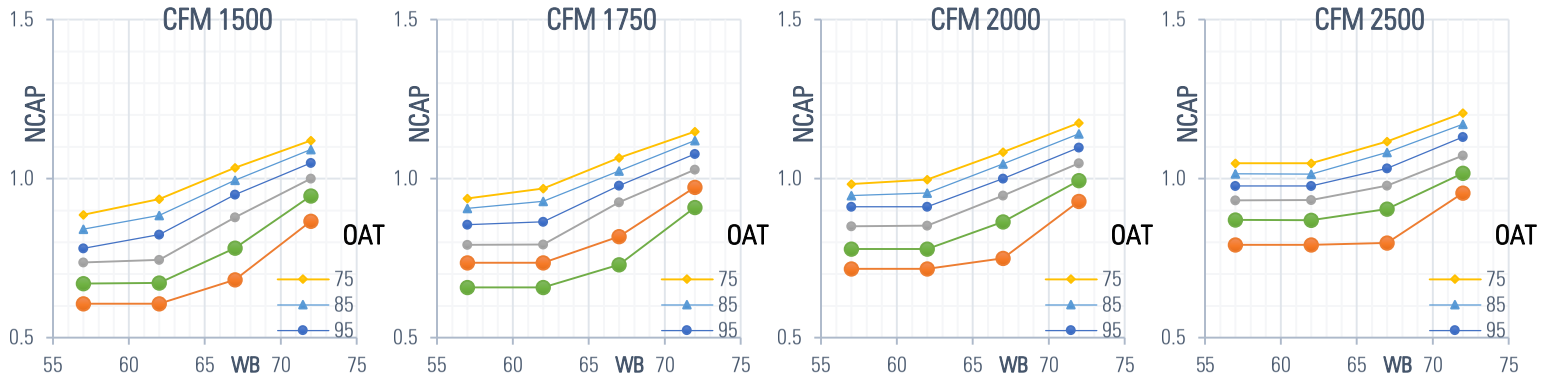

(b) Fixed CFM and DB, vary OAT: Cooling capacity plots

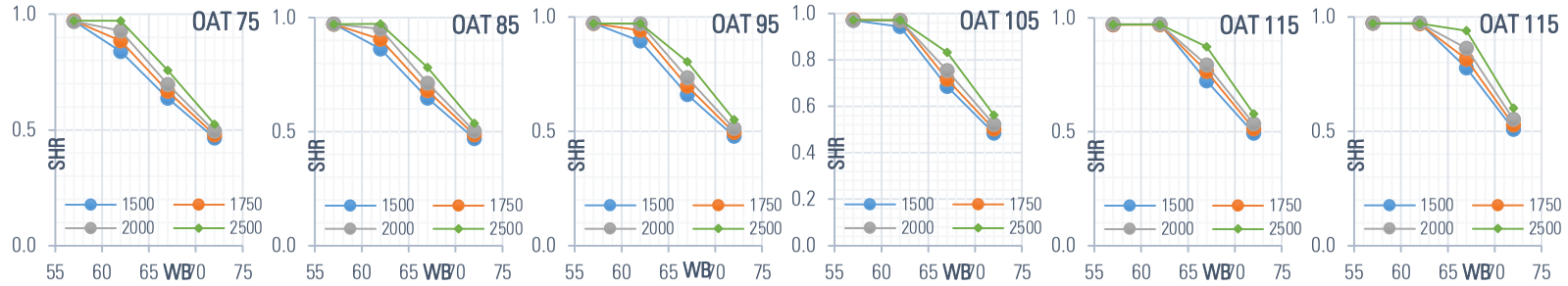

(c) Fixed OAT and DB, vary CFM: SHR plots

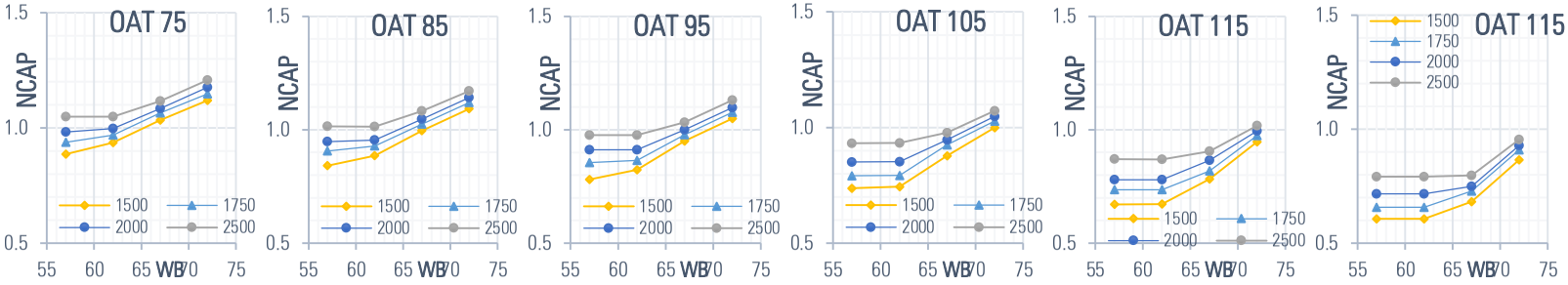

(d) Fixed OAT and DB, vary CFM: Cooling capacity plots

Figure F-2 Carrier RTU model CHP48H006 Normalized capacity and SHR performance plots

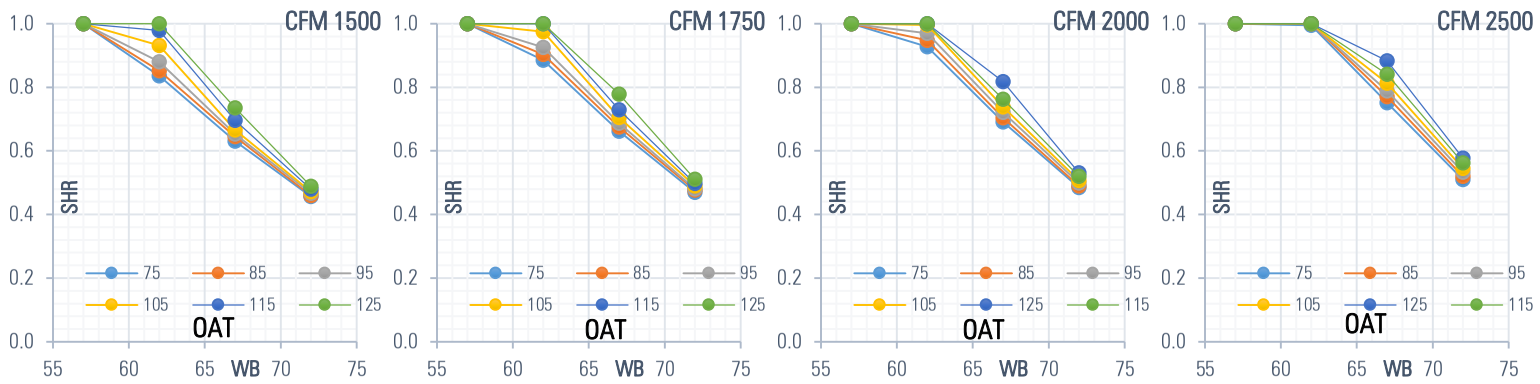

(a) Fixed CFM and DB, vary OAT: SHR plots

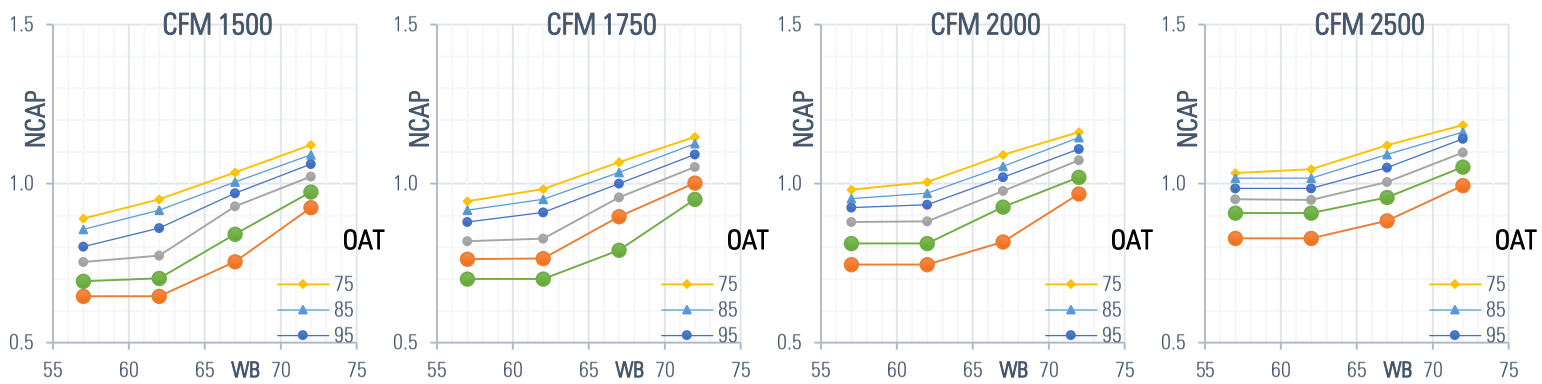

(b) Fixed CFM and DB, vary OAT: Cooling capacity plots

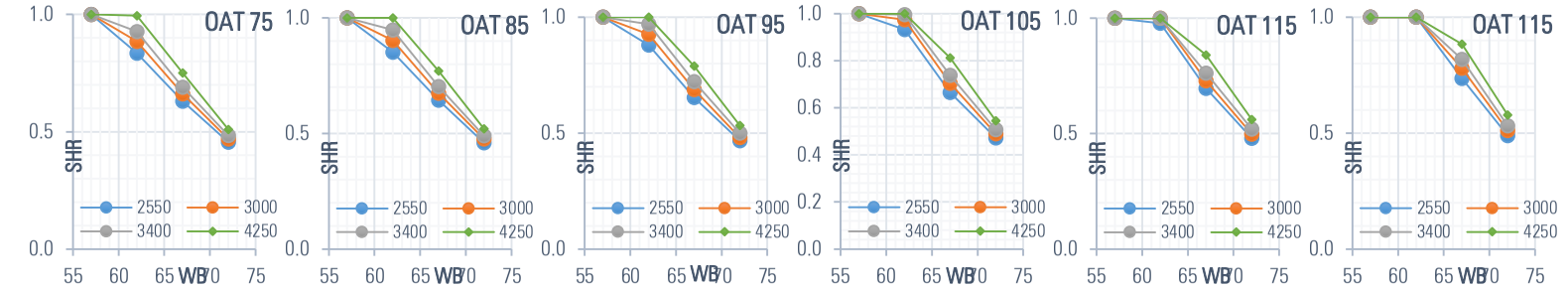

(c) Fixed OAT and DB, vary CFM: SHR plots

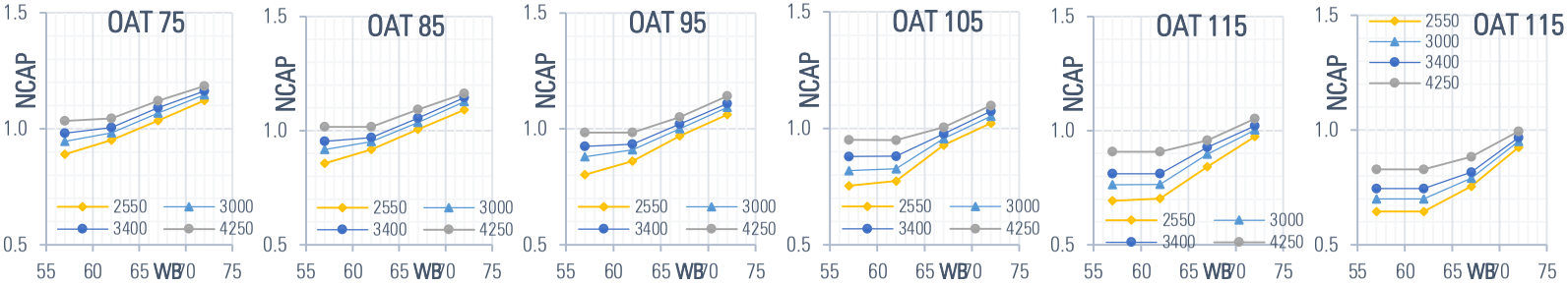

(d) Fixed OAT and DB, vary CFM: Cooling capacity plots

Figure F-3 Carrier RTU model CHP48H012 Normalized capacity and SHR performance plots

Table F-4 Trane RTU-PRC048-T/YHC037E3 (3 ton) performance data

T/YHC037E3		Ambient Temperature																		Ambient Temperature											
		85						95						105						115						125					
Air	Ent	Entering Wet Bulb																		Entering Wet Bulb											
CFM	DB	61		67		73		61		67		73		61		67		73		61		67		73		61		67		73	
		CAP	SHC	CAP	SHC	CAP	SHC	CAP	SHC	CAP	SHC	CAP	SHC	CAP	SHC	CAP	SHC	CAP	SHC	CAP	SHC	CAP	SHC	CAP	SHC	CAP	SHC	CAP	SHC	CAP	SHC
600	75	28.6	22	32.2	16.8	37	9.1	26.7	20.9	30.1	15.9	34.7	8.5	24.7	19.7	27.9	15	32.3	7.7	22.6	18.4	25.6	13.9	29.7	6.8	20.4	17.1	23.1	12.7	27.1	5.8
600	80	29.1	25.3	32.1	21.5	36.3	15.2	27.2	24.1	30	20.5	34	14.4	25.3	22.8	27.9	19.4	31.7	13.5	23.2	21.4	25.6	18.2	29.1	12.5	21	19.9	23.1	16.9	26.5	11.4
600	85	29.9	27.9	32.3	25.5	36	20.5	28.1	26.6	30.3	24.3	33.7	19.5	26.1	25.2	28.2	23.1	31.4	18.5	24.1	23.6	25.9	21.8	28.9	17.4	21.9	21.9	23.5	20.3	26.3	16.1
600	90	31	29.8	32.9	28.7	36	25	29.2	28.3	30.9	27.4	33.8	24	27.3	26.8	28.8	26	31.4	22.8	26.3	26.3	26.5	24.6	29	21.5	23.9	23.9	24.2	23	26.4	20.2
720	75	30.2	23.7	33.7	18.2	38.3	10.3	28.3	22.5	31.5	17.3	36	9.5	26.2	21.2	29.2	16.2	33.5	8.7	24	19.9	26.8	15.1	30.8	7.7	21.7	18.4	24.3	13.8	28.1	6.6
720	80	30.9	27.3	33.8	23.2	37.8	16.6	29	26	31.6	22.1	35.5	15.7	26.9	24.6	29.4	20.9	33	14.7	24.7	23.1	27	19.6	30.4	13.6	22.4	21.5	24.5	18.2	27.7	12.4
720	85	31.8	30.1	34.2	27.3	37.7	22.1	29.9	28.7	32	26.1	35.3	21.1	27.9	27.1	29.8	24.8	32.9	19.9	25.8	25.5	27.4	23.4	30.3	18.7	23.5	23.5	25	21.8	27.6	17.4
720	90	33.1	32.2	34.9	30.8	37.8	26.8	31.3	30.6	32.8	29.4	35.5	25.7	29.3	28.9	30.6	28	33.1	24.4	28	28	28.2	26.4	30.5	23.1	25.5	25.5	25.8	24.7	27.9	21.6
840	75	31.7	25.2	35	19.5	39.5	11.3	29.7	24	32.8	18.5	37.1	10.5	27.5	22.6	30.4	17.3	34.5	9.5	25.3	21.2	27.9	16.1	31.8	8.5	22.9	19.6	25.3	14.7	29	7.3
840	80	32.5	29	35.3	24.7	39.2	17.8	30.5	27.6	33	23.5	36.8	16.8	28.4	26.2	30.7	22.2	34.2	15.8	26.1	24.6	28.2	20.8	31.5	14.6	23.7	22.9	25.6	19.3	28.7	13.3
840	85	33.6	32.1	35.8	29.1	39.2	23.5	31.6	30.6	33.6	27.8	36.8	22.4	29.5	28.9	31.3	26.4	34.2	21.2	27.3	27.2	28.8	24.8	31.6	19.9	24.9	24.9	26.3	23.2	28.8	18.5
840	90	35.1	34.4	36.7	32.7	39.5	28.5	33.1	32.7	34.5	31.3	37.1	27.3	31	31	32.2	29.7	34.6	25.9	29.5	29.5	29.8	28.1	31.9	24.5	27	27	27.2	26.3	29.2	22.9
960	75	33	26.6	36.2	20.7	40.6	12.2	30.9	25.3	33.9	19.5	38	11.3	28.7	23.9	31.4	18.3	35.4	10.2	26.3	22.3	28.8	17	32.6	9.1	23.8	20.7	26.1	15.5	29.6	7.8
960	80	34	30.7	36.6	26	40.4	18.9	31.9	29.2	34.3	24.8	37.9	17.8	29.7	27.6	31.8	23.4	35.2	16.7	27.3	25.9	29.3	21.9	32.4	15.4	24.9	24.2	26.6	20.4	29.5	14
960	85	35.2	33.9	37.3	30.6	40.5	24.9	33.2	32.3	35	29.2	38	23.7	31	30.6	32.6	27.7	35.4	22.4	28.7	28.7	30	26.1	32.6	21	26.2	26.2	27.4	24.4	29.8	19.4
960	90	36.8	36.4	38.3	34.5	40.9	30	34.8	34.7	36	33	38.5	28.7	32.6	32.6	33.6	31.3	35.9	27.3	30.8	30.8	31.1	29.6	33.2	25.7	28.2	28.2	28.5	27.7	30.3	24.1
1080	75	34.2	27.9	37.2	21.7	41.4	12.9	32	26.5	34.8	20.4	38.8	11.9	29.6	24.9	32.2	19.1	36	10.8	27.2	23.3	29.6	17.7	33.2	9.5	24.6	21.6	26.8	16.1	30.1	8.2
1080	80	35.3	32.1	37.7	27.3	41.4	19.9	33.1	30.6	35.3	25.9	38.8	18.7	30.8	28.9	32.8	24.4	36	17.4	28.3	27.1	30.2	22.9	33.2	16.1	25.8	25.3	27.4	21.2	30.2	14.6
1080	85	36.7	35.6	38.6	32.1	41.7	26	34.5	33.9	36.2	30.6	39.1	24.7	32.2	32.1	33.7	29	36.4	23.3	29.8	29.8	31.1	27.3	33.5	21.8	27.3	27.3	28.3	25.5	30.6	20.2
1080	90	38.4	38.3	39.7	36.1	42.3	31.4	36.3	36.3	37.4	34.5	39.7	30	34	34	34.9	32.8	37	28.5	32	32	32.3	31	34.2	26.9	29.3	29.3	29.6	29	31.3	25.1
1200	75	35.1	29	38	22.5	42.1	13.5	32.9	27.5	35.5	21.2	39.4	12.4	30.4	25.9	32.9	19.8	36.5	11.2	27.9	24.1	30.1	18.3	33.6	9.9	25.2	22.3	27.2	16.6	30.5	8.4
1200	80	36.4	33.4	38.7	28.3	42.2	20.6	34.1	31.8	36.2	27	39.5	19.4	31.7	30	33.6	25.3	36.7	18.1	29.2	28.2	30.9	23.7	33.7	16.6	26.6	26.2	28	21.9	30.7	15
1200	85	37.9	37.1	39.7	33.3	42.6	27	35.7	35.4	37.2	31.8	40	25.6	33.3	33.3	34.6	30.1	37.2	24.2	30.8	30.8	31.9	28.3	34.2	22.6	28.2	28.2	29.1	26.4	31.2	20.9
1200	90	39.8	39.8	41	37.6	43.4	32.6	37.6	37.6	38.6	35.9	40.7	31.1	35.7	35.7	36	34.1	38	29.5	33	33	33.3	32.2	35.1	27.8	30.2	30.2	30.5	30.2	32.1	26
1320	75	35.9	30	38.7	23.2	42.6	13.9	33.5	28.3	36.1	21.8	39.8	12.7	31	26.6	33.4	20.3	36.9	11.4	28.4	24.8	30.5	18.7	33.8	10	25.7	22.9	27.5	17	30.6	8.5
1320	80	37.3	34.6	39.5	29.2	42.9	21.3	35	32.9	36.9	27.7	40.1	20	32.5	31	34.2	26	37.2	18.5	29.9	29.1	31.4	24.3	34.1	17	27.1	27.1	28.5	22.5	31	15.3
1320	85	39	38.5	40.6	34.5	43.4	27.9	36.7	36.7	38.1	32.8	40.7	26.4	34.2	34.2	35.4	31	37.8	24.9	31.7	31.7	32.6	29.2	34.8	23.2	29	29	29.7	27.2	31.7	21.4
1320	90	41.1	41.1	42.1	39	44.3	33.7	38.8	38.8	39.6	37.2	41.6	32.1	36.6	36.6	36.9	35.3	38.7	30.4	33.8	33.8	34.2	33.3	35.8	28.6	31	31	31.3	31.1	32.7	26.7
1440	75	36.5	30.8	39.1	23.8	42.9	14.2	34.1	29.1	36.5	22.3	40	12.9	31.5	27.3	33.7	20.7	37	11.5	28.8	25.4	30.7	19	33.9	10	25.9	23.4	27.7	17.2	30.6	8.4
1440	80	38.1	35.6	40.1	30	43.3	21.8	35.6	33.8	37.5	28.4	40.5	20.4	33.1	31.9	34.7	26.6	37.5	18.8	30.4	29.9	31.8	24.8	34.4	17.2	27.6	27.6	28.7	22.9	31.1	15.5
1440	85	39.9	39.8	41.4	35.4	44.1	28.6	37.5	37.5	38.8	33.7	41.2	27	35	35	36	31.8	38.3	25.4	32.3	32.3	33.1	29.9	35.2	23.6	29.5	29.5	30.1	27.8	31.9	21.8
1440	90	42.1	42.1	43	40.1	45.1	34.6	39.7	39.7	40.4	38.3	42.3	33	37.3	37.3	37.7	36.3	39.4	31.2	34.5	34.5	34.8	34.2	36.3	29.3	31.9	31.9	31.9	31.9	33.1	27.3

Table F-5 Trane RTU-PRC048-T/YHC047E3 (4 ton) performance data

T/YHC047E3		Ambient Temperature																		Ambient Temperature											
		85						95						105						115						125					
CFM	DB	Entering Wet Bulb																		Entering Wet Bulb											
	F	61		67		73		61		67		73		61		67		73		61		67		73		61		67		73	
		CAP	SHC	CAP	SHC	CAP	SHC	CAP	SHC	CAP	SHC	CAP	SHC	CAP	SHC	CAP	SHC	CAP	SHC	CAP	SHC	CAP	SHC	CAP	SHC	CAP	SHC	CAP	SHC	CAP	SHC
800	75	39.2	30	44	22.7	50.4	12	36.9	28.6	41.4	21.7	47.5	11.2	34.3	27.1	38.6	20.4	44.4	10.3	31.6	25.5	35.6	19.1	41.2	9.2	29	23.9	32.8	17.7	38.1	8.1
800	80	39.9	34.6	43.9	29.2	49.6	20.4	37.6	33.1	41.3	28	46.7	19.4	35.1	31.4	38.5	26.6	43.7	18.3	32.4	29.6	35.6	25.1	40.4	17	29.8	28	32.8	23.6	37.4	15.8
800	85	41	38.3	44.3	34.7	49.2	27.7	38.7	36.6	41.7	33.3	46.4	26.6	36.2	34.7	39	31.7	43.4	25.3	33.6	32.8	36.1	30	40.2	23.9	31	30.9	33.3	28.5	37.2	22.5
800	90	42.6	40.9	45.2	39.2	49.3	34	40.3	39	42.6	37.6	46.5	32.7	37.9	37	39.9	35.8	43.5	31.2	35.2	34.9	37	34	40.3	29.6	33.9	33.9	34.2	32.3	37.4	28.2
960	75	41.5	32.3	46.1	24.7	52.3	13.7	39	30.9	43.4	23.6	49.3	12.8	36.4	29.3	40.5	22.2	46.1	11.7	33.6	27.5	37.4	20.8	42.8	10.5	30.9	25.9	34.4	19.4	39.6	9.3
960	80	42.4	37.3	46.2	31.5	51.7	22.3	40	35.7	43.5	30.2	48.7	21.2	37.3	33.9	40.6	28.7	45.6	20	34.5	32	37.6	27	42.2	18.7	31.9	30.2	34.7	25.5	39.1	17.4
960	85	43.7	41.2	46.8	37.3	51.6	29.9	41.3	39.4	44.2	35.8	48.6	28.7	38.7	37.5	41.3	34.1	45.5	27.3	35.9	35.4	38.3	32.3	42.2	25.8	33.3	33.3	35.4	30.7	39.1	24.4
960	90	45.5	44.1	47.9	42	51.9	36.5	43.1	42.1	45.2	40.3	49	35.1	40.6	40	42.4	38.5	45.9	33.5	37.8	37.8	39.4	36.5	42.6	31.9	36.2	36.2	36.6	34.8	39.5	30.3
1120	75	43.6	34.5	48	26.5	54	15.1	41	32.9	45.1	25.2	50.9	14.1	38.2	31.2	42.1	23.8	47.6	13	35.3	29.4	38.9	22.3	44.1	11.7	32.5	27.6	35.9	20.7	40.9	10.4
1120	80	44.7	39.7	48.3	33.6	53.6	24	42.1	38	45.5	32.2	50.5	22.9	39.4	36.1	42.5	30.6	47.3	21.6	36.5	34.1	39.3	28.8	43.8	20.1	33.7	32.3	36.3	27.2	40.6	18.7
1120	85	46.2	43.9	49.1	39.7	53.7	32	43.7	42	46.3	38	50.6	30.6	41	40	43.4	36.3	47.4	29.1	38.1	37.8	40.2	34.4	44	27.5	35.4	35.4	37.3	32.6	40.8	26
1120	90	48.2	47.1	50.4	44.7	54.2	38.8	45.7	45	47.6	42.9	51.2	37.3	43	42.8	44.7	41	48	35.7	40.2	40.2	41.6	38.9	44.6	33.9	38.3	38.3	38.6	37	41.4	32.2
1280	75	45.4	36.4	49.6	28.1	55.5	16.4	42.7	34.7	46.6	26.7	52.2	15.2	39.8	32.9	43.5	25.2	48.8	14	36.8	31	40.2	23.5	45.3	12.6	33.9	29.2	37.1	21.9	41.9	11.2
1280	80	46.7	41.9	50.2	35.5	55.3	25.6	44	40.1	47.2	33.9	52.1	24.3	41.2	38.1	44.1	32.2	48.7	22.9	38.1	36	40.8	30.4	45.2	21.3	35.3	34.1	37.8	28.7	41.8	19.8
1280	85	48.5	46.5	51.2	41.8	55.6	33.8	45.8	44.4	48.3	40.1	52.4	32.3	43	42.3	45.2	38.2	49.1	30.7	40	40	41.9	36.2	45.5	29	37.2	37.2	38.9	34.4	42.2	27.4
1280	90	50.7	49.9	52.7	47.2	56.3	40.9	48.1	47.8	49.8	45.3	53.2	39.3	45.3	45.3	46.7	43.2	49.9	37.6	42.3	42.3	43.5	41	46.3	35.7	40.1	40.1	40.5	39.1	43.1	33.9
1440	75	46.9	38.1	51	29.5	56.7	17.4	44.1	36.4	47.9	28	53.3	16.2	41.2	34.5	44.7	26.4	49.8	14.8	38	32.4	41.3	24.6	46.1	13.3	35	30.5	38	22.9	42.7	11.8
1440	80	48.5	44	51.8	37.2	56.7	26.9	45.7	42	48.7	35.5	53.4	25.5	42.7	39.9	45.5	33.7	49.9	24	39.6	37.7	42.1	31.7	46.3	22.3	36.6	35.7	38.9	30	42.8	20.7
1440	85	50.5	48.8	53	43.8	57.2	35.4	47.7	46.6	50	42	53.9	33.8	44.8	44.4	46.8	40	50.5	32.1	41.6	41.6	43.4	37.9	46.8	30.3	38.7	38.7	40.3	36	43.4	28.6
1440	90	52.9	52.5	54.7	49.4	58.2	42.8	50.2	50.2	51.7	47.4	54.9	41.1	47.2	47.2	48.6	45.3	51.5	39.2	44.1	44.1	45.2	43	47.9	37.2	41.7	41.7	42.1	41	44.5	35.4
1600	75	48.3	39.7	52.2	30.7	57.7	18.2	45.4	37.8	49	29.1	54.2	16.9	42.3	35.8	45.6	27.3	50.6	15.4	39	33.6	42.1	25.4	46.8	13.8	35.9	31.6	38.8	23.7	43.2	12.2
1600	80	50	45.8	53.2	38.6	57.9	28	47.1	43.7	***50***	***36.8***	54.5	26.5	44	41.5	46.7	34.9	50.9	24.9	40.8	39.2	43.1	32.9	47.1	23.1	37.7	37.1	39.9	31	43.6	21.4
1600	85	52.2	50.9	54.6	45.5	58.6	36.8	49.3	48.6	51.5	43.6	55.2	35.1	46.3	46.3	48.2	41.5	51.7	33.3	43.1	43.1	44.7	39.3	47.9	31.4	40.1	40.1	41.4	37.3	44.4	29.6
1600	90	54.9	54.9	56.5	51.4	59.8	44.5	52	52	53.4	49.3	56.4	42.7	49	49	50.1	47.1	52.9	40.7	46.2	46.2	46.7	44.7	49.2	38.6	43	43	43.4	42.6	45.7	36.7
1760	75	49.4	41	53.1	31.6	58.4	18.8	46.3	39	49.8	29.9	54.8	17.4	43.1	36.9	46.3	28.1	51.1	15.8	39.8	34.6	42.7	26.1	47.2	14.1	36.6	32.5	39.2	24.2	43.5	12.4
1760	80	51.3	47.4	54.3	39.9	58.9	28.9	48.3	45.2	51	38	55.3	27.3	45.1	42.9	47.6	36	51.6	25.6	41.8	40.5	43.9	33.8	47.7	23.7	38.6	38.3	40.5	31.9	44.1	21.9
1760	85	53.7	52.7	56	47.1	59.8	38	50.7	50.4	52.7	45	56.3	36.2	47.6	47.6	49.3	42.9	52.6	34.3	44.2	44.2	45.7	40.5	48.7	32.3	41.1	41.1	42.3	38.5	45.1	30.4
1760	90	56.6	56.6	58.1	53.3	61.2	46	53.6	53.6	54.9	51.1	57.7	44.1	50.5	50.5	51.5	48.7	54	42	47.4	47.4	47.9	46.2	50.2	39.8	44.1	44.1	44.6	44	46.6	37.8
1920	75	50.2	42.1	53.8	32.4	58.9	19.2	47.1	40	50.4	30.6	55.2	17.7	43.8	37.8	46.8	28.6	51.4	16	40.3	35.4	43	26.5	47.4	14.2	37	33.2	39.5	24.6	43.6	12.4
1920	80	52.4	48.8	55.2	40.9	59.6	29.6	49.3	46.5	51.8	38.9	55.9	27.9	46	44.1	48.2	36.8	52.1	26.1	42.5	41.6	44.5	34.6	48.1	24.1	39.2	39.2	41	32.5	44.4	22.2
1920	85	55	54.4	57.1	48.4	60.7	38.9	51.9	51.9	53.7	46.3	57.1	37.1	48.6	48.6	50.2	44	53.3	35.1	45.2	45.2	46.5	41.6	49.3	32.9	42	42	43	39.4	45.6	30.9
1920	90	58.1	58.1	59.4	54.9	62.4	47.3	55	55	56.1	52.6	58.7	45.2	51.8	51.8	52.6	50.1	55	43.1	48.4	48.4	48.9	47.5	51	40.7	45	45	45.4	45.2	47.3	38.7

Table F-6 Trane RTU-PRC048-T/YHC067E3 (5 ton) performance data

5 Ton T/YHC067E		Ambient Temperature																		Ambient Temperature											
		85						95						105						115						125					
CFM	DB	Entering Wet Bulb																		Entering Wet Bulb											
	F	61		67		73		61		67		73		61		67		73		61		67		73		61		67		73	
		CAP	SHC	CAP	SHC	CAP	SHC	CAP	SHC	CAP	SHC	CAP	SHC	CAP	SHC	CAP	SHC	CAP	SHC	CAP	SHC	CAP	SHC	CAP	SHC	CAP	SHC	CAP	SHC	CAP	SHC
1000	75	47.6	36.8	53.6	28.2	61.6	15.4	44.5	35	50.2	26.7	57.9	14.3	41.3	33	46.6	25.1	54	13.1	37.8	30.9	42.8	23.4	49.9	11.7	34.2	28.7	38.9	21.5	45.7	10.1
1000	80	48.4	42.5	53.4	36.1	60.5	25.5	45.4	40.5	50	34.4	56.8	24.2	42.2	38.3	46.5	32.6	52.9	22.7	38.8	36	42.8	30.6	48.9	21.1	35.2	33.5	38.9	28.5	44.7	19.4
1000	85	49.9	46.9	53.8	42.7	59.9	34.4	46.8	44.7	50.5	40.9	56.3	32.9	43.7	42.3	47	38.8	52.5	31.2	40.3	39.8	43.4	36.6	48.5	29.4	36.8	36.8	39.5	34.3	44.3	27.4
1000	90	51.9	50.1	54.9	48.1	60	42	48.9	47.7	51.6	46	56.4	40.3	45.8	45.1	48.1	43.8	52.6	38.4	42.5	42.3	44.5	41.4	48.7	36.4	40.3	40.3	40.8	38.9	44.6	34.2
1200	75	50.3	39.7	56	30.7	63.8	17.5	47.1	37.7	52.5	29.1	60	16.3	43.7	35.6	48.8	27.3	55.9	14.9	40.1	33.4	44.9	25.5	51.7	13.4	36.4	31	40.8	23.4	47.4	11.7
1200	80	51.4	45.7	56.1	38.9	62.9	28	48.2	43.5	52.6	37.1	59.1	26.5	44.8	41.2	48.9	35.1	55.1	24.9	41.3	38.8	45.1	33.1	51	23.2	37.7	36.2	41.1	30.8	46.7	21.3
1200	85	53	50.5	56.8	45.9	62.6	37.2	49.9	48.1	53.3	43.9	58.9	35.5	46.6	45.6	49.7	41.7	54.9	33.7	43.1	42.9	45.9	39.4	50.8	31.7	39.5	39.5	42	37	46.6	29.7
1200	90	55.3	54	58.1	51.6	62.9	45.1	52.2	51.4	54.7	49.4	59.2	43.2	49	48.7	51.1	47	55.3	41.2	45.5	45.5	47.4	44.5	51.3	39.1	43	43	43.5	41.8	47	36.8
1400	75	52.7	42.3	58.2	32.9	65.7	19.4	49.3	40.2	54.5	31.2	61.7	18	45.8	38	50.7	29.3	57.6	16.5	42.1	35.6	46.7	27.3	53.3	14.8	38.3	33.1	42.5	25.1	48.8	13
1400	80	54	48.7	58.5	41.5	65.1	30.2	50.7	46.4	54.9	39.5	61.1	28.6	47.2	43.9	51.1	37.4	57	26.8	43.6	41.3	47.1	35.2	52.8	25	39.8	38.6	43	32.8	48.3	23
1400	85	55.9	53.7	59.5	48.8	65	39.7	52.7	51.2	55.9	46.6	61.2	37.9	49.3	48.6	52.1	44.3	57.1	35.9	45.7	45.7	48.2	41.9	52.9	33.9	41.9	41.9	44.2	39.3	48.5	31.6
1400	90	58.5	57.6	61	54.8	65.6	47.9	55.3	54.9	57.5	52.5	61.8	45.9	51.9	51.9	53.8	50	57.8	43.8	48.3	48.3	49.9	47.3	53.6	41.5	45.4	45.4	45.9	44.5	49.2	39.1
1600	75	54.8	44.7	60	34.9	67.3	21	51.3	42.5	56.2	33	63.2	19.5	47.7	40.1	52.3	31	59	17.8	43.9	37.6	48.2	28.9	54.5	16	39.9	34.9	43.9	26.6	49.9	14.1
1600	80	56.4	51.3	60.6	43.8	67	32.1	52.9	48.9	56.9	41.7	62.9	30.4	49.3	46.3	53	39.5	58.7	28.5	45.6	43.6	48.9	37.1	54.3	26.5	41.7	40.8	44.7	34.6	49.7	24.4
1600	85	58.5	56.7	61.8	51.4	67.2	41.9	55.2	54.1	58.1	49.1	63.2	40	51.6	51.3	54.3	46.7	59	37.9	47.9	47.9	50.2	44.1	54.6	35.7	44	44	46	41.4	50.1	33.4
1600	90	61.3	60.9	63.6	57.8	68	50.5	58	58	60	55.3	64	48.4	54.5	54.5	56.2	52.7	59.9	46.1	50.8	50.8	52.2	49.9	55.6	43.7	47.6	47.6	48	47	51.1	41.1
1800	75	56.6	46.8	61.6	36.6	68.7	22.3	53	44.4	57.7	34.6	64.4	20.7	49.2	41.9	53.6	32.5	60	18.9	45.3	39.3	49.4	30.2	55.5	17	41.2	36.5	44.9	27.8	50.8	14.9
1800	80	58.4	53.8	62.4	45.8	68.5	33.8	54.9	51.2	58.6	43.6	64.4	31.9	51.2	48.5	54.6	41.3	60	29.9	47.3	45.7	50.4	38.8	55.5	27.8	43.3	42.7	46	36.2	50.8	25.5
1800	85	60.9	59.5	63.9	53.8	69	43.9	57.4	56.7	60.1	51.4	64.9	41.9	53.7	53.7	56.1	48.8	60.6	39.7	49.9	49.9	52	46.1	56.1	37.3	45.9	45.9	47.6	43.3	51.5	34.9
1800	90	63.9	63.9	66	60.5	70.1	52.9	60.5	60.5	62.2	57.9	66	50.6	56.8	56.8	58.3	55.1	61.8	48.2	53.6	53.6	54.2	52.2	57.3	45.6	49.4	49.4	49.9	49.2	52.8	42.9
2000	75	58.1	48.6	62.9	38.1	69.7	23.4	54.4	46.1	58.8	36	65.4	21.6	50.5	43.5	54.6	33.7	60.8	19.7	46.5	40.7	50.3	31.3	56.2	17.7	42.3	37.8	45.7	28.7	51.3	15.5
2000	80	60.2	55.9	64	47.6	69.8	35.2	56.5	53.2	60	45.3	65.5	33.2	52.7	50.4	55.8	42.8	61.1	31.1	48.7	47.4	51.5	40.2	56.4	28.8	44.5	44.3	47	37.4	51.6	26.4
2000	85	62.9	62	65.7	55.9	70.6	45.7	59.3	59.1	61.8	53.4	66.3	43.5	55.5	55.5	57.7	50.7	61.9	41.2	51.5	51.5	53.4	47.9	57.3	38.7	47.4	47.4	49	44.9	52.6	36.1
2000	90	66.2	66.2	68	63	71.9	54.9	62.6	62.6	64.1	60.2	67.7	52.5	58.9	58.9	60.1	57.3	63.3	50	55.3	55.3	55.8	54.3	58.8	47.3	50.9	50.9	51.5	51.1	54.1	44.5
2200	75	59.3	50.2	63.9	39.3	70.5	24.3	55.5	47.6	59.7	37	66	22.3	51.5	44.8	55.4	34.6	61.4	20.3	47.3	41.9	50.9	32.1	56.6	18.1	43	38.9	46.3	29.4	51.6	15.8
2200	80	61.7	57.9	65.2	49.2	70.9	36.3	57.9	55	61.1	46.7	66.4	34.2	54	52.1	56.9	44.1	61.8	32	49.8	49	52.4	41.3	57.1	29.6	45.5	45.5	47.8	38.4	52.2	27
2200	85	64.7	64.3	67.2	57.8	71.9	47.2	60.9	60.9	63.2	55.1	67.5	44.8	57	57	58.9	52.3	62.9	42.4	52.9	52.9	54.5	49.3	58.2	39.8	48.7	48.7	50	46.2	53.3	37
2200	90	68.2	68.2	69.8	65.1	73.5	56.7	64.5	64.5	65.8	62.3	69.1	54.2	60.7	60.7	61.6	59.2	64.6	51.6	56.7	56.7	57.2	56.1	60	48.7	52.7	52.7	52.7	52.7	55.1	45.8
2400	75	60.3	51.6	64.6	40.3	70.9	24.8	56.3	48.8	60.3	37.9	66.3	22.8	52.2	45.9	55.9	35.3	61.6	20.6	47.9	42.9	51.2	32.7	56.7	18.3	43.5	39.7	46.5	29.8	51.6	15.8
2400	80	62.9	59.5	66.2	50.5	71.6	37.2	59	56.6	62	47.9	67	35	54.9	53.5	57.6	45.1	62.3	32.6	50.7	50.2	53	42.2	57.5	30.1	46.3	46.3	48.3	39.2	52.4	27.4
2400	85	66.1	66.1	68.4	59.4	72.8	48.4	62.3	62.3	64.3	56.6	68.3	45.9	58.2	58.2	59.9	53.6	63.7	43.4	54	54	55.4	50.5	58.8	40.6	49.7	49.7	50.7	47.3	53.8	37.7
2400	90	69.9	69.9	71.3	67.1	74.7	58.3	66.1	66.1	67.1	64.1	70.2	55.7	62.2	62.2	62.8	60.9	65.6	52.9	57.8	57.8	58.4	57.6	60.8	49.9	53.7	53.7	53.7	53.7	55.9	46.8

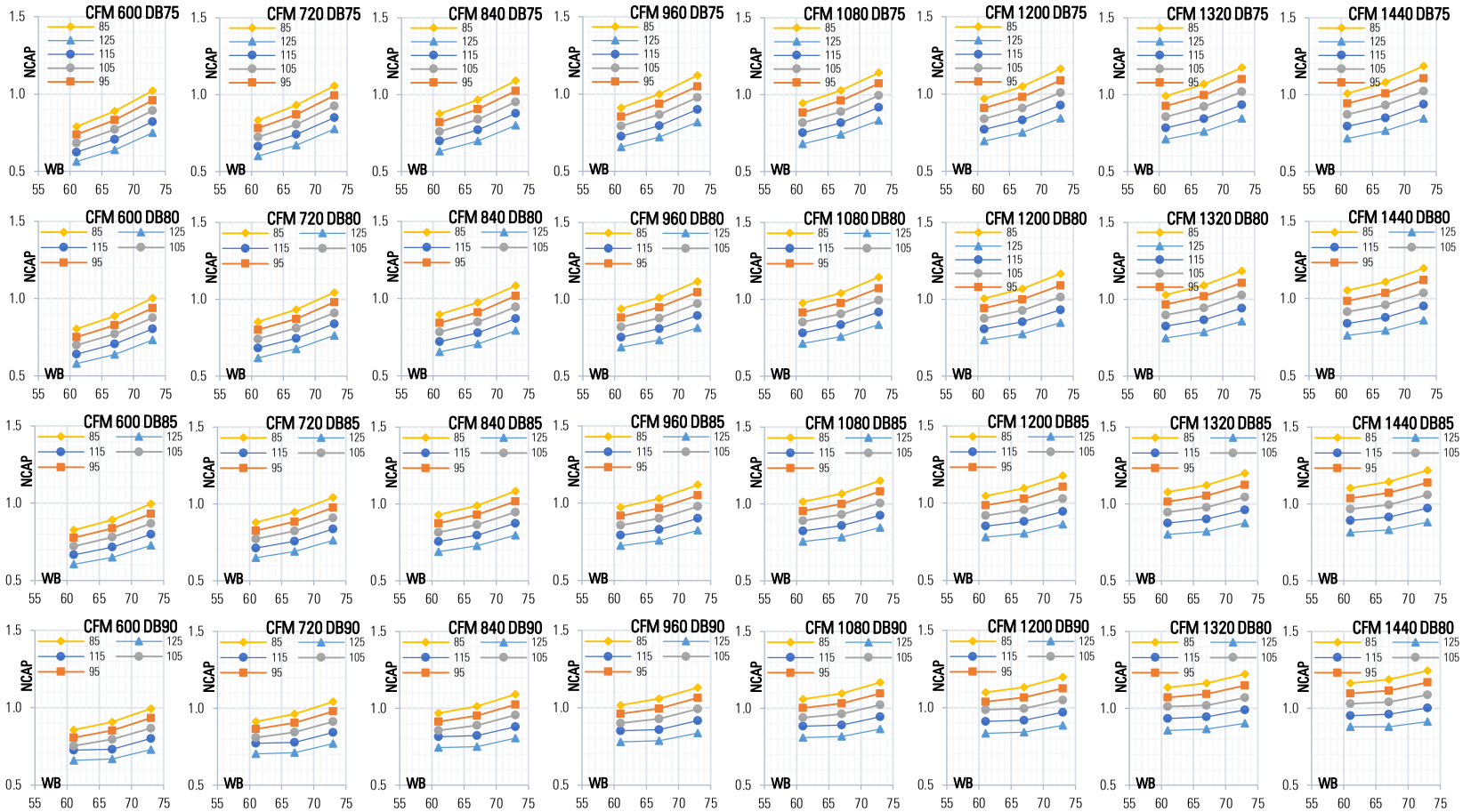

(a) Fixed CFM and DB, vary OAT: Cooling capacity plots

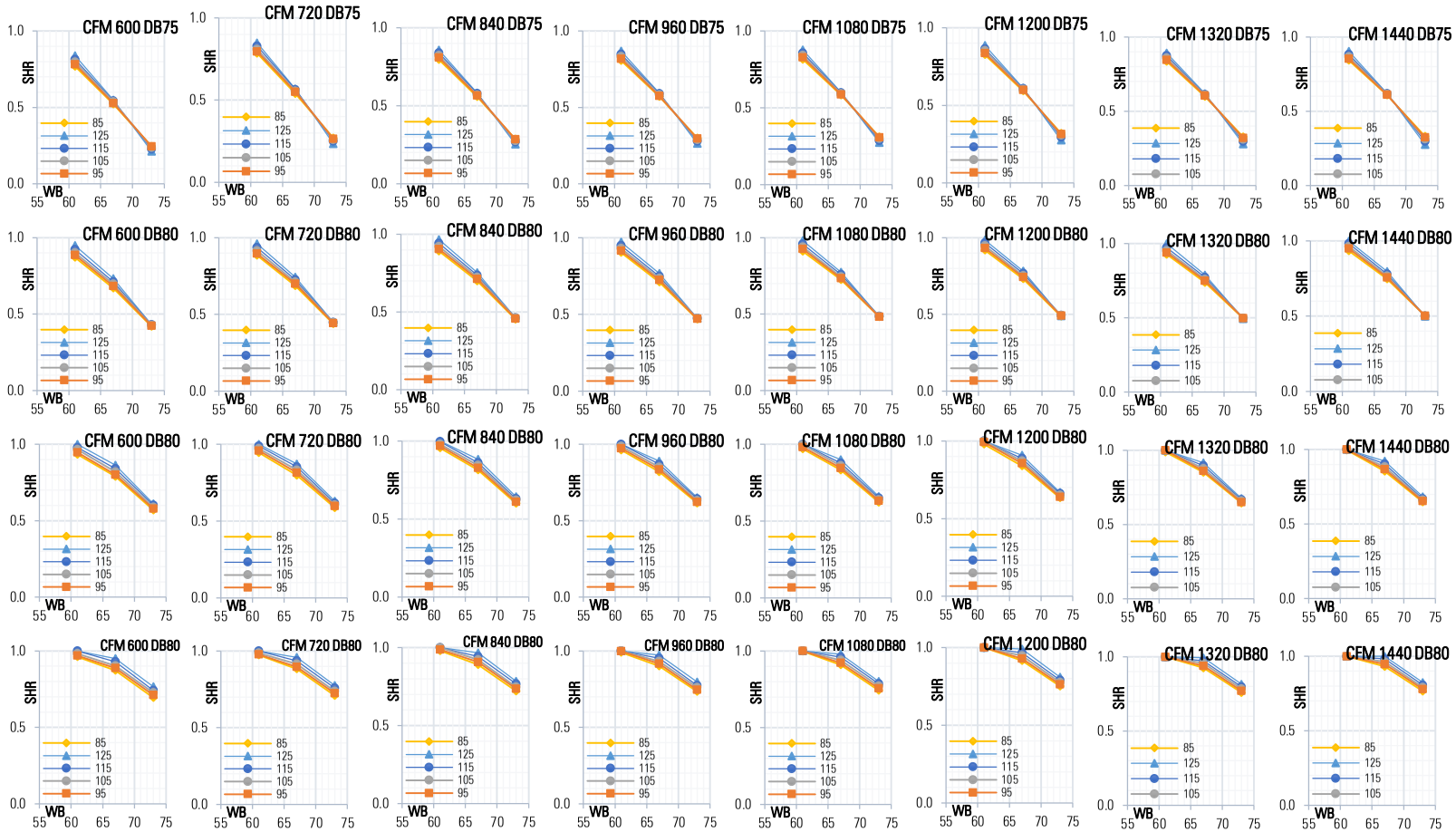

(b) Fixed CFM and DB, vary OAT: Cooling capacity plots

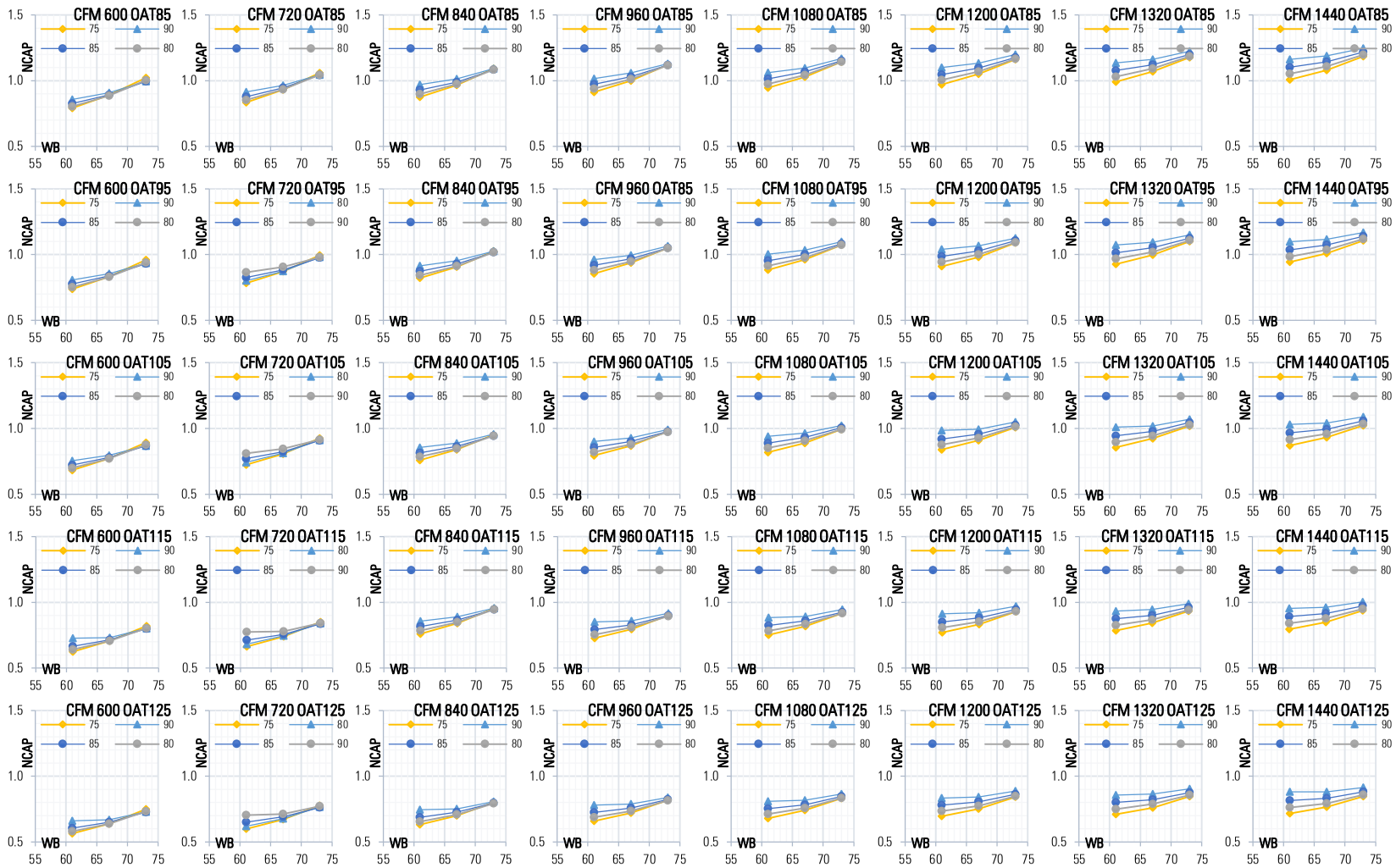

(c) Fixed OAT and CFM, vary DB: Cooling capacity plots

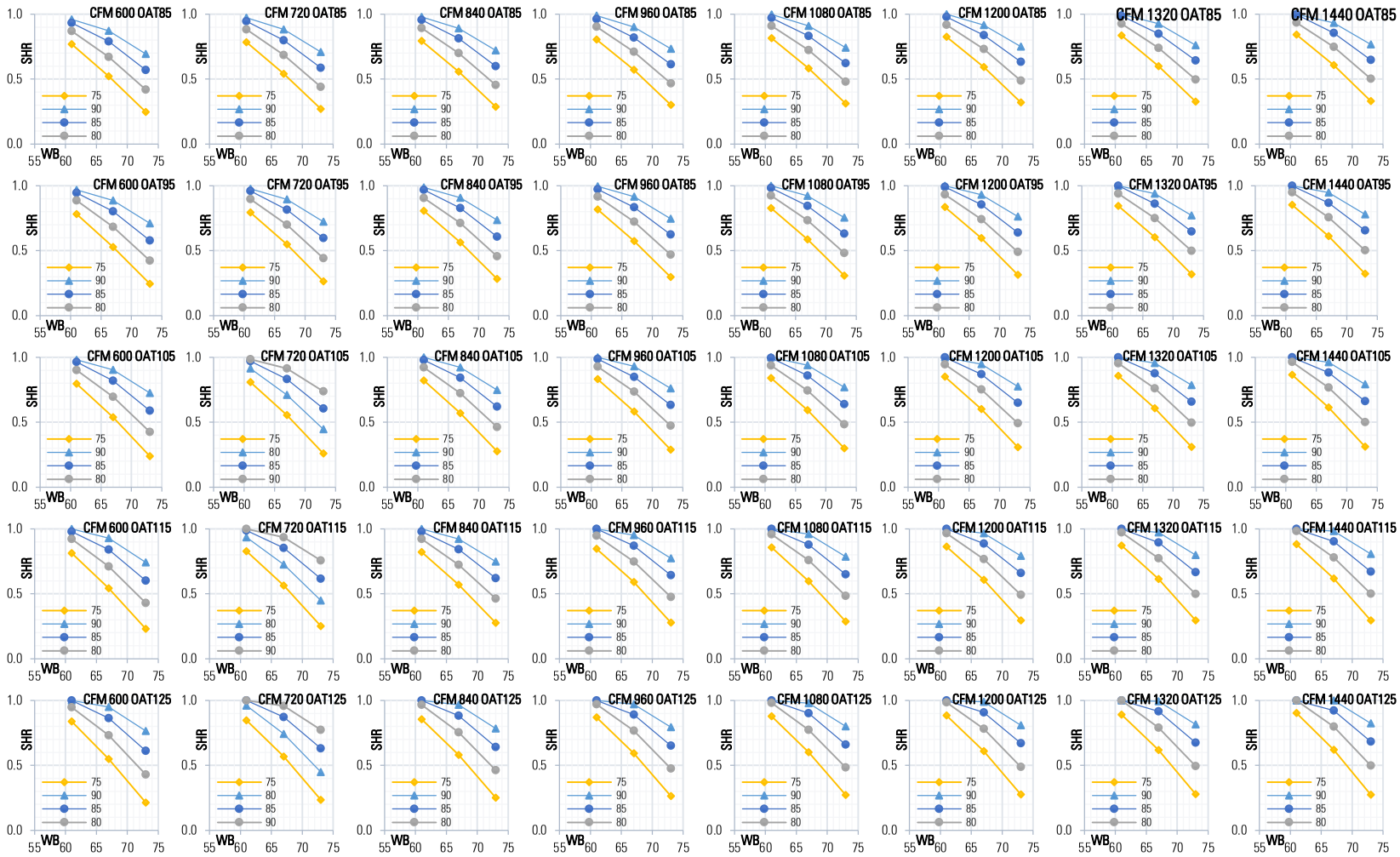

(d) Fixed OAT and CFM, vary DB: SHR plots

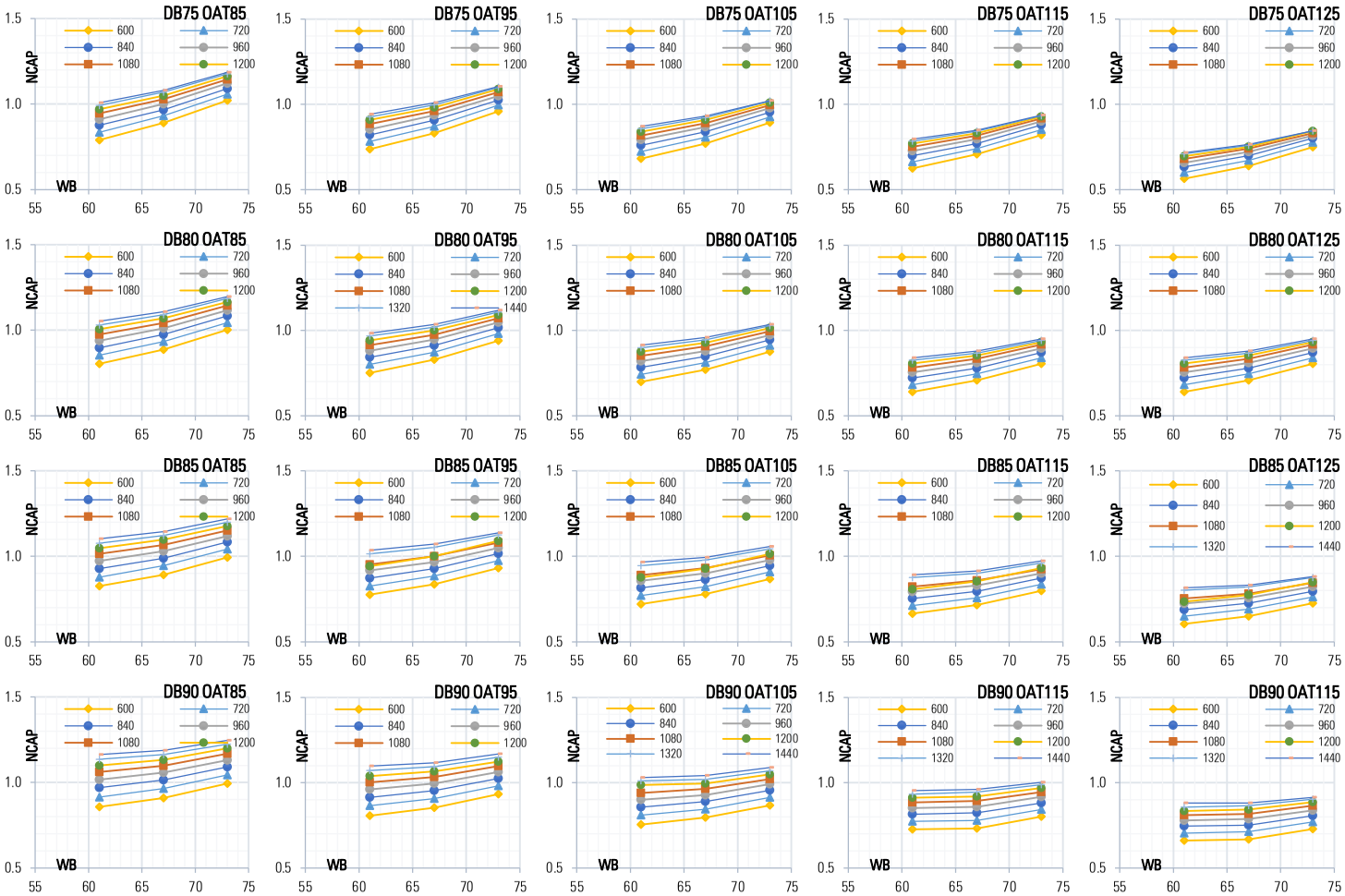

(e) Fixed OAT and DB, vary CFM: Cooling capacity plots

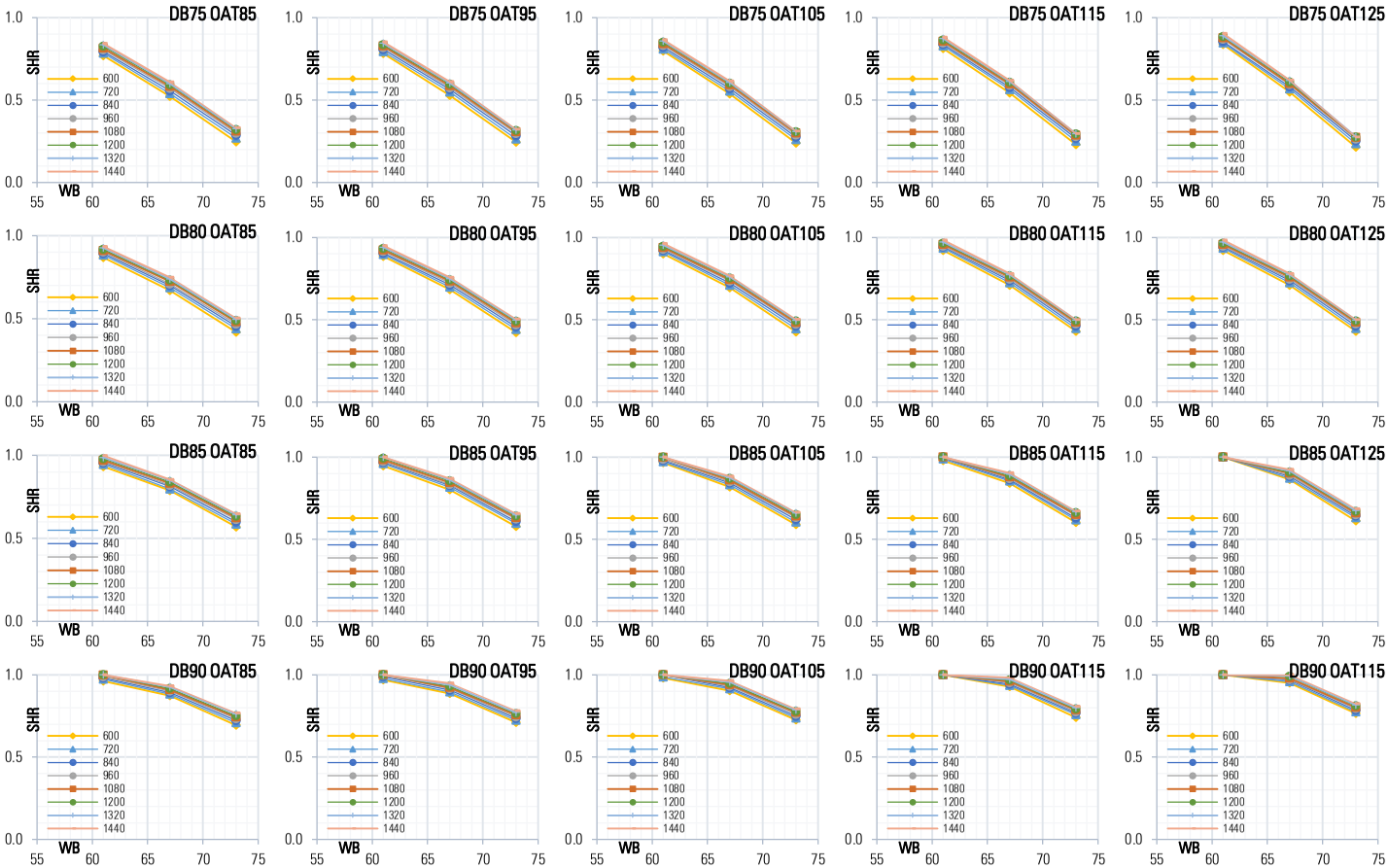

(f) Fixed OAT and DB, vary CFM: SHR plots

Figure F-4 Trane RTU model PRC048K T/YHC037E3 model 3 Tons Normalized capacity and SHR performance plots

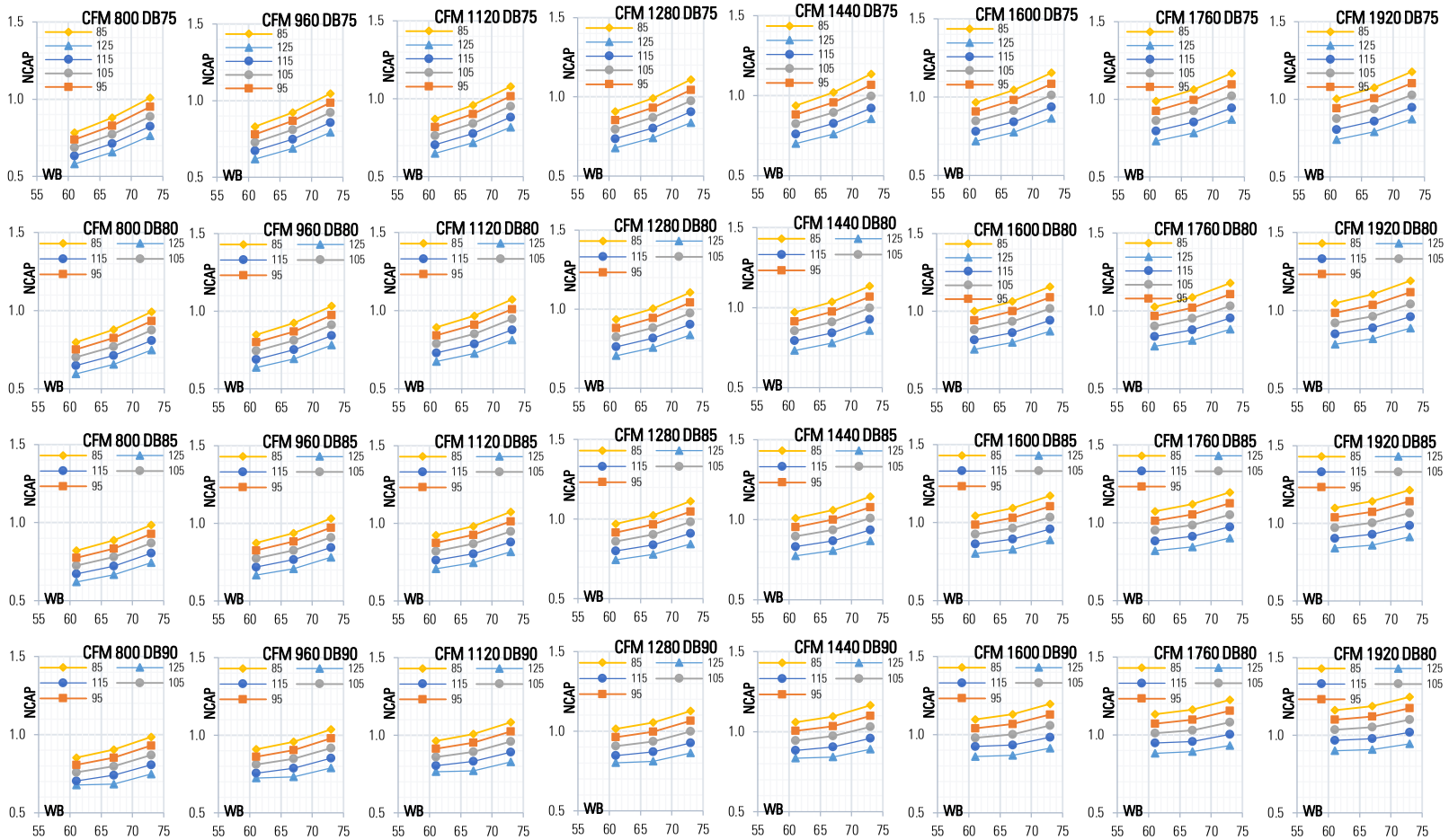

(a) Fixed CFM and DB, vary OAT: Cooling capacity plots

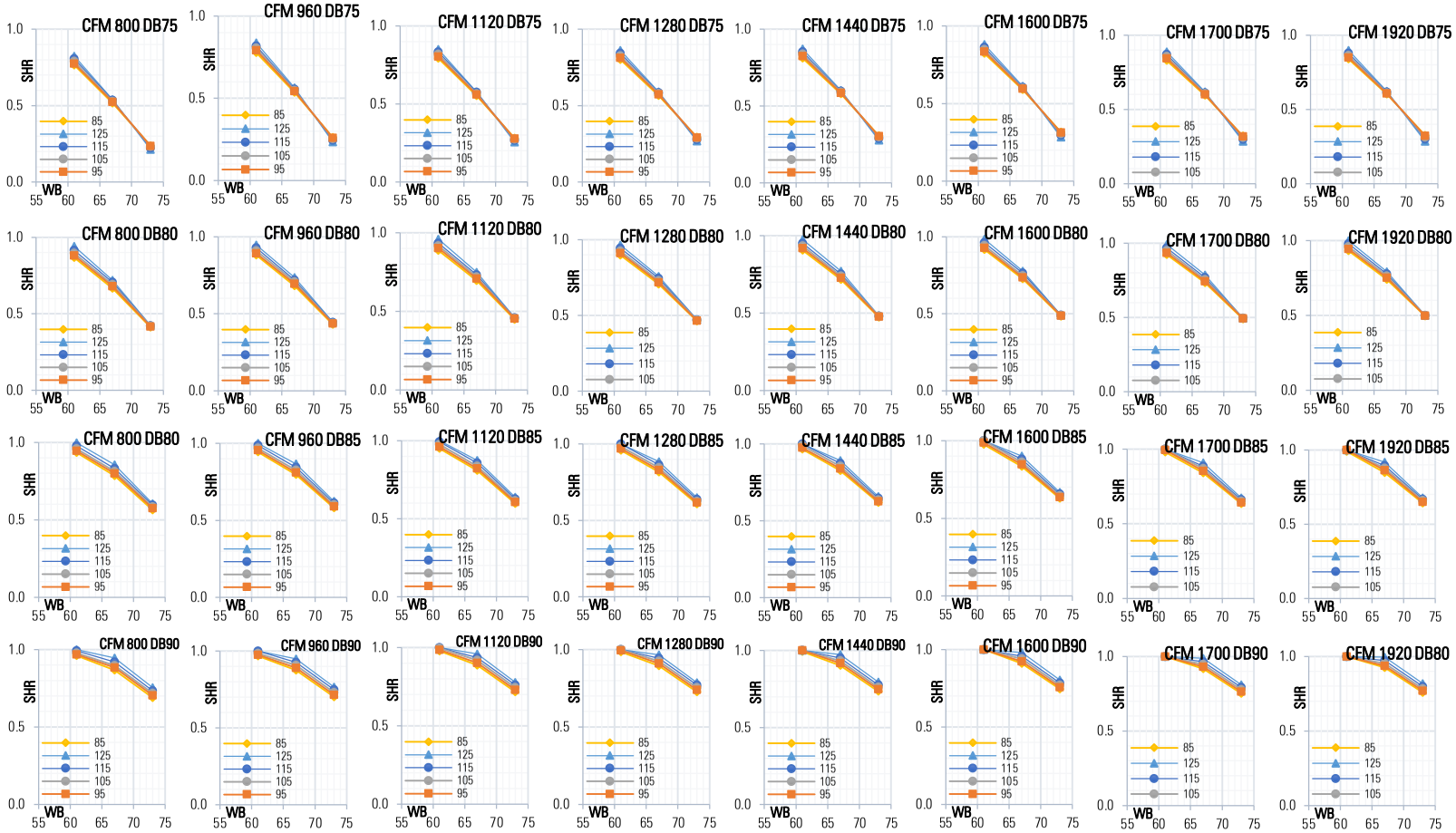

(b) Fixed CFM and DB, vary OAT: SHR plots

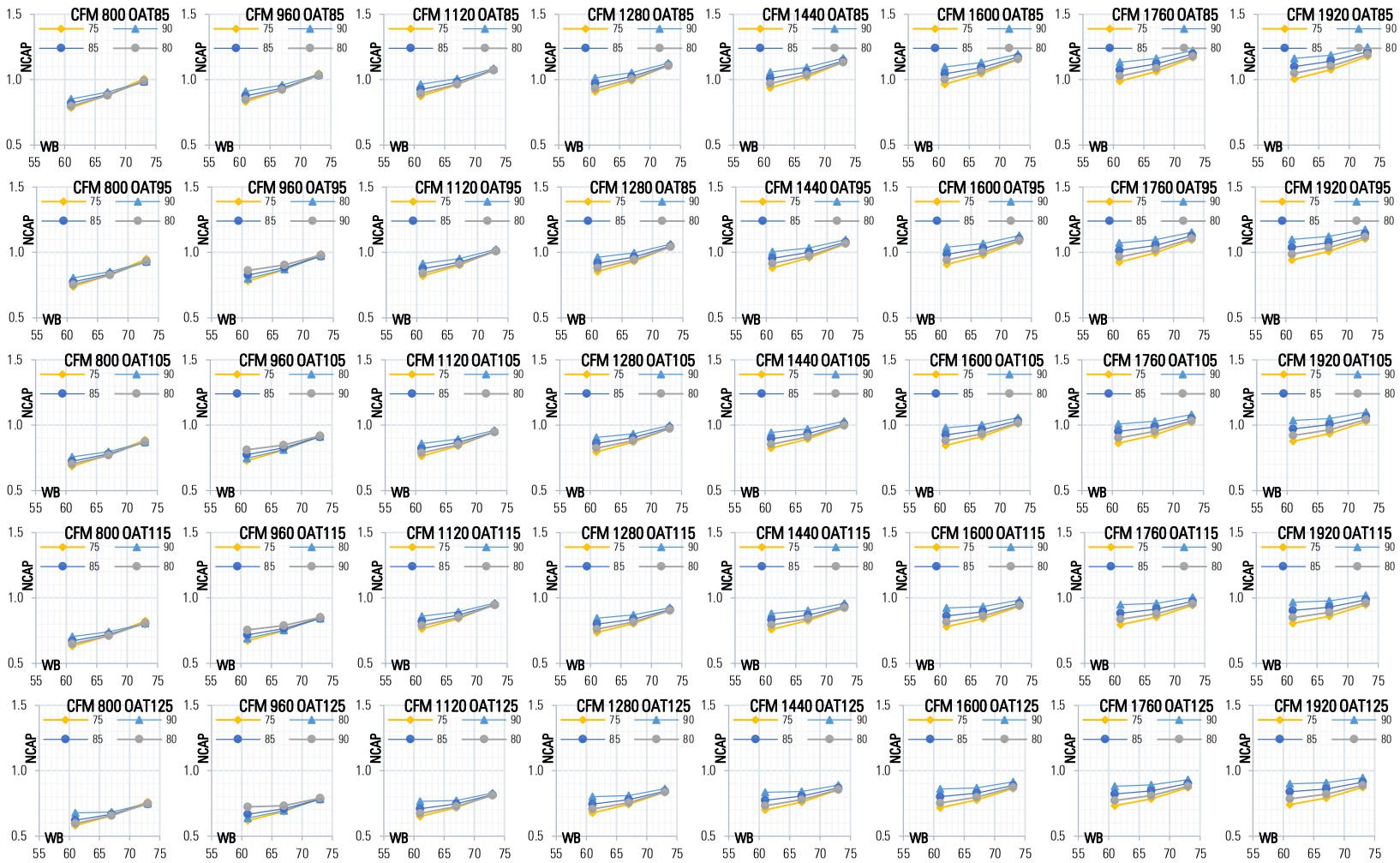

(c) Fixed OAT and CFM, vary DB: Cooling capacity plots

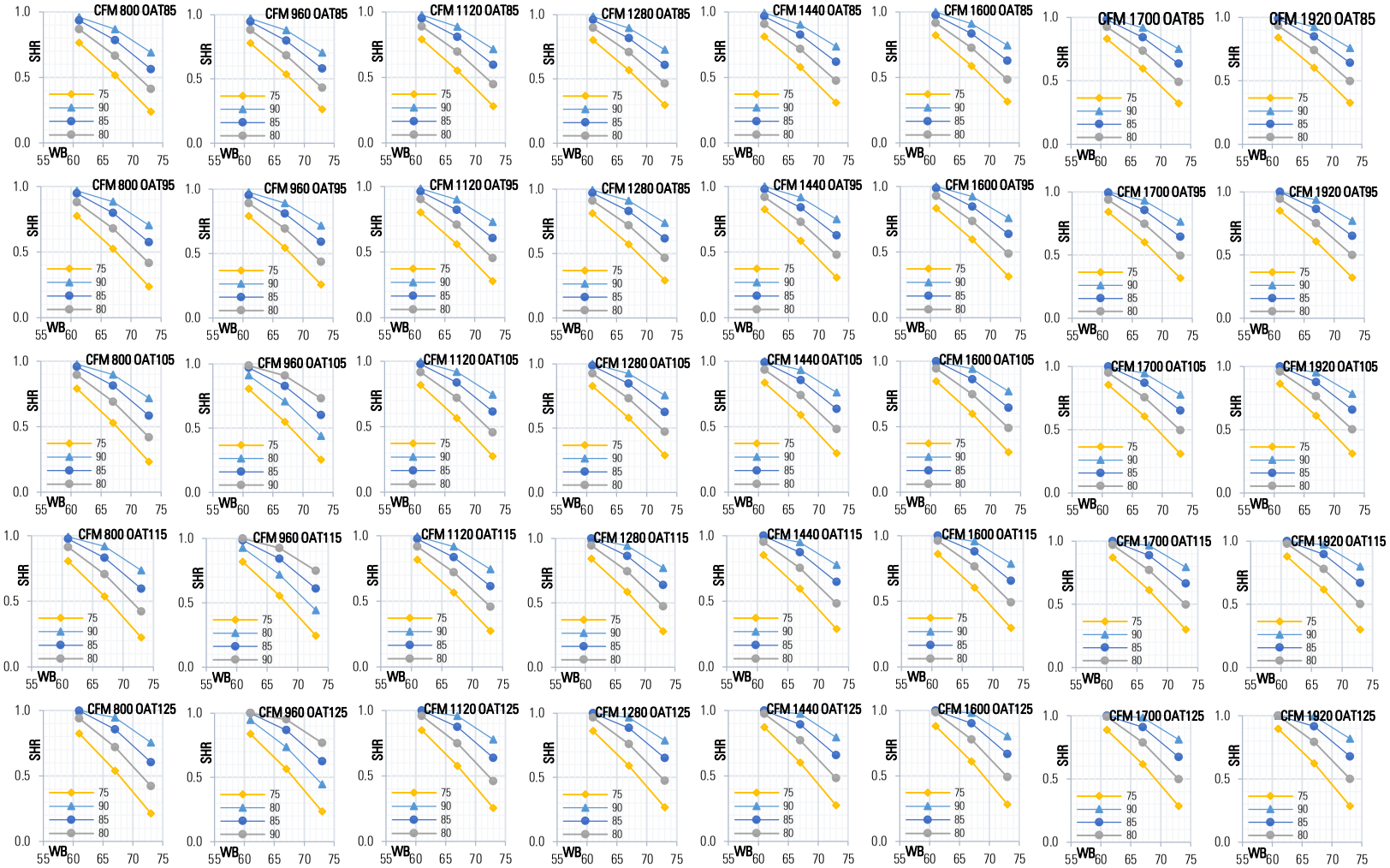

(d) Fixed OAT and CFM, vary DB: Cooling capacity plots

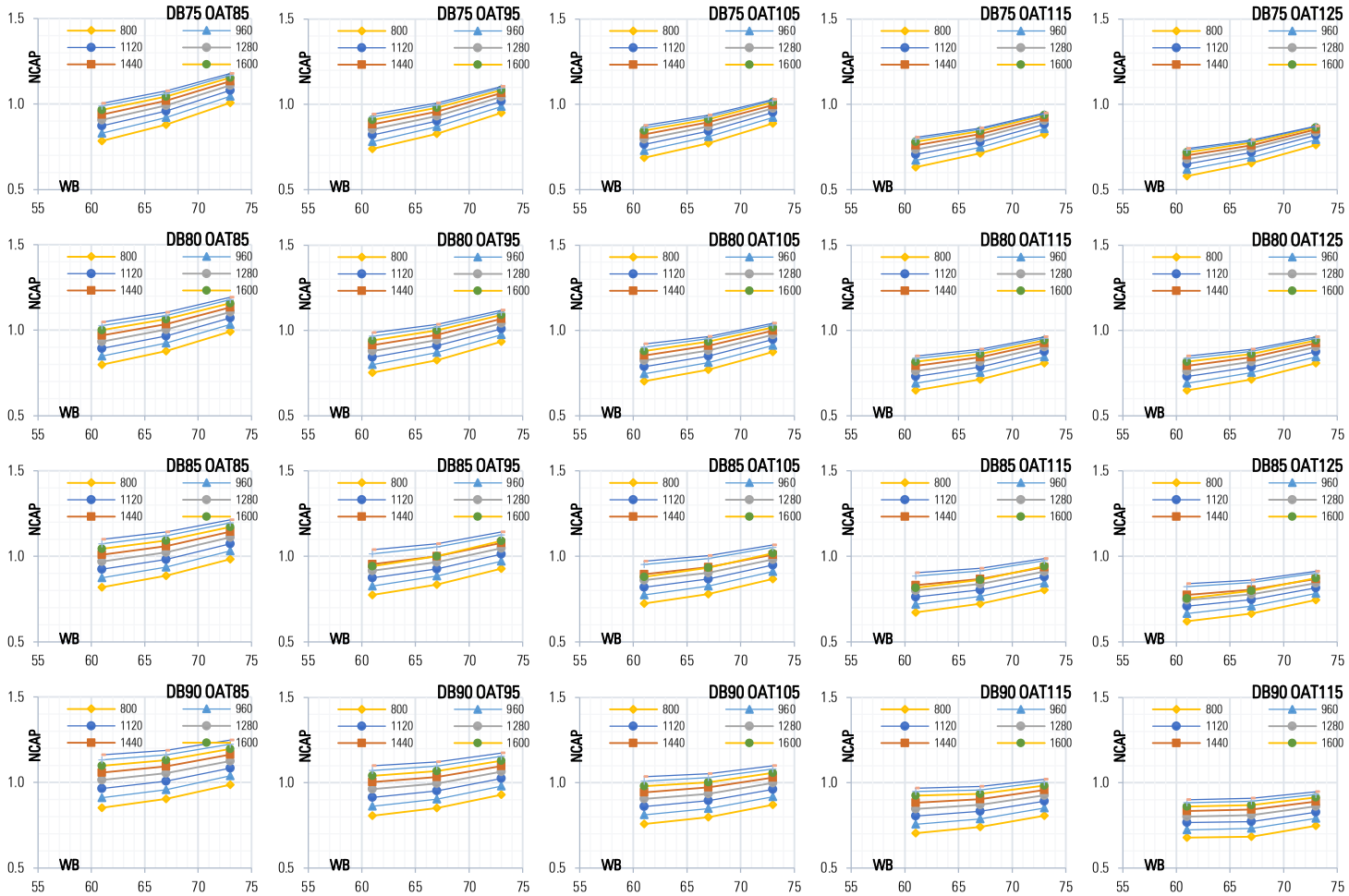

(e) Fixed OAT and DB, vary CFM: Cooling capacity plots

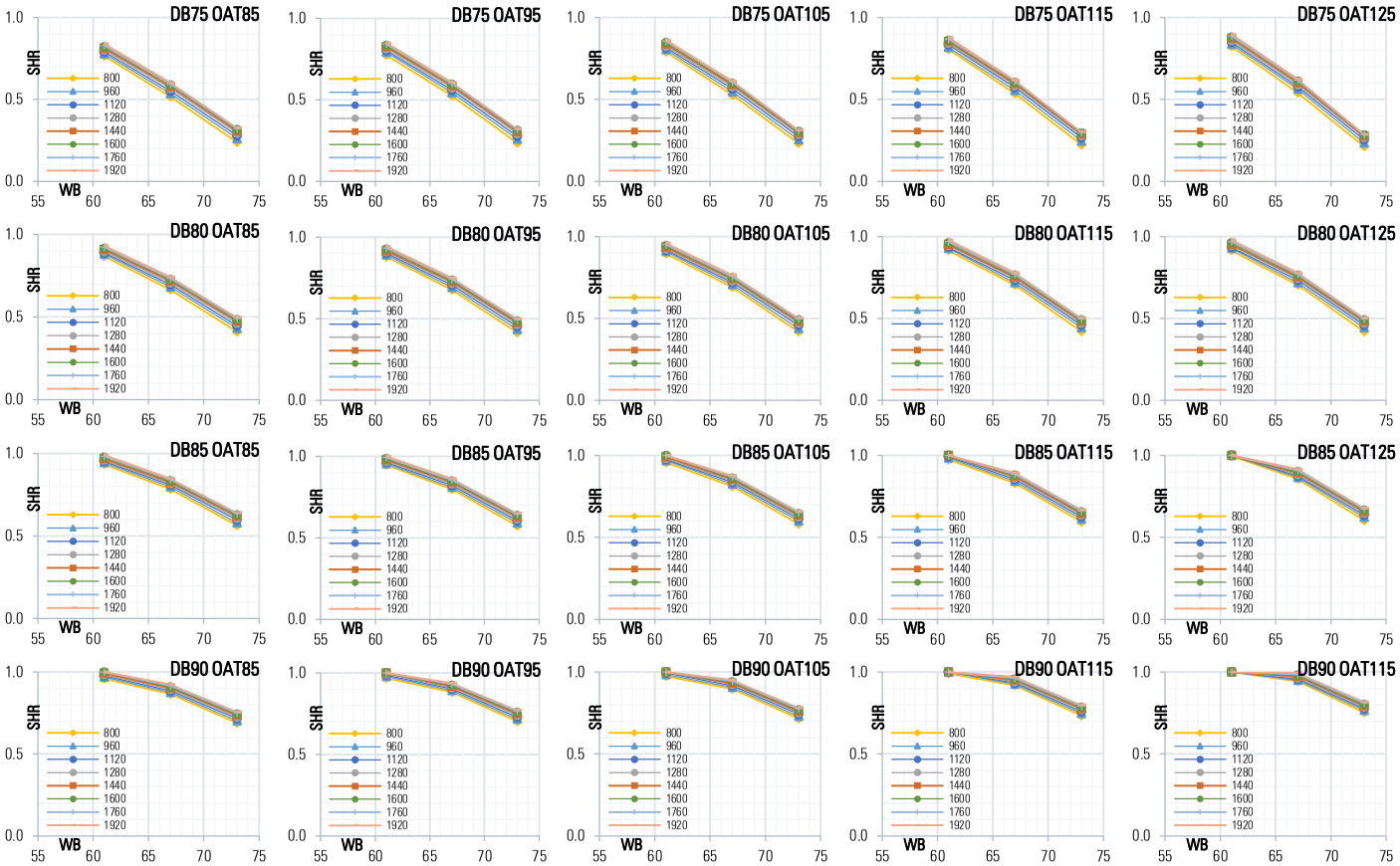

(f) Fixed OAT and DB, vary CFM: SHR plots

Figure F-5 Trane RTU model PRC048K T/YHC047E3 4 Ton Normalized capacity and SHR performance plots

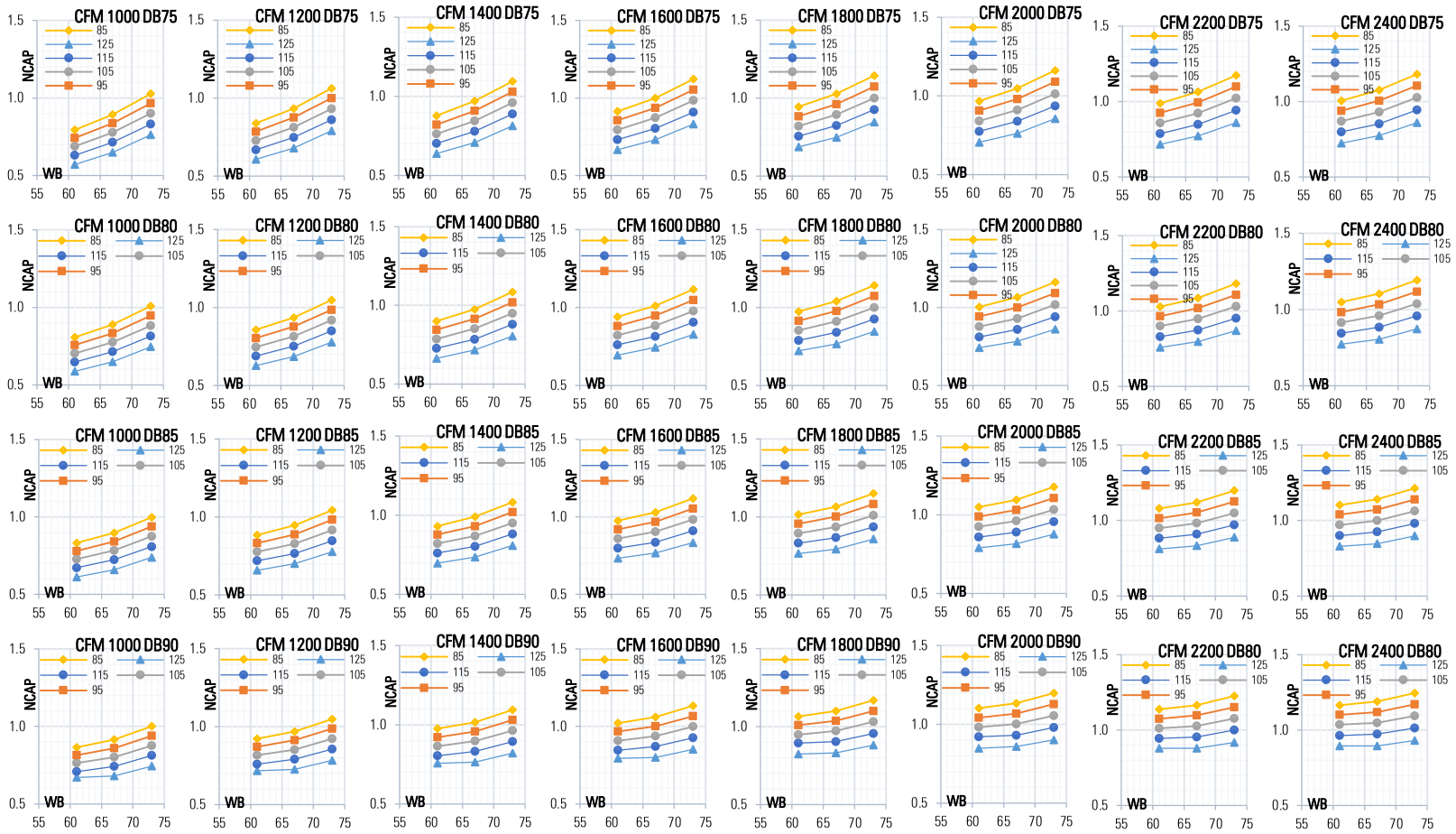

(a) Fixed CFM and DB, vary OAT: Cooling capacity plots

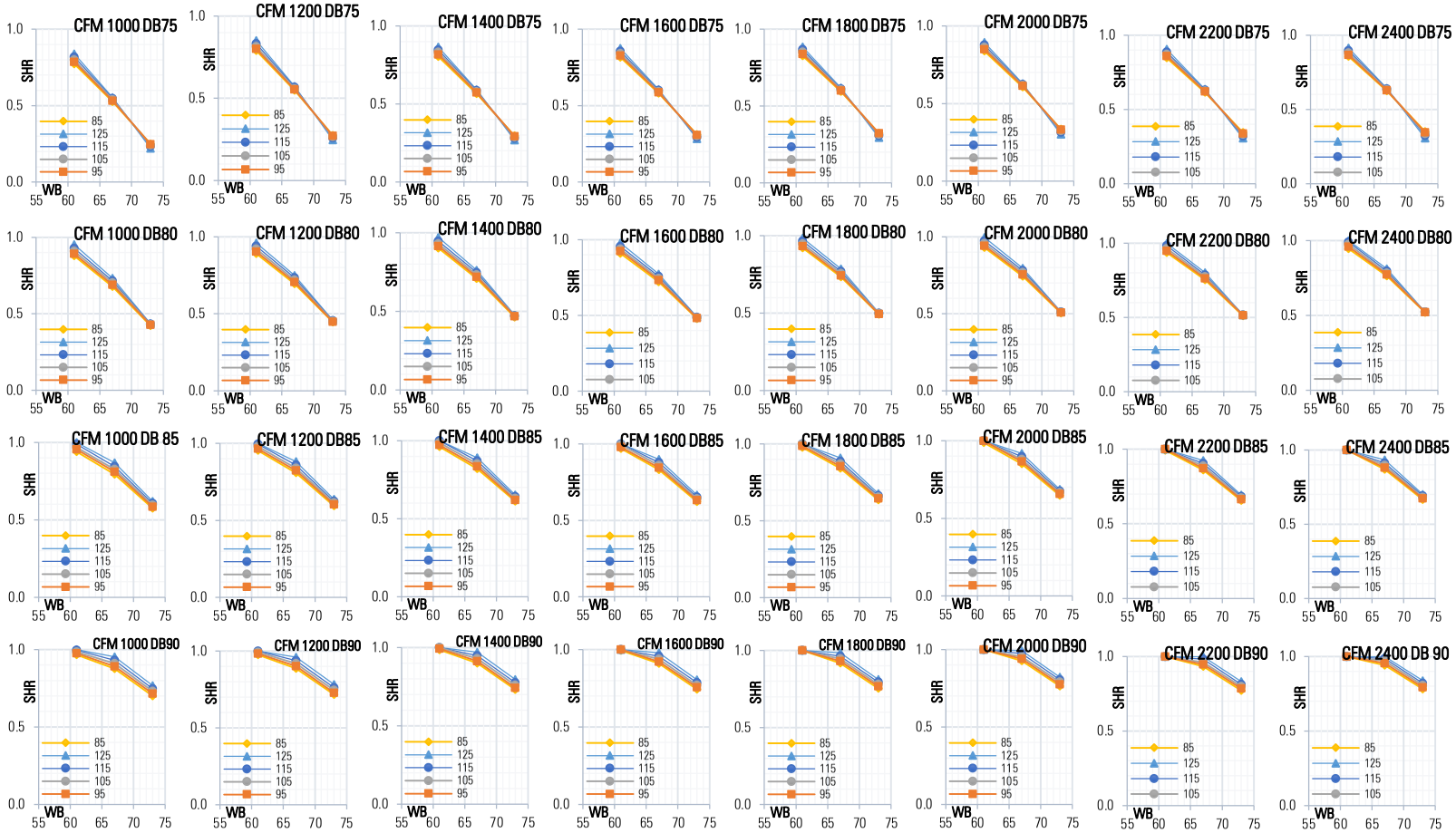

(b) Fixed CFM and DB, vary OAT: Cooling capacity plots

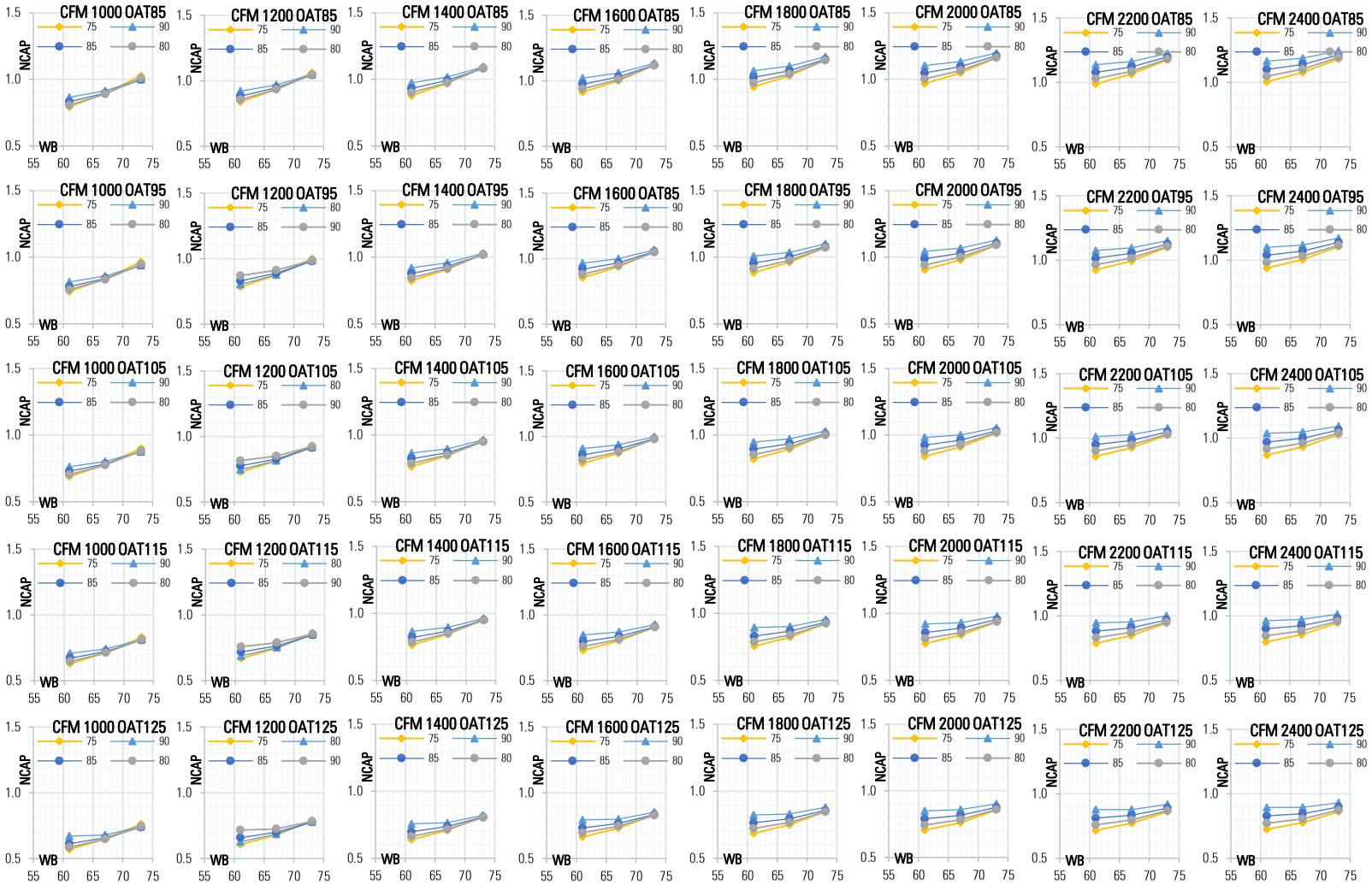

(c) Fixed OAT and DB, vary CFM: Cooling capacity plots

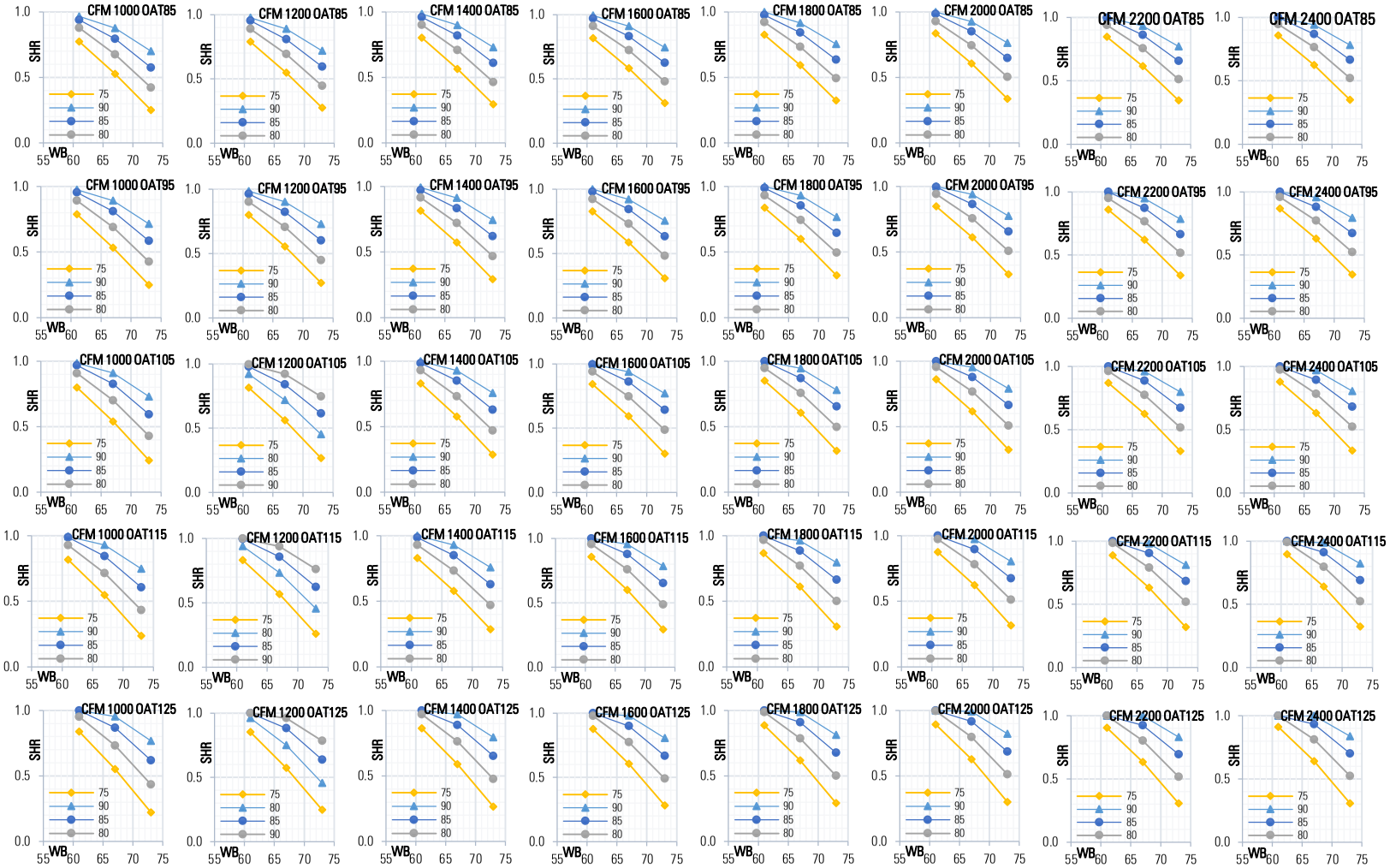

(d) Fixed OAT and CFM, vary DB: Cooling capacity plots

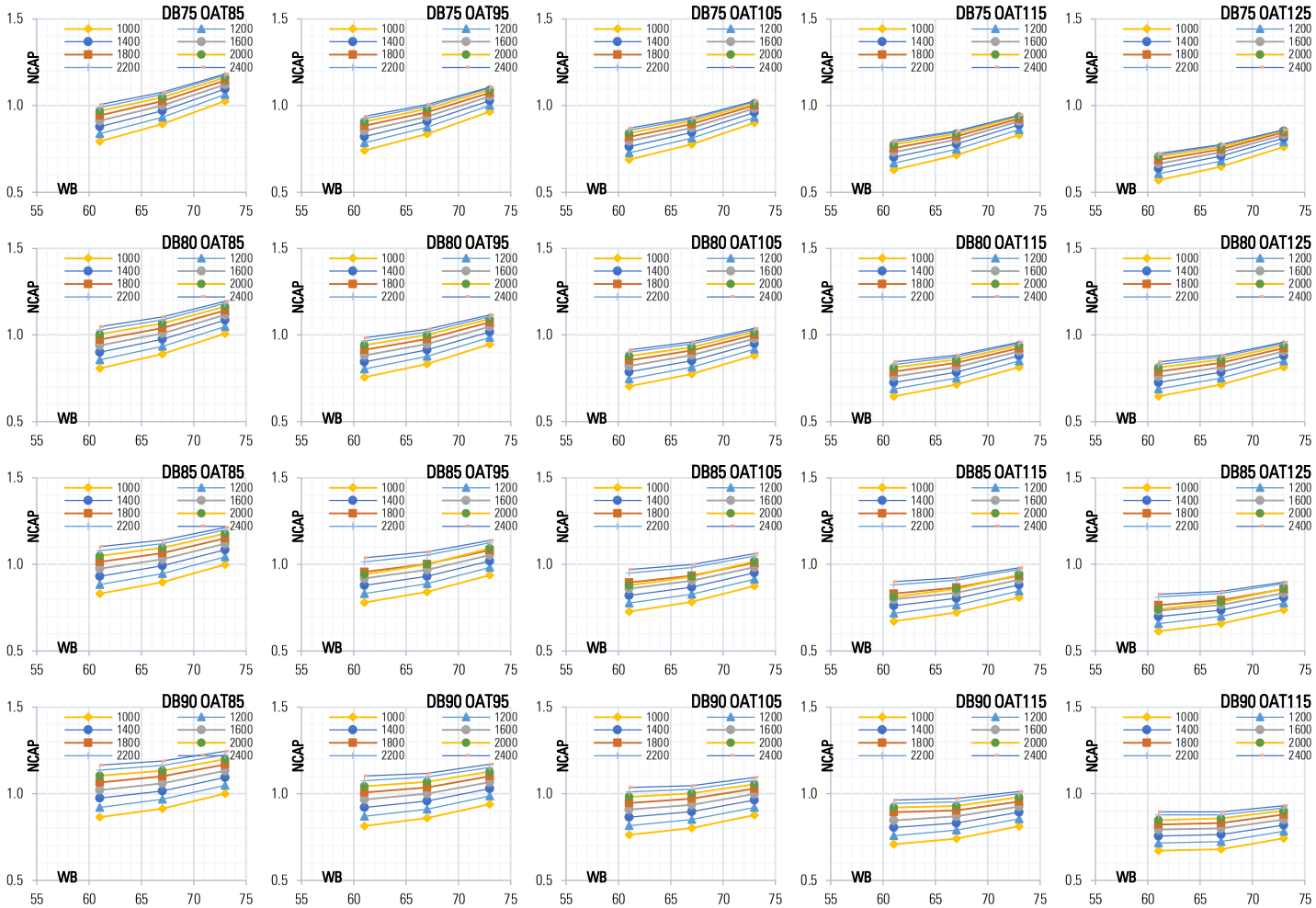

(e) Fixed OAT and CFM, vary DB: Cooling capacity plots

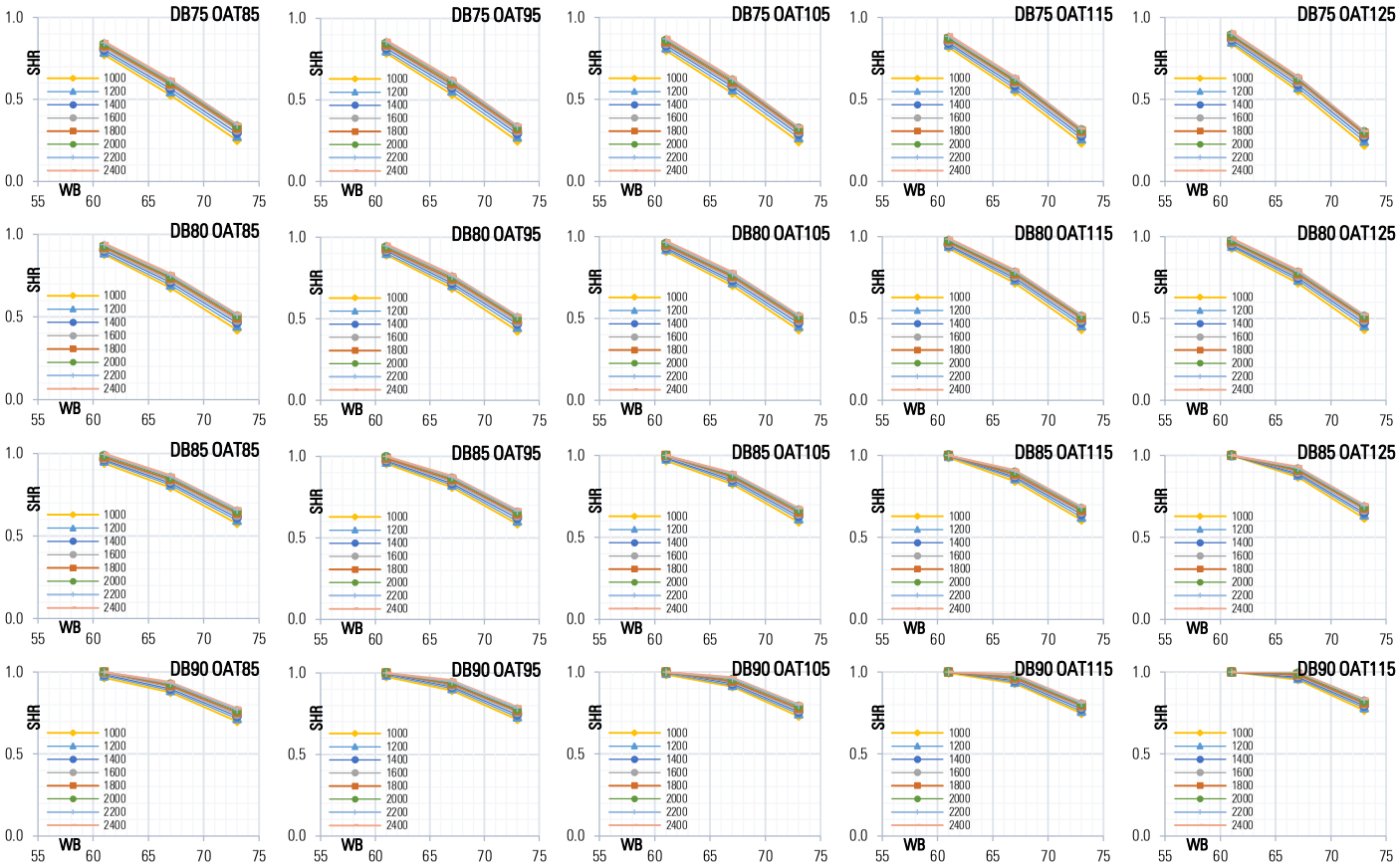

(f) Fixed OAT and DB, vary CFM: SHR plots

Figure F-6 Trane RTU model PRC048K T/YHC067E3 (5 Ton) Normalized capacity and SHR performance plots

APPENDIX G LOCAL OPTIMIZED CRITICAL POINTS OF VARIOUS COOLING CONDITIONS

Table G-1 An RTU's cooling performance data.

OAT		85						95						105						115					
CFM	WB	61	61	67	67	73	73	61	61	67	67	73	73	61	61	67	67	73	73	61	61	67	67	73	73
x100	ºF	MBH	SHC	MBH	SHC	MBH	SHC	MBH	SHC	MBH	SHC	MBH	SHC	MBH	SHC	MBH	SHC	MBH	SHC	MBH	SHC	MBH	SHC	MBH	SHC
63	75	195	171	213	127	224	83	182	164	206	124	219	80.1	169	158	195	119	213	76.1	155	151	181	113	204	71.8
	80	200	200	214	157	226	114	191	191	207	156	221	112	180	180	196	153	214	110	168	168	183	147	205	106
	85	211	211	217	188	229	140	204	204	209	188	223	139	195	195	199	186	216	139	184	184	187	182	206	137
	90	219	219	220	217	230	164	214	214	214	214	225	167	207	207	207	207	218	169	198	198	198	198	208	168
70	75	199	181	215	131	225	84.7	187	176	208	129	221	81.4	174	169	198	125	215	77.7	160	160	185	119	206	73.4
	80	206	206	217	164	228	116	198	198	210	164	222	114	188	188	200	162	216	113	176	176	187	157	207	110
	85	216	216	220	197	230	144	210	210	213	198	225	144	202	202	204	198	218	145	192	192	192	192	209	144
	90	224	224	224	224	233	172	219	219	219	219	227	173	212	212	212	212	221	177	204	204	204	204	211	177
77	75	203	191	217	135	226	86.1	192	187	211	138	222	82.9	178	178	201	131	216	79.2	165	165	188	126	208	75
	80	211	211	219	169	229	118	204	204	212	171	224	117	194	194	203	170	218	116	183	183	191	167	209	114
	85	220	220	222	203	232	147	214	214	216	207	226	148	207	207	207	207	220	150	197	197	197	197	211	150
	90	226	226	226	226	235	176	223	223	222	222	229	179	216	216	216	216	223	184	208	208	208	208	214	186
84	75	206	199	218	138	227	87.8	195	195	212	143	223	84.3	183	183	203	136	217	80.6	171	171	190	132	209	76.5
	80	214	214	221	174	230	120	208	208	214	178	226	120	199	199	205	178	219	119	188	188	194	176	211	117
	85	222	222	224	210	233	150	217	217	218	215	228	151	211	211	211	211	222	155	202	202	202	202	213	156
	90	229	229	229	229	236	181	225	225	225	225	231	184	220	220	219	219	225	190	212	212	212	212	216	193

Table G-2 Critical plots based on local optimization of maximized R square values at 85°f of Outdoor air temperature

Calculation table at OAT = 85ºF

Cond.	CFM	DB	OAT	WB	CAP	SHC	NCFM	SHR	NCAP
Guess	6300	75	85	57.87	187	187	360	1	0.89
	6300	75	85	61	195	171	360	0.88	0.93
	6300	75	85	67	213	127	360	0.60	1.01
	6300	75	85	73	224	83	360	0.37	1.07
Crit	6300	75	85	57.87	187	187	360	1	0.89

	NCAP			SHR			Obj.
Cond.	m	c	r^2	m	c	r^2	
Initial	0.012	0.227	0.981	-0.042	3.451	0.981	
Optimized	0.012	0.206	0.990	-0.042	3.451	0.998	0.998
rel_dev	2.5%	9.1%	0.9%	0.0%	0.0%	1.7%	

Cond	CFM	DB	OAT	WB	CAP	SHC	NCFM	SHR	NCAP
	6300	80	85	61	200	200	360	1.00	0.95
Guess	6300	80	85	61.00	200	200	360	1.00	0.95
	6300	80	85	67	214	157	360	0.73	1.02
	6300	80	85	73	226	114	360	0.50	1.08
Crit	6300	80	85	61.00	200	200	360	1	0.95

	NCAP			SHR			Objective
Cond.	m	c	r^2	m	c	r^2	
initial cod.	0.010	0.381	0.998	-0.038	3.293		
Opt cond	0.010	0.323	0.998	-0.041	9.838	0.998	0.998
rel_dev							

Cond	CFM	DB	OAT	WB	CAP	SHC	NCFM	SHR	NCAP
	6300	85	85	61	211	211	360	1.00	1.00
Guess	6300	85	85	63.86	211	211	360	1.00	1.00
	6300	85	85	67	217	188	360	0.87	1.03
	6300	85	85	73	229	140	360	0.61	1.09
Crit	6300	85	85	63.86	211	211	360	1	1.00

	NCAP			SHR			Objective
Cond.	m	c	r^2	m	c	r^2	
initial cod.	0.010	0.395	1.000	-0.043	3.714		
Opt cond	0.009	0.405	1.000	-0.043	3.714	1.000	1.000
rel_dev							

CFM,DB,OAT

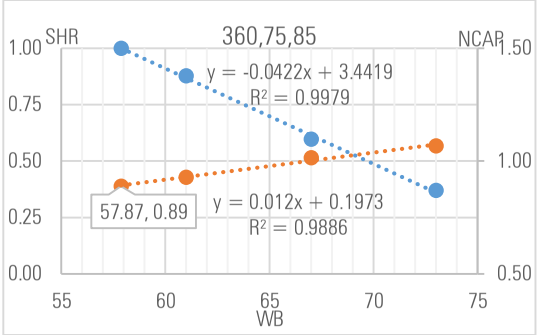

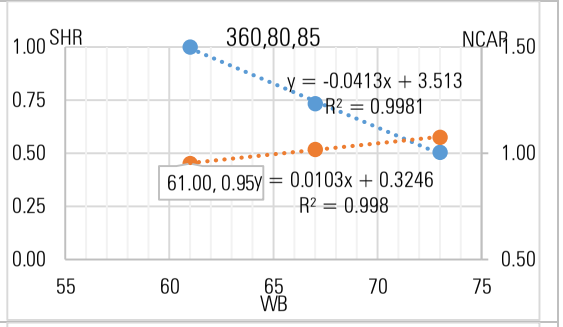

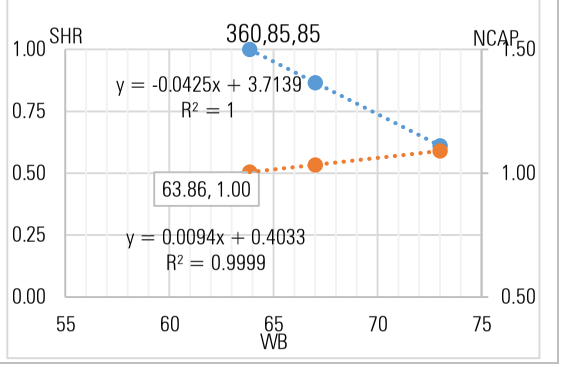

Calculation table at OAT = 85ºF

Cond	CFM	DB	OAT	WB	CAP	SHC	NCFM	SHR	NCAP
	6300	90	85	61	219	219	360	1.00	1.04
Guess	6300	90	85	66.70	219	219	360	1.00	1.04
	6300	90	85	67	220	217	360	0.99	1.05
	6300	90	85	73	230	164	360	0.71	1.10
Crit	6300	90	85	66.70	219	219	360	1	1.04

	NCAP			SHR			Objective
Cond.	m	c	r^2	m	c	r^2	
initial cod.	0.008	0.516	0.998	-0.046	4.038		
Opt cond	0.008	0.501	1.000	-0.046	4.038	1.000	1.000
rel_dev							

Cond.	CFM	DB	OAT	WB	CAP	SHC	NCFM	SHR	NCAP
Guess	7000	75	85	57.87	192	192	400	1	0.92
	7000	75	85	61	199	181	400	0.91	0.95
	7000	75	85	67	215	131	400	0.61	1.02
	7000	75	85	73	225	84.7	400	0.38	1.07
Crit	7000	75	85	57.87	191	191	400	1	0.91

	NCAP			SHR			Objective
Cond.	m	c	r^2	m	c	r^2	
initial cod.	0.010	0.318	0.983	-0.044	3.619	0.983	
Opt cond	0.011	0.301	0.990	-0.043	3.480	0.995	0.995
rel_dev	2.3%	5.6%	0.7%	4.3%	3.9%	1.2%	

Cond	CFM	DB	OAT	WB	CAP	SHC	NCFM	SHR	NCAP
	7000	80	85	61	206	206	400	1.00	0.98
Guess	7000	80	85	61.07	206	206	400	1.00	0.98
	7000	80	85	67	217	164	400	0.76	1.03
	7000	80	85	73	228	116	400	0.51	1.09
Crit	7000	80	85	61.07	206	206	400	1	0.98

	NCAP			SHR			Objective
Cond.	m	c	r^2	m	c	r^2	
initial cod.	0.009	0.448	1.000	-0.041	3.514		
Opt cond	0.009	0.445	1.000	-0.041	3.514	1.000	1.000
rel_dev							

CFM,DB,OAT

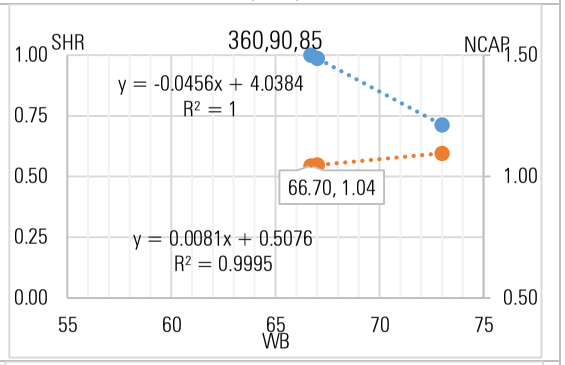

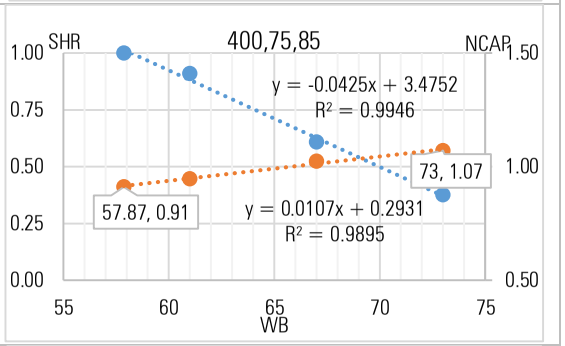

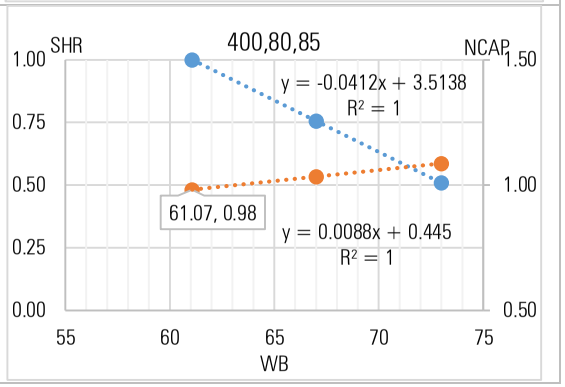

Calculation table at OAT = 85ºF

Cond	CFM	DB	OAT	WB	CAP	SHC	NCFM	SHR	NCAP
	7000	85	85	61	216	216	400	1.00	1.03
Guess	7000	85	85	64.67	216	216	400	1.00	1.03
	7000	85	85	67	220	197	400	0.90	1.05
	7000	85	85	73	230	144	400	0.63	1.10
Crit	7000	85	85	64.67	216	216	400	1	1.03

	NCAP			SHR			Objective
Cond.	m	c	r^2	m	c	r^2	
initial cod.	0.008	0.516	1.000	-0.045	3.903		
Opt cond	0.008	0.512	1.000	-0.045	3.903	1.000	1.000
rel_dev							

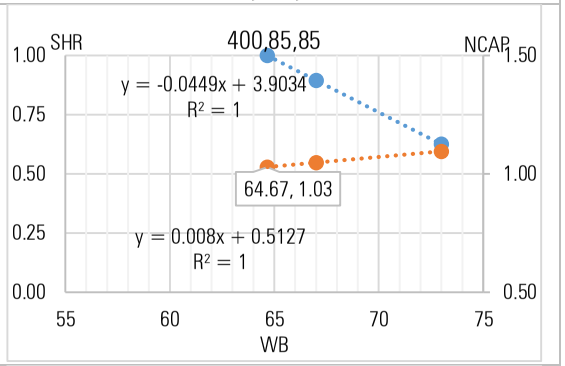

Cond.	CFM	DB	OAT	WB	CAP	SHC	NCFM	SHR	NCAP
Guess	7700	75	85	59.46	200	200	440	1	0.95
	7700	75	85	61	203	191	440	0.94	0.97
	7700	75	85	67	217	135	440	0.62	1.03
	7700	75	85	73	226	86.1	440	0.38	1.08
Crit	7700	75	85	59.46	199	199	440	1	0.95

	NCAP			SHR			Objective
Cond.	m	c	r^2	m	c	r^2	
initial cod.	0.009	0.410	0.984	-0.047	3.787	0.984	
Opt cond	0.009	0.396	0.989	-0.047	3.787	0.996	0.996
rel_dev	2.1%	3.5%	0.4%	0.0%	0.0%	1.2%	

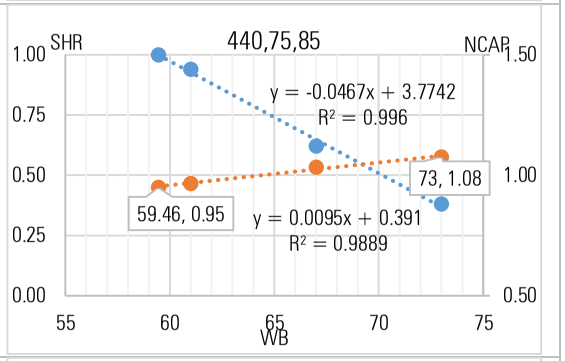

Cond	CFM	DB	OAT	WB	CAP	SHC	NCFM	SHR	NCAP
	7700	80	85	61	211	211	440	1.00	1.00
Guess	7700	80	85	61.66	211	211	440	1.00	1.00
	7700	80	85	67	219	169	440	0.77	1.04
	7700	80	85	73	229	118	440	0.52	1.09
Crit	7700	80	85	61.66	211	211	440	1	1.00

	NCAP			SHR			Objective
Cond.	m	c	r^2	m	c	r^2	
initial cod.	0.008	0.511	0.999	-0.043	3.635		
Opt cond	0.008	0.538	0.999	-0.043	3.635	1.000	1.000
rel_dev							

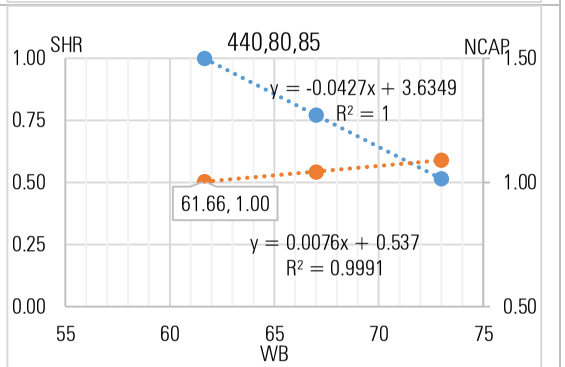

CFM,DB,OAT

Calculation table at OAT = 85ºF

Cond	CFM	DB	OAT	WB	CAP	SHC	NCFM	SHR	NCAP
	7700	85	85	61	220	220	440	1.00	1.05
Guess	7700	85	85	65.17	220	220	440	1.00	1.05
	7700	85	85	67	222	203	440	0.91	1.06
	7700	85	85	73	232	147	440	0.63	1.10
Crit	7700	85	85	65.17	220	220	440	1	1.05

	NCAP			SHR			Objective
Cond.	m	c	r^2	m	c	r^2	
initial cod.	0.008	0.525	0.995	-0.047	4.050		
Opt cond	0.007	0.560	0.997	-0.047	4.050	1.000	1.000
rel_dev							

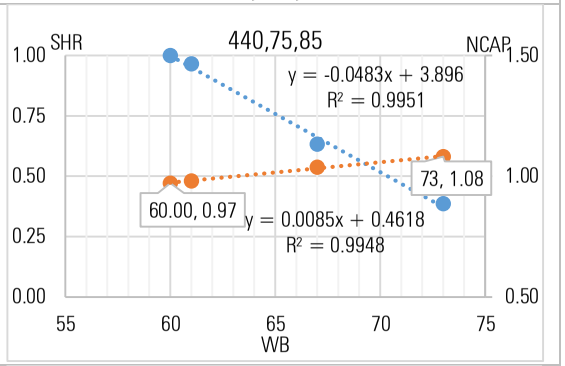

	CFM	DB	OAT	WB	CAP	SHC	NCFM	SHR	NCAP
Guess	8400	75	85	60.00	204	204	480	1	0.97
	8400	75	85	61	206	199	480	0.97	0.98
	8400	75	85	67	218	138	480	0.63	1.04
Crit	8400	75	85	73	227	87.8	480	0.39	1.08
	8400	75	85	60.00	204	204	480	1	0.97

	NCAP			SHR			Objective
Cond.	m	c	r^2	m	c	r^2	
initial cod.	0.008	0.473	0.993	-0.048	3.910	0.993	
Opt cond	0.008	0.464	0.995	-0.048	3.910	0.995	0.995
rel_dev	1.4%	1.8%	0.2%	0.0%	0.0%	0.2%	

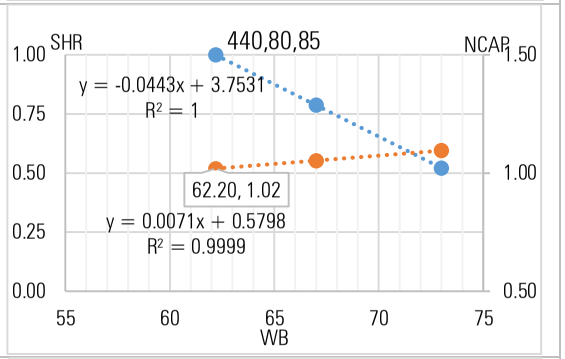

Cond	CFM	DB	OAT	WB	CAP	SHC	NCFM	SHR	NCAP
	8400	85	85	61	222	222	480	1.00	1.06
Guess	8400	85	85	65.72	222	222	480	1.00	1.06
	8400	85	85	67	224	210	480	0.94	1.07
	8400	85	85	73	233	150	480	0.64	1.11
Crit	8400	85	85	65.72	222	222	480	1	1.06

	NCAP			SHR			Objective
Cond.	m	c	r^2	m	c	r^2	
initial cod.	0.007	0.588	1.000	-0.049	4.217		
Opt cond	0.007	0.585	1.000	-0.049	4.217	1.000	1.000
rel_dev							

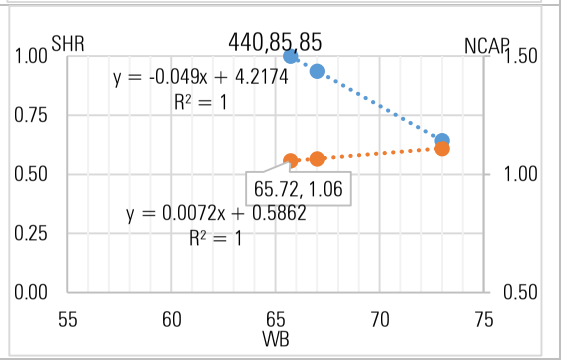

Table G-3 Critical plots based on local optimization of maximized R square values at 95°f of Outdoor air temperature

Calculation table at OAT = 95ºF

Cond.	CFM	DB	OAT	WB	CAP	SHC	NCFM	SHR	NCAP
Guess	6300	75	95	58.55	174	174	360	1	0.83
	6300	75	95	61	182	164	360	0.90	0.87
	6300	75	95	67	206	124	360	0.60	0.98
	6300	75	95	73	219	80.1	360	0.37	1.04
Crit	6300	75	95	58.55	173	173	360	1	0.82

	NCAP			SHR			Objective
Cond.	m	c	r^2	m	c	r^2	
Initial	0.015	-0.029	0.971	-0.045	3.622	0.971	
Optimized	0.015	-0.061	0.982	-0.045	3.622	0.997	0.997
rel_dev	3.0%	111.1%	1.1%	0.0%	0.0%	2.7%	

CFM,DB,OAT

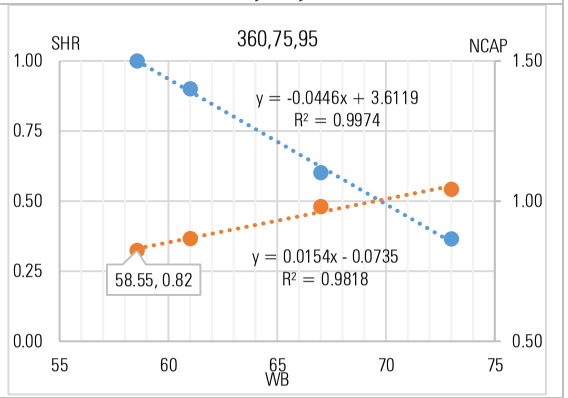

Cond	CFM	DB	OAT	WB	CAP	SHC	NCFM	SHR	NCAP
	6300	80	95	61	191	191	360	1.00	0.91
Guess	6300	80	95	61.01	191	191	360	1.00	0.91
	6300	80	95	67	207	156	360	0.75	0.99
	6300	80	95	73	221	112	360	0.51	1.05
Crit	6300	80	95	61.01	191	191	360	1	0.91

	NCAP			SHR			Objective
Cond.	m	c	r^2	m	c	r^2	
Initial	0.011	0.241	0.998	-0.041	3.510		
Optimized	0.012	0.183	0.998	-0.041	3.510	1.000	1.000
rel_dev							

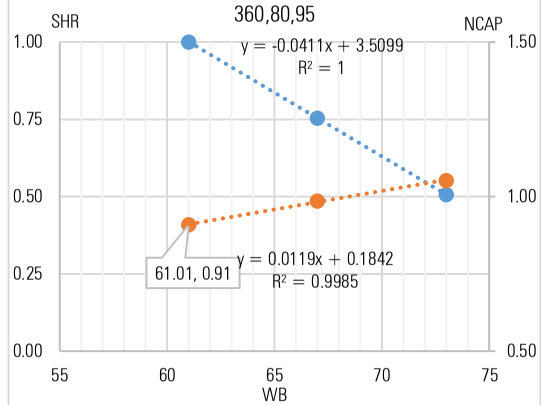

Calculation table at OAT = 95ºF

Cond	CFM	DB	OAT	WB	CAP	SHC	NCFM	SHR	NCAP
	6300	85	95	61	204	204	360	1.00	0.97
Guess	6300	85	95	64.82	204	204	360	1.00	0.97
	6300	85	95	67	209	188	360	0.90	1.00
	6300	85	95	73	223	139	360	0.62	1.06
Crit	6300	85	95	64.82	204	204	360	1	0.97

	NCAP			SHR			Objective
Cond.	m	c	r^2	m	c	r^2	
Initial	0.011	0.251	1.000	-0.046	3.984		
Optimized	0.011	0.254	1.000	-0.046	3.984	1.000	1.000
rel_dev							

CFM,DB,OAT

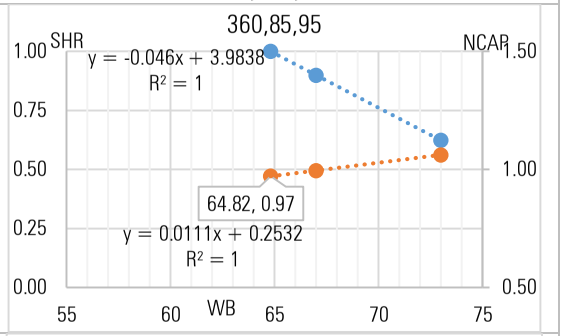

	CFM	DB	OAT	WB	CAP	SHC	NCFM	SHR	NCAP
Guess	7000	75	95	59.53	183	183	400	1	0.87
	7000	75	95	61	187	176	400	0.94	0.89
	7000	75	95	67	208	129	400	0.62	0.99
Crit	7000	75	95	73	221	81.4	400	0.37	1.05
	7000	75	95	59.53	182	182	400	1	0.87

	NCAP			SHR			Objective
Cond.	m	c	r^2	m	c	r^2	
Initial	0.013	0.067	0.982	-0.048	3.853	0.982	
Optimized	0.014	0.045	0.987	-0.048	3.853	0.997	0.997
rel_dev	2.3%	33.8%	0.5%	0.0%	0.0%	1.5%	

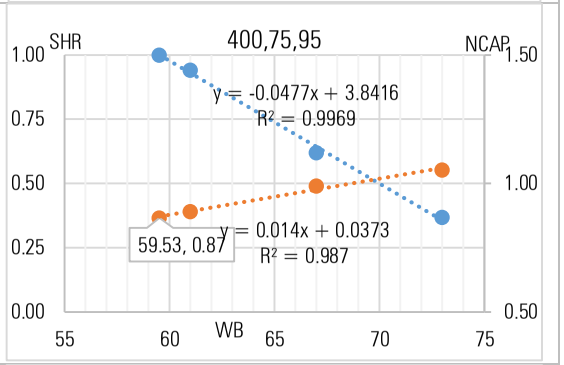

Cond	CFM	DB	OAT	WB	CAP	SHC	NCFM	SHR	NCAP
	7000	80	95	61	198	198	400	1.00	0.94
Guess	7000	80	95	62.09	198	198	400	1.00	0.94
	7000	80	95	67	210	164	400	0.78	1.00
	7000	80	95	73	222	114	400	0.51	1.06
Crit	7000	80	95	62.09	198	198	400	1	0.94

	NCAP			SHR			Objective
Cond.	m	c	r^2	m	c	r^2	
Initial	0.010	0.362	0.997	-0.045	3.767		
Optimized	0.010	0.295	0.997	-0.045	3.767	1.000	1.000
rel_dev							

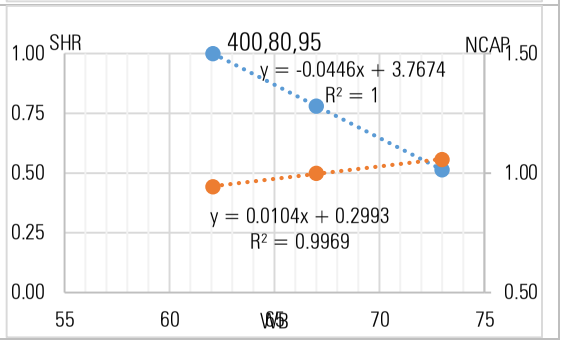

Calculation table at OAT = 95ºF

Cond	CFM	DB	OAT	WB	CAP	SHC	NCFM	SHR	NCAP
	7000	85	95	61	210	210	400	1.00	1.00
Guess	7000	85	95	65.54	210	210	400	1.00	1.00
	7000	85	95	67	213	198	400	0.93	1.01
	7000	85	95	73	225	144	400	0.64	1.07
Crit	7000	85	95	65.54	210	210	400	1	1.00

	NCAP			SHR			Objective
Cond.	m	c	r^2	m	c	r^2	
Initial	0.010	0.376	1.000	-0.048	4.163		
Optimized	0.010	0.373	1.000	-0.048	4.163	1.000	1.000
rel_dev							

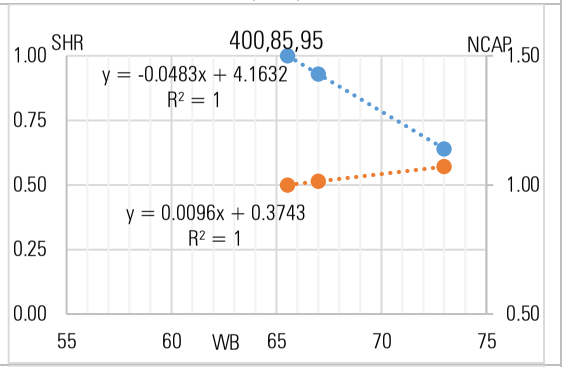

	CFM	DB	OAT	WB	CAP	SHC	NCFM	SHR	NCAP
Guess	7700	75	95	60.35	190	190	440	1	0.91
	7700	75	95	61	192	187	440	0.97	0.91
	7700	75	95	67	211	138	440	0.65	1.00
Crit	7700	75	95	73	222	82.9	440	0.37	1.06
	7700	75	95	60.35	190	190	440	1	0.90

	NCAP			SHR			Objective
Cond.	m	c	r^2	m	c	r^2	
Initial	0.012	0.188	0.977	-0.050	4.027	0.977	
Optimized	0.012	0.166	0.982	-0.050	4.027	0.999	0.999
rel_dev	2.5%	11.7%	0.5%	0.0%	0.0%	2.3%	

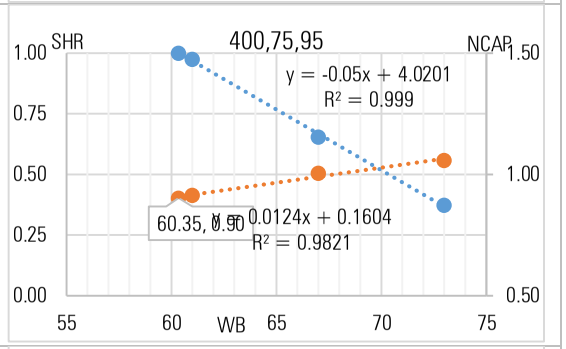

Cond	CFM	DB	OAT	WB	CAP	SHC	NCFM	SHR	NCAP
	7700	80	95	61	204	204	440	1.00	0.97
Guess	7700	80	95	62.92	204	204	440	1.00	0.97
	7700	80	95	67	212	171	440	0.81	1.01
	7700	80	95	73	224	117	440	0.52	1.07
Crit	7700	80	95	62.92	204	204	440	1	0.97

	NCAP			SHR			Objective
Cond.	m	c	r^2	m	c	r^2	
Initial	0.010	0.371	1.000	-0.047	3.981		
Optimized	0.009	0.377	1.000	-0.047	3.981	1.000	1.000
rel_dev							

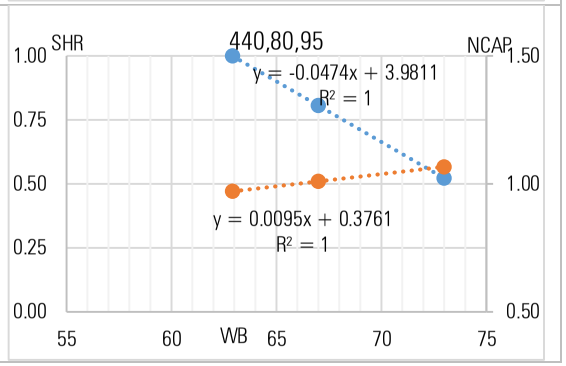

Calculation table at OAT = 95ºF

Cond	CFM	DB	OAT	WB	CAP	SHC	NCFM	SHR	NCAP
	7700	85	95	61	214	214	440	1.00	1.02
Guess	7700	85	95	66.18	214	214	440	1.00	1.02
	7700	85	95	67	216	207	440	0.96	1.03
	7700	85	95	73	226	148	440	0.65	1.08
Crit	7700	85	95	66.18	214	214	440	1	1.02

	NCAP			SHR			Objective
Cond.	m	c	r^2	m	c	r^2	
Initial	0.008	0.497	0.998	-0.051	4.347		
Optimized	0.008	0.477	0.999	-0.051	4.347	1.000	1.000
rel_dev							

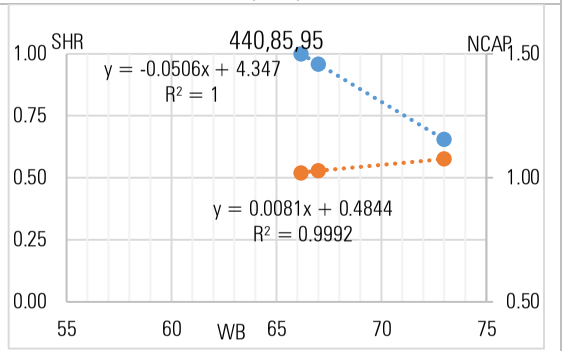

Cond	CFM	DB	OAT	WB	CAP	SHC	NCFM	SHR	NCAP
	8400	75	95	61	195	195	480	1.00	0.93
Guess	8400	75	95	61.00	195	195	480	1.00	0.93
	8400	75	95	67	212	143	480	0.67	1.01
	8400	75	95	73	223	84.3	480	0.38	1.06
Crit	8400	75	95	61.00	195	195	480	1	0.93

	NCAP			SHR			Objective	1.000
Cond.	m	c	r^2	m	c	r^2		1
Initial	0.009	0.425	0.985	-0.049	3.985			TRUE
Optimized	0.011	0.251	0.985	-0.052	4.162	0.999	0.999	TRUE
rel_dev								32767

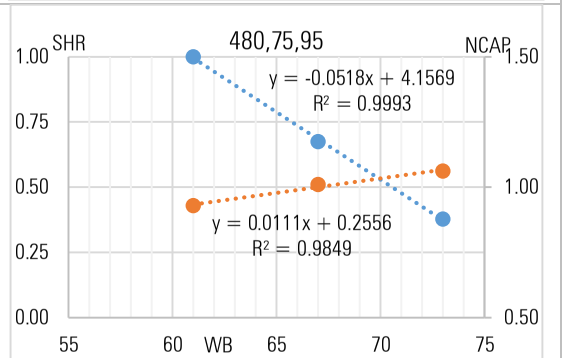

Cond	CFM	DB	OAT	WB	CAP	SHC	NCFM	SHR	NCAP
	8400	80	95	61	208	208	480	1.00	0.99
Guess	8400	80	95	63.64	208	208	480	1.00	0.99
	8400	80	95	67	214	178	480	0.83	1.02
	8400	80	95	73	226	120	480	0.53	1.08
Crit	8400	80	95	63.64	208	208	480	1	0.99

	NCAP			SHR			Objective
Cond.	m	c	r^2	m	c	r^2	
Initial	0.010	0.381	0.999	-0.050	4.191		
Optimized	0.009	0.404	0.999	-0.050	4.191	1.000	1.000
rel_dev							

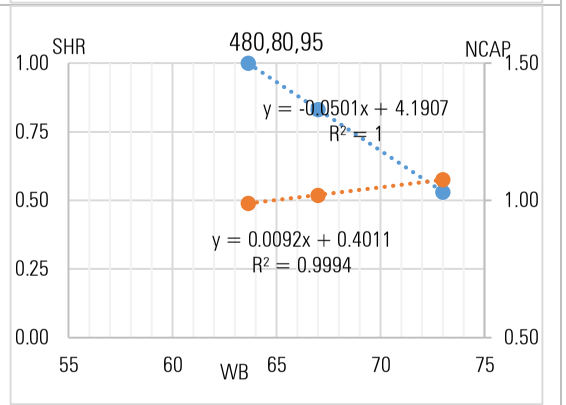

CFM,DB,OAT

Calculation table at OAT = 95ºF

Cond	CFM	DB	OAT	WB	CAP	SHC	NCFM	SHR	NCAP
	8400	85	95	61	217	217	480	1.00	1.03
Guess	8400	85	95	66.75	217	217	480	1.00	1.03
	8400	85	95	67	218	215	480	0.99	1.04
	8400	85	95	73	228	151	480	0.66	1.09
Crit	8400	85	95	66.75	217	217	480	1	1.03

	NCAP			SHR			Objective
Cond.	m	c	r^2	m	c	r^2	
Initial	0.008	0.506	0.998	-0.054	4.604		
Optimized	0.008	0.489	0.999	-0.054	4.604	1.000	1.000
rel_dev							

CFM,DB,OAT

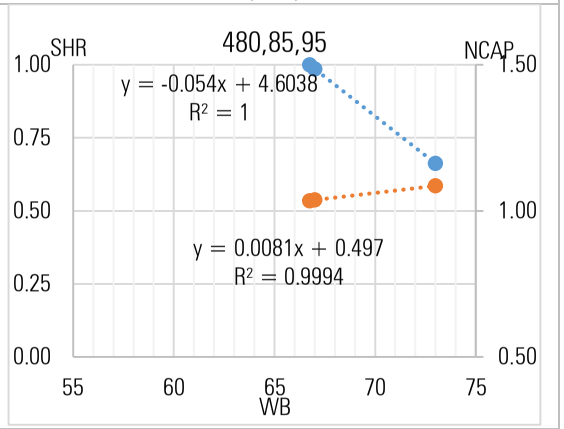

Table G-4 Critical plots based on local optimization of maximized R square values at 105°F of Outdoor air temperature

Calculation table at OAT = 105ºF

Cond.	CFM	DB	OAT	WB	CAP	SHC	NCFM	SHR	NCAP
Guess	6300	75	105	59.40	163	163	360	1	0.78
	6300	75	105	61	169	158	360	0.93	0.80
	6300	75	105	67	195	119	360	0.61	0.93
	6300	75	105	73	213	76.1	360	0.36	1.01
Crit	6300	75	105	59.40	162	162	360	1	0.77

	NCAP			SHR			Objective
Cond.	m	c	r^2	m	c	r^2	
Initial	0.017	-0.260	0.989	-0.048	3.871	0.989	
Optimized	0.018	-0.283	0.992	-0.048	3.871	0.997	0.997
rel_dev	1.8%	8.8%	0.3%	0.0%	0.0%	0.8%	

CFM,DB,OAT

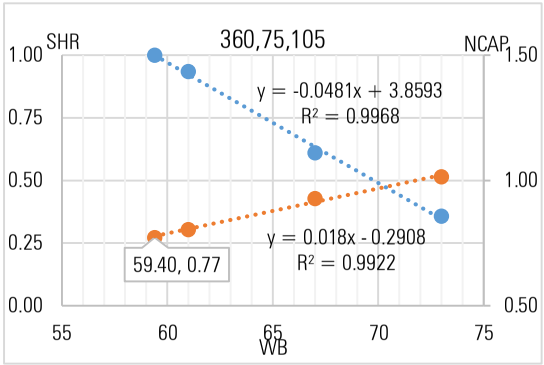

Cond	CFM	DB	OAT	WB	CAP	SHC	NCFM	SHR	NCAP
	6300	80	105	61	180	180	360	1.00	0.86
Guess	6300	80	105	62.06	180	180	360	1.00	0.86
	6300	80	105	67	196	153	360	0.78	0.93
	6300	80	105	73	214	110	360	0.51	1.02
Crit	6300	80	105	62.06	180	180	360	1	0.86

	NCAP			SHR			Objective
Cond.	m	c	r^2	m	c	r^2	
Initial	0.014	-0.024	1.000	-0.044	3.758		
Optimized	0.015	-0.060	1.000	-0.044	3.758	1.000	1.000
rel_dev							

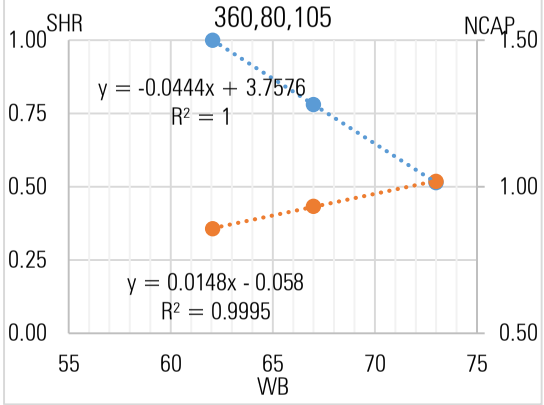

Calculation table at OAT = 105ºF

Cond	CFM	DB	OAT	WB	CAP	SHC	NCFM	SHR	NCAP
	6300	85	105	61	195	195	360	1.00	0.93
Guess	6300	85	105	65.65	195	195	360	1.00	0.93
	6300	85	105	67	199	186	360	0.93	0.95
	6300	85	105	73	216	139	360	0.64	1.03
Crit	6300	85	105	65.65	195	195	360	1	0.93

	NCAP			SHR			Obj.
Cond.	m	c	r^2	m	c	r^2	
Initial	0.013	0.044	1.000	-0.049	4.186		
Optimized	0.014	0.038	1.000	-0.049	4.186	1.000	1.000
rel_dev							

CFM,DB,OAT

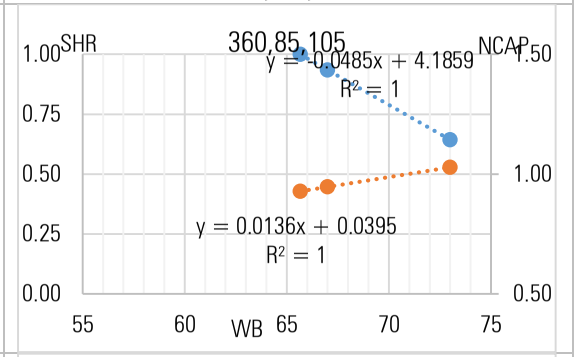

Cond.	CFM	DB	OAT	WB	CAP	SHC	NCFM	SHR	NCAP
Guess	7000	75	105	57.87	163	163	400	1	0.78
	7000	75	105	61	174	169	400	0.97	0.83
	7000	75	105	67	198	125	400	0.63	0.94
	7000	75	105	73	215	77.7	400	0.36	1.02
Crit	7000	75	105	57.87	162	162	400	1	0.77

	NCAP			SHR			Obj.
Cond.	m	c	r^2	m	c	r^2	
Initial	0.016	-0.164	0.990	-0.051	4.071	0.990	
Optimized	0.017	-0.185	0.994	-0.045	3.630	0.977	0.977
rel_dev	1.7%	12.6%	0.4%	11.9%	10.8%	1.4%	

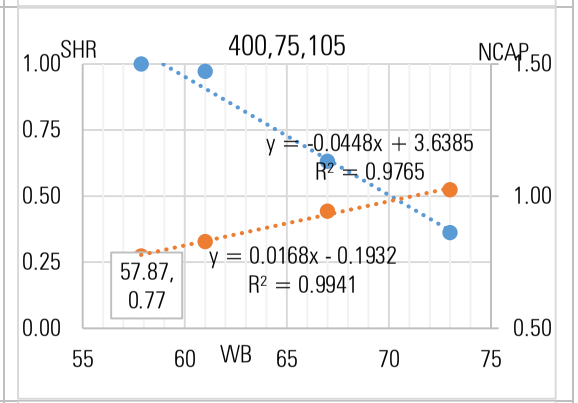

Cond	CFM	DB	OAT	WB	CAP	SHC	NCFM	SHR	NCAP
	7000	80	105	61	188	188	400	1.00	0.90
Guess	7000	80	105	63.03	188	188	400	1.00	0.90
	7000	80	105	67	200	162	400	0.81	0.95
	7000	80	105	73	216	113	400	0.52	1.03
Crit	7000	80	105	63.03	188	188	400	1	0.90

	NCAP			SHR			Objective
Cond.	m	c	r^2	m	c	r^2	
Initial	0.013	0.102	0.999	-0.048	4.013		
Optimized	0.013	0.057	0.999	-0.048	4.013	1.000	1.000
rel_dev							

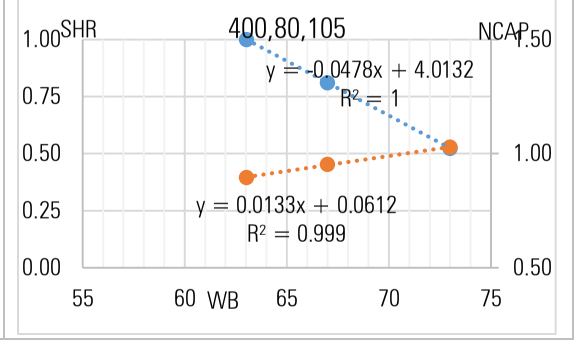

Calculation table at OAT = 105ºF

Cond.	CFM	DB	OAT	WB	CAP	SHC	NCFM	SHR	NCAP
Guess	7700	75	105	60.80	177	177	440	1	0.84
	7700	75	105	61	178	178	440	1.00	0.85
	7700	75	105	67	201	131	440	0.65	0.96
	7700	75	105	73	216	79.2	440	0.37	1.03
Crit	7700	75	105	60.80	177	177	440	1	0.84

	NCAP			SHR			Objective
Cond.	m	c	r^2	m	c	r^2	
Initial	0.015	-0.072	0.985	-0.053	4.219	0.985	
Optimized	0.015	-0.094	0.988	-0.053	4.219	0.998	0.998
rel_dev	1.9%	29.6%	0.3%	0.0%	0.0%	1.2%	

Cond	CFM	DB	OAT	WB	CAP	SHC	NCFM	SHR	NCAP
	7700	80	105	61	194	194	440	1.00	0.92
Guess	7700	80	105	63.81	194	194	440	1.00	0.92
	7700	80	105	67	203	170	440	0.84	0.97
	7700	80	105	73	218	116	440	0.53	1.04
Crit	7700	80	105	63.81	194	194	440	1	0.92

	NCAP			SHR			Objective
Cond.	m	c	r^2	m	c	r^2	
Initial	0.012	0.169	0.999	-0.051	4.247		
Optimized	0.012	0.136	0.999	-0.051	4.247	1.000	1.000
rel_dev							

Cond	CFM	DB	OAT	WB	CAP	SHC	NCFM	SHR	NCAP
	8400	75	105	61	183	183	480	1.00	0.87
Guess	8400	75	105	61.00	183	183	480	1.00	0.87
	8400	75	105	67	203	136	480	0.67	0.97
	8400	75	105	73	217	80.6	480	0.37	1.03
Crit	8400	75	105	61.00	183	183	480	1	0.87

	NCAP			SHR			Objective
Cond.	m	c	r^2	m	c	r^2	
Initial	0.011	0.222	0.990	-0.050	4.003		
Optimized	0.013	0.048	0.990	-0.052	4.195	0.999	0.999
rel_dev							

CFM,DB,OAT

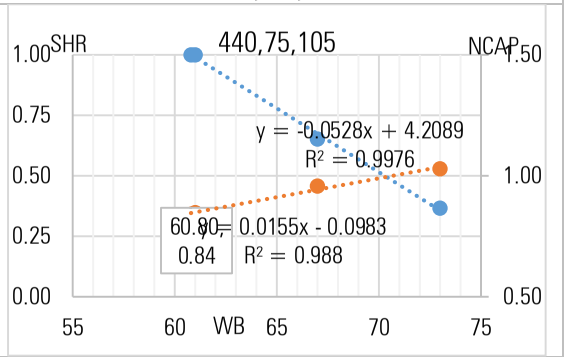

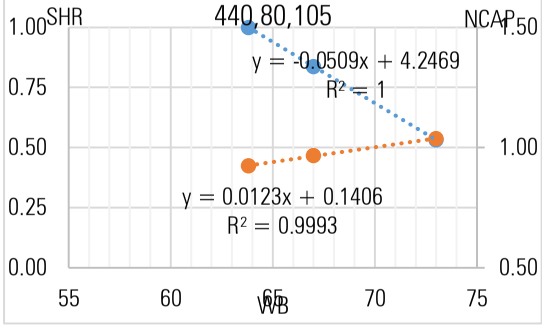

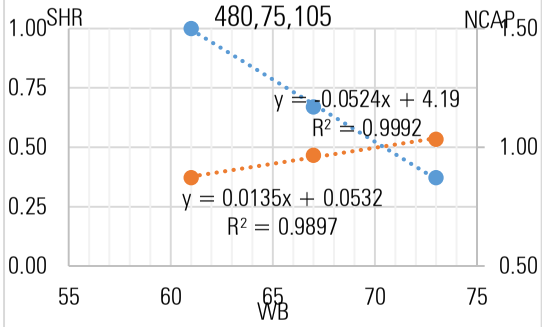

Calculation table at OAT = 105ºF

Cond	CFM	DB	OAT	WB	CAP	SHC	NCFM	SHR	NCAP
	8400	80	105	61	199	199	480	1.00	0.95
Guess	8400	80	105	64.57	199	199	480	1.00	0.95
	8400	80	105	67	205	178	480	0.87	0.98
	8400	80	105	73	219	119	480	0.54	1.04
Crit	8400	80	105	64.57	199	199	480	1	0.95

	NCAP			SHR			Objective
Cond.	m	c	r^2	m	c	r^2	
Initial	0.011	0.232	1.000	-0.054	4.496		
Optimized	0.011	0.221	1.000	-0.054	4.496	1.000	1.000
rel_dev							

CFM,DB,OAT

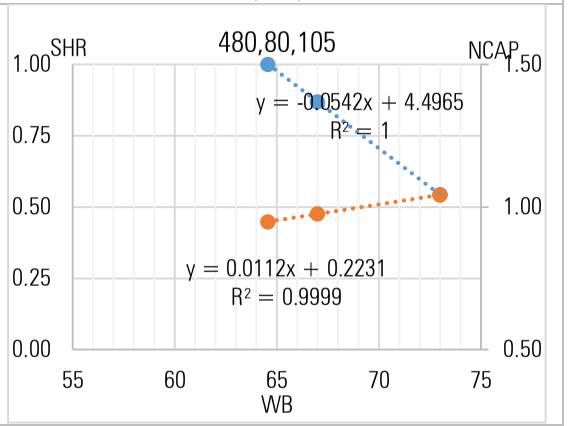

Table G-5 Critical plots based on local optimization of maximized R square values at 115°F of Outdoor air temperature

Calculation table at OAT = 115ºF

Cond.	CFM	DB	OAT	WB	CAP	SHC	NCFM	SHR	NCAP
Guess	6300	75	105	59.40	163	163	360	1	0.78
	6300	75	105	61	169	158	360	0.93	0.80
	6300	75	105	67	195	119	360	0.61	0.93
	6300	75	105	73	213	76.1	360	0.36	1.01
Crit	6300	75	105	59.40	162	162	360	1	0.77

	NCAP			SHR			Objective
Cond.	m	c	r^2	m	c	r^2	
Initial	0.017	-0.260	0.989	-0.048	3.871	0.989	
Optimized	0.018	-0.283	0.992	-0.048	3.871	0.997	0.997
rel_dev	1.8%	8.8%	0.3%	0.0%	0.0%	0.8%	

CFM,DB,OAT

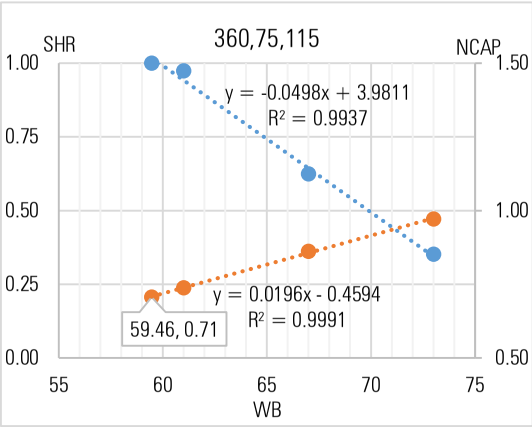

Cond.	CFM	DB	OAT	WB	CAP	SHC	NCFM	SHR	NCAP
Guess	6300	75	115	59.46	149	149	360	1	0.71
	6300	75	115	61	155	151	360	0.97	0.74
	6300	75	115	67	181	113	360	0.62	0.86
	6300	75	115	73	204	71.8	360	0.35	0.97
Crit	6300	75	115	59.46	148	148	360	1	0.71

	NCAP			SHR			Objective
Cond.	m	c	r^2	m	c	r^2	
Initial	0.019	-0.448	0.999	-0.052	4.137	0.999	
Optimized	0.020	-0.457	0.999	-0.050	3.988	0.994	0.994
rel_dev	0.6%	1.9%	0.0%	3.9%	3.6%	0.5%	

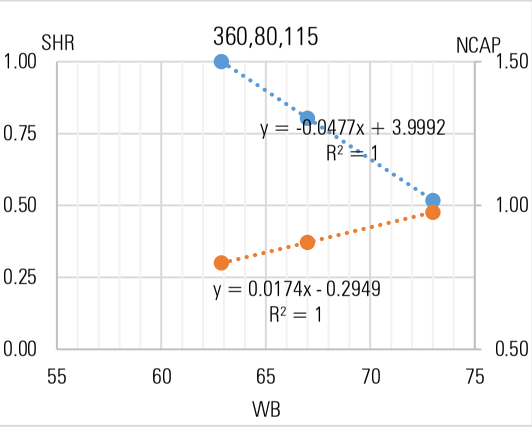

Calculation table at OAT = 115ºF

Cond	CFM	DB	OAT	WB	CAP	SHC	NCFM	SHR	NCAP
	6300	90	115	61	168	168	360	1.00	0.80
Guess	6300	90	115	62.88	168	168	360	1.00	0.80
	6300	90	115	67	183	147	360	0.80	0.87
	6300	90	115	73	205	106	360	0.52	0.98
Crit	6300	90	115	62.88	168	168	360	1	0.80

	NCAP			SHR			Objective	1.000
Cond.	m	c	r^2	m	c	r^2		1
Initial	0.017	-0.298	1.000	-0.048	3.999			TRUE
Optimized	0.017	-0.295	1.000	-0.048	3.999	1.000	1.000	TRUE
rel_dev								32767

CFM,DB,OAT

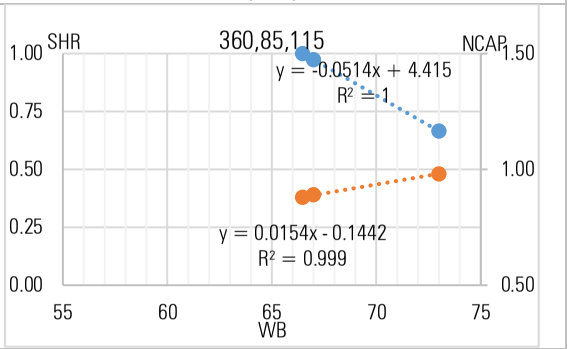

Cond	CFM	DB	OAT	WB	CAP	SHC	NCFM	SHR	NCAP
	6300	90	115	61	184	184	360	1.00	0.88
Guess	6300	90	115	66.48	184	184	360	1.00	0.88
	6300	90	115	67	187	182	360	0.97	0.89
	6300	90	115	73	206	137	360	0.67	0.98
Crit	6300	90	115	66.48	185	185	360	1	0.88

	NCAP			SHR			Objective	1.000
Cond.	m	c	r^2	m	c	r^2		1
Initial	0.015	-0.120	0.997	-0.051	4.415			TRUE
Optimized	0.016	-0.162	0.999	-0.051	4.415	1.000	1.000	TRUE
rel_dev								32767

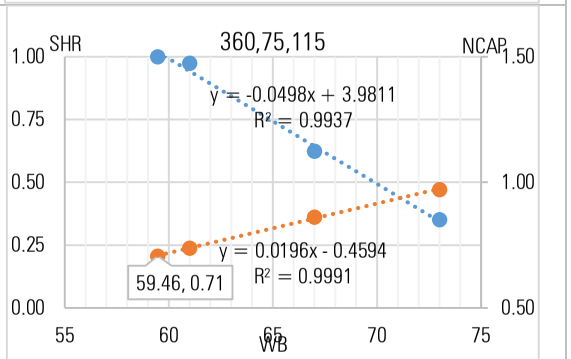

	63	80	168	168	183	147	205	106

Cond	CFM	DB	OAT	WB	CAP	SHC	NCFM	SHR	NCAP
	6300	80	115	61	168	168	360	1.00	0.80
Guess	6300	80	115	62.88	168	168	360	1.00	0.80
	6300	80	115	67	183	147	360	0.80	0.87
	6300	80	115	73	205	106	360	0.52	0.98
Crit	6300	80	115	62.88	168	168	360	1	0.80

	NCAP			SHR			Objective	1.000
Cond.	m	c	r^2	m	c	r^2		1
Initial	0.017	-0.298	1.000	-0.048	3.999			TRUE
Optimized	0.017	-0.295	1.000	-0.048	3.999	1.000	1.000	TRUE
rel_dev								32767

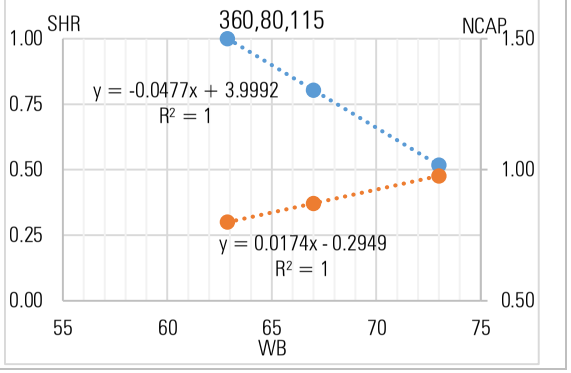

Calculation table at OAT = 115ºF

Cond	CFM	DB	OAT	WB	CAP	SHC	NCFM	SHR	NCAP
	6300	85	115	61	184	184	360	1.00	0.88
Guess	6300	85	115	66.48	184	184	360	1.00	0.88
	6300	85	115	67	187	182	360	0.97	0.89
	6300	85	115	73	206	137	360	0.67	0.98
Crit	6300	85	115	66.48	185	185	360	1	0.88

	NCAP			SHR			Objective	1.000
Cond.	m	c	r^2	m	c	r^2		1
Initial	0.015	-0.120	0.997	-0.051	4.415			TRUE
Optimized	0.016	-0.162	0.999	-0.051	4.415	1.000	1.000	TRUE
rel_dev								32767

Cond	CFM	DB	OAT	WB	CAP	SHC	NCFM	SHR	NCAP
	7000	75	115	61	160	160	400	1.00	0.76
Guess	7000	75	115	61.00	160	160	400	1.00	0.76
	7000	75	115	67	185	119	400	0.64	0.88
	7000	75	115	73	206	73.4	400	0.36	0.98
Crit	7000	75	115	61.00	160	160	400	1	0.76

	NCAP			SHR			Objective	1.000
Cond.	m	c	r^2	m	c	r^2		1
Initial	0.017	-0.236	0.997	-0.048	3.847			TRUE
Optimized	0.018	-0.352	0.997	-0.054	4.272	0.996	0.996	TRUE
rel_dev								32767

Cond	CFM	DB	OAT	WB	CAP	SHC	NCFM	SHR	NCAP
	7000	80	115	61	176	176	400	1.00	0.84
Guess	7000	80	115	63.88	176	176	400	1.00	0.84
	7000	80	115	67	187	157	400	0.84	0.89
	7000	80	115	73	207	110	400	0.53	0.99
Crit	7000	80	115	63.88	176	176	400	1	0.84

	NCAP			SHR			Objective	1.000
Cond.	m	c	r^2	m	c	r^2		1
Initial	0.016	-0.173	1.000	-0.051	4.281			TRUE
Optimized	0.016	-0.192	1.000	-0.051	4.281	1.000	1.000	TRUE
rel_dev								32767

CFM,DB,OAT

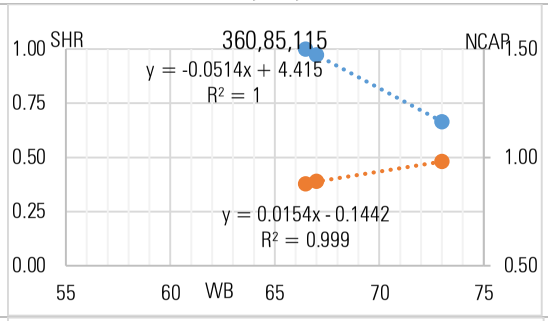

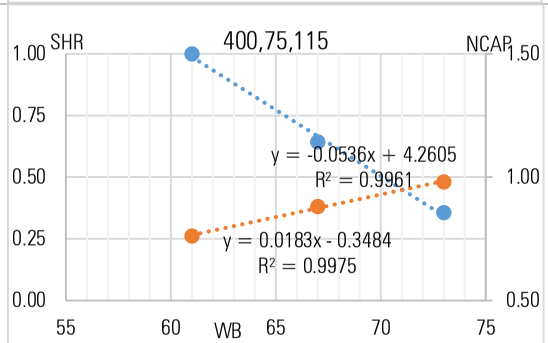

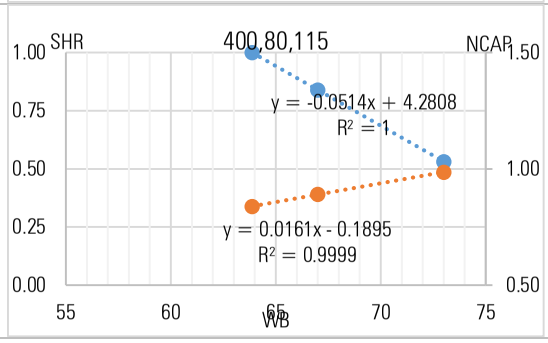

Calculation table at OAT = 115ºF

Cond	CFM	DB	OAT	WB	CAP	SHC	NCFM	SHR	NCAP
	7700	75	115	61	165	165	440	1.00	0.79
Guess	7700	75	115	61.00	165	165	440	1.00	0.79
	7700	75	115	67	188	126	440	0.67	0.90
	7700	75	115	73	208	75	440	0.36	0.99
Crit	7700	75	115	61.00	165	165	440	1	0.79

	NCAP			SHR			Objective	1.000
Cond.	m	c	r^2	m	c	r^2		1
Initial	0.016	-0.168	0.998	-0.052	4.128			TRUE
Optimized	0.017	-0.255	0.998	-0.053	4.250	1.000	1.000	TRUE
rel_dev								32767

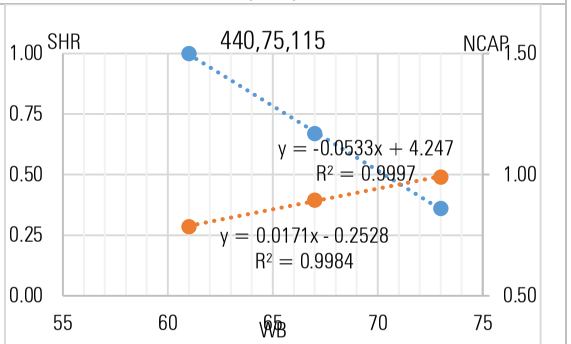

Cond	CFM	DB	OAT	WB	CAP	SHC	NCFM	SHR	NCAP
	7700	80	115	61	183	183	440	1.00	0.87
Guess	7700	80	115	64.71	183	183	440	1.00	0.87
	7700	80	115	67	191	167	440	0.87	0.91
	7700	80	115	73	209	114	440	0.55	1.00
Crit	7700	80	115	64.71	183	183	440	1	0.87

	NCAP			SHR			Objective	1.000
Cond.	m	c	r^2	m	c	r^2		1
Initial	0.014	-0.048	0.999	-0.055	4.547			TRUE
Optimized	0.015	-0.085	0.999	-0.055	4.547	1.000	1.000	TRUE
rel_dev								32767

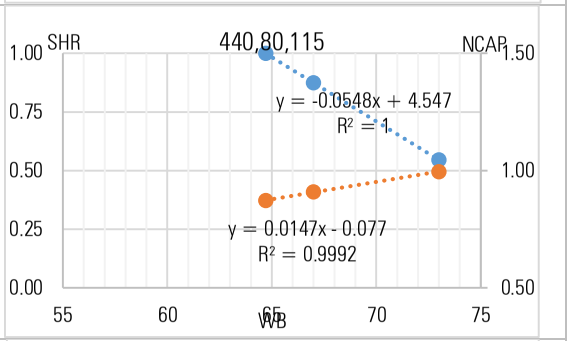

Cond	CFM	DB	OAT	WB	CAP	SHC	NCFM	SHR	NCAP
	8400	75	85	61	171	171	480	1.00	0.81
Guess	8400	75	85	61.43	171	171	480	1.00	0.81
	8400	75	85	67	190	132	480	0.69	0.90
	8400	75	85	73	209	76.5	480	0.37	1.00
Crit	8400	75	85	61.43	171	171	480	1	0.81

	NCAP			SHR			Objective	1.000
Cond.	m	c	r^2	m	c	r^2		1
Initial	0.015	-0.106	1.000	-0.055	4.365			TRUE
Optimized	0.016	-0.146	1.000	-0.055	4.365	1.000	1.000	TRUE
rel_dev								32767

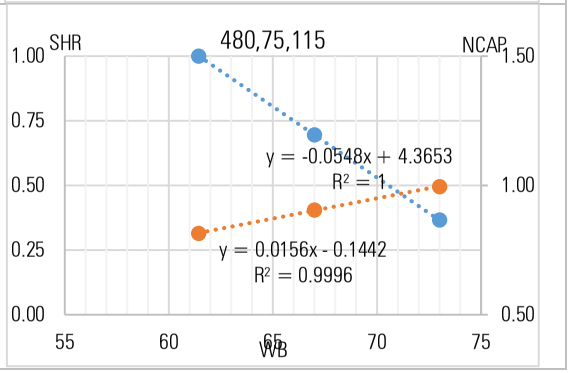

CFM,DB,OAT

Calculation table at OAT = 115ºF

Cond	CFM	DB	OAT	WB	CAP	SHC	NCFM	SHR	NCAP
	8400	80	115	61	188	188	480	1.00	0.90
Guess	8400	80	115	65.42	188	188	480	1.00	0.90
	8400	80	115	67	194	176	480	0.91	0.92
	8400	80	115	73	211	117	480	0.55	1.00
Crit	8400	80	115	65.42	188	188	480	1	0.90

	NCAP			SHR			Objective	1.000
Cond.	m	c	r^2	m	c	r^2		1
Initial	0.013	0.020	0.997	-0.059	4.846			TRUE
Optimized	0.014	-0.031	0.998	-0.059	4.846	1.000	1.000	TRUE
rel_dev								32767

CFM,DB,OAT

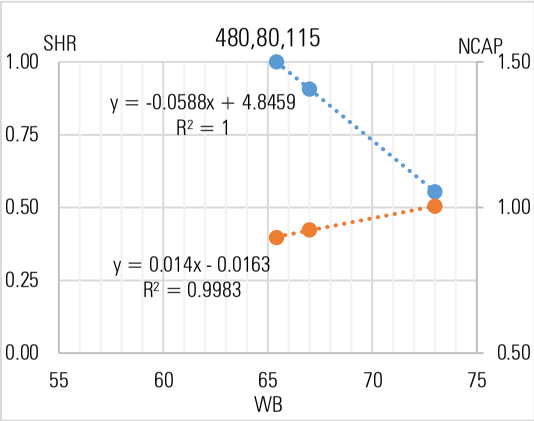

APPENDIX H GLOBAL OPTIMIZED CRITICAL POINTS OF CARRIER MODEL 25HBB18 WITH FIXED DB OF 80°F

Table H-1 Cooling Performance data of 25HBB18

DB = 80		CONDENSER ENTERING AIR TEMPERATURES ° F (° C)											
CFM	WB	75		85		95		105		115		125	
	°F	CAP	SHC	CAP	SHC	CAP	SHC	CAP	SHC	CAP	SHC	CAP	SHC
25HBB318A30 Outdoor Section With FY4ANF018 Indoor Section													
525	72	20.67	10.5	19.67	10.1	18.62	9.67	17.52	9.26	16.35	8.83	15.07	8.36
525	67	18.85	13	17.92	12.6	16.94	12.2	15.91	11.7	14.81	11.3	13.62	10.8
525	62	17.17	15.5	16.31	15.1	15.42	14.6	14.49	14.1	13.59	13.6	12.68	12.7
525	57	16.59	16.6	15.91	15.9	15.18	15.2	14.41	14.4	13.59	13.6	12.68	12.7
600	72	21.03	10.9	19.99	10.5	18.89	10.1	17.76	9.71	16.55	9.28	15.23	8.81
600	67	19.19	13.8	18.22	13.4	**17.2**	13	16.13	12.5	15.01	12.1	13.78	11.6
600	62	17.53	16.6	16.65	16.1	15.76	15.8	14.93	14.9	14.06	14.1	13.1	13.1
600	57	17.25	17.3	16.52	16.5	15.75	15.8	14.94	14.9	14.06	14.1	13.1	13.1
675	72	21.29	11.4	20.22	11	19.09	10.6	17.93	10.2	16.69	9.71	15.34	9.24
675	67	19.44	14.5	18.44	14.1	17.39	13.7	16.3	13.3	15.14	12.8	13.89	12.3
675	62	17.84	17.7	17.02	17	16.21	16.2	15.36	15.4	14.45	14.5	13.44	13.4
675	57	17.79	17.8	17.02	17	16.22	16.2	15.36	15.4	14.45	14.5	13.44	13.4

Table H-2 SHR and cooling performance data of 25HBB18

CFM	WB	75	75	85	85	95	95	105	105	115	115	125	125
	°F	SHR	CAP	SHR	CAP	SHR	CAP	SHR	CAP	SHR	CAP	SHR	CAP
25HBB318A30 Outdoor Section With FY4ANF018 Indoor Section													
525	72	0.506	20.67	0.511	19.67	0.519	18.62	0.529	17.52	0.54	16.35	0.555	15.07
525	67	0.689	18.85	0.702	17.92	0.718	16.94	0.738	15.91	0.762	14.81	0.793	13.62
525	62	0.902	17.17	0.923	16.31	0.947	15.42	0.974	14.49	1	13.59	1	12.68
525	57	1	16.59	1	15.91	1	15.18	1	14.41	1	13.59	1	12.68
600	72	0.519	21.03	0.527	19.99	0.536	18.89	0.547	17.76	0.561	16.55	0.578	15.23
600	67	0.718	19.19	0.734	18.22	0.753	**17.2**	0.776	16.13	0.803	15.01	0.839	13.78
600	62	0.944	17.53	0.966	16.65	1	15.76	1	14.93	1	14.06	1	13.1
600	57	1	17.25	1	16.52	1	15.75	1	14.94	1	14.06	1	13.1
675	72	0.534	21.29	0.543	20.22	0.554	19.09	0.566	17.93	0.582	16.69	0.602	15.34
675	67	0.747	19.44	0.766	18.44	0.788	17.39	0.813	16.3	0.844	15.14	0.883	13.89
675	62	0.992	17.84	1	17.02	1	16.21	1	15.36	1	14.45	1	13.44
675	57	1	17.79	1	17.02	1	16.22	1	15.36	1	14.45	1	13.44

Table H-3 Estimated inflection points calculation tables.

INFLECTION POINT	**OAT (F)**					
CFM	**75**	**85**	**95**	**105**	**115**	**125**
525	59.91	60.46	61.00	61.59	61.59	63.24
600	60.94	61.43	62.00	62.76	62.76	67.24
675	61.85	62.42	63.04	63.68	63.68	67.24
NCAP						
525	0.95	0.91	0.87	0.83	0.83	0.73
600	0.99	0.95	0.91	0.86	0.86	0.78
675	1.02	0.98	0.93	0.88	0.88	0.79
SHR SLOPE (m)						
525	-0.04	-0.04	-0.04	-0.05	-0.05	-0.05
600	-0.04	-0.04	-0.05	-0.05	-0.05	-0.07
675	-0.05	-0.05	-0.05	-0.05	-0.05	-0.07

Table H-4 Estimated inflection points calculation tables.

Global optimized points calculation Table

Cond.	CFM	DB	OAT	WB	TCC	TSC	NCFM	SHR	NCAP
Guess	525	80	75	59.91	16.59	16.59	362	1	0.95
	525	80	75	72.00	20.67	10.45	362	0.506	1.19
	525	80	75	67.00	18.85	12.98	362	0.689	1.08
	525	80	75	62.00	17.17	15.48	362	0.902	0.99
	525	80	75	57.00	16.59	16.59	362	1	0.95
Crit	**525**	**80**	**75**	**59.91**	**16.57**	**16.57**	**362**	**1**	**0.95**

	NCAP			SHR			Obj.
Cond.	m	c	r^2	m	c	r^2	
Initial	0.020	-0.260	0.999	-0.040	3.357	0.998	
Opt	0.020	-0.217	0.998	-0.041	3.447	0.998	0.996
rel_dev	0.030	0.168	0.001	0.032	0.027	0.000	

Cond.	CFM	DB	OAT	WB	TCC	TSC	NCFM	SHR	NCAP
Guess	600	80	75	60.94	17.25	17.25	414	1	0.99
	600	80	75	72.00	21.03	10.92	414	0.519	1.21
	600	80	75	67.00	19.19	13.77	414	0.718	1.10
	600	80	75	62.00	17.53	16.55	414	0.944	1.01
	600	80	75	57.00	17.25	17.25	414	1	0.99
Crit	**600**	**80**	**75**	**60.94**	**17.24**	**17.24**	**414**	**1**	**0.99**

	NCAP			SHR			Obj.
Cond.	m	c	r^2	m	c	r^2	
Initial	0.020	-0.240	0.999	-0.042	3.578	0.999	
Opt	0.020	-0.210	0.999	-0.043	3.643	0.998	0.997
rel_dev	0.020	0.124	0.001	0.021	0.018	0.000	

CFM, DB, OAT

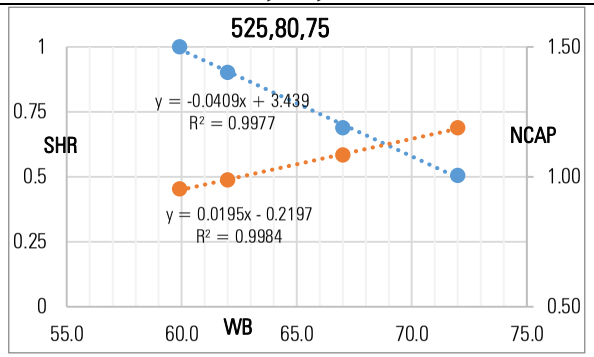

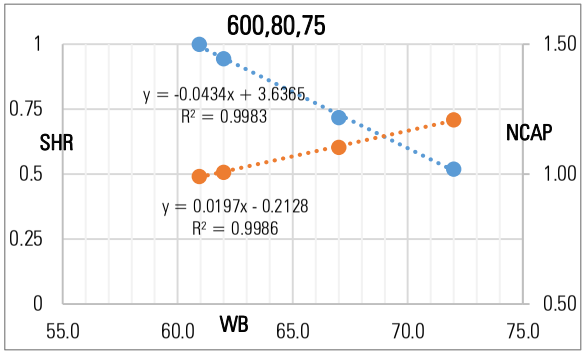

Global optimized points calculation Table

Cond.	CFM	DB	OAT	WB	TCC	TSC	NCFM	SHR	NCAP
Guess	675	80	75	61.85	17.79	17.79	466	1	1.02
	675	80	75	72.00	21.29	11.37	466	0.534	1.22
	675	80	75	67.00	19.44	14.53	466	0.747	1.12
	675	80	75	62.00	17.84	17.70	466	0.992	1.03
	675	80	75	57.00	17.79	17.79	466	1.000	1.02
Crit	**675**	**80**	**75**	**61.85**	**17.81**	**17.81**	**466**	**1**	**1.02**

	NCAP			SHR			Obj.
Cond.	m	c	r^2	m	c	r^2	
Initial	0.020	-0.204	0.998	-0.046	3.832	0.998	
Opt	0.020	-0.194	0.999	-0.046	3.856	0.999	0.997
rel_dev	0.007	0.050	0.000	0.007	0.006	0.000	

Cond.	CFM	DB	OAT	WB	TCC	TSC	NCFM	SHR	NCAP
Guess	525	80	85	60.46	15.91	15.91	362	1	0.91
	525	80	85	72.00	19.67	10.06	362	0.511	1.13
	525	80	85	67.00	17.92	12.58	362	0.702	1.03
	525	80	85	62.00	16.31	15.06	362	0.923	0.94
	525	80	85	57.00	15.91	15.91	362	1	0.91
Crit	**525**	**80**	**85**	**60.46**	**15.89**	**15.89**	**362**	**1**	**0.91**

	NCAP			SHR			Obj.
Cond.	m	c	r^2	m	c	r^2	
Initial	0.019	-0.260	0.999	-0.041	3.477	0.998	
Opt	0.019	-0.225	0.999	-0.042	3.556	0.998	0.996
rel_dev	0.025	0.135	0.001	0.026	0.023	0.000	

Cond.	CFM	DB	OAT	WB	TCC	TSC	NCFM	SHR	NCAP
Guess	600	80	85	61.43	16.52	16.52	414	1	0.95
	600	80	85	72.00	19.99	10.53	414	0.527	1.15
	600	80	85	67.00	18.22	13.37	414	0.734	1.05
	600	80	85	62.00	16.65	16.09	414	0.966	0.96
	600	80	85	57.00	16.52	16.52	414	1	0.95
Crit	**600**	**80**	**85**	**61.43**	**16.52**	**16.52**	**414**	**1**	**0.95**

	NCAP			SHR			Obj.
Cond.	m	c	r^2	m	c	r^2	
Initial	0.019	-0.233	0.999	-0.044	3.692	0.999	
Opt	0.019	-0.211	0.999	-0.045	3.744	0.999	0.997
rel_dev	0.016	0.095	0.000	0.017	0.014	0.000	

CFM, DB, OAT

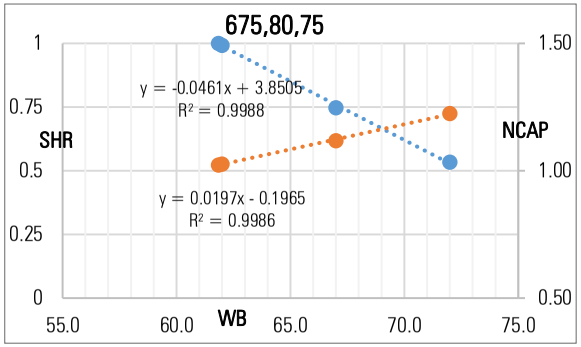

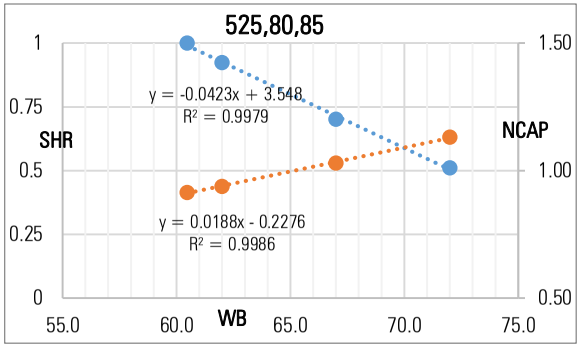

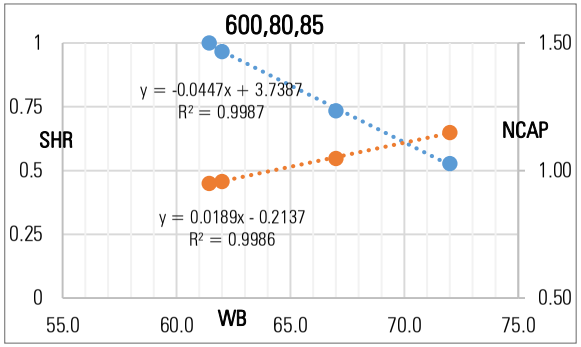

Global optimized points calculation Table

Cond.	CFM	DB	OAT	WB	TCC	TSC	NCFM	SHR	NCAP
Guess	675	80	85	62.42	17.02	17.02	466	1	0.98
	675	80	85	72.00	20.22	10.97	466	0.543	1.16
	675	80	85	67.00	18.44	14.12	466	0.766	1.06
	675	80	85	62.00	17.02	17.02	466	1.000	0.98
	675	80	85	57.00	17.02	17.02	466	1.000	0.98
Crit	**675**	**80**	**85**	**62.42**	**17.02**	**17.02**	**466**	**1**	**0.98**

		NCAP			SHR			Obj.	
Crit									0.997
	Cond.	m	c	r^2	m	c	r^2		1
	Initial	0.020	-0.311	1.000	-0.045	3.757	1.000		TRUE
	Opt	0.019	-0.222	0.998	-0.048	3.978	0.998	0.997	TRUE
	rel_dev	0.061	0.287	0.002	0.069	0.059	0.002		####

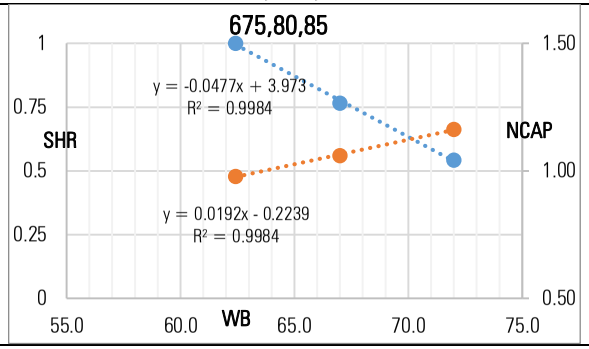

Cond.	CFM	DB	OAT	WB	TCC	TSC	NCFM	SHR	NCAP
Guess	525	80	95	61.00	15.18	15.18	362	1	0.87
	525	80	95	72.00	18.62	9.67	362	0.519	1.07
	525	80	95	67.00	16.94	12.17	362	0.718	0.97
	525	80	95	62.00	15.42	14.61	362	0.947	0.89
	525	**80**	**95**	**57.00**	**15.18**	**15.18**	**362**	**1**	**0.87**
Crit	525	80	95	61	15.17	15.17	362.1	1	0.872

		NCAP			SHR			Obj.
	Cond.	m	c	r^2	m	c	r^2	
	Initial	0.018	-0.254	0.999	-0.043	3.602	0.998	
	Opt	0.018	-0.228	0.999	-0.044	3.664	0.998	0.997
	rel_dev	0.019	0.101	0.000	0.020	0.017	0.000	

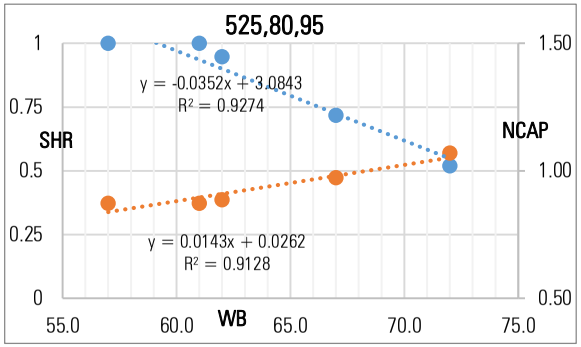

Cond.	CFM	DB	OAT	WB	TCC	TSC	NCFM	SHR	NCAP
Guess	600	80	95	62.00	15.75	15.75	414	1	0.91
	600	80	95	72.00	18.89	10.13	414	0.536	1.09
	600	80	95	67.00	17.20	12.95	414	0.753	0.99
	600	80	95	62.00	15.76	15.76	414	1.000	0.91
	600	80	95	57.00	15.75	15.75	414	1	0.91
Crit	**600**	**80**	**95**	**62.00**	**15.78**	**15.78**	**414**	**1**	**0.91**

		NCAP			SHR			Obj.	
									0.997
	Cond.	m	c	r^2	m	c	r^2		1
	Initial	0.018	-0.210	0.998	-0.046	3.875	0.999		TRUE
	Opt	0.018	-0.202	0.998	-0.047	3.894	0.999	0.997	TRUE
	rel_dev	0.006	0.035	0.000	0.006	0.005	0.000		TRUE

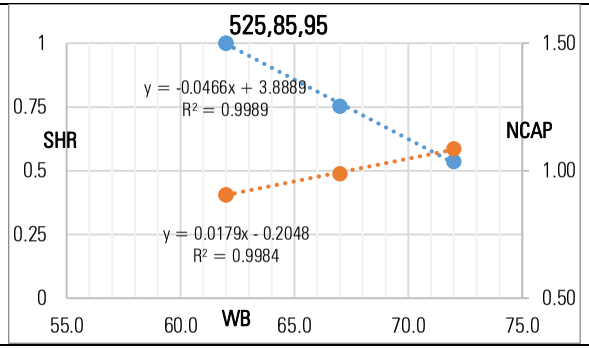

Global optimized points calculation Table

Cond.	CFM	DB	OAT	WB	TCC	TSC	NCFM	SHR	NCAP
Guess	675	80	95	63.04	16.22	16.22	466	1	0.93
	675	80	95	72.00	19.09	10.57	466	0.554	1.10
	675	80	95	67.00	17.39	13.70	466	0.788	1.00
	675	80	95	62.00	16.21	16.21	466	1.000	0.93
	675	80	95	57.00	16.22	16.22	466	1.000	0.93
Crit	**675**	**80**	**95**	**63.04**	**16.21**	**16.21**	**466**	**1**	**0.93**

Crit

	NCAP			SHR			Obj.	
Cond.	m	c	r^2	m	c	r^2		
Initial	0.020	-0.310	1.000	-0.047	3.925	1.000		TRUE
Opt	0.018	-0.233	0.998	-0.050	4.132	0.998	0.997	TRUE
rel_dev	0.055	0.250	0.002	0.062	0.053	0.002		TRUE

0.997
1

Cond.	CFM	DB	OAT	WB	TCC	TSC	NCFM	SHR	NCAP
Guess	525	80	105	61.59	14.41	14.41	362	1	0.83
	525	80	105	72.00	17.52	9.26	362	0.529	1.01
	525	80	105	67.00	15.91	11.74	362	0.738	0.91
	525	80	105	62.00	14.49	14.12	362	0.974	0.83
	525	80	105	57.00	14.41	14.41	362	1	0.83
Crit	**525**	**80**	**105**	**61.59**	**14.41**	**14.41**	**362**	**1**	**0.83**

Crit

	NCAP			SHR			Obj.
Cond.	m	c	r^2	m	c	r^2	
Initial	0.017	-0.334	1.000	-0.048	3.985	1.000	
Opt	0.016	-0.267	0.998	-0.051	4.202	0.998	0.997
rel_dev	0.056	0.202	0.002	0.063	0.054	0.002	

Cond.	CFM	DB	OAT	WB	TCC	TSC	NCFM	SHR	NCAP
Guess	675	80	105	62.76	14.94	14.94	466	1	0.86
	675	80	105	72.00	17.76	9.71	466	0.547	1.02
	675	80	105	67.00	16.13	12.51	466	0.776	0.93
	675	80	105	62.00	14.93	14.93	466	1.000	0.86
	675	80	105	57.00	14.94	14.94	466	1	0.86
Crit	**675**	**80**	**105**	**62.76**	**14.93**	**14.93**	**466**	**1**	**0.86**

Crit

	NCAP			SHR			Obj.	
Cond.	m	c	r^2	m	c	r^2		
Initial	0.019	-0.328	1.000	-0.046	3.842	1.000		TRUE
Opt	0.018	-0.245	0.998	-0.049	4.073	0.998	0.996	TRUE
rel_dev	0.062	0.253	0.002	0.070	0.060	0.002		####

0.996
1

CFM, DB, OAT

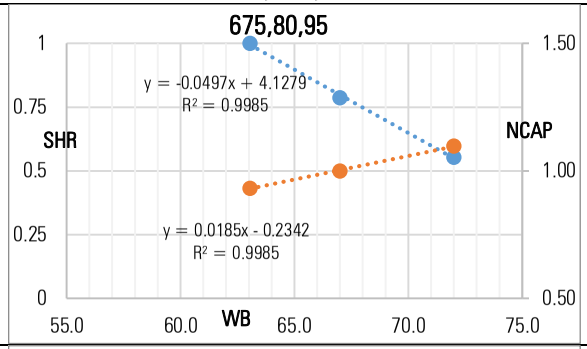

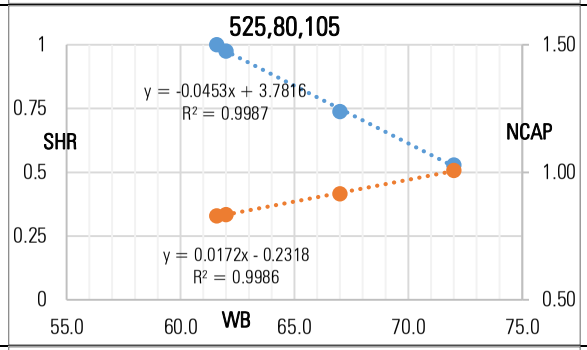

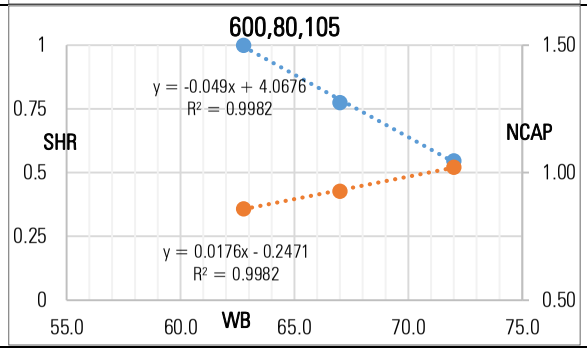

Global optimized points calculation Table

Cond.	CFM	DB	OAT	WB	TCC	TSC	NCFM	SHR	NCAP
Guess	675	80	105	63.68	15.36	15.36	466	1	0.88
	675	80	105	72.00	17.93	10.15	466	0.566	1.03
	675	80	105	67.00	16.30	13.25	466	0.813	0.94
	675	80	105	62.00	15.36	15.36	466	1.000	0.88
	675	80	105	57.00	15.36	15.36	466	1.000	0.88
Crit	**675**	**80**	**105**	**63.68**	**15.35**	**15.35**	**466**	**1**	**0.88**

Crit		NCAP			SHR			Obj.	0.997
	Cond.	m	c	r^2	m	c	r^2		1
	Initial	0.019	-0.319	1.000	-0.049	4.120	1.000		TRUE
	Opt	0.018	-0.254	0.999	-0.052	4.307	0.999	0.997	TRUE
	rel_dev	0.048	0.202	0.001	0.053	0.045	0.001		####

Cond.	CFM	DB	OAT	WB	TCC	TSC	NCFM	SHR	NCAP
Guess	675	80	115	61.59	14.41	14.41	466	1	0.83
	675	80	115	72.00	17.52	9.26	466	0.529	1.01
	675	80	115	67.00	15.91	11.74	466	0.738	0.91
	675	80	115	62.00	14.49	14.12	466	0.974	0.83
	675	80	115	57.00	14.41	14.41	466	1	0.83
Crit	**675**	**80**	**115**	**61.59**	**14.41**	**14.41**	**466**	**1**	**0.83**

Crit		NCAP			SHR			Obj.
	Cond.	m	c	r^2	m	c	r^2	
	Initial	0.019	-0.326	1.000	-0.042	3.543	1.000	
	Opt	0.017	-0.229	0.998	-0.045	3.793	0.998	0.996
	rel_dev	0.073	0.298	0.002	0.083	0.071	0.002	

Cond.	CFM	DB	OAT	WB	TCC	TSC	NCFM	SHR	NCAP
Guess	675	80	115	62.76	14.94	14.94	466	1	0.86
	675	80	115	72.00	17.76	9.71	466	0.547	1.02
	675	80	115	67.00	16.13	12.51	466	0.776	0.93
	675	80	115	62.00	14.93	14.93	466	1.000	0.86
	675	80	115	57.00	14.94	14.94	466	1	0.86
Crit	**675**	**80**	**115**	**62.76**	**14.93**	**14.93**	**466**	**1**	**0.86**

Crit		NCAP			SHR			Obj.	0.996
	Cond.	m	c	r^2	m	c	r^2		1
	Initial	0.019	-0.328	1.000	-0.046	3.842	1.000		TRUE
	Opt	0.018	-0.245	0.998	-0.049	4.073	0.998	0.996	TRUE
	rel_dev	0.062	0.253	0.002	0.070	0.060	0.002		####

CFM, DB, OAT

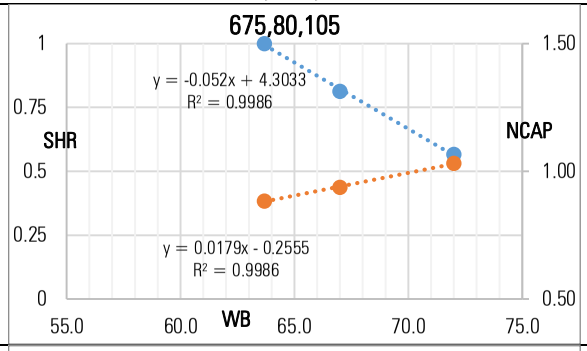

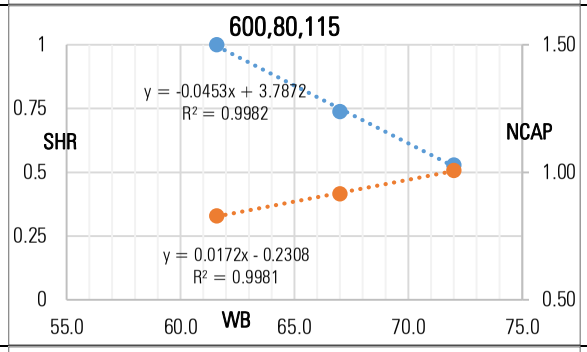

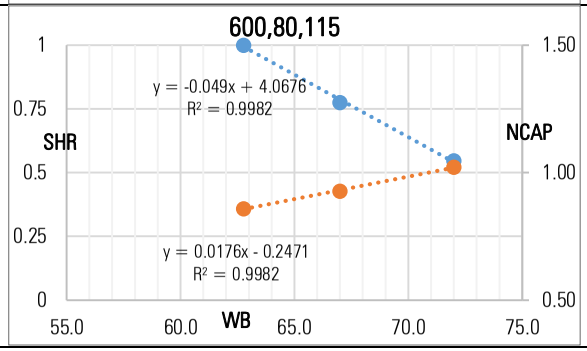

Global optimized points calculation Table

Cond.	CFM	DB	OAT	WB	TCC	TSC	NCFM	SHR	NCAP
Guess	675	80	115	63.68	15.36	15.36	466	1	0.88
	675	80	115	72.00	17.93	10.15	466	0.566	1.03
	675	80	115	67.00	16.30	13.25	466	0.813	0.94
	675	80	115	62.00	15.36	15.36	466	1.000	0.88
	675	80	115	57.00	15.36	15.36	466	1.000	0.88
Crit	**675**	**80**	**115**	**63.68**	**15.35**	**15.35**	**466**	**1**	**0.88**

Crit		NCAP			SHR			Obj.	0.997
	Cond.	m	c	r^2	m	c	r^2		1
	Initial	0.019	-0.319	1.000	-0.049	4.120	1.000		TRUE
	Opt	0.018	-0.254	0.999	-0.052	4.307	0.999	0.997	TRUE
	rel_dev	0.048	0.202	0.001	0.053	0.045	0.001		TRUE

CFM, DB, OAT

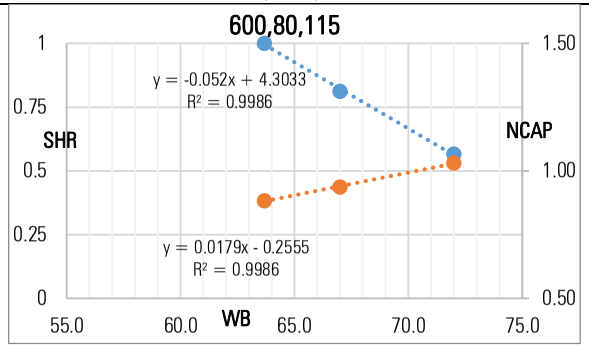

Cond.	CFM	DB	OAT	WB	TCC	TSC	NCFM	SHR	NCAP
Guess	525	80	125	63.24	12.68	12.68	362	1	0.73
	525	80	125	72.00	15.07	8.36	362	0.555	0.87
	525	80	125	67.00	13.62	10.80	362	0.793	0.78
	525	80	125	62.00	12.68	12.68	362	1.000	0.73
	525	80	125	57.00	12.68	12.68	362	1	0.73
Crit	**525**	**80**	**125**	**63.24**	**12.67**	**12.67**	**362**	**1**	**0.73**

Crit		NCAP			SHR			Obj.
	Cond.	m	c	r^2	m	c	r^2	
	Initial	0.017	-0.334	1.000	-0.048	3.985	1.000	
	Opt	0.016	-0.267	0.998	-0.051	4.202	0.998	0.997
	rel_dev	0.056	0.202	0.002	0.063	0.054	0.002	

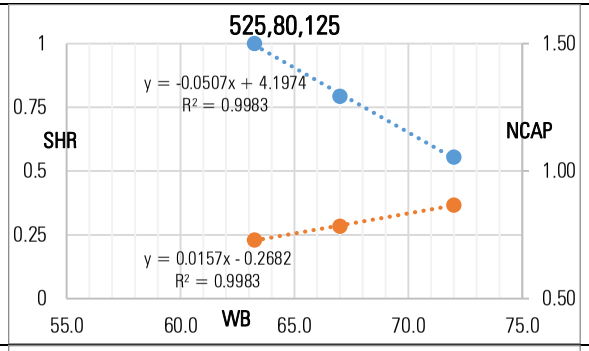

Cond.	CFM	DB	OAT	WB	TCC	TSC	NCFM	SHR	NCAP
Guess	600	80	125	67.24	13.1	13.1	414	1	0.75
	600	80	125	72.00	15.23	8.81	414	0.578	0.88
	600	80	125	67.00	13.78	11.56	414	0.839	0.79
	600	80	125	62.00	13.10	13.10	414	1.000	0.75
	600	80	125	57.00	13.10	13.10	414	1	0.75
Crit	**600**	**80**	**125**	**67.24**	**13.51**	**13.51**	**414**	**1**	**0.78**

Crit		NCAP			SHR			Obj.	0.723
	Cond.	m	c	r^2	m	c	r^2		1
	Initial	0.017	-0.325	1.000	-0.052	4.329	1.000		####
	Opt	0.021	-0.619	0.876	-0.069	5.513	0.825	0.723	TRUE
	rel_dev	0.245	0.905	0.124	0.316	0.274	0.175		####

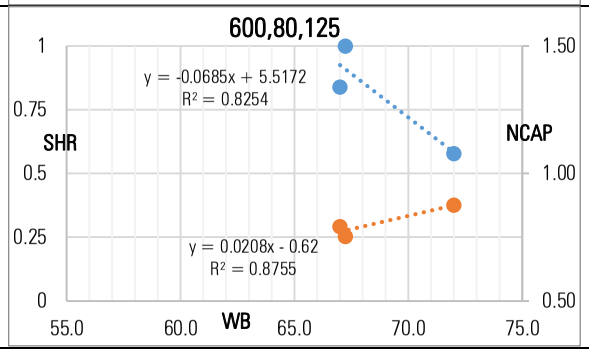

Global optimized points calculation Table

Cond.	CFM	DB	OAT	WB	TCC	TSC	NCFM	SHR	NCAP
Guess	675	80	125	67.24	13.44	13.44	466	1	0.77
	675	80	125	72.00	15.34	9.24	466	0.602	0.88
	675	80	125	67.00	13.89	12.27	466	0.883	0.80
	675	80	125	62.00	13.44	13.44	466	1.000	0.77
	675	80	125	57.00	13.44	13.44	466	1.000	0.77
Crit	**675**	**80**	**125**	**67.24**	**13.73**	**13.73**	**466**	**1**	**0.79**

Crit		NCAP			SHR			Obj.	0.83
	Cond.	m	c	r^2	m	c	r^2		1
	Initial	0.017	-0.319	1.000	-0.056	4.649	1.000		####
	Opt	0.020	-0.522	0.928	-0.069	5.537	0.894	0.830	TRUE
	rel_dev	0.170	0.640	0.072	0.219	0.191	0.106		TRUE

CFM, DB, OAT

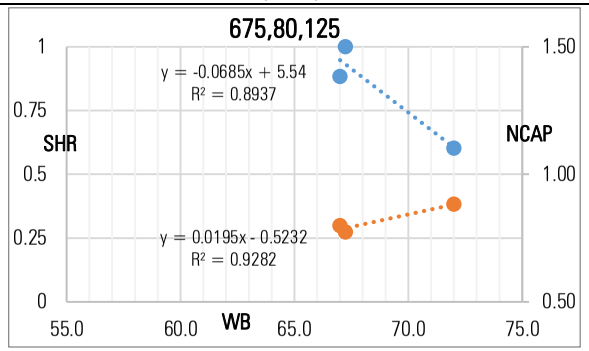

Table H-5 25HBB318 critical point estimation table for normalized plots of Figure F1

CFM	WB	NCAP	WB	NCAP	WB	NCAP	WB	NCAP	WB	NCAP	WB	NCAP
525	72	1.189	72	1.131	72	1.071	72	1.007	72	0.94	72	0.867
525	67	1.084	67	1.03	67	0.974	67	0.915	67	0.852	67	0.783
525	62	0.987	62	0.938	62	0.887	62	0.833	62	0.781	63.24	0.73
525	59.91	0.95	60.46	0.91	61.00	0.87	61.59	0.83	61.59	0.83	62	0.729
525	57	0.954	57	0.915	57	0.873	57	0.829	57	0.781	57	0.729
600	72	1.209	72	1.15	72	1.086	72	1.021	72	0.952	72	0.876
600	67	1.104	67	1.048	67	0.989	67	0.928	67	0.863	67.24	0.78
600	62	1.008	62	0.957	62	0.906	62.76	0.86	62.76	0.86	67	0.792
600	60.94	0.99	61.43	0.95	62.00	0.91	62	0.859	62	0.809	62	0.753
600	57	0.992	57	0.95	57	0.906	57	0.859	57	0.809	57	0.753
675	72	1.224	72	1.163	72	1.098	72	1.031	72	0.96	72	0.882
675	67	1.118	67	1.06	67	1	67	0.937	67	0.871	67.24	0.79
675	62	1.026	62	0.979	63.04	0.93	63.68	0.88	63.68	0.88	67	0.799
675	61.85	1.02	62.42	0.98	62	0.932	62	0.883	62	0.831	62	0.773
675	57	1.023	57	0.979	57	0.933	57	0.883	57	0.831	57	0.773
CFM	**WB**	**SHR**	**WB**	**SHR**	**WB**	**SHR**	**WB**	**SHR**	**WB**	**SHR**	**WB**	**SHR**
525	78.11	0.26	78.11	0.26	78.11	0.26	78.11	0.26	78.11	0.26	78.11	0.26
525	72.00	0.51	72.00	0.51	72.00	0.52	72.00	0.53	72.00	0.54	72.00	0.55
525	67.00	0.69	67.00	0.70	67.00	0.72	67.00	0.74	67.00	0.76	67.00	0.79
525	62.00	0.90	62.00	0.92	62.00	0.95	62.00	0.97	62.00	1.00	63.24	1.00
525	59.91	1.00	60.46	1.00	61.00	1.00	61.59	1.00	61.59	1.00	62.00	1.00
525	57.00	1.00	57.00	1.00	57.00	1.00	57.00	1.00	57.00	1.00	57.00	1.00
600	78.11	0.26	78.11	0.26	78.11	0.26	78.11	0.26	78.11	0.26	78.11	0.26
600	72.00	0.52	72.00	0.53	72.00	0.54	72.00	0.55	72.00	0.56	72.00	0.58
600	67.00	0.72	67.00	0.73	67.00	0.75	67.00	0.78	67.00	0.80	67.24	0.84
600	62.00	0.94	62.00	0.97	62.00	1.00	62.76	1.00	62.76	1.00	67.00	1.00
600	60.94	1.00	61.43	1.00	62.00	1.00	62.00	1.00	62.00	1.00	62.00	1.00
600	57.00	1.00	57.00	1.00	57.00	1.00	57.00	1.00	57.00	1.00	57.00	1.00
675	78.11	0.26	78.11	0.26	78.11	0.26	78.11	0.26	78.11	0.26	78.11	0.26
675	72.00	0.53	72.00	0.54	72.00	0.55	72.00	0.57	72.00	0.58	72.00	0.60
675	67.00	0.75	67.00	0.77	67.00	0.79	67.00	0.81	67.00	0.84	67.24	0.88
675	62.00	0.99	62.00	1.00	63.04	1.00	63.68	1.00	63.68	1.00	67.00	1.00
675	61.85	1.00	62.42	1.00	62.00	1.00	62.00	1.00	62.00	1.00	62.00	1.00
675	57.00	1.00	57.00	1.00	57.00	1.00	57.00	1.00	57.00	1.00	57.00	1.00

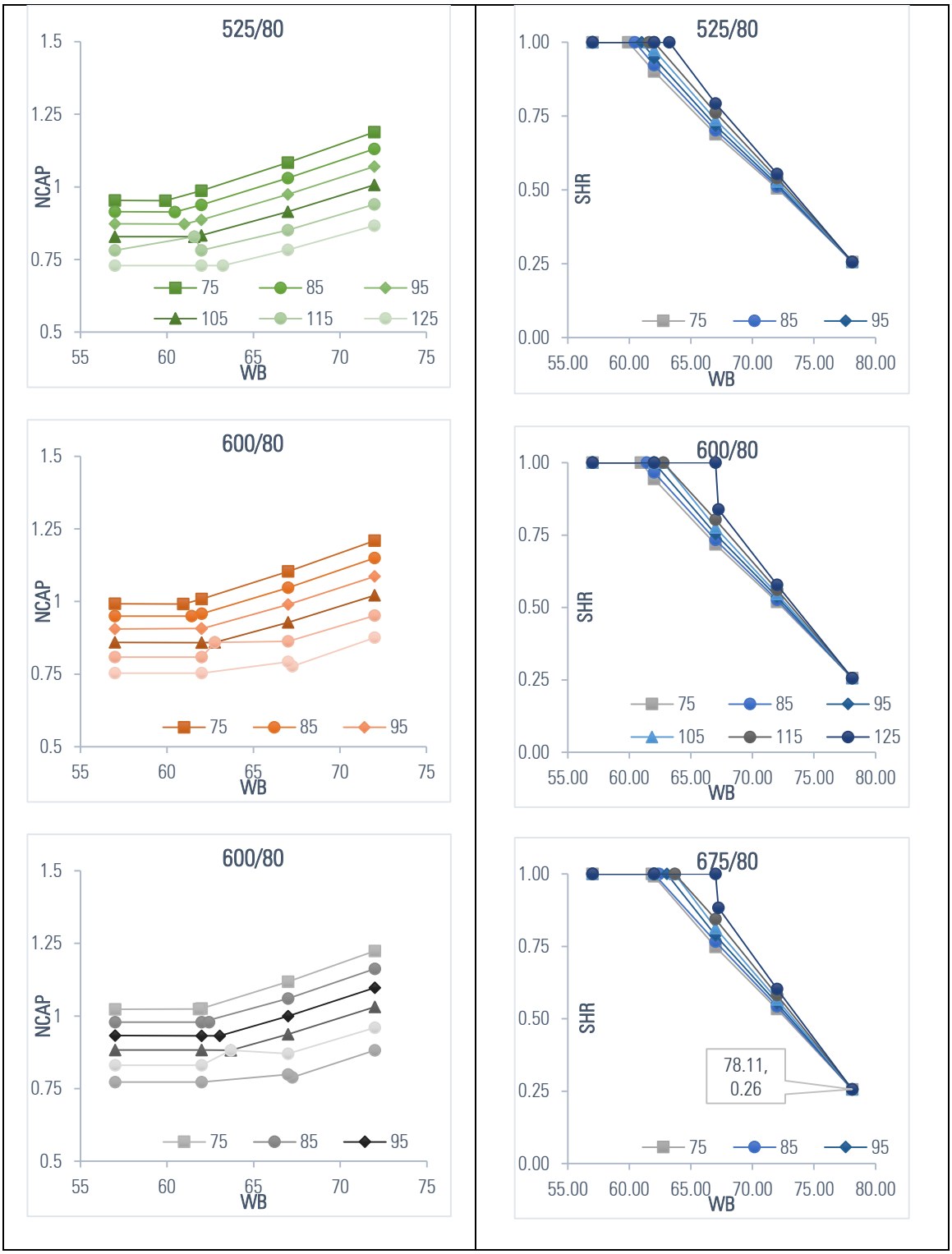

Figure H-1 25HBB318 critical point estimation normalized plots